Modelling and Optimization of Competitive Bio-sorption of Copper and Lead Ions Using Fruit Peels

A thesis submitted in fulfilment of the academic requirements for the degree of

Doctor of Engineering

Durban University of Technology

Faculty of Engineering and Built Environment

Chemical Engineering

By

Felicia Omolara Afolabi

September 2022

Supervisors: Prof P. Musonge

Prof B. F. Bakare

Declaration

I Felicia Omolara Afolabi, hereby declare that the content presented in this thesis entitled "Modeling and optimization of competitive bio-sorption of heavy metals using fruit peels" is a record of my own research work conducted with the intention of obtaining the degree of Doctoral of Engineering in Chemical Engineering at the Durban University of Technology (DUT). The content of this research work has not been previously published or written by another person for the award of any other degree at DUT or at any other educational institution. Moreover, I declare that the content presented in this thesis does not violate any copyright as all the work of others has been indicated accordingly by means of in-text referencing and a comprehensive list of references has been listed at the end of this thesis.

Author: Afolabi Felicia Omolara

Signature: Date: 20 September 2022

Co – Supervisor: Prof Babatunde Bakare

Signature: Date: 20 September 2022

Supervisor: Prof Paul Musonge

Signature: Date: 20/September 2022

Acknowledgments

Firstly, I would like to appreciate my Lord God Almighty for His grace, divine enablement, and love towards me during this academic journey. Many people have shown immeasurable help and support to me in the process of this Doctoral study as such I would like to appreciate them. To my supervisors, I want to say thank you for the opportunity to undertake this study under your supervision. Thank you for your tutelage and support.

My special appreciation goes to Ms. Zimbini Ngcingwana of the Chemistry Department, University of Kwazulu-natal, Pietermaritzburg campus for assisting to analyze my samples. Mrs. Ope Alabi and Ms. Samantha Govender of the Department of Food Science for their assistance with the use of some equipment in their laboratory.

I wish to appreciate the Durban University of Technology, Mangosuthu University of Technology, the National Research Foundation, and the Institute of Systems Science for their financial support. My appreciation also goes to the HoD and staff of the Chemical Engineering Department, my fellow postgraduate students (Dr. Martha Achisa, Jeremiah, Donald, Emmanuel, Edward, Charlene, Sli, Lindi, Elon, and Anietie).

My gratitude goes to Dr. and Mrs. Bunmi Oyekunle, Rev(Dr) and Pst(Mrs) Samuel Bunmi Olajire, Pastor Olu Victor, Prophet Ajala, and Dr(Mrs) Yemisi Oyegbile for their prayers, words of encouragement, and support.

My heartfelt gratitude goes to my mum, siblings, and the Afolabi family. Thank you for your prayers, support, and for believing in me.

Finally, I sincerely appreciate my lovely husband and friend (Olusegun Afolabi) and my princesses (Oluwatoni and Oluwatomisona). Thank you for your immeasurable love and understanding. You have made this possible. Thank you for standing by me. I love you!

Dedication

This research work is dedicated to God Almighty for His mercies and faithfulness over my life. I also dedicate this work to my late daddy (Pa Thomas Adeyemi Ilori). I appreciate your fatherly care. I love you, daddy.

Publications

Some publications have resulted from this study which is in the form of peer-reviewed journal articles and peer-reviewed conference papers.

PUBLISHED JOURNAL ARTICLES

1. **Afolabi, FO.,** Musonge P., Bakare, BF. 2020. Evaluation of lead (II) removal from wastewater using banana peels. optimization study. *Polish Journal of Environmental Studies*, 30 (2), 1-10.
2. **Afolabi, FO.,** Musonge P., Bakare, BF. 2021. Bio-sorption of a bi-solute system of copper and lead ions onto banana peels. characterization and optimization. *Journal of Environmental Health Science and Engineering.*
3. **Afolabi, FO.**, Musonge P., Bakare, BF. 2021. Bio-sorption of copper and lead ions in single and binary systems onto banana peels. *Cogent Engineering*, 8 (1), 1886730.
4. **Afolabi, FO.,** Musonge P., Bakare, BF. 2021. Application of the response surface methodology in the removal of Cu^{2+} and Pb^{2+} from aqueous solution using orange peels. *Scientific Africa*, 13: e00931.
5. **Afolabi, FO.,** Musonge P., Bakare, BF. 2022. Adsorption of copper and lead ions in a binary system oto orage peels: Optimizatio, Equilirium ad Kietic study. Sustainability 2022, 14, 10860. https://doi.org/10.3390/su141710860.

PEER-REVIEWED CONFERENCE AND PUBLICATION (ORAL PRESENTATION)

1. **Afolabi, FO,** Musonge P., Bakare, BF. 2021. Bio-sorption of Cu^{2+} ion from wastewater using (Musa acuminata) banana peels. Conference proceedings presented at *International Conference on Green Technologies for Sustainable Development (GTSD-2021), Schedule for Virtual International Conference, March 9-11, 2021 Gujarat, India*.
2. **Afolabi, FO.,** Musonge P., Bakare, BF. 2020. Bio-sorption of Cu^{2+} and Pb^{2+} ions onto Citrus sinensis (Orange) peels. Conference Proceedings presented at the *18^{th} International Conference on Science, Engineering, Technology, and Waste*

Management. Volume 1, ISBN: 978-93-86878-46-5, Nov. 16-17, 2020, Johannesburg, South Africa.

3. **Afolabi, FO.,** Musonge P., Bakare, BF. 2018. The Performance of Banana Peels in the removal of Cu^{2+} and Pb^{2+} ions from Wastewater. Conference Proceedings presented at the *Third International Conference on Composite, Bio-composites, and Nanocomposites (ICCBN), Advanced in Composite, Bio-composite and Nanocomposites Volume 3, 7-9 November 2018, Port Elizabeth, South Africa*.

Other output

1. **Afolabi, FO.,** Musonge P., Bakare, BF. 2019. Evaluation of Lead (II) Pb^{2+} removal from Wastewater using Banana Peels: Optimization study. Conference Proceedings presented at the *4^{th} Interdisciplinary Research and Innovation Conference. 17-20 September 2019, Durban, South Africa*.

Awards and Honours

- Best paper presented at International Conference on Green Technologies for Sustainable Development (GTSD-2021).
- Best Oral Presenter at the 11th Annual SAIChE KZN Research, Mangosuthu University of Technology, Umlazi, Durban, South Africa: 2019.

Abstract

The application of various agricultural-based materials as adsorbents for the removal of heavy metal ions from aqueous solutions has attracted the interest of many researchers. Many studies have been conducted on the removal of heavy metals from wastewater using the bio-sorption process with a focus on wastewater containing single solutes. In addition, the existing column adsorption models were developed to describe the dynamic behaviour of single solute bio-sorption processes. However, the application of a linear driving force model which makes use of batch experimental results to describe the bio-sorption process in a fixed-bed has not been reported for binary solute systems. In this study, the performance of orange and banana peels was investigated for the removal of copper and lead ions from wastewater in both single and binary systems. These bio-sorbents were used in their natural form.

The characterization of the bio-sorbents before and after adsorption was achieved using analytical techniques. Fourier Transform Infrared Spectroscopy (FTIR) was used to determine the functional groups present on the surface of the bio-sorbents. The results showed that the bio-sorbents contain various functional groups such as carboxyl, hydroxyl, carbonyl, aminyl, and alkyl groups that enhanced the adsorption process. After adsorption, there were significant shifts in the peaks representing hydroxyl and carboxyl groups which were common to both bio-sorbents. Therefore, it was concluded that ion exchange is the sorption mechanism responsible for the adsorption of metal ions. The Scanning Electron Microscopy with Energy Dispersive X-ray Spectroscopy (SEM/EDS) was used to determine the morphological structure and the elemental composition of the bio-sorbents. The surfaces of the bio-sorbents showed an irregular, and microporous structure while the elemental composition revealed the presence of carbon, oxygen, hydrogen, and potassium. The surfaces of the bio-sorbents became uniform, smooth, and covered after the adsorption and the EDS showed the presence of adsorbed metal ions. The X-ray diffractometer (XRD) which explained the crystallinity of the bio-sorbents showed that both bio-sorbents are amorphous. The values of the point of zero charge (pHpzc) for orange and banana peels obtained were 3.85 and 4.83 respectively. This revealed that the surfaces of both bio-sorbents were acidic and therefore suitable for the adsorption of cations.

The design of experiments (DOE) was employed in the batch study to investigate the interactive effect of the operating parameters, and a 2^4 full factorial design was used to generate the experimental runs. The factors studied and their ranges are initial concentration (10 – 100 mg/L), solution pH (2 - 6), adsorbent dosage (0.1 – 1 g), and particle size (75 – 455 µm), for the single solute system. The interaction of the factors was studied using response surface methodology (RSM) with the central composite design (CCD). The highest removal of lead and copper for orange peels was 99.75% and 98.53% while 99.32% and 98.12% were obtained for lead and copper using banana peels. The results showed that both bio-sorbents have a high affinity for lead and copper while the order of influence of the factors gave adsorbent dosage > pH > initial concentration > particle size for the bio-sorption of copper and lead using both bio-sorbents. The optimum pH of 5.5 was obtained for both metals hence three factors (initial concentration, adsorbent dosage, and particle size) with the same parameter range specified for a single solute were considered for the binary solute interactive study using the same method. The initial concentration of the metal ions in the binary system was in the ratio of 1:1. In most of the experimental runs, the percentage yield of lead was higher than copper. The highest removal for lead and copper was 98.85 % and 87.32 % for orange peels, while for banana peels, lead was 97.85 % and copper was 97.6 %.

The isotherm and kinetic studies of single and binary systems of copper and lead were carried out using both bio-sorbents. The Langmuir isotherm fitted the adsorption data signifying a monolayer adsorption mechanism while the pseudo-second-order model fitted the kinetic data which suggested the chemisorption process for both bio-sorbents in single and binary systems. The adsorption of lead was higher than copper in both single and binary systems and the adsorption of copper was sensitive to the co-existence of lead in binary systems. Orange peels bio-sorbent performed slightly better than banana peels hence, it was chosen for the dynamic column studies

The fixed bed experiments were conducted to investigate the effect of column parameters such as flow rate (1 and 3 mL/min), initial concentration (10, 50, and 100 mg/L), and bed height (1 and 3 cm). The results showed that the performance of the bed was improved with an increase in the bed height while the volume of solution treated at breakthrough decreased with an increase in flow rate for both metals in a single solute system. The Thomas, Yoon Nelson, and Bohart Adams models were applied to the experimental data. The Thomas and Yoon Nelson

models performed well with a high coefficient of correlation ($R^2 > 0.9$) and the lowest mean absolute error value of less than 0.1.

The breakthrough curves for the binary solution of copper and lead showed slightly different shapes than the single solute system. This can be ascribed to the influence of the co-existence of metal ions which led to competition for the limited binding sites on the bio-sorbent. The breakthrough time decreased with an increased initial concentration for both metal ions in the binary system. However, the breakthrough curves representing copper bio-sorption, reached the breakthrough point faster than lead suggesting a lower affinity of copper to bind to the active site. The bio-sorption capacity of lead was consistently higher than copper for all the initial concentrations considered.

A mathematical model was developed for the binary solute system of copper and lead. The model was developed from the mass balance equation of the solid and liquid phases of an elemental section of the column. An assumption of axially dispersed plug flow was made, and a linear driving force (LDF) was used to describe the intraparticle mass transfer. The partial differential equation obtained from the mass conservation equation was discretized to form an ordinary differential equation (ODE) using the finite difference method. The resulting ODEs were solved using the ode15s solver in MATLAB. The mathematical model results followed a similar trend with the experimental results, such that the breakthrough curve of copper reached the breakthrough point faster than lead for all the initial concentrations considered. The model results showed that the mathematical model based on the linear driving force can be used to describe the dynamic behaviour of a bi-solute fixed-bed adsorption column. The mathematical model performed well at high initial concentrations. The Thomas model gave the lowest mean absolute error (MAE) value of 0.08 while the mathematical model gave an MAE value of 0.9 which explains the deviation of the models from the experimental results.

In conclusion, the equilibrium isotherm studies carried out in the batch experiments were used to assess the adsorption capacity of the bio-sorbent which was used in the LDF expression of the model. Hence, this study has demonstrated that the mathematical model developed for the binary system is suitable for predicting the breakthrough curves using batch experimental results

Table of contents

List of Tables

List of Figures

Glossary and Acronyms

AMD	Acid mine drainage
ANOVA	Analysis of variance
BET	Braunner Emmett Teller
BOD	Biochemical Oxygen Demand
BP	Banana peel
BTC	Breakthrough curve
COD	Chemical Oxygen Demand
EDS	Electron Dispersive Spectroscopy
EPA	Environmental Protection Agency
FTIR	Fourier Transform Infrared Spectroscopy
LDF	Linear driving force
MAE	Mean Absolute Error
MP-AES	Micro-plasma Atomic Emission Spectrophotometer
MTZ	Mass Transfer Zone
ODE	Ordinary Differential Equation
OP	Orange peel
PZC	Point of zero charge

RMSE	Root Mean Squared Error
SANS	South African National Standards
SEM	Scanning electron microscopy
WHO	World Health Organization
XRD	X – Ray Diffraction

List of Notations

K_L	Langmuir adsorption constant	1/mg
K_F	Freundlich constant related to adsorption capacity	(mg/ g)
K	Reaction rate constant	mg/L/min
K_1	Rate constant of pseudo first-order adsorption model	(1/min)
K_2	Pseudo-second-order rate constant	gm/g/min
R_L	Separation factor	
R^2	Correlation coefficient	
m	Mass of adsorbents	g
n	Adsorption intensity	
C_0	Initial concentration of contaminant	mg/L
C	Final concentration of metal at time	mg/L
t	Reaction time	min, h
t_b	Breakthrough time	min
t_b^{id}	Ideal breakthrough time	min
C_e	Equilibrium concentration of metal at time t	mg/L
q_e	Mass of metal adsorbed at equilibrium	mg/g
q_t	Adsorbate uptake at time t	mg/g

q_{max}	Maximum metal adsorption at equilibrium	mg/g

CHAPTER 1

1. Introduction

1.1 Background and Research Motivation

Water is a major constituent of all living matter. A clean and adequate supply of water is essential for household, agricultural, industrial, forestry, and recreational use. An increase in household population, economic development, expansion in agriculture, irrigation farming, and forestry are some of the factors contributing to the fresh water supply to millions of people in South Africa. Furthermore, the average annual rainfall in South Africa is below the world's average rainfall per year and is not evenly distributed across the regions in the country (Liu *et al.* 2017).

Water is a source of life for plants, animals as well as human beings. There is a rapid increase in population growth while the availability of clean water is decreasing. Human beings cannot do without water in a single day; we use water for many purposes such as generation of electricity, growing of crops, drinking, and washing, etc. Water is very critical and cannot be compared with many natural resources, however, the challenges of water pollution are becoming alarming and severe. Water quality problems and availability are approaching a catastrophic level. A way to avoid this impending calamity is to guide against contamination of the various sources of water such, as rivers, streams, oceans, and lakes. These water sources are mostly threatened by increasing industrial activities (Singh N.B *et al.* 2018). Increasing technological activities leading to the generation of heavy metals have exposed the aquatic environment to metal ion concentrations beyond the allowable limit expected in the environment, animals, and human life. South Africa is one of many countries that is rich in mineral resources, however, mining of these mineral resources poses serious challenges such as contamination of groundwater and surface water arising from acid mine drainage (AMD). Therefore, mining industries are considered as a major source of heavy metals as presented in **Figure 1.1**. Heavy metals are toxic and poisonous metallic elements that are released into the environment during mineral extraction activities. Some of these heavy metals of concern include; zinc, copper, iron, manganese, lead, nickel, chromium, cadmium, aluminum (Raouf MS and Raheim ARM 2016).

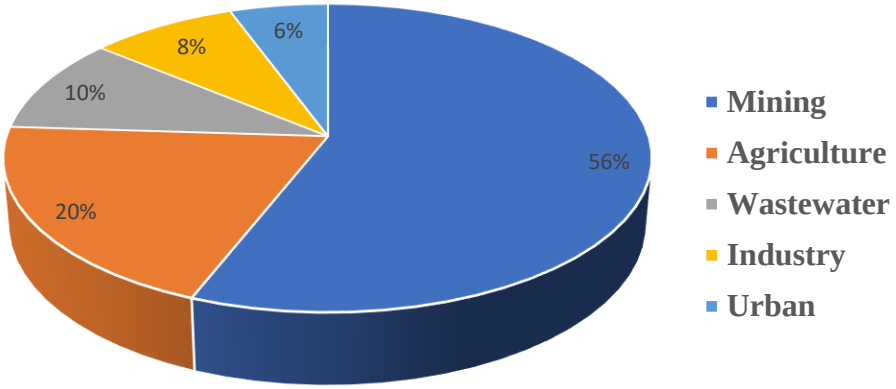

Figure 1.1: Wastewaters containing heavy metals generated in developed countries (Araujo *et al.* 2013)

Heavy metals contribute to a variety of adverse health effects due to their acute and chronic impact on human and aquatic life through water. Thus, considering the environmental, ecological, and health threats associated with heavy metals, there is a need for innovative and effective technologies for the removal of heavy metals from wastewater to a limit that will not pose any significant risks to public health. Wastewater treatment can be categorized into three stages namely: primary, secondary, and tertiary stages (Sonune and Ghate 2004; Raouf MS and Raheim ARM 2016). The primary treatment stage removes suspended solids and oil from wastewater, the secondary treatment stage is used to remove biodegradable wastes while the tertiary treatment stage removes the non-biodegradable wastes. The non-biodegradable wastes are toxic and create severe health and environmental hazard hence, these wastes must be removed from wastewater before discharge into the water bodies. Some of the methods used for tertiary wastewater treatment are membrane separation, ion exchange, precipitation, electrolysis, solvent extraction, and adsorption. However, these methods have common drawbacks which are the high cost of operation and expertise (Volesky 1990; Afroze and Sen 2018). However, adsorption technology has been proven to be less expensive, simple, versatile, and robust over a wide range of applications. The efficiency and performance of an adsorption process are greatly determined by the choice of adsorbent. Many conventional adsorbents have been used for wastewater treatment such as activated carbon, silica gel, activated alumina, and zeolites (Issabayeva, Aroua and Sulaiman 2008; Ismael, Melegy and Kratochvíl 2012; Gupta

et al. 2016; Kumar and Jena 2016; Shi *et al.* 2018). Nevertheless, these adsorbents are highly expensive which has led researchers into a quest for low-cost adsorbents (Barakat 2011). Recently, agricultural wastes have gained the interest of researchers as they are readily available, low-cost, and underutilized. Hence, agricultural wastes are used as bio-sorbent for the removal of heavy metals from wastewater in this study.

1.2 Problem Statement

The scarcity of water is made worse in South Africa by the surface and underground water pollution. The major pollutants of the aquatic environment are from industrial effluents. Effluents from open and abandoned mines, metallurgical plants, and mine residues can cause adverse pollution to the water body. Mining industries produce acid mine drainage (AMD) which has become a major environmental challenge facing the industry. AMD contains metals such as; cadmium, lead, copper, arsenic, iron, and zinc which are hazardous to human health. AMD generated in mining industries will become an environmental, economic, and social burden in the future if left unattended (Naidu *et al.* 2019). Therefore, treatment of mine drainage to a level that does not affect the aquatic environment and human lives is necessary.

Several methods have been used for the treatment of wastewater containing heavy metal ions. Conventional methods such as ion exchange, membrane filtration, oxidation, precipitation, etc., mostly used for removal of heavy metals from wastewater have disadvantages associated with them such as expensive cost of chemicals, incomplete removal of metal ions, production of a large volume of sludge, inability to handle a large volume of wastewater, requires a high level of expertise and high energy requirement. Hence, innovative, and more effective technologies are needed which can reduce metal ion concentration to a minimal level that is environmentally friendly less operating cost.

The adsorption process has become a more preferred option for the removal of heavy metals from wastewater. Adsorption technology is an attractive alternative because of its inherent low cost, efficiency, profitability, and ease of operation (Demirbas 2008; Bilal *et al.* 2021). Activated carbon is an effective adsorbent that has been widely used for the removal of heavy metals present in wastewater. However, it is highly expensive and the cost increases with the quality (Suhas *et al.* 2016). In addition, regeneration of spent carbon is expensive and therefore not practical for industrial scale because it produces excessive sludge hence leading to loss of

adsorbent. As a result of these disadvantages, the use of locally available, underutilized, low-cost adsorbents obtained from agricultural wastes namely; orange and banana peels are used in this study. Although many agricultural wastes have been used for the adsorption of various heavy metals from wastewater, most of the published work has reported a single metal system in both batch and column studies investigating one factor at a time. In addition, the existing breakthrough models were developed based on a single solute system hence, it is important to develop a model to describe the breakthrough curve behaviour of solution containing more than one solute since it is very rare for wastewater to contain a single solute. It is important to emphasize that orange and banana peels were used in their natural form without any form of modification and regeneration of these adsorbents is not within the scope of this work.

1.3 Justification

Bananas and oranges are in high consumption worldwide. Oranges are the biggest citrus type in South Africa and account for 60 % of the citrus fruits produced from approximately 45,000 hectares of cultivated land. South Africa produces an average of 416.5 thousand metric tons and 1.5 Million mega tons of bananas and oranges respectively annually, some of which are exported and used to produce fruit juice (Akpomie and Conradie 2020). Unwanted peels of banana and orange generate a huge quantity of waste from households, markets, and restaurants, which are disposed of on dumping sites. These wastes can be used as low-cost, readily available, and eco-friendly adsorbents for the removal of copper and lead from wastewater thereby reducing the environmental pollution.

The presence of heavy metals in water poses a serious threat to human and aquatic life, as well as the environment. Toxic heavy metals include arsenic, cadmium, chromium, copper, lead, manganese, nickel and mercury (Singh N.B *et al.* 2018). Among these pollutants, lead and copper are the most common heavy metals found in wastewater. They have severe environmental impacts on the waterbodies worldwide (Tang *et al.* 2019). These heavy metals are generated from industries, such as electroplating, electrolytic deposition, printing, pigments and explosives manufacturing, production of coatings, milling, and etching (Sen *et al.* 2019). The presence of lead and copper ions in low concentrations of water is a risk to human life.

Much work has been reported on the use of banana and orange peels for the treatment of wastewater. No work has been reported on the use of these bio-sorbents for the competitive

bio-sorption of Cu^{2+} and Pb^{2+} from wastewater in batch and column mode to the best knowledge of the author. Most of the works reported on batch adsorption studies considered the effect of one-factor-at-a-time also known as OFAT. This method is time-consuming especially when many operating parameters are involved. To the best of the author's knowledge, no work has been reported on the interactive effect of various operating parameters on the bi-solute system of Cu^{2+} and Pb^{2+} using banana and orange peels in a batch mode. It is therefore important and interesting to study the interactive effects of the operating variables in both single and binary systems using response surface methodology (RSM) in batch mode. Although batch results can be used to determine the adsorption capacity of an adsorbent and the adsorption mechanism, these data are not enough for large-scale treatment systems. Therefore, a laboratory-scale fixed-bed column study is important to describe the breakthrough curve behavior which is typical of an industrial treatment plant. Hence, this research work focused on both batch and column adsorption experiments. Both adsorbents were used for batch study thereafter, the adsorbent with the highest sorption capacity was used for the column study. In addition, to the best of the author's knowledge, no work has been reported on the competitive adsorption of Cu^{2+} and Pb^{2+} using banana and orange peels in a fixed-bed column. Various dynamic models have been applied to describe the behavior of a fixed-bed column; however, these existing models are only applicable to a single solute system. Hence, it is necessary to develop a suitable model for the binary solute system which was an area of focus for this research work.

1.4 Hypothesis

The following hypothesis was proposed for this study:

- Real wastewater contains more than one heavy metal, hence; the heavy metals are expected to compete for active sites which may affect the adsorption of one heavy metal in the presence of the other and vice versa.
- It is expected that the batch experimental data are efficient for developing a suitable model for the breakthrough curve of binary solute adsorption in a fixed-bed column.

1.5 Aim and Objectives

The overall aim of the study is focused on modeling and optimization of competitive bio-sorption of heavy metals using fruit peels (banana and orange peels).

The specific objectives are as follows.

- ❖ To determine the characteristics of the bio-sorbents before and after adsorption using analytical techniques (FTIR, SEM-EDS, XRD, and BET) and the point of zero charge (pHpzc) of the bio-sorbents.
- ❖ To optimize the interactive effects of process parameters such as pH, initial concentration, adsorbent dosage, and particle size on the single and bi-solute adsorption of Cu^{2+} and Pb^{2+} using orange and banana peels
- ❖ To determine the equilibrium and kinetic parameters of single and binary bio-sorption of Cu^{2+} and Pb^{2+} using orange and banana peels.
- ❖ To study the effect of initial concentration, flow rate, and bed height on the single and binary bio-sorption of Cu^{2+} and Pb^{2+} using a fixed-bed column.
- ❖ To develop a suitable model for binary solute competitive adsorption breakthrough curve.

1.6 Thesis Outline

This thesis consists of eleven chapters which are organized as outlined in **Table 1.1**.

Table 1.1: Thesis outline

Chapter	Outline
1: Introduction	This chapter states the problem of water scarcity associated with environmental pollution. Industrial activities generating a high concentration of contaminants are highlighted and the impact on the aquatic system. The chapter also explains the conventional wastewater treatment approach briefly. Adsorption techniques and various types of adsorbents are also briefly discussed. In addition, the adsorption method is explained, with a focus on recent studies that have applied bio-sorbents for the treatment of wastewater. The reason for the competitive adsorption of heavy metals is also

	emphasized. This chapter also includes the aim and objectives of this study as well as the thesis outline.
2: **Literature review**	This chapter provides a detailed review of wastewater properties, sources, and effects of heavy metals, wastewater treatment methods, and their drawbacks. Further still, reasons for choosing adsorption for this study, factors affecting adsorption mechanism, and the gaps in the literature are pointed out. Finally, an overview of experimental design techniques with response surface methodology is elaborated.
3: **Materials and Methods**	This chapter is divided into five sections according to the specific objectives of this study. The first section explains the analytical techniques used for the characterization of the bio-sorbents before and after adsorption. The second section has two parts concerning the two bio-sorbents chosen for this study. The first part of the second section describes the interactive effects and optimization of operating parameters in single and binary bio-sorption of Cu^{2+} and Pb^{2+} using banana peels while the second part discusses the same objective using orange peels. The third section is also divided into two parts based on the bio-sorbents. The first part describes the isotherm and kinetic study of Cu^{2+} and Pb^{2+} in single and binary systems using banana peels while the second part presents the same objective using orange peels. The fourth section explains the effect of initial concentration, flow rate, and bed height on single and binary bio-sorption of Cu^{2+} and Pb^{2+} using a fixed-bed column. Finally, the last section presents a mathematical model developed for the binary solute breakthrough curve.

4: **Results of characterization of the bio-sorbents before and after adsorption**	This chapter explained the characterization results of orange and banana peels obtained before and after adsorption. The pore size, pore volume, and pHpzc were also discussed.
5: **Results and discussion on the interactive effect and optimization of operating parameters using CCD-RSM**	Chapter five is devoted to the results obtained from the interactive effect and bio-sorption optimization of operating parameters using banana and orange peels in a single solute system. The data derived from the experimental design comprised of the actual and predicted values, as well as the regression model equations, were also explained. In conclusion, the results obtained from the application of response surface methodology were also presented.
6: **Results and discussion of equilibrium study of Cu^{2+} and Pb^{2+} in single and binary systems.**	This chapter presents the results obtained from the equilibrium study of the heavy metals in both single and binary systems using banana and orange peels. The Langmuir and Freundlich isotherms are used to describe the adsorption study in both single and binary systems. The results obtained were validated using statistical error analysis.
7: **Results and discussion of the**	This chapter presents the results obtained from the kinetic study of the heavy metals in both single and binary systems using banana and orange peels. The models used to describe the mechanism of

kinetic study of Cu^{2+} and Pb^{2+} in single and binary systems.	adsorption for the kinetic studies are pseudo-first-order and pseudo-second-order models.
8: **Results and discussion on the effect of operating parameters in fixed bed column**	Chapter eight presents the results obtained from the effect of operating parameters in the fixed bed column using the best-performed bio-sorbent in the batch studies. The results of the effect of the operating parameters in single and binary bio-sorption of the heavy metals are discussed and the breakthrough experimental data were fitted with different dynamic models namely; Thomas, Yoon-Nelson, and Bohart-Adams models.
9: **Results and discussion on the experimental breakthrough curve of binary solute of Cu^{2+} and Pb^{2+}.**	In this chapter, the competitive adsorption of copper and lead ions was investigated by varying initial metal concentrations in a fixed-bed column. The behavior and the parameters of the breakthrough curves were explained.
10: **Results and discussion on the mathematical modelling of binary breakthrough curve model.**	Chapter ten presents the mathematical model of the binary breakthrough curve model. The model test and validation are also discussed here.

11: **Conclusions and Recommendations**	Findings and conclusions drawn from the bio-sorption of copper and lead using orange and banana peels are presented based on each of the specific objectives outlined. Finally, some research recommendations were suggested for further work on the adsorption of heavy metals from wastewater in both batch and column studies.

CHAPTER 2

2. Literature Review

This chapter is divided into four main sections. In the first section, the sources of water pollution and the different types of pollutants present in wastewater are discussed. The health risks associated with heavy metals and various wastewater treatment methods are elaborated. The second section discusses the different types of adsorbents that can be used for the removal of heavy metals from wastewater. It also explains the mechanisms of adsorption and the factors affecting adsorption. The third section reviews the equilibrium and kinetic models that are used in the batch study to determine the adsorption capacity of an adsorbent and the rate of reaction. The process parameters involved in a fixed-bed adsorption column as well as the empirical models used to estimate the behavior of breakthrough curves are discussed. The last section discusses the application of the design of the experiment in the bio-sorption of heavy metals.

2.1 Sources of Water Pollution

The world is faced with severe threats of water pollution because of various human activities. The generation of large volumes of wastewater, scarcity of water due to reduced rainfall, and misuse of water resources have increased the challenge of water for humankind. There are different types of water pollutants as summarized in **Figure 2.1**.

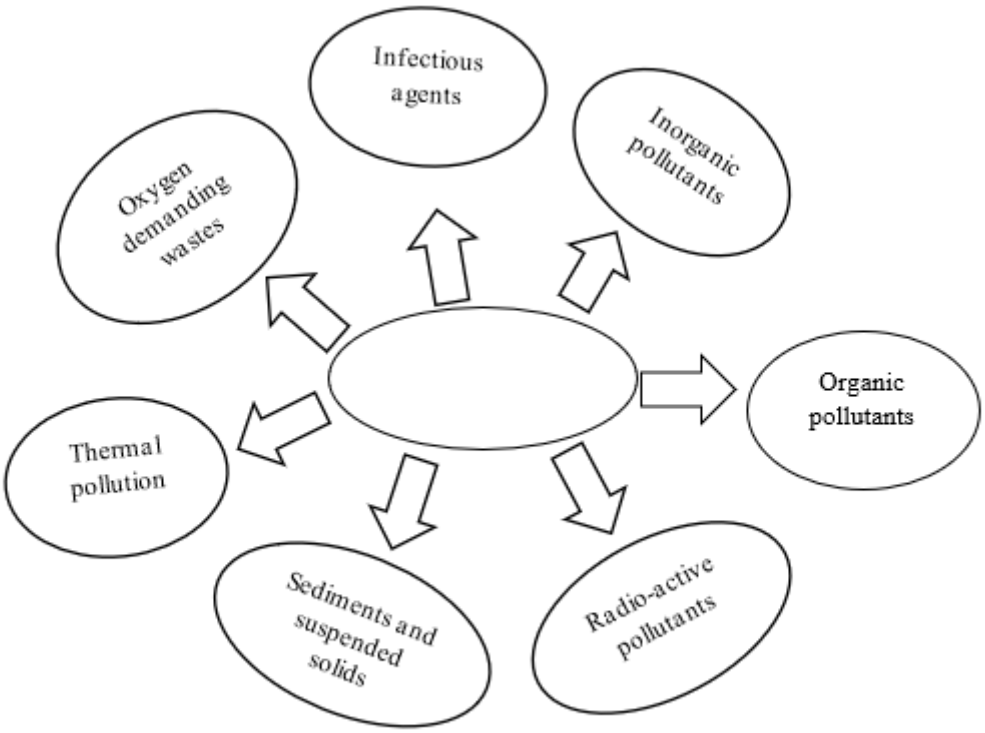

Figure 2.1: Different types of water pollutants (Raouf MS and Raheim ARM 2016)

The sources of water pollution can either be a point or non-point source. The point sources are traceable to a particular activity while the non-point source diffuses into the aquatic ecosystem without a traceable discharge source (Singh N.B *et al.* 2018). The traceable pollutants emanate from factories, sewage systems, coal mines, oil wells, power plants, etc, releasing tons of heavy metals and toxic sludge into water bodies. Many industries produce and discharge wastes comprising various heavy metals into the environment. The major sources of heavy metal pollution are metal plating, mining, smelting, battery manufacturing, tanneries, petroleum refining, pesticides, pigment manufacturing, printing paint manufacture (Salman H. Abbas *et al.* 2014; Singh N.B *et al.* 2018).

2.2 Wastewater Properties

Knowledge of wastewater characteristics is important in the treatment, design, and disposal facilities as well as engineering improvement of the industrial processes. This section, therefore, gives information on the chemical and physical properties of wastewater from

various sources. However, emphasis is laid on wastewater mainly containing heavy metals. In addition, the wastewater classification is based on their various compositions.

2.2.1 Biodegradable wastewater

The characteristic of wastewater depends on the source of the wastewater. Wastewater emanating from food processing industries and municipal wastewater plants contains contaminants of various types which are generally termed biodegradable. The effluent composition of the industrial food processing unit is greatly influenced by the number of raw materials, manufacturing processes, and the type of products involved (Obotey Ezugbe and Rathilal 2020). Biological oxygen demand (BOD) reduction is required in the majority of biodegradable wastewater due to the presence of organic matter such as sugars, starch, and protein. Also, suspended solids and oils can be present in such types of wastewaters.

2.2.2 Non-biodegradable wastewater

With the rapid change in technologies, industrial processes produce effluents that are becoming difficult and tedious to manage. This wastewater is termed non-biodegradable because of its composition. The characteristics of non-biodegradable wastewater are acidity, toxic metals, high total solids mainly mineral matter. In addition, the wastewater can have a high chemical oxygen demand COD to BOD ratio and different metal sulfides. Some industrial wastes and their major characteristics are presented in **Table 2.1.**

Table 2.1 Industrial wastes and major characteristics

Industrial wastes	Major Characteristics
Textile	Highly alkaline, colored, COD, temperature, high suspended solids
Leather goods	High total solids, hardness, salt sulfides, chromium, pH, precipitated lime, and BOD
Laundry trades	High turbidity, alkalinity, and organic solids

Canned goods	High in suspended solids, colloidal products, and dissolved organic matter
Dairy	High in dissolved organic matter, mainly protein, fat, and lactose
Meat and poultry beverages	High in dissolved and suspended organic matter, blood, other proteins, and fats
Brewed and distilled beverages	High in dissolved organic solids, containing nitrogen and fermented starches or their products
Beet sugar	High in dissolved and suspended organic matter, containing sugar and protein
Pharmaceutical products	High in suspended and dissolved organic matter
Yeast	High in solids (mainly organic) and BOD
Pickles	Variable pH, high suspended solids, color, and organic matter
Coffee	High BOD and suspended solids
Fish	Very high BOD, total organic solids, and odour
Glass	Red colour, alkaline non-settleable suspended solids
Fuel oil use	High in emulsified and dissolved oils
Rubber	High BOD and odour, high suspended solid, variable pH, high chlorides
Cane sugar	Variable pH, organic matter with relatively high BOD of carbonaceous nature

Palm oil	High BOD, COD, solids and total fats, and low pH
Pulp and paper	High or low pH, colour, high suspended colloidal and dissolved solids, inorganic filters
Photographic	Alkaline, containing various organic and inorganic reducing agents
Steel	Low pH, acids, cyanogen, phenol, ore, coke, limestone, alkali, oils, mill scale, and fine suspended solids
Metal – plated	Acid, metals, toxic, low volume, mainly a mineral matter
Oil fields and refineries	High dissolved salts from the field; high BOD, odour, phenol, and sulfur compounds from refinery
Petrochemical	High COD, TDS, metals, COD/BOD ratio
Cement	Heated cooling water, suspended solids, some inorganic salts
Asbestos	Suspended asbestos and mineral solids
Paint and inks	Contain organic solids from dyes, resins, oils, solvents, etc
Pesticides	High organic matter, benzene ring structure, toxic to bacteria and fish, acid
Organic	Varied types of organic chemicals

2.3 Health Risks Associated with Heavy Metals

Industrial effluent units are the main sources of heavy metal pollution which pose a significant risk to the environment as well as to public health (Barakat 2011; Singh N.B *et al.* 2018). Mercury (Hg), Chromium (Cr), Lead (Pb), Copper (Cu), Nickel (Ni), Iron (Fe), Cadmium (Cd), Manganese (Mn), and Arsenic (Ar) are heavy metals commonly detected in industrial wastewater originating from petroleum refining, tanneries, paint and adhesive industries, electroplating industry, rubber industry, industrial emissions, textile manufacturing, galvanizing, copper refineries, wood preservatives, pulp, and paper processing unit, mining industries, smelting and photographic industry (Krstić, Urošević and Pešovski 2018). Contamination of these dangerous, hazardous, and toxic heavy metals with surface water, groundwater, air, and sediments causes significant problems to human health and the environment at large. Each heavy metal is associated with different symptoms and risks to human health as presented in **Table 2.1** below.

Due to the health risks associated with these heavy metals, many countries have introduced stringent legislation to regulate water pollution. Maximum permissible limits have been set by different regulatory organizations such as World Health Organization (WHO), United States Environmental Protection Agency (USEPA) and European Union (EU), South African National Standard (SANS) to ensure proper discharge of toxic heavy metals into the aquatic system (Nour T. Abdel-Ghani and El-Chaghaby 2014). **Table 2.1** summarizes the source of some heavy metals, their permissible limits as specified by WHO and USEPA as well as risks associated with human health.

Table 2.1: Sources of heavy metals, permissible limits, and effects on human health (Barakat 2011; Araujo *et al.* 2013; Raouf MS and Raheim ARM 2016; Singh N.B *et al.* 2018)

Heavy metals	Sources	Permissible Limits (ppm)		Toxic effect
		WHO	US EPA	
Lead	Mining, paint, pigments, electroplating, manufacturing of batteries, burning of coal	0.01	0.015	Anemia, brain damage, anorexia, malaise, loss of appetite, liver, kidney, gastrointestinal damage, mental retardation in children
Copper	Plating, copper polishing, paint, printing operations	2.0	1.3	Neurotoxicity and acute toxicity, dizziness, diarrhea
Cadmium	Plastic, welding, pesticide, fertilizer, mining, refining	0.003	0.01	Kidney damage, bronchitis, Gastrointestinal disorder, bone marrow, cancer, lung insufficiency, hypertension, Itai-Itai disease, weight loss

Iron	Steel making, iron industries, mining, metal corrosion	0.3	0.3	Damage to the nervous system, nausea, abdominal pain, vomiting, seizure
Nickel	Porcelain enameling, non-ferous metal, paint formulation, electroplating	0.07	0.20	Chronic bronchitis, reduced lung function, lung cancer
Arsenic	Smelting, mining, rock sedimentation, pesticides	0.01	0.05	Bronchitis, dermatitis, bone marrow depression, hemolysis, hepatomegaly
Chromium	Textile, dyeing, paints and pigments, steel fabrication	0.05	0.05	Carcinogenic, mutagenic, teratogenicity, epigastria pain nausea, vomiting, severe diarrhea, producing lung tumors
Manganese		0.4	0.5	A high concentration of manganese causes neurological problems through drinking water

2.4 Wastewater Treatment Methods

Wastewater treatment processes can be classified into three stages namely, primary, secondary, and tertiary or advanced processes. The primary treatment stage takes care of suspended solids, grease, and oils from wastewater. The secondary treatment process is usually used to remove the biodegradable materials from wastewater; this is referred to as a biodegradation process while the tertiary treatment stage is used mostly to remove non-biodegradable materials from wastewater. Non-biodegradable wastes pose a serious threat to the environment and the removal of these contaminants can only be achieved through tertiary treatment methods (Orts *et al.* 2019).

Tertiary wastewater treatment methods is a process containing unit operations designed to improve the effluent quality of the secondary treatment process (Sonune and Ghate 2004; Ahmed and Ahmaruzzaman 2016). The methods commonly used for the removal of heavy metal ions from wastewater include electrolytic extraction, chemical precipitation, ion exchange, reverse osmosis, coagulation, chemical oxidation and reduction, dilution, air stripping, , solvent extraction, electrodialysis, cementation, steam stripping, adsorption etc. The advantages and disadvantages of each of these methods will be discussed as this research work is focused on the treatment of wastewater that has passed through a secondary treatment plant but needs to be treated further to meet the allowable discharge limit.

2.4.1 Chemical precipitation

Chemical precipitation is a technology mostly used for the removal of dissolved metal ions from wastewater. This technique makes use of precipitating agents such as calcium hydroxide, ferrous sulfate, sodium hydroxide to convert the metal ions into insoluble particles. The particles formed are then allowed to settle and removed through filtration (Gunatilake 2015). This technology requires unit operations such as coagulation/flocculation, precipitation, neutralization, solid/liquid separation, and dewatering. The chemical precipitation method is easy, simple to operate and economical, however, it might not be suitable and applicable for some end-users because it is not versatile (Nguyen *et al.* 2013). One major challenge of this technique is that it generates sludge that contains solid residue and the disposal method is landfilling which does not meet World Health Organization (WHO) and the South African

National Standards (SANS) policies. Hence, a license is required from the environmental management body for the disposal of the produced sludge. Furthermore, another disadvantage of the precipitation technique is that the solubility of the precipitate determines the metal ion concentration of the treated water (Huang *et al.* 2019).

2.4.2 Ion exchange

Ion-exchange is a process that involves the exchange of ions between the molecules in the liquid phase and the porous solid. This technique is mostly used in water treatment plants. In the ion exchange process, synthetic organic resins are commonly used as ion exchangers to remove metal ions from an aqueous solution (Gunatilake 2015). These ion exchange resins are insoluble solid substances with a high potential of absorbing positively or negatively charged ions from an aqueous solution and replace with an equal number of other ions having the same charges. Cation exchange resins are used to remove Ca^{2+} and Mg^{2+} from 'hard' water, these resins are mostly used in residential houses, water plant factories where drinking water is produced, municipal water treatment plants and also by industries producing ultra-pure water (Li *et al.* 2019). Ion-exchange can effectively remove heavy metal ions even though, the resins are highly expensive. Another drawback in the use of the ion-exchange technique is the disposal of regenerated solutions which could also be very costly (Singh N.B *et al.* 2018).

2.4.3 Membrane separation techniques

This technique can be used to remove suspended solids, organic compounds, and inorganic pollutants from an aqueous solution. Membrane separation processes are driven by mechanisms such as pressure, concentration, electrical and temperature differences. Pressure-driven separation includes ultrafiltration (UF), reverse osmosis (RO) and nanofiltration (NF); concentration driven separation is termed diffusion dialysis; electrically driven separation is referred to as electrodialysis while temperature difference driven separation is called membrane distillation. The pressure-driven mechanism is also referred to as membrane filtration which encompasses (RO, UF, and NF), this process is usually used to remove chemical oxygen dissolved (COD), colour, total dissolved solids (TDS) and heavy metals from wastewater. The choice of a suitable type of membrane filtration for a process depends on the particle size that can be retained (Gunatilake 2015). This process can be used to effectively achieve solid free effluents thus making this method efficient for wastewater treatment. Furthermore, the

membrane separation technique has advantages such as compact system, easy to operate and maintain as well as less use of chemicals.

Despite these advantages, the membrane separation technique has its demerits which include; inability to handle low molecular weight materials which can be linked to ultrafiltration and also high energy usage/consumption which is common in reverse osmosis (Nguyen *et al.* 2013; Bera, Godhaniya and Kothari 2021). Another drawback of the membrane separation process is membrane fouling which usually results in flux decline, this happens because of clogging of organic and inorganic substances on the membrane pores. The effects of membrane fouling on the membrane separation process include reduction in the efficiency of the membrane which could also shorten the membrane life and reduction of the effluent/treated water production (Obotey Ezugbe and Rathilal 2020).

2.4.4 Oxidation process

Ozone is a strong oxidant used for water and wastewater treatment. When ozone dissolves in water, it tends to react with many organic compounds either directly or indirectly. Direct reaction of ozone results in molecular ozone while indirect oxidation occurs by formation of secondary oxidants especially hydroxyl radicals which are also referred to as free radical species. Therefore, ozone and hydroxyl radicals are powerful oxidants, capable of oxidizing several compounds (Schrank *et al.* 2017). Ozonation is used in the coagulation/flocculation process for the removal of inorganic compounds (Mella *et al.* 2017)

Ozone has been used by many researchers for the treatment of phenols, pesticides, dyes (Khamparia and Jaspal 2017). One of the main disadvantages of ozone treatment is that it can generate unwanted by-products which can be hazardous to health if not properly controlled, for example, bromate and formaldehyde. In addition, ozone is not efficient for the removal of minerals and salts in solution (Khamparia and Jaspal 2017).

2.4.5 Coagulation and flocculation

Coagulation and flocculation are mostly considered together, these methods are used to remove suspended particles that cannot be trapped by sedimentation or filtration. The particles are referred to as colloids with sizes usually less than 1 µm. These particles always increase the colour and turbidity of water due to their poor settling properties. They are metal oxides, clays,

proteins as well as some organic compounds. Interaction of these negatively charged substances with colloidal particles and water hinders them from aggregating and settling in still water. Most of the time, positively charged colloids or multi-valent ions such as alum and ferric salts are added as chemical coagulants to aggregate the particles (Bilal *et al.* 2013; Asante-Sackey *et al.* 2020).

Coagulation is a chemical reaction between a chemical or coagulant and water. Cationic coagulants are used to reduce the negative charge of the colloids (zeta potential) to positive charges thereby encouraging the colloidal materials in the water to form small aggregates called flocs. These flocs then attract suspended matter. Flocculation is a gentle and slow mixing of water to help the formation and settling of flocs. The coagulation and flocculation method can be used for treating wastewater from various sources such as industrial, sewage sludge, and wastewater from municipal treated plants (Chiban *et al.* 2012; Kweinor Tetteh and Rathilal 2018). In general, this method is not economical for the treatment of a large volume of wastewater considering the cost of chemicals that will be used. The method also generates sludge which could be difficult to dispose of (Ahmed and Ahmaruzzaman 2016).

2.4.6 Electrochemical method

This method makes use of electrical energy, the electricity can be applied in various ways such as electrodeposition, electrocoagulation, and electro floatation (Bilal *et al.* 2013; Kweinor Tetteh and Rathilal 2018; Tang *et al.* 2019). This method has also been applied to industrial wastewater generated from the textile industry, beef effluent, and distillery (Sala and Gutiérrez-Bouzán 2014; Orts *et al.* 2019; Sen *et al.* 2019). The electrochemical method is highly expensive as it requires sophisticated equipment and a high level of maintenance.

Other methods of removing heavy metals from wastewater include complexation, solvent extraction, and cementation, however, they have challenges such as generation of sludge, slow kinetics, and low selectivity. Therefore, among these methods adsorption has emerged to be more efficient because of its simplicity and cost-effectiveness (Malik, Jain and Yadav 2017).

2.4.7 Adsorption

Adsorption is a surface process used to remove substances from fluid phases. It could also be defined as the accumulation of dissolved substances at an interface or between phases. The

adsorption process allows diversity in operation, design and produces treated water of high quality. In the treatment of water, adsorption has been used efficiently for the removal of single and multiple solutes where molecules or ions are removed from the liquid phase onto a solid surface. The solid surfaces are characterized as active sites and energetically heterogeneous which can attract the solutes. Adsorbates are dissolved substances that get adsorbed on a solid phase called Adsorbent. When properties of the liquid phase such as temperature, pH, and concentration are changed, adsorbed species from the solid surface can be released and then transferred back into the liquid phase. This process is known as desorption. Therefore, the adsorption process is reversible, and regeneration of adsorbents is possible by proper desorption methods (Abd-Talib *et al.* 2020).

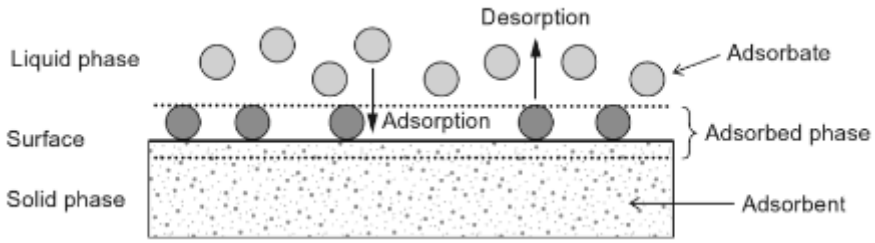

Figure 2.2: Adsorption terms (Worch 2012)

The adsorption process can be classified into physical or chemical. It can also involve a combination of both (Sulyman, Namiesnik and Gierak 2017). Physical adsorption occurs when the attraction force between the solid surface and the adsorbed metal ion is bound together by van der Waals force or hydrogen bonding. This type of adsorption occurs by an electrostatic force between the metal solution and the atoms present in the solid material. These forces are weak hence, the reaction is reversible (Gupta, Kumar and Gaur 2009; Abd-Talib *et al.* 2020). Besides this, no activation energy is required as equilibrium is reached within a short time. While chemical adsorption is the transfer of electrons which results in the formation of a chemical bond between the adsorbate and the solid adsorbent. The force of attraction between the adsorbate and the solid surface is greater and the heat liberated during the reaction is also greater compared to physical adsorption. Covalent bonds between the adsorbate and the adsorbent are referred to as weak chemical adsorption while the ionic bonds are referred to as strong chemical adsorption. Chemisorption is an irreversible process. The adsorption process usually follows the steps below:

(i) Mass transfer: the adsorbate molecules at the boundary layer move towards the solid particles/adsorbent.

(ii) Intraparticle diffusion: diffusion of the adsorbate molecules from the particle surface to the inner surface of the porous adsorbent.

(iii) The adsorbate molecules move to the active sites of the adsorbent pores

(iv) The overall adsorption rate is generally explained by either film formation or intra particle diffusion or both. This step occurs speedily compared to the previous steps.

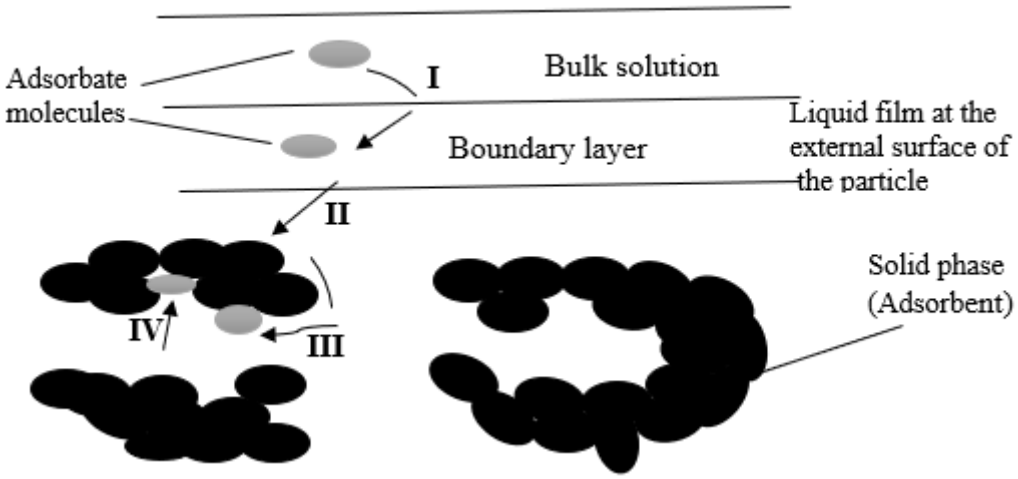

Figure 2.3: Adsorption mechanism using microporous adsorbents (Sulyman, Namiesnik and Gierak 2017)

Adsorption is mostly used for the removal of heavy metals from various industrial effluents. The efficiency of an adsorption process solely depends on the physical and chemical properties of the adsorbent and adsorbate chosen as well as operating conditions such as the concentration of the adsorbate, pH, temperature, adsorbent dose, agitation speed, contact time (Arunakumara, Walpola and Yoon 2013). The choice of an adsorbent is always a prerequisite for the design and development of an adsorption column. Different types of adsorbents have been used for treating industrial wastewater.

2.5 Types of Adsorbents

Adsorbents can be classified as conventional and non- conventional adsorbents. Conventional adsorbents can also be referred to as commercial adsorbents while non-conventional adsorbents are referred to as low-cost adsorbents.

2.5.1 Conventional adsorbents

2.5.1.1 Activated carbon

Activated carbons are microporous carbonaceous adsorbents widely used for industrial wastewater treatment. Activated carbons are majorly generated from raw materials containing carbon such as wood, petroleum, lignite, coal, peat, nut shells as well as synthetic polymers. It is characterized by a large surface area, microporous structure, high-pitched adsorption efficiency, and a high level of surface reactivity thus making it a renowned adsorbent. Activated carbon exhibits a wide range of internal surface areas ranging from 500-1500 m^2/g, this is efficient for water treatment as it allows larger molecules to be adsorbed on the inner surface (De Gisi *et al.* 2016). The manufacturing process of activated carbon consists of a charring or carbonization step in which the majority of the non-carbon materials are volatilized at high temperatures by pyrolysis. The temperature range is usually between 600 - 1200 ^0C, this results in about 60-70 % mass reduction of the material. The fine pore structure of activated carbons is developed during the activation process. Organic raw materials such as wood, wood charcoal, peat, and coconut shell undergo an initial carbonization process which helps to convert the cellulose structure into carbonaceous material. The use of chemicals in the activation process makes recycling highly expensive and reduces the properties of the products. Hence, activated carbons usually used for water treatment are produced through alternative processes termed physical, thermal, or gas activation.

In the gas activation process, the carbon-rich materials used as raw materials already exhibit a certain degree of porosity. During activation, the carbon-rich materials meet activation gas (steam, CO_2, or air) at high temperatures (800 ^0C – 1000 ^0C). This activity opens new pores on the material surface and enlarges the existing pores. In chemical activation, the char is soaked with chemicals and then allowed to burn at high temperatures. The chemicals usually used are strong acids and bases (sulfuric acid, phosphoric acid, zinc chloride, potassium thiocyanate, potassium hydroxide), which help to improve the pore structure (Yakout and El-Deen 2016). The advantages of chemical activation include simplicity and good development of pore structure (Dąbrowski *et al.* 2005; Pap *et al.* 2018). The macropore is the pathway through which adsorption molecules are transported to the mesopore after which they finally get to the micropore. The macropore and mesopore are referred to as the transport pathway which enhances the adsorption process, they are used for the adsorption of larger molecules.

2.5.1.2 Silica gel

Silica gel is usually obtained from the coagulation of colloidal silicic acid, which leads to the creation of porous and non-crystalline granules of various sizes. Silica gel exhibits a higher surface area when compared with alumina, which varies from 250 – 900 m^2/g (Gupta *et al.* 2009; Younes *et al.* 2019).

2.5.1.3 Zeolites

Zeolites are aluminosilicates derived from aqueous solutions of silicon and aluminum compounds under hydrothermal conditions. The aluminosilicates structure consists of water and exchangeable alkaline as well as alkaline earth metal cations (such as Ca, Mg, Na, and K) in their framework. Zeolites have a porous structure described by windows and caves of definite sizes. They are characterized by good thermal and mechanical stability; hence they possess high ion exchange and size-selective adsorption capacities. Zeolites can be classified as synthetic or natural. Natural zeolites are non-porous while synthetic zeolites are porous with great structure. The application of zeolites involves different techniques of synthesizing zeolites which are expensive and not economical.

2.5.1.4 Activated alumina

Activated alumina is a granulated form of aluminum oxide. It can be obtained when aluminum ore is treated to a level that it becomes porous and highly adsorptive. Activated alumina has been used effectively as an adsorbent at the point of use application. It absorbs pollutants present in the wastewater. One major drawback of using activated alumina in wastewater treatment is that it requires strong acid and base solutions for regeneration.

2.5.2 Non- conventional adsorbents

Non-conventional adsorbents are also referred to as low-cost adsorbents. South Africa is a country that has agricultural wastes and industrial by-products locally available in abundance. Waste materials generated from these agricultural products increase yearly, hence the conversion of these waste materials into adsorbents for wastewater treatment would assist to minimize the cost of waste disposal and provide an alternative to commercial adsorbents (Kurniawan *et al.* 2006; Burakov *et al.* 2018). Agricultural waste materials are abundant in

nature, bio-degradable, and readily available thus making them economical and eco-friendly (Raouf MS and Raheim ARM 2016).

- They are readily available
- They have good adsorption capacity
- They can be regenerated
- Generation of non-toxic sludge
- Easy to modify
- They are less challenging to dispose of after adsorption.

The low-cost adsorbent can be divided into three major categories as shown in **Figure 2.4** below.

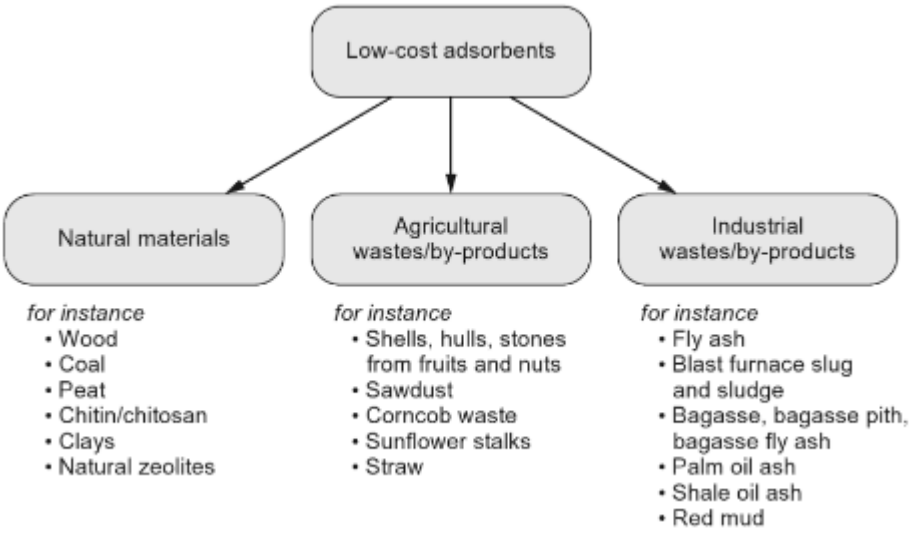

Figure 2.4: Classification of low-cost adsorbent (Singh N.B *et al.* 2018).

2.5.2.1 Industrial wastes

Industrial wastes are part of the low-cost adsorbents exploited for the removal of heavy metals from polluted wastewater. These waste materials are produced as by-products or remains of industrial processes. Often, they might undergo minimal treatment processes to improve their adsorptive capacity. Industrial waste materials are locally available, abundant in nature, inexpensive, and have high-performance capacity hence, they are a better substitute for commercial adsorbents (Bhatt and Singh 2018). Several industrial by-products have been utilized for the removal of heavy metals from wastewater. Spent coffee waste was used for

heavy metals and dyes removal from wastewater, fly ash, blast furnace slag, tea waste, bagasse ash, flax meal (Podstawczyk *et al.* 2015), coffee waste, and red mud. Many of these waste materials constitute a variety of disposal challenges because of bulk volume and physical nature.

Blast furnace slag is a by-product of industrial activities from the steel plant. Many researchers have utilized this waste for the removal of heavy metals from an aqueous solution. Medina *et al.* (2020) studied the removal of Pb^{2+} from an aqueous solution onto a blast furnace slag and fly ash-based adsorbent synthesized using the hydrothermal method. Nguyen *et al.* (2018) investigated the removal of five heavy metals from wastewater using iron industry blast furnace slag waste and a coal industry fly ash waste. The adsorption capacity of the metals was in the order Pb > Cu > Cd, Zn, Cr.

2.5.2.2 Living and dead biomass

This living and dead biomass are algae, fungi, yeast, and bacteria. Several studies have reported their adsorption capacity for various heavy metals. Algae are promising bio-sorbents, they are known for their high adsorption potential and are abundantly available in seas and oceans. The algae cell wall is composed of polysaccharides such as chitin, xylan, mannan, and alginic acid (Tavana, Pahlavanzadeh and Zarei 2020). These components combine with protein to form functional groups such as hydroxyl, aminyl, sulfonyl, amino, and imidazole for the biosorption of heavy metals and other organic compounds found in wastewater (Singh N.B *et al.* 2018). Green algae waste biomass obtained from marine green algae was used as a bio-sorbent for the removal of lead, cadmium, and cobalt from an aqueous solution. The effect of the operating parameters such as temperature, contact time, and solution pH was studied. The results showed that marine green algae can be used for the removal of metal ions. Brown algae *Sargassum* species were used as free and immobilized bio-sorbents for the adsorption of nickel and copper from an aqueous solution. The algae were immobilized by ionic polymerization using the calcium chloride solution drip method. The adsorption capacity of copper was higher than a nickel in both free and immobilized algae (Barquilha *et al.* 2017).

Fungi and yeast are excellent biomass for the removal of heavy metals from wastewater, they are generated industrially. The bio-sorption of these waste biomass also depends on their cell wall, which is made up of polysaccharides, glucans, chitins, and proteins. The functional groups providing binding sites for heavy metals are hydroxyl, amino, carboxylate, phosphate,

and sulfate groups. The bio-sorption mechanisms are physical adsorption, complexation, and ion exchange (Gupta *et al.* 2020).

Bacteria have also been used as bio-sorbents for the removal of various heavy metals. Their unique features such as tiny size, pervasive, and ability to grow at different environmental conditions have shown that they are good bio-sorbents. Bacteria are composed of polysaccharides and functional groups such as carboxyl, amino, sulfate, and phosphate that enhance heavy metals bio-sorption. Gorman-Lewis, Martens-Habbena and Stahl (2019) described copper adsorption onto *Nitrosococcus oceani* C-107 (*N. Oceani*) and *Nitrosomonas europea* C-31 (*N. Europacea*) ad archaeal species *Nitrosopumilus maritimus* (*N. Maritimus*). Modeling competitive copper complexation between *N. maritimus* and two organic acids, to mimic dissolved organic carbon, showed that *N. maritimus* could compete with nitrilotriacetic acid and triethylenetetramine under conditions like experimental measurements of copper adsorption. These results suggest that selectivity of the *N. maritimus* surface may confer some advantage in low-copper environments.

2.5.2.3 Agricultural wastes

Agricultural products have become a basis for generating the most abundant renewable resources available worldwide while agricultural wastes (fruit peels, vegetables, and residues) are regarded as garbage and have no usefulness anywhere (Bilal *et al.* 2021). Agricultural wastes are rich sources for low-cost adsorbents which show great potential for adsorption study after processing. These agricultural waste materials consist of basic components such as hemicellulose, lipids, proteins, lignin, simple sugars, water, starch, and hydrocarbons, containing different types of functional groups such as; carbonyl, phenolic, amino, carboxylic, alcoholic, ketone, and sulphonyl groups (Saka, Şahin and Küçük 2012; Raouf MS and Raheim ARM 2016). These functional groups are usually present on the surface of bio-sorbents, they have an affinity for heavy metal ions to form complexes that immobilize the pollutants through reactions of chemisorption, adsorption on the surface, complexation, ion exchange, and pore diffusion.

In the past few decades, several agricultural wastes have been explored as low-cost adsorbents for wastewater treatment. These include olive stones, hazelnut husk, rice husk (Ahmad, Ee and Baharudin 2016), corn (Mahmoud 2016), bagasse (Vera *et al.* 2018), eggshell (Harripersadth *et al.* 2020), sunflower waste, orange peel (Amin, Alazba and Amin 2017), potato peels

(Guechi and Hamdaoui 2016), tea waste (Amarasinghe and Williams 2007), maize leaf (Babarinde, Babalola and Sanni 2006), Punica granatum peel (Bhatnagar and Minocha 2010), banana peel (Deshmukh *et al.* 2017), cashew nutshell (Kumar *et al.* 2011), mango biomass (Ashraf *et al.* 2011), moringa oleifera seed (Araujo *et al.* 2013), moringa pods (Matouq *et al.* 2015a), almond shell (Ronda *et al.* 2013), pine sawdust (Semerjian 2018), lemon peel (Bhatnagar, Minocha and Sillanpää 2010), Java plum and amaltash seed (Giri *et al.* 2021) etc. Agricultural wastes are used for the removal of heavy metals from wastewater either in their natural or modified form. In the natural form, the waste material is washed, dried, ground and sieved to achieve the desired particle size and then stored in an airtight container for use in adsorption studies (De Gisi *et al.* 2016). While, the modified form undergoes various modification methods such as pre-treatment, binding group enhancement, locking or elimination of functional group, polymer grafting, other compound loadings, and microwave activation (Pathak Pranav, Mandavgane Sachin and Kulkarni Bhaskar 2015). The main aim of modification is to improve and reinforce the functional groups on the surface of the bio-sorbent thereby increasing the amount of the active sites. However, modified bio-sorbents are expensive due to processing cost as compared to natural bio-sorbents. Therefore, the study focused on the use of agricultural waste in its natural form.

Fruit peels are agricultural waste materials that are low-cost, bio-degradable, environmentally friendly, and locally available. However, these peels could become a nuisance to the environment if not properly disposed of. This research work, therefore, studied the feasibility of using banana and orange peels as adsorbents. The world's annual production of bananas exceeds 100 million tons, out of which 40 million tons of banana peels remain vastly unused (Mondal and Roy 2018). Many researchers have explored the possibilities of using these fruit peels for the removal of pollutants from wastewater. It is well expected that this work would lessen the environmental irritations when utilized for the removal of various heavy metals from industrial wastewater.

2.5.2.3.1 Previous studies using banana and orange peels

Kamsonlian *et al.* (2011) explained the bio-sorption mechanism of pollutants using the characterization of banana and orange peels. Energy dispersive atomic x-ray (EDAX) revealed the presence of carbon, oxygen, sodium, aluminum, calcium, magnesium, potassium, sodium, and silica on the surface of the peels. Fourier transform infrared (FTIR) showed the presence

of an aliphatic group, carboxylic acid group, and a carbonyl group. Scanning electron microscopy (SEM) of banana and orange peels showed that the peels have an irregular and porous surface. The author concluded that banana and orange peels would be efficient for heavy metal ion adsorption (Kamsonlian *et al.* 2011). These results are similar to work reported by (Memon *et al.* 2008; Akpomie and Conradie 2020).

Anwar *et al.* (2010) reported the adsorption of lead and cadmium on banana peels in batch mode. The operating parameters studied were adsorbent dosage, pH, contact time, and agitation speed. The maximum capacity of banana peels for cadmium and lead were 5.71 and 2.18 mg/g as evaluated by Langmuir isotherm at pH 3 and 5 respectively

Hossain *et al.* (2012) carried out a batch adsorption study using banana peels for the removal of Cu^{2+} from wastewater. Copper adsorption showed a high association with Langmuir and Freundlich isotherm model while the pseudo-second-order kinetic model was well fitted with the experimental kinetic data. The author reported that 1 g of banana peel adsorbed 28 mg of copper in a favourable condition. The author observed that the adsorption capacity of copper declined when pH decreased below 2 but increased as pH increased from 2 to 6. Liu *et al.* (2012) explained the optimal conditions for the preparation of banana peels in removing copper from water. The author submitted that the morphological structure of banana peels was rough and heterogenous with lots of pores. The highest adsorption capacity of banana peels was obtained at a drying temperature of 120 ^{0}C. Mondal (2016) investigated natural banana peels for the removal of fluoride from an aqueous solution through a batch study. The author reported that maximum adsorption of fluoride was obtained at pH 4 and pHpzc 5.63. The kinetic data were fitted with pseudo-second-order. Oyewo, Onyango and Wolkersdorfer (2016) reported the application of banana peels nano sorbent for the adsorption of radioactive minerals from real mine water. The same author studied the performance of nanostructured banana peels in lanthanide-laden mine water treatment. The author confirmed that the FTIR of banana peels after adsorption showed carboxylic and amine groups as functional groups responsible for metal ions removal. The Langmuir adsorption capacity was 27.1 mg/g, 34.13 mg/g for uranium, and 45.5 mg/g, 10.10 mg/g for thorium in synthetic and real mine water respectively while it was 47.8 mg/g for lanthanum and 52.6 mg/g for gadolinium.

Perez-Marin *et al.* (2007) explained the adsorption of cadmium from aqueous solutions using orange waste. The authors observed that the adsorption capacity of the bio-sorbent increased

as solution pH increased from 4 – 6, with maximum adsorption capacity of 0.4, 0.14, and 0.43 mmol/g respectively. The same authors explored the potential of orange waste to remove chromium from an aqueous solution in batch and continuous mode. The authors also reported that the adsorbent dosage and pH increased with the percentage removal of chromium while the maximum sorption capacity was in the range of 0.57 mmol/g to 1.44 mmol/g. The continuous study was represented by the bed depth service time (BDST) model (Pérez Marín *et al.* 2009). Schiewer and Balaria (2009) reported the bio-sorption of lead by orange peels in a batch mode. The FTIR revealed that the carboxylic group was responsible for the adsorption of lead as there was a significant shift in the peak after adsorption. Equilibrium was achieved in 30 min to 2 h while the second-order kinetic model gave a better fit.

Gönen and Serin (2012) studied the adsorption of nickel from an aqueous solution using an orange peel. The study investigated the effect of pH, initial concentration of nickel ion, and adsorbent dosage on the removal of nickel. The pH value was 5.0 while the percentage removal of nickel increased with a decrease in initial concentration and increase in the adsorbent dosage. Rajput *et al.* (2015) investigated the removal of lead from an aqueous solution using orange waste. The results gave optimum conditions for maximum removal of lead as pH 7, contact time 90 min. adsorbent dosage 0.6g/100 mL and concentration of 10 ppm with 78 % efficiency. Ali Gh. Khamseh and Ghorbanian (2018) reported the experimental and modelling investigation of thorium bio-sorption by orange peel in a continuous fixed-bed column. The parameters studied were bed heights, initial concentration, and flow rates while the experimental results were compared with Thomas, Yoon Nelson, and Modified Dose-Response (MDR) models. The author reported that the MDR model showed better results.

Guiza (2017) reported the adsorption of copper from an aqueous solution using cellulosic waste orange peel. The adsorption equilibrium followed the Freundlich adsorption isotherm model while the maximum adsorption capacity of the bio-sorbent for copper ions was 63 mg/g. Kumar *et al.* (2018) reported an equilibrium study of dried orange peel for copper ion removal from water. The effects of pH, initial concentration, adsorbent dosage, and temperature were investigated for the removal of copper. The optimum removal of copper was favoured by a slightly acidic solution (pH 6) while the equilibrium data were well fitted with Langmuir and Freundlich isotherm models. This implies that adsorption occurred on both mono and multilayer surfaces.

In these studies, orange and banana peel's efficiency has been reported for heavy metal removal. However, most of the studies investigated the effects of the operating parameters with one factor at a time. In addition, the effect of metal coexistence in wastewater and the interactive effect of the operating parameters are not reported to the best of the author's knowledge. It is highly unlikely to find wastewater that contains a single metal ion hence, the investigation of the competitive effect of binary solute will give information on the adsorption capacity of the bio-sorbents in the presence of more than one solute.

2.6 Mechanisms involve in Bio-sorption

Bio-sorbents consist of multi-functional surfaces; hence, there are various methods through which metal ions can be entrapped on the surface of a sorbent. Many factors affect the adsorption mechanism of metal ions in a solution. The quantity of adsorbent used determines the availability of binding sites on the surface of the adsorbent. Therefore, the adsorbent dosage has a great influence on the percentage removal of the metal ions. Other factors include the type of bio-sorbent, properties of the metal solution, and environmental parameters (pH and temperature). The adsorption mechanism is, therefore, a complex process that needs to be properly understood. It is important to discuss the adsorption mechanism to have in-depth knowledge of the process, which can be useful for the future improvement of the system. The mechanism of bio-sorption may be classified under the following sub-headings.

2.6.1 Physical adsorption

Physical adsorption occurs when the attraction force between the solid surface and the adsorbed metal ion is bound together by van der Waals' forces. This type of adsorption mainly occurs by van der Waal's electrostatic force between the metal solution and the atoms present in the solid material. These forces are weak hence, the reaction is reversible. The adsorption of cadmium onto banana peels was reported to be a physical process (Deshmukh *et al.* 2017).

2.6.2 Ion exchange

Ion exchange is a chemical process wherein a metal ion in a solution is exchanged with the surface charge of a solid particle. It is an essential aspect of the adsorption process which gives interactive behaviour between metal ions and the functional groups present on the solid surface

(Abd-Talib *et al.* 2020). Bio-sorbents consist of exchangeable cation sites. Chao, Chang and Nieva (2014) found out that biosorption of Cu, Ni, Cd, and Pb onto citrus maxima peel, passion fruit, and sugarcane bagasse increased in the order Pb > Cd > Cu > Ni proportionally to the ionic radius of the metals.

2.6.3 Complexation

This is an adsorption mechanism in which metal ions in a solution react with the active groups of a solid material leading to the complex formation on the surface of the substance (Pala *et al.* 2021). Metal ion binding could occur with a single ligand or because of chelation.

2.6.4 Precipitation

Precipitation can be classified as metabolism and non-metabolism dependent. Precipitation may occur on the surface of the bio-sorbent as well as in the solution. Furthermore, if precipitation is metabolic dependent then certain compounds have been produced by a microorganism in the presence of toxic metals which make precipitation possible. In another case, it could be as a result of chemical interaction between the metal ions and the biomass surface hence, precipitation is non-metabolism dependent (Veglio and Beolchini 1997; Nleya, Simate and Ndlovu 2016).

2.7 Factors Affecting Bio-sorption

Many physical and chemical factors affect the adsorption process of heavy metals from wastewater which are pH, initial metal ion concentration, temperature, adsorbent dosage, particle size, ionic strength, etc. These factors control the overall performance of a bio-sorption process. The influence of each of the factors is discussed below.

2.7.1 pH

The pH value is a very important parameter that controls the rate of adsorption as well as the adsorption capacity of an adsorbent. The pH greatly influences the metal solution chemistry and the surface chemistry on the binding sites of the adsorbents as well as competition between metallic ions in solution (Abbas *et al.* 2014; Dada *et al.* 2017). The surface pH of an adsorbent also affects the pH as it relates to the functional group activity. The pH_{pzc} (point of zero charge) of an adsorbent is also an important factor. The surface of an adsorbent becomes positively

charged at pH < pH_{pzc}, negatively charged at pH > $pH_{pzc,}$ and neutral at pH = pH_{pzc} (Pathak Pranav, Mandavgane Sachin and Kulkarni Bhaskar 2015; Ahmed and Ahmaruzzaman 2016). The adsorption capacity of cations increases with increasing solution pH while it decreases for anionic metals. The surface charge of a bio-sorbent becomes positive at a lower pH leading to competition between the H^+ ions and the metal cations resulting in a decrease in bio-sorption capacity. At an increased pH value, the bio-sorbent surface becomes negatively charged, bio-sorption of metal ions is favoured as a result of electrostatic interaction (Nguyen *et al.* 2013; Liu and Lian 2019). In general, heavy metal ion uptake increases significantly from 2-6 for most bio-sorbents. At higher pH, metal ions have a tendency to form hydroxides which leads to precipitation (Badessa, Wakuma and Yimer 2020).

2.7.2 Temperature

The mobility of metal ions in solution is enhanced by an increase in temperature which in turn increases the rate of adsorption. As the temperature of the solution increases, the viscosity of the solution decreases and increases the random movement of the ions in the solution. Therefore, changes in the solution temperature will not only affect the rate of metal diffusion but also the metal ions solubility (Park, Yun and Park 2010; Qiu *et al.* 2021). However, the increase in temperature of the adsorption process using microbial living cells can endanger the microorganisms and as such decrease the metal uptake (Corda and Kini 2019). Adsorption study is usually performed in the laboratory within the range of 25 ^{0}C – 30 ^{0}C as higher temperature might cause physical damage to the bio-sorbent (Beni and Esmaeili 2020). In addition, adsorption efficiency remains the same at this temperature. The temperature analysis of an adsorption process can also give an in-depth understanding of thermodynamic parameters which include entropy, enthalpy, and energy involved in the adsorption phenomena.

2.7.3 Adsorbent dose

The adsorbent dose helps to determine the adsorbent capacity. The quantity of adsorbent used determines the availability of binding sites on the surface of the adsorbent and thus the extent of adsorption (Pathak Pranav, Mandavgane Sachin and Kulkarni Bhaskar 2015; Hong *et al.* 2018). During adsorption, the percentage removal of metal ions increases with increased adsorbent dose until equilibrium is reached. At equilibrium, an increase in adsorbent dose has no significant impact on the percentage removal of the adsorbate. The equilibrium point is also said to be the optimum condition for the solid and liquid in the solution.

2.7.4 Contact time

This is the time required for an adsorption process to attain equilibrium. An increase in contact time increases the adsorption efficiency until equilibrium is reached. An equilibrium state is reached when the adsorbent is saturated with metal ions. The effect of contact time was studied on the removal of copper ions using sawdust. Equilibrium was reached at a contact time of 3h with maximum efficiency of 96 % and gradually decreased to 87 % after 24 h (Semerjian 2018).

2.7.5 Initial metal concentration

Initial metal ion concentration is a salient factor in the adsorption process. It provides the power needed to surmount all mass transfer barriers between a metal ion in an aqueous solution and the solid material during the adsorption process. Many researchers have reported that the adsorption capacity of bio-sorbent increases with increasing initial metal ion concentration however, the percentage removal decreases for a fixed adsorbent dosage. Matouq *et al.* (2015b) reported that the removal of Chromium ions with varying initial concentrations at 20 ^{0}C increased when the initial concentration was increased from 25 to 100 mg/L. At a higher initial concentration, the amount of metal ions in solution are higher compared with the available active sites, thereby decreasing the percentage removal of the metal ions. Therefore, an increase in the adsorbent dosage increases the active sites leading to an increase in metal ion uptake (Matouq *et al.* 2015a). In addition, Semerjian (2018) reported that an increase in copper ion concentration from 1 to 50 mg/L resulted in a decrease in the percentage removal of the metal ion while the adsorption capacity increased from 0.09 to 5.12 mg/g. The bio-sorption capacity of chemically modified orange peel and date palm fibres and the hybrid adsorbent were studied for varying initial metal concentrations of copper, lead, and arsenic from 20 – 80 mg/L (Amin, Alazba and Amin 2017). The results showed that the amount of metal ions adsorbed at equilibrium increased for all the metal ions when the initial concentration increased from 20 – 80 mg/L using orange peel, date palm fibre, and the hybrid (DPF – OP). The percentage removal however decreased for all the metal ions with increasing initial metal concentration from 20 – 80 mg/L with all the bio-sorbents. In general, percentage removal decreases when initial metal concentration increases because of saturation of the active sites on the surface of the bio-sorbent.

2.7.6 Method of preparation

The nature of the bio-sorbent is also an important factor that could be determined from the preparation methods adopted for the bio-sorbent. Different modification methods can be used to enhance the characteristics of a bio-sorbent. A physical modification that includes heat treatment (such as drying, boiling, autoclaving, and freezing) and size reduction (such as, cutting, grinding, and crushing). A chemical modification comprises acid treatment, alkali treatment, oxidation with organic solvents, and treatment with metal salts (Marín *et al.* 2010; Pathak Pranav, Mandavgane Sachin and Kulkarni Bhaskar 2015). Cell modification includes enhancing the binding group, graft polymerization, and elimination of inhibiting groups. Finally, pyrolysis to reduce bio-sorbent to activated carbon is also a modification method (Bhatnagar and Minocha 2010; Qiu *et al.* 2021). All these methods can be used to improve the binding properties as well as the biosorption capacity of the bio-sorbent. However, in this study, the bio-sorbents used underwent physical modification, drying, and size reduction. The bio-sorbents were used in their natural state without the addition of any chemicals.

2.7.7 Particle size

An increase in the surface area gives rise to several available binding sites for adsorption hence adsorption capacity increases with a smaller particle size of adsorbents. The smaller particle size of an adsorbent could be used for batch adsorption to achieve higher percentage removal however, the reasonable particle size must be used in fixed bed study to reduce porosity. Amin, Alazba and Amin (2017) studied the effect of particle size of modified date palm fibres, orange peels, and the DPF – OP hybrid ranging from 45 – 251 µm for the biosorption of copper, lead, and arsenic. The results showed significantly higher adsorption of the metal ions with 45 µm particle size of the bio-sorbents compared to the 251 µm. In addition, the percentage removal of the metal ions decreased by 40 – 60 % when the particle size of the bio-sorbents was increased from 45 to 251 µm.

2.7.8 Ionic strength

Real wastewater usually contains not only heavy metals but other metal ions such as Na^{+}, Ca^{+}, $K^{+,}$ and Mg^{+}. Therefore, the chloride form (NaCl, $CaCl_2$, KCl, $MgCl_2$) of these metals is added to wastewater to determine the ionic strength of the heavy metals in the bio-sorption process. Mostly, adsorption decreases with the increasing ionic strength of an aqueous solution. When

metal ions and a bio-sorbent come in contact in an aqueous solution, they are enclosed by an electrical double layer because of electrostatic interaction.

2.7.9 Selectivity

There is a tendency for a bio-sorbent to have a preference for some heavy metals over others (Medellin-Castillo *et al.* 2017). A comparative study of lead removal was carried out using spinach, coffee, and tea extracts (Lathan *et al.* 2013). The result showed that the bio-sorbents affinity for lead ions was in the order Spinach > Coffee > Tea. Hossain *et al.* (2014) reported that the cabbage had a higher affinity for lead in the single, binary, ternary and quaternary sorption system of copper, lead, zinc, and cadmium ions. The order of the adsorption preference of the metal ions onto cabbage waste was $Pb^{2+} > Cd^{2+} > Cu^{2+} > Zn^{2+}$ in single metal system while it was $Pb^{2+} > Cd^{2+} > Zn^{2+} > Cu^{2+}$ for multi- solute system. Martín-Lara *et al.* (2016) reported higher selectivity of the pine cone shell for Pb^{2+} over Cu^{2+} ions in both batch and column experiments.

2.7.10 Co-existence of ions

Ronda *et al.* (2013) studied the effect of Pb^{2+} on the biosorption of Cu^{2+} by an almond shell in a binary solute system. It was reported that Cu^{2+} equilibrium uptake was reduced in the presence of Pb^{2+} which suggests that there was a competition between the cations in solution for active sites on the surface of the almond shell. The bio-sorption uptake capacities of pine cone shells for Cu^{2+} and Pb^{2+} were slightly inhibited by the presence of Pb^{2+} and Cu^{2+} respectively. However, the pine cone shell had a higher affinity for Pb^{2+} than Cu^{2+} (Martín-Lara *et al.* 2016). In the competitive bio-sorption of Cd^{2+} and Pb^{2+} on chilli seeds, Pb^{2+} showed strong antagonism in the competitive adsorption of Cd^{2+}. However, the competitive adsorption of Pb^{2+} was not affected by Cd^{2+} in the co-existence of the metal ions (Medellin-Castillo *et al.* 2017).

2.7.11 Surface area

Surface area increases with a decrease in particle size. A higher surface area gives more number of binding sites for adsorption. Small particle size lowers the mass transfer driving force per unit area of adsorbent particles, which increases the uptake and saturation capacity per unit mass of bio-sorbent. Pathak, Mandavgane and Kulkarni (2017) reported that the surface area

of banana peels and orange peels are 0.65 m^2/g and 1.03 m^2/g respectively. The low surface area is possibly due to the operational complexity of degassing lignocellulosic samples which is a characteristic feature of carbonacceous materials.

2.8 Equilibrium Isotherm Models

Adsorption isotherm is a plot that shows the quantity of solute removed from an aqueous solution at equilibrium, constant temperature, and pH. Adsorption equilibrium is expressed as the ratio of the adsorbed amount of solute to the amount of solute remaining in the solution, it gives essential physicochemical data for assessing the applicability of the adsorption process as a unit operation. The equation below gives expression of equilibrium metal uptake q_e,

$$q_e = \frac{(C_o - C_e)V}{M} \qquad (2.1)$$

Where V represents the volume of the solution, C_0 and C_e are the initial and final/equilibrium concentration of the solution and M is the mass of the adsorbent.

For equilibrium to be reached, the aqueous solution must be in contact with the adsorbent. At equilibrium, the solute concentration in the solution and sorbate at the interface are in dynamic balance. Prediction of a suitable isotherm model for an adsorption process is important for the design and optimization of a batch adsorption system. Adsorption data has been fitted into a wide variety of equilibrium isotherm models like Langmuir, Freundlich, Temkin, Sips (Langmuir-Freundlich), Dubinin-Raduskevich, Tóth, Redliche-Peterson, Harkins-Jura, Flory-Huggins, Koble-Corrigan, Khan, Hill, and Radke-Prausnitz isotherm (Singh N.B *et al.* 2018). These isotherm models can be divided into two categories; two-parameter and three-parameter isotherm. Langmuir, Freundlich, Temkin, Dubinin-Raduskevich, and Flory-Huggins, Hill are two-parameter isotherms while Toth, Sips, Redliche-Peterson, Koble-Corrigan, and Harkins-Jura are three-parameter isotherms. However, the most used isotherm models are Langmuir and Freundlich models as they are simple and easy to interpret. Therefore, this research work used Langmuir and Freundlich isotherm models.

2.8.1 Langmuir isotherm model

Langmuir (1918) developed the isotherm model to explain the gas-solid adsorption onto activated carbon. Also referred to as ideal localized monolayer model. In the formulation of this isotherm model, the following assumptions were made; monolayer coverage (adsorbed layer is one molecule in thickness), adsorption can only occur at a fixed number of definitely localized sites, the surface adsorption sites are identical and equivalent, no lateral interaction of adsorbed molecules with neighboring molecules and the adsorption process is reversible (Febrianto *et al.* 2009; Foo and Hameed 2010). Application of these assumptions with a kinetic principle (rate of adsorption and desorption from the surface is equal), the Langmuir equation can be formulated as follows.

$$q_e = q_{max} \frac{K_L C_e}{1 + K_L C_e} \qquad (2.2)$$

Often, the equation is written in linear form as follows (Febrianto *et al.* 2009)

$$\frac{1}{q_e} = \left(\frac{1}{K_L q_{max}}\right)\frac{1}{C_e} + \frac{1}{q_{max}} \qquad (2.3)$$

$$\frac{C_e}{q_e} = \frac{1}{q_{max}} C_e + \frac{1}{K_L q_{max}} \qquad (2.4)$$

Where q_{max} is the maximum/saturation adsorption capacity of the adsorbent to produce a complete monolayer coverage (mg/g), q_e is the amount adsorbed at equilibrium (mg/g), K_L is the Langmuir adsorption constant (L/mg) and C_e is the supernatant concentration of the aqueous solution at equilibrium (mg/l). A plot of C_e/q_e vs. C_e is expected to be linear provided the model fits the experimental data well, where $1/(q_{max}.K_L)$ is the intercept and $1/q_{max}$ is the slope. These can be obtained from the graph.

The Langmuir isotherm can be described by a separation factor R_L. It is a dimensionless constant also referred to as an equilibrium constant (Juang, Wu and Tseng 1997).

$$R_L = \frac{1}{1 + K_L C_e} \quad (2.5)$$

The value of R_L is used to characterize the adsorption system such that, when $R_L > 1$, the adsorption is unfavorable, $R_L = 1$ means adsorption is linear, $R_L < 1 > 0$ denotes adsorption is favorable while $R_L = 0$ means adsorption is irreversible.

2.8.2 Freundlich isotherm model

Freundlich isotherm is an empirical model which explains the reversible, non-ideal adsorption process not controlled by the formation of a monolayer. It relates to multilayer adsorption with exponential distribution of active sites and energies over a heterogeneous surface of an adsorbent, each active site has bond energy (Febrianto *et al.* 2009). The quantity adsorbed is the total of the adsorption on all the sites with stronger binding sites being filled first, until an exponential reduction in the adsorption energy as the adsorption process goes to completion. The model equation for single solute adsorption can be represented as follows,

$$q = K C_f^{1/n} \quad (2.6)$$

Where K and n are Freundlich constants which show adsorption capacity and adsorption intensity respectively. 'n' value of between 1 and 10 for Freundlich isotherm, indicates that the adsorption process is thermodynamically favorable. The linearized form of the equation gives,

$$log\, q = log\, K + \frac{1}{n} log\, C_f \quad (2.7)$$

The Langmuir and Freundlich isotherms are based on single component adsorption. Since wastewater usually consists of more than one pollutant, it is imperative to consider isotherm models for competitive adsorption.

2.9 Competitive Equilibrium Models

Adsorption of heavy metals in a real system account for more than one component, therefore, adsorption equilibria involving competition between the different metal ions is necessary for a deeper understanding of the system and industrial-scale design purpose. Competitive equilibrium models are used to account for the adsorption capacity of each metal ion present in a solution. The equilibrium metal uptake q_e for a metal ion "i" in multi-metal solution is expressed as,

$$q_{i,e} = \frac{(C_{i,o} - C_{i,e})V}{M} \qquad (2.8)$$

Where $C_{i,0}$ and $C_{i,e}$ are the initial and final/equilibrium concentration of component i, V is the volume of the solution and M is the mass of the adsorbent.

Langmuir and Freundlich isotherm models have been modified to fit the competitive effect of metal ions in solution.

2.9.1 Competitive Langmuir isotherm model

Langmuir isotherm was modified to multi-metals isotherm by the introduction of some parameters/interaction factors (Padilla-Ortega, Leyva-Ramos and Flores-Cano 2013; Hossain *et al.* 2014). This model is referred to as the extended or competitive Langmuir model developed by Butler and Ockrent (1936). Its assumption is the same as Langmuir isotherm model which assumes the surface of the adsorbent is homogenous for energy and that all the sites adsorb either solute equally (Mihalache *et al.* 1998).

$$q_{e,i} = \frac{q_{m,i} K_{L,i} C_{e,i}}{1 + \sum_{j=1}^{N} K_{L,j} C_{e,j}} \qquad (2.9)$$

Where, $q_{e,i}$ and $q_{m,i}$ are the equilibrium adsorption capacity and maximum adsorption capacity of metal "i" (mg/g), $C_{e,i}$ is the equilibrium concentration of metal 'i' (mg/L), $K_{L,i}$ is

the Langmuir isotherm constant for metal 'i', while, j denotes the number of metal ions in the solution.

2.10 Adsorption Kinetics

The rate-limiting step in an adsorption process can be determined by contact time experimental results. A complete adsorption process includes mass transfer which encompasses steps such as film or external diffusion, pore diffusion, surface diffusion, and adsorption on the pore surface. The overall adsorption process may be controlled by any of these steps or a combination of one or more steps. Each step possesses resistance to the adsorption rate therefore if one step contributes dominantly to the overall adsorption resistance such that reducing the other two resistances only slightly increases the adsorptive uptake rate, then, the step is referred to as the rate-controlling step (Tan and Hameed 2017). The adsorption kinetics of a process depends on factors such as; adsorbent and type of adsorbate as well as the experimental factors such as temperature and pH (Regti *et al.* 2017). The most used adsorption kinetic models include the pseudo-first-order, pseudo-second-order, intraparticle diffusion, and Elovich model. However, for this study, pseudo-first-order and pseudo-second-order kinetic models are used.

2.10.1 Pseudo first order (PFO) kinetics

The pseudo-first-order kinetic equation was developed by Lagergren in 1898 for the adsorption of oxalic and malonic acid onto charcoal (Lagergren 1898). It is generally expressed as.

$$\frac{dq}{dt} = K_1(q_e - q_t) \qquad (2.10)$$

Where q_e and q_t are the amounts of solute adsorbed (mg/g) at equilibrium and at any time t (min) respectively, K_1 is the pseudo-first-order kinetic rate constant (min^{-1}). Upon integration of the equation above with the initial conditions of $q_t = 0$ when $t = 0$, gives a linear equation as stated.

$$log(q_e - q_t) = log\, q_e - \frac{K_1}{2.303} t \qquad (2.11)$$

Plotting $\log(q_e - q_t)$ against t gives a straight line that passes through the origin with a slope K_1.

2.10.2 Pseudo-second order (PSO) kinetic model

The Pseudo-second order model assumes that the adsorption uptake is the second order for the available sites (Ys *et al.* 1999). The rate equation for the pseudo-second-order model was developed by Ho (1999), as given

$$\frac{dq_1}{dt} = K_2(q_e - q_t)^2 \qquad (2.12)$$

Where K_2 is the pseudo-second-order rate constant ($gmg^{-1}min^{-1}$). Other parameters have the same meaning as in the pseudo-first-order model. The integrated form of the equation with the boundary conditions, $t = 0$ to t and $q_t = 0$ to q_t gives.

$$\frac{1}{(q_e - q_t)} = \frac{1}{q_e} + K_2 t \qquad (2.13)$$

The equation can be re-arranged to obtain the linearized form.

$$\frac{t}{q_t} = \frac{1}{K_2 q_e^2} + \frac{1}{q_e} t \qquad (2.14)$$

The plot of t/q_t against t gives a straight line for pseudo-second-order kinetics. $1/q_e$ is the slope and $1/K_2 q_e^2$ is the intercept.

2.11 Adsorption in Fixed Bed Column

Several studies on heavy metal adsorption in batch systems have been described in the literature. However, in the practical industrial operation of large-scale adsorption processes, a dynamic or continuous flow fixed-bed column is always preferred. In the continuous adsorption study, an amount of an adsorbent is charged into the column which forms the bed through which the aqueous solution passes. As the adsorbate passes through the bed, it meets a fresh part of the adsorbent continuously and a new equilibrium is established all along. However, due to limited contact time with a part of the adsorbent, an actual equilibrium is not achieved. The mass transfer zone or the adsorption zone is the zone where adsorption takes place within the adsorbent bed. The mass transfer zone travels through the column with a velocity slower than the solution velocity during the adsorption process. The movement of the mass transfer zone through the column is greatly determined by the strength of the adsorbate. The higher the adsorption of the adsorbate, the greater the margin between the mass transfer zone velocity and the solution velocity. The mass transfer zone moves downwards as the solution passes through the column continuously, a time t_b is reached when the adsorption zone has moved to the bottom of the column hence, increasing the concentration of the adsorbate at the exit of the column. In practice, column operation is usually disturbed when the effluent concentration rises to a certain level known as the breakthrough point, above this level, it is not ideal to continue the operation. The breakthrough time, t_b, is the time at which the adsorbate occurs at the effluent. As the adsorption progresses, the mass transfer zone moves downwards thus increasing the concentration of the adsorbate in the effluent. A point is reached at which the mass transfer zone is completely out of the column. At this point, the adsorbent in the column is completely used up and no adsorbate uptake takes place in the column then the fixed bed is saturated, and the time related to this is called the saturation time, t_s.

A breakthrough curve is always used to represent the adsorption process in a fixed bed column study. It can also be explained as the time at which the effluent concentration exceeds the breakthrough limit of 0.05, while the exhaustion time is the time at which the effluent concentration is 95 % of the initial concentration. The breakthrough curve is the plot of effluent concentration C_t/C_0 vs time.

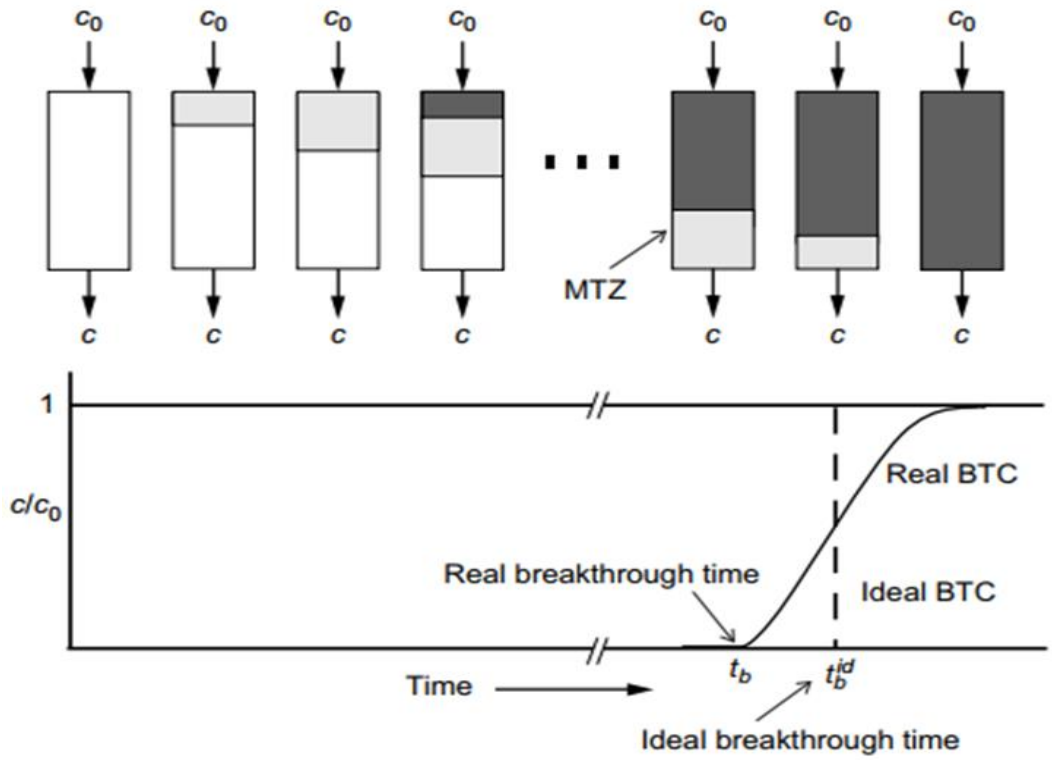

Figure 2.5: Showing movement of mass transfer zone in an absorber and the breakthrough curve (Worch 2012).

2.12 Process Parameters for Column Study

Fixed adsorption study is mostly conducted with synthesized wastewater containing metal ions as adsorbate to be treated by adsorbents. The effect of process parameters such as initial metal concentration, flow rate, solution pH, bed height of column, adsorbent particle size, and temperature of the system can be investigated in a column study. All these parameters are important for determining the performance of an adsorbent in a dynamic process. However, out of these process parameters, initial metal ion concentration, bed height of column, and flow rate are most considered and feasible parameters reported by many researchers on the removal of different types of pollutants from wastewater.

2.12.1 Initial metal ion concentration

Adsorption occurs rapidly at the initial stage due to the availability of a huge amount of vacant active sites on the adsorbent. As the initial concentration increases thereafter, the driving force required to overcome the mass transfer resistance in the liquid phase increases, and the active sites on the surface of the adsorbent is exhausted faster thereby decreasing the volume of

effluent treated. Breakthrough and exhaustion time occur faster with increasing initial metal ion concentration while breakpoint time decreases with increasing initial concentration (Moyo, Pakade and Modise 2017; Saravanan, Kumar and Yaswanthraj 2017).

2.12.2 Flow rate

The adsorption efficiency in the column increases with an increasing flow rate resulting in a faster saturation of the adsorbent bed. At a lower flow rate, the contact time of the adsorbent with the liquid phase is much thereby leading to increased adsorption in the column. Generally, breakthrough time occurs faster with increased flow rate while saturation of the adsorbent bed increases significantly at a lower flow rate. Therefore, the highest efficiency of the column is obtained at a lower influent flow rate (Abdolali *et al.* 2017).

2.12.3 Bed Height

The breakthrough and saturation time is slower with an increase in bed height. This can be explained with more adsorbent which leads to more available active binding sites at increased bed height consequently increasing the removal efficiency in the column. The contact between the adsorbate and the adsorbent increases with increasing bed height therefore, the volume of effluent treated increases with bed height (Abdolali *et al.* 2017; Patel 2019).

2.12.4 Particle size

Adsorption is a surface phenomenon and the adsorption efficiency depends on the adsorbent surface area. However, a reasonable size of adsorbent is used in column study to avoid the problem with liquid-solid separation. Hence, the smaller particle size of the adsorbent is not studied because of the high-pressure drop in the column (Zou, Zhao and Zhu 2012; Amin, Alazba and Shafiq 2017a). Breakthrough and exhaustion time is slower with increasing adsorbent particle size.

2.12.5 pH

The solution pH greatly depends on the adsorbate and the adsorbent. Generally, high removal efficiency is achieved at acidic pH while the highest removal of some metal ions is achieved at alkaline pH.

2.12.6 Temperature

The adsorption capacity decreases with increasing temperature. High temperature enhances diffusion of the adsorbate in the column hence low breakthrough and exhaustion time is obtained (Ye *et al.* 2018).

2.13 Evaluation of Breakthrough Curve and Mathematical Models

The efficiency of a fixed bed column is explained through the concept of the breakthrough curve. The breakthrough time, as well as the shape of the breakthrough curve, are very essential characteristics for describing the operation and the dynamic output of an adsorption column. The results are stated in terms of maximum column capacity, q_{total} (mg), the equilibrium metal uptake, q_{eq} (mg/g) and the percentage adsorption yield, $\%Y$.

$$q_{total} = \frac{QA}{1000} = \frac{Q}{1000} \int_{t=0}^{t=total} C_{ad}\, dt \qquad (2.15)$$

Where A is the area under the curve, Q is the volumetric flow rate (mLmin^{-1}), t is the total flow time (min) and C_{ad} is the adsorbed concentration (mg/L).

$$q_{eq} = \frac{q_{total}}{X} \qquad (2.16)$$

Where x is the mass of the adsorbent (g).

The amount of metal sent to the column in mg is given as M_{total} ;

$$M_{total} = \frac{C_o Q t_{total}}{1000} \qquad (2.17)$$

$$The\ total\ metal\ removal\ (\%) = \frac{q_{total}}{M_{total}} * 100 \qquad (2.18)$$

2.13.1 Thomas Model

Thomas (1944)is one of the most widely used to estimate the adsorptive capacity of adsorbents and to predict the breakthrough curve. This model assumes that adsorption kinetics follows pseudo-second-order, which relates to Langmuir isotherm at equilibrium and a plug flow with no axial dispersion (Aksu and Gönen 2004; Chatterjee and Schiewer 2011; Chatterjee, Mondal and De 2018).

$$\frac{C_t}{C_o} = \frac{1}{1 + \ exp^{\left(\frac{K_{TH}}{Q}(q_o m - C_o V_{eff})\right)}} \qquad (2.19)$$

The linearized form of the equation is.

$$ln\left[\left(\frac{C_o}{C_t}\right) - 1\right] = \left(\frac{K_{TH} q_o m}{Q}\right) - \left(\frac{K_{TH} C_o V_{eff}}{Q}\right) \qquad (2.20)$$

Where, K_{TH} is the Thomas constant (mL/mg-min), q_0 is the maximum solid-phase concentration of the solute/equilibrium uptake of the metal ion (mg/g), $V_{eff}$is the effluent volume (mL), m is the mass of the loaded adsorbent (g), Q is the flow rate (mL/min), C_0 is the influent concentration (mg/L), C_t is the effluent concentration at time t, (mg/L). The plot of $\ln\left[\left(\frac{C_0}{C_t}\right) - 1\right]$ against time, t gives a straight line.

2.13.2 Adams-Bohart Model

This model was developed by Adams and Bohart in 1920. It was first applied to the gas-solid systems and later extended to other kinds of systems (Bohart and Adams 1920). This model is used to check the dynamic behaviour of the column, it assumes irreversible adsorption; adsorption of solute is directly proportional to the concentration of solute in the bulk solution

and residual adsorptive capacity of the adsorbent. Also, it assumes ideal plug flow with no axial dispersion (Calero *et al.* 2009; Chu 2010; Chatterjee and Schiewer 2011; Chatterjee, Mondal and De 2018). The equation is as stated below.

$$\frac{C_t}{C_o} = \frac{e^{K_{AB}C_o t}}{e^{(K_{AB}N_o Z/U_o)} - 1 + e^{K_{AB}C_o t}} \quad (2.21)$$

The linearized form of the equation is given as.

$$ln\left(\frac{C_t}{C_o}\right) = K_{AB}\, C_o t - K_{AB} N_o \left(\frac{Z}{U_o}\right) \quad (2.22)$$

Where K_{AB} is the kinetic constant in L/mgmin, N_0 is the maximum volumetric sorption capacity in mg/L, C_t is the solute concentration in the liquid phase at time t in min, C_0 is the initial concentration of the metal ion in solution in mg/L, U_0 is the superficial velocity in cm/min, Z is the bed depth/bed height in cm. The plot of $\ln\left(\frac{C_t}{C_0}\right)$ versus t gives a straight line and K_{AB} and N_0 are obtained from the slope and intercept of the graph.

2.13.3 Yoon-Nelson Model

Yoon and NELSON (1984) established a model based on the adsorption of gases in activated coal. This model assumes that the decrease rate in the probability of adsorption of adsorbate molecule is directly proportional to the probability of adsorbate sorption as well as the probability of the sorbate breakthrough on the sorbent with no axial dispersion (Calero *et al.* 2009). The equation below depicts the model.

$$\frac{C_o}{C_t} = \frac{1}{1 + e^{K_{YN}(\tau - t)}} \quad (2.23)$$

The linear form of the equation is represented in the next equation,

$$ln\left(\frac{C_t}{C_o - C_t}\right) = K_{YN}t - \tau K_{YN} \quad (2.24)$$

Where Y_{AB} is the Yoon-Nelson rate constant (min^{-1}) and τ is the time at which effluent concentration reaches 50% of the initial concentration.

2.14 Recent Studies on Fixed-bed Column Adsorption using Bio-sorbents

A fixed-bed column has been used for the removal of various heavy metal ions from wastewater. However, wastewater usually contains more than a single pollutant therefore, researchers have recently considered multi-solute adsorption for industrial-scale using fixed-bed columns. This section will therefore review recent studies on single, binary, and multi-solute adsorption in fixed bed columns using various bio-sorbents.

Abdolali *et al.* (2017) studied the continuous sorption of Cd^{2+}, Cu^{2+}, $Pb^{2+,}$ and Zn^{2+} from wastewater in a single metal solute using a mini glass column 100 cm long and inner radius of 22 mm with varying bed height (9.5, 21, 31 cm). A combination of tea waste, maple leaves, and mandarin peel was used for the adsorption study and the solution pH was maintained at the optimum value of 5.5. The best adsorption capacity was a flow rate of 10 mL/min and a bed height of 31 cm while Thomas and Dose-response best described the adsorption process. Biswas and Mishra (2015) conducted a fixed-bed column adsorption study with a glass column of 2.54 cm internal diameter and 10 cm height using rubberwood sawdust for Pb^{2+} removal from an aqueous solution. The effect of process parameters such as flow rate (10, 15, and 20 mL/min), bed height (2, 5, and 7 cm), initial concentration (10, 20, and 30 mg/L), and pH (3.1, 5.2, and 6.4) was investigated. Chao, Chang and Nieva (2014) investigated the effect of pH and flow rate on the biosorption of Cu^{2+}, Cd^{2+}, Ni^{2+} and Pb^{2+} metal ions using citrus maxima peel, passion fruit shell, and sugarcane bagasse. The Thomas model was used to determine the adsorption capacity of the bio-sorbents.

Ali Gh. Khamseh and Ghorbanian (2018) studied the effect of sorbent diameter, flow rate, bed height, and feed inlet concentration on the breakthrough modeling of thorium biosorption on orange peels in a fixed-bed column. The breakthrough point decreased with decreasing bed height, an increasing inlet concentration, and flow rate. The experimental results were fitted by the Thomas, Yoon Nelson, and Modified Dose-Response (MDR) models. The MDR model

showed better results. Harripersadth (2021) studied the removal of Pb^{2+} from an aqueous solution using sugarcane bagasse, eggshells, and the combination of both in different ratios. The results showed an improvement in bed performance with an increase in bed height. The Thomas and Yoon-Nelson model was used to interpret the breakthrough curves. Both models showed good fits. Vera *et al.* (2018) studied the removal of Pb^{2+} and Cd^{2+} in a column of 1.5 cm internal diameter and height of 50 cm using sugarcane bagasse. The breakthrough curves of the single and binary component system were explained by Thomas, Yoon-Nelson, and Dose-Response models. The biosorption of Pb^{2+} by sugarcane bagasse was significantly influenced by the presence of Cd^{2+}. The Thomas and Yoon-Nelson model successfully fitted the breakthrough curves for the single and binary component system, however, the Thomas model performed better. Martín-Lara *et al.* (2016) reported the binary bio-sorption of Cu^{2+} and Pb^{2+} onto pinecone shells using a packed bed of 15 mm internal diameter and 230 mm length. The effect of the competition of Cu^{2+} and Pb^{2+} ions for binding sites of pinecone shell and operating parameters such as flow rate, inlet $Cu^{2+,}$ and Pb^{2+} concentration, and bed height were investigated. The breakthrough curves for bi-component solutions gave distinct shapes than those obtained for mono-component results. Escudero-Oñate, Poch and Villaescusa (2017) described the competitive sorption of Cu^{2+}, Ni^{2+}, Pb^{2+}, and Cd^{2+} onto grape stalks wastes in ternary mixtures. A model based on the Homogenous surface diffusion model was developed to explain the competitive sorption of the four metal ions. Dong and Lin (2017) examined the competitive adsorption of Pb^{2+} and Zn^{2+} from an aqueous solution using modified beer lees. The effect of operating parameters such as bed height, initial concentration, and the flow rate was explained by the breakthrough curves of binary Pb^{2+} and Zn^{2+} bio-sorption. The Thomas, bed depth service time (BDST), and Yoon-Nelson models were used to predict the removal of Pb^{2+} and Zn^{2+} in the bio-sorption system. Arim *et al.* (2018) modelled the breakthrough curves of Cr^{3+} removal from synthetic effluent using pine bark by a mechanistic approach, empirical models, and multivariate regression analysis. The authors contend that the fitting through the empirical models (Bohart-Adams, Thomas, and Yoon-Nelson) are better than the mechanistic model.

The existing dynamic models were developed for single solute systems and assumed negligible axial dispersion in the column adsorption. Practically, wastewater contains more than one solute, hence it is necessary to develop a model that explains the dynamic adsorption of binary solute in a fixed bed column with the selected bio-sorbent.

2.15 Response Surface Methodology

Bio-sorption is a process that involves various operating parameters which greatly influence the process performance. Depending on the number of parameters, the bio-sorption process could be a complex one to analyze. Therefore, mathematical models are employed to predict and optimize the system. Optimization is a method used to predict the best combination of process parameters that gives the highest process efficiency which leads to improved performance of the process design. In the bio-sorption process, optimization helps to determine the specific operating conditions which give the best process performance in terms of removal efficiency or uptake capacity. Mostly, adsorption experiments are carried out investigating one factor while other process parameters remain constant. The method is known as one factor at a time (OFAT). Some of the advantages of OFAT are: it is very easy to understand, less complex, and needs less training for the readers to interpret the experimental results. However, the application of OFAT has reduced while many researchers prefer to make use of the factorial design method for the following reasons.

- OFAT method does not allow the evaluation of the interaction between variables.
- There is a lack of randomization which results in incomplete conclusions.
- The forecast of the response surface is enhanced in a factorial design.

Response surface methodology is a set of statistical techniques which explain the relationship between many independent variables and one or more responses or yields. This approach was developed by (Box and Wilson 1951), it has been in use since then for the design of experiments. The results obtained from the deigned experimental runs are fitted into mathematical models such as linear, quadratic, polynomial while statistical methods are used to verify the model. The design of experiment (DOE) is an efficient tool in the field of engineering. DOE is used to study the effects of various operating parameters with few experimental runs, the experimental results obtained are then combined in a mathematical model. Thereafter, the model is used for optimization and interpretation of the results. DOE increases the efficiency of a process, reduces the number of experimental runs, reduces the cost of materials, saves time, considers the important parameters in the process (Montgomery 2009). There are six stages involved in the optimization process using RSM as listed below,

- Choosing of independent variables and the required responses

- Choosing an experimental design approach
- Performance of experiments and obtaining of results.
- Fitting of the model equation into experimental data.
- Generation of response graphs and verification of the model (ANOVA)
- Prediction of the optimum conditions.

2.15.1 Choosing of independent variables and the required responses.

The first step is to determine the most significant variables as well as their ranges. In the case of the biosorption batch study, the important variables influencing the adsorption capacity are pH, initial concentration of the metal ion, adsorbent dosage, temperature, agitation speed, and contact time. However, if the biosorption is done in a continuous mode, the significant variables are flow rate, initial concentration of the metal, bed height, pH, and the particle size of the adsorbent. It is important to choose the most significant process variables and for this purpose preliminary experiments become necessary. Some of the design methods used to select variables that have the main effect on the output are, the two-level full or fractional factorial design, the Plackett-Burman (PB), and the Minimum Run Equireplicated Resolution design (Cao *et al.* 2010). The merits of these design methods include a huge decrease in the experimental runs and high resolution. The selection of a good range of variables enhances the possibility of identifying the response optimum conditions.

2.15.2 Choosing the experimental design approach

This step deals with the design of an experiment with the determination of the points at which the response will be estimated. Many researchers have applied various design methods for optimizing the biosorption process, the most generally used being the Box-Behnken design (BBD), central composite design (CCD), Doehlert Matrix (D), Plackett-Burman (PB) design, full or fractional factorial designs. These methods have been used for the optimization of biosorption processes with various variables using engineering software such as Design Expert (Stat-Ease, Inc), Minitab (Minitab Inc.), Statistica (StatSoft), JMP (SAS), and MATLAB (Mathworks).

2.15.2.1 Full factorial design (FFD)

Full factorial experimental design is one in which all input variables are set at two levels. FFD considers all likely combinations of variables with multiple levels. The application of FFD has major drawbacks with fitting into second or higher-order polynomial models. Optimization is mostly improved upon using a second-order model when a three-level factorial design is chosen which helps to estimate higher-order interactive effects between different factors. To deal with this deficiency, a central composite design (CCD) approach was developed.

2.15.2.2 Central composite design (CCD)

This method gives a reduced number of experimental runs than FFD and produces information as much as the 3^n full factorial design. In addition, CCD gives excellent predictions of linear and quadratic interactive effects of variables influencing the process. The CCD comprises of full factorial or fractional factorial design at two levels (2^n), the centre points (cp) which connote the midpoint of the factors, and the axial points (2n), which relies on certain properties preferred for the design and the number of variables selected (Myers, Montgomery and Anderson-Cook 2016). The CCD can be categorized into three types: CCI (inscribed central composite), CCC (circumscribed central composite), and CCF (Face-Centred Composite), which depends on the position of the axial points. The choice of the right type of CCD depends on the area of operability and the interested region (Witek-Krowiak *et al.* 2014). The CCD uses a wider range of variables and is more sophisticated than other design approaches. Therefore, for the batch adsorption study in this work, CCD was used to optimize and study the interactive effects of the process variables.

2.15.3 Experimental data fitting and response graph analysis

This deals with the fitting of the model equation to experimental data and obtaining response graphs. The model fitting comprises two steps: coding of the experimental data and regression. In RSM, coded input values are used to represent the models like +1, 0, and -1 rather than the actual values (Witek-Krowiak *et al.* 2014). The coded values of the experimental data are generated using the general equation below and then fitted to a chosen model using least square methods.

$$y_i = \frac{y_{i-} y_{co}}{\Delta y_i} \qquad (2.25)$$

The response is represented in a graph which could be a three–dimensional plot or contour plot. This graphical representation helps to identify curvature on the response surface and makes it faster to predict whether the optimal value is within the experimental range.

2.15.4 Model verification (ANOVA)

The analysis of variance (ANOVA) is a set of statistical techniques and mathematical functions used to identify the significant variables and their effects on the system in a multi-variable system. It also provides information on the accuracy of the fit and the significance of the experimental results. The parameters used to measure the significance of the variables are F-value and p-value. The co-efficient F-value is obtained from the quotient of the co-efficient mean square and the residual mean square. When the p-value of a variable is lower than 0.05, the variable is termed significant.

2.15.5 Prediction of optimum conditions

In a system involving one response, the optimization can be obtained using calculus. However, when multiple responses are involved, the values can be optimized simultaneously. In this case, the desirability function is required to determine the best optimum conditions. The equation for the desirability function is stated as,

$$D = \left(\prod\nolimits_{i=1}^{m} d_i\right)^{1/m} \qquad (2.26)$$

Where d_i is the desirability of i-th response. The desirability value ranges from $d_i = 0$ for unacceptable value to $d_i = 1$ which is the maximum value.

2.16 Conclusions

There are many techniques applicable for the removal of heavy metals from wastewater. However, adsorption has gained the interest of researchers in the past decades. This technique has been proven to be efficient for the removal of heavy metals present in wastewater. These

heavy metals are hazardous and bio-accumulated in the food chain. Their detection has been due to the development of sophisticated analytical technologies that are efficient for quantifying these contaminants at low concentrations.

The main sources of heavy metals have been linked to different industrial activities. Industrial activities such as mining produce wastewater refer to as acid mine drainage, which is acidic and affects the plant, animal, and human health when it enters surface water. Copper and lead are some of the predominant heavy metals usually found in acid mine drainage (Naidu *et al.* 2019). Therefore, it is important to treat this wastewater to the point that it causes no harm to the environment. Industrial wastewater treatment methods are highly expensive with a high level of expertise hence adsorption is mostly used as it is less expensive.

The present study focused on the treatment of wastewater using readily available waste as a way of reducing environmental pollution and the treatment cost. Hence, these heavy metals will be investigated at low concentrations.

Based on this background, the aim of the present study was focused on the modeling and optimization of competitive bio-sorption of copper and lead ions using orange and banana peels. The interactive effect of the operating parameters was studied in batch mode and a mathematical model was developed to describe the breakthrough curve of a binary solute system in a fixed bed column.

CHAPTER 3

3 Materials and methods

This chapter presents the materials and methods used to accomplish the objectives stated for this study.

Section **3.1** is based on bio-sorbent preparation and characterization. Sections **3.1.1** to **3.1.3** present the methods and materials used for the preparation of the bio-sorbents while section **3.1.4** explains the methods used for the characterization of the bio-sorbents. This study explores two modes of operation, which are batch and continuous mode. The batch mode is presented in sections **3.2** to **3.4** while the continuous mode is presented in sections **3.5** to **3.**6.

The second objective of this study entails the optimization of operating parameters with banana and orange peels using the design of experiments. The materials and methods used to accomplish the second objective are explained in section **3.2**. The third objective of this study encompasses the adsorption kinetic and isotherm studies of single and binary metal systems of Pb^{2+} and Cu^{2+} using banana and orange peels. The materials and methods employed for the third objective are detailed in sections **3.3** to **3.4**. Section **3.5** describes how fixed bed experiment studies were performed as well as the kinetic models used to explain the adsorption mechanism, which is the third objective of the study. Further still, derivation of mathematical model for binary solutes is presented in section **3.6**. Sections **3.5** and **3.6** form objectives 4 and 5 of the study, respectively.

3.1 Bio-sorbent Preparation and Characterization

3.1.1 Biomass processing

The ripened banana and orange peels were collected from a nearby market in Durban, KwaZulu Natal, South Africa. The biomass was washed several times with distilled water to get rid of dust, stone, and other impurities. The peels were dried at 80 ^{0}C for 24 hr. The samples were crushed using a milling machine, then washed with distilled water to remove the colour, and dried at 50 ^{0}C for 24 hr. They were then grounded into powder using a coffee blender and sieved into different particle sizes ranging from 75 – 455 µm. The samples were then labeled

and stored in an airtight container for use. These bio-sorbents (banana and orange peels) were prepared separately without any pre-treatment.

3.1.2 Synthetic Solution

All the reagents used in this research work were of analytical grade supplied by Sigma Chemical Company (South Africa). The stock solutions of Copper and Lead were prepared from metal nitrate salts ($Cu(NO_3)_2.7H_2O$ and $PbNO_3$) in distilled water. The required concentrations were obtained by diluting the stock solution. Dilute H_2SO_4 and NaOH were used to adjust the pH of the solution.

3.1.3 Other consumables

Whatman filter paper of 150 mm diameter was purchased from Shalom laboratory in Durban, South Africa. The filter paper was used to filter samples after the adsorption process. Also, syringe filters with a pore size of 0.45 µm were purchased from Anatech analytical technology in Durban, South Africa. The syringe filters were used to further remove suspended particles from the samples before analysis. Syringes of 10 ml volume were used alongside the syringe filters.

3.1.4 Equipment

Table 3.1 shows the list of the equipment, purpose, and model of the equipment. The equipment was used to measure parameters such as; pH, the mass of bio-sorbent, mixing of the solution and quantity of metal ion adsorbed.

Table 3.1: List of the major equipment used

Equipment	Model	Purpose
Digital pH Meter	Edge^{pH} HI 2002	pH measurement
Conventional oven	Scientific 221	For drying samples
Weighing balance	Highland^{TM} HCB602H	Measuring adsorbent mass
Jar test	VELP JLT6	Consistent mixing of solution
Linear shaker	Orbital shaker 262	For mixing
Micro-plasma atomic emission spectrophotometer (MP-AES)	MY 18379001	Analytes quantity

3.1.5 Characterization of bio-sorbents

The following characterizations (poit of zero charge, FT-IR, SEM-EDS, XRD and BET) were carried out on banana and orange peels as described in sections 3.1.5.1 to 3.1.5.4.

3.1.5.1 Point of zero charge (pHpzc)

The point of zero charge of an adsorbent is determined to know the surface charge of the adsorbent. It is the point at which the surface of the adsorbent has zero net charge, it is usually denoted as pH_{PZC}. At this pH, the positive charge of the surface sites of the bio-sorbent is equal to the negative charge. An understanding of pHpzc helps to hypothesize the ionization

of the functional groups present on the surface of the bio-sorbent and their interactions with the metal ions in the solution.

The pHpzc was be determined by using 50 ml of 0.1 N KNO_3 solution, the initial pH of the solution (pH_i) ranging from 2 to 12 was adjusted using 0.1 M HCl or 0.1 M NaOH solution. 0.5 g of adsorbent is added to the series of beakers containing solutions with different pH values. The solution is mixed in a shaker for 48 hours at 120 rpm under room temperature. The final pH of the solution (pH_f) in each of the beakers is measured. The change in pH (ΔpH) which is the difference between the initial pH and the final pH ($pH_i - pH_f$) is plotted against the initial pH (pH_i). The point at which the curve intercepts the (pH_i axis) line is the pHpzc.

3.1.5.2 Fourier Transform Infrared Spectroscopy (FT-IR)

This is used to determine the active sites and the functional groups present on the surface of the adsorbents. FT-IR gives the characterization of the adsorbents as their chemical structure. The spectrum of a sample is referred to as fingerprint. Oftentimes, it becomes difficult to identify a material through its spectrum, however, the presence and absence of a particular group can be determined by the presence or absence of absorption at a specific wavelength (R. W. Cahn Frs 2005).

IR spectroscopy signifies radiation between two vibration states, whose wavelength (λ) ranges from 30 to 3µ (1µ= 10^{-3}mm) of the electromagnetic spectrum while the energy differences range from 1 – 10 Kcal mol^{-1}. The IR spectra are always presented as the plot of absorption (% of transmission) or transmittance against the wavelength (cm^{-1}) (A. Streitwieser and C. H. Heathcock 1989). The functioal groups present on the surface of banana and orange peel powder were determined using FT-IR (Perkin Elmer, Frontier, USA).

3.1.5.3 Scanning Electron Microscopy – Energy Dispersive X-Ray Spectroscopy (SEM-EDS)

This is used to determine the morphology of a material on a nanometer (nm) to micrometer (µm) scale, to obtain magnified three-dimensional images of their surfaces. A very fine beam of electrons is focused on the specimen which scans through the specimen by the scan coils. There are three types of electronic signals which can be emitted from the surface of the

specimen subjected to the incident beam: backscattered electrons with energy close to that of the incident beam, secondary electrons which possess kinetic energy less than 50 eV, and Auger electrons created by de-excitation of the atoms (J. I. Goldstein *et al.* 2003). The de-excitation of atoms also creates a photon within an emission area ranging from x-ray to visible. The detector gathers and converts the radiation of importance that leaves the specimen into an electrical signal for adjustment and exhibition by the signal processing electronics to establish an image (B. Imelik and J. C. Vedrine 1994; P. J. Goodhew, J. Humphreys and Beanland 2001). The surface morphology of banana and orange peel powder was determined using (FEI Nova NanoSEM 230) scanning electron microscope supported by energy dispersive x-ray analyzer (EDX) (Oxford X-Max detector and INCA software).

3.1.5.4 X-ray Diffraction

A Phillips PW 3830/40 Generator with a PW 3710 mpd control X-ray diffraction system using the Xpert data collector software was used to identify the crystalline materials of the biomass. The measurements were done continuously on a J-J scan in locked coupled mode and the tube was Cu-Ka radiation (lKa1=1.5406Å). The measurement range was 6° to 60° with an increment (D2J: 0.034°).

3.1.5.5 Surface area, pore volume and pore size (BET)

The surface area, pore volume and pore size distribution of the adsorbents were obtained by measuring the nitrogen adsorption–desorption isotherms using a surface area and porosity analyzer (Micromeritics TriStar 3000). Brunnaer–Emmett–Teller surface area (BET m^2/g) and total pore volume (Vt, cm^3/g at STP) were thus obtained by the Nitrogen adsorption data according to BET theory. The pore size distribution was calculated based on differential pore volume of Barrett–Joyner–Halenda (BJH) adsorption–desorption isotherm data.

3.2 Optimization of Operating Parameters using Design of Experiment

3.2.1 Design of experiments

The design of the experiment was done using Design Expert (11.1.0.1) software to obtain the required experimental design matrix and to optimize the adsorption process with the available experimental runs. The aim was to obtain the optimum values of the operating parameters as

well as the significant factors that yield maximum efficiency of the heavy metal removal. Besides, the data obtained were used to develop regression models for each of the responses (Pb^{2+} and Cu^{2+}) removal to establish the interactive effects of the input parameters on the adsorption process. Some of the steps followed in Design Expert are listed below;

(i) Construction of the experimental design matrix: This makes use of the input parameters and the parameters range to generate the experimental runs required to obtain the desired response (yield) as the output value.

(ii) Statistical analysis of experimental data and response modelling: This involves analysis of the experimental data to obtain the yield. The model graphs obtained include; actual versus predicted value, 3D surface plots, and contour plots. These graphs explain the interactive effects of the input variables and the model fitness of the adsorption process. The analysis of variance (ANOVA) is used to validate the model, while the coefficient of determination (R^2) explains the correlation between the predicted and the experimental values.

(iii) Process optimization: Different levels of the input variables were combined to obtain the best conditions that give a maximum response. However, multiple variables can be optimized simultaneously using numerical and graphical representations.

3.2.2 Central composite design (CCD)

The three levels full factorial central composite design (CCD) with face-centered was used (Myers, Montgomery and Anderson-Cook 2016). The single metal optimization study with four input variables generated 30 experimental runs including 6 replicates while the binary metal ions with three input variables generated 20 experimental runs. MATLAB version R2019a was used to obtain the surface response plot of the binary solute system. Table 3-2 depicts the level of the input variables and the experimental range. The following steps were followed.

(i) The adsorption study requires an optimization process.

(ii) The input variable levels and ranges were selected and the number of center points.

(iii) The responses were determined as the removal efficiency of the metal ions in the solution.

(iv) The central composite design was used to generate the experimental matrix.

(v) The randomized experimental runs were followed for each experiment and the corresponding responses were obtained.

(vi) The response data were entered and statistically analyzed.

(vii) The regression models were generated and validated by comparing the predicted and experimental results obtained while the optimum conditions for the operating parameters and the most influential variable were also deduced.

(viii) Interpretation of the results and recommendations were done.

Table 3.2: Experimental design conditions and variable levels using CCD

Bio-sorbent	**Solution**	**Input variables**	**Coded levels**		
			-1	**0**	**1**
Banana peels	Single Cu	X1:Initial concentration (mg/L)	10	55	100
	Single Pb	X2: pH	2	4	6
		X3:Adsorbent dosage (g)	0.1	0.55	1
		X4: Particle size (µm)	75	250	455
	Binary solute Cu-Pb	X1: Initial concentration (mg/L)	10	55	100
		X2: Adsorbent dosage (g)	0.1	0.55	1
		X3: Particle size (µm)	75	250	455
Orange peels	Single solute Cu and Pb	X1:Initial concentration (mg/L)	10	55	100
		X2: pH	2	4	6
		X3:Adsorbent dosage (g)	0.1	0.55	1
		X4: Particle size (µm)	75	250	455
	Binary solute Cu – Pb	X1: Initial concentration (mg/L)	10	55	100
		X2: Adsorbent dosage (g)	0.1	0.55	1
		X3: Particle size (µm)	75	250	455

3.2.3 Adsorption study experiment

The adsorption experiments were carried out with varying initial concentrations of each of the metal ions in a single system and both metals in a binary system, pH, adsorbent dosage, and particle size. The experiments were done using a 250 mL conical flask containing 100 mL solution with initial concentration ranging from (10 – 100 mg/L) of each Cu^{2+}, Pb^{2+} or mixture of both and solution pH ranging from 2 – 6 for solutions containing either Cu^{2+} or Pb^{2+}. However, the optimized pH obtained for the single metal studies was used for the binary solute system thereby reducing the number of experimental runs. The adsorbent dosage and the particle size varied from (0.1 – 1 g) and (75 – 455 µm) respectively. The conical flasks were sealed with foil and placed on the linear orbital shaker and shaken at 180 rpm for 120 min. The solutions were then filtered using Whatman filter paper (150 mm), the filtrate was filtered again using 0.45 µm syringe filters. Thereafter, the filtrate was analyzed using MP-AES. The quantity adsorbed, percentage removal of each metal ion in solution as well as the overall removal efficiency of the binary solute was calculated using Equations 3.1, 3.2, and 3.3 respectively.

$$q_e = \frac{(C_o - C_e)V}{M} \tag{3.1}$$

$$\%\ Removal\ of\ metal\ ion = \frac{(C_0 - C_e)}{C_0} * 100 \tag{3.2}$$

$$Overall\ \%\ Removal\ of\ solutes = \frac{\left(C_{0,Cu+Pb} - C_{e,Cu+Pb}\right)}{C_{0,Cu+Pb}} * 100 \tag{3.3}$$

Where; q_e is the amount of metal ion adsorbed, C_0 is the initial concentration of metal in the solution (mg/L), C_e is the final concentration of metal in the solution after adsorption (mg/L), V is the volume of the solution (L), M is the mass of the adsorbent (g), $C_{0,Cu+Pb}$ is the initial

concentrations of Pb^{2+} and Cu^{2+} in the solution (mg/L) and $C_{e,Cu+Pb}$ is the final concentration of Pb^{2+} and Cu^{2+} in the solution after adsorption (mg/L).

3.2.4 Procedure for quantitative metal ion analysis

The metal quantity adsorbed for all the samples was determined with the aid of a Micro plasma atomic emission spectrophotometer (MP-AES) at specified wavelengths 368.346 and 283.305 nm. The calibration curves (intensity versus concentration) showed working ranges with a correlation coefficient of 0.9999 for all the standards prepared.

3.3 Adsorption kinetic Studies

The kinetic studies were done with a single and binary solute of Cu^{2+} and Pb^{2+}. A dosage of 1g of bio-sorbent was added to a 1 L solution containing Cu^{2+} or Pb^{2+} with an initial concentration of 10 mg/L, 55 mg/L, and 100 mg/L. The solution was agitated for 24 h at 180 rpm while samples were withdrawn at specified intervals (0.25, 0.5, 1, 2, 3, 4, 5, 6, and 24 h). The samples were filtered using Whatman filter paper and syringe filters of 0.45 µm. The samples were then analyzed using MP-AES. All experiments were conducted at room temperature, 27 ^{0}C and the amount of Cu^{2+} and Pb^{2+} adsorbed was calculated using Equation 3.1. All the experiments were conducted in triplicate, while the average of the values was reported.

The kinetic studies provide insight into the time required for the adsorption process to reach equilibrium and the mechanism of the adsorption process. Two kinetic models were used in this study namely, pseudo-first-order and pseudo-second-order models as discussed in chapter two, section 2.10.

3.4 Adsorption Isotherm Studies

The single solute isotherm experiments were conducted with an initial concentration of Cu^{2+} or Pb^{2+} ranging from 10 – 200 mg/L. A dosage of 0.5 g of bio-sorbent was added to the solution and agitated at 180 rpm for 2 h. The binary solute isotherm experiments were done with a mixture of Cu^{2+} and Pb^{2+} containing initial concentration in the ratio 1:1, all other procedures for a single solute isotherm study were followed. The amount of Pb^{2+} and Cu^{2+} adsorbed was

calculated using Equation 3. All isotherm study experiments were conducted at optimum pH of 5 and in triplicate while the mean values were reported.

For equilibrium to be reached, the aqueous solution must be in contact with the adsorbent for enough time. At equilibrium, the solute concentration in the solution and sorbate at the interface becomes the same that is, they are in dynamic balance. Prediction of a suitable isotherm model for an adsorption process is important for the design and optimization of an adsorption system. The experimental results were fitted with the Langmuir and Freundlich isotherm models as discussed in chapter two, section 2.8.

3.5 Fixed bed Column Study

The batch adsorption studies do not give complete information on the industrial application of wastewater treatment. Therefore, batch equilibrium and kinetic studies are always supported by continuous studies to determine the contact time, bio-sorbent efficiency, exhaustion time, mass transfer zone, and most importantly scale-up for industrial treatment plants. These parameters are characteristics of the breakthrough adsorption curve. The continuous adsorption studies were carried out at room temperature with a fixed bed column made of glass material. The column had an internal diameter of 2.5 cm and a height of 50 cm as shown in **Figure 3.1**. The column was designed mainly for this study, it has a spout that allows passage of the effluent. The experiments were performed in a downward flow mode which provides maximum contact between the bio-sorbent and the adsorbates in the inlet stream. A peristaltic pump was used to achieve the desired flow rate. The column was packed with glass beads of 25 mm to the height of 2 cm at the top then followed by glass wool of 1 cm to make the bed compact and give mechanical support to the adsorbent bed. The desired amount of adsorbent was loaded and 1 cm thick glass wool was placed at the bottom followed by a 1 cm glass bead to prevent adsorbent loss. To get rid of air trapped in the bed, distilled water was passed through the column for 3 h before starting the experiments. This ensured that the adsorbent bed was fully wetted and void of air.

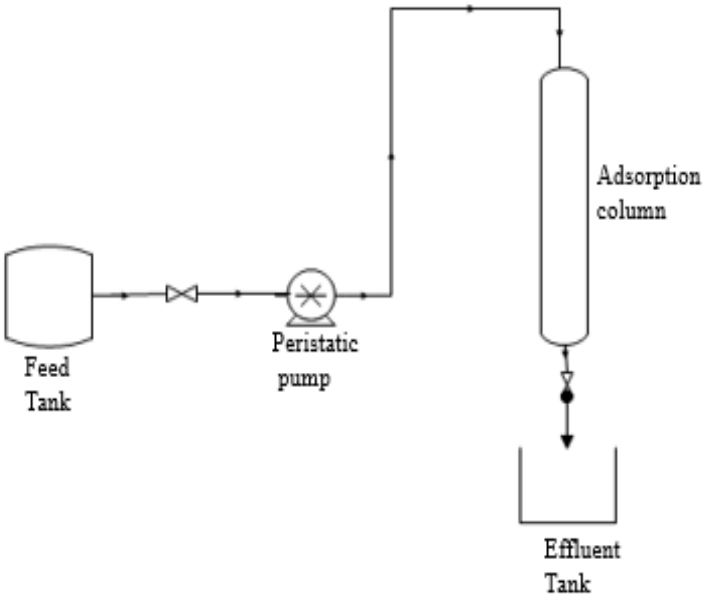

Figure 3.1: Fixed bed column experimental set up

Each experimental run was carried out with an inlet feed of a determined volumetric flow rate, initial concentration, and pH as shown in **Table 3.3**. The pH of the solution was kept constant as already determined in the batch studies. The flow rate was adjusted using a calibrated peristaltic pump (Flexflo A1N11E-4T). The adsorbent dosage variation was used to achieve different bed height values. Samples were collected at the bottom of the column every 30 min for the first 5 h then at an hour interval and analyzed for metal ions concentration. Each metal ion was studied individually and then in a binary system. In the case of competitive adsorption of Cu^{2+} and Pb^{2+}, the initial concentration of the metal ions was at the ratio of 1:1. All experiments were carried out in duplicate and the average values were used for further calculations. This helped to determine the influence and sensitivity of the co-existence of the metal ions. The column experiments were carried out to investigate the effect of operating parameters such as initial metal ion concentration, bed height, and flow rate on the process efficiency. The experimental data were fitted with Thomas, Yoon Nelson, and Bohart-Adams models as discussed in chapter two, section 2.13.

Table 3.3: Process variables and experimental runs for fixed bed column

Variable parameters	Value/range	Adsorbent/ metal ion	pH	Bed height Cm	Initial concentration mg/L	Flow rate mL/min
Bed height (cm)	1, 3	OP - Cu^{2+} OP – Pb^{2+} OP-Cu-Pb	5	-	50	3
Initial concentration (mg/L)	10, 50, 100	OP - Cu^{2+} OP – Pb^{2+} OP-Cu-Pb	5	2	-	3
Flow rate (mL/min)	1, 3	OP - Cu^{2+} OP – Pb^{2+} OP-Cu-Pb	5	2	50	-

3.6 Mathematical Modelling of Binary Solutes Breakthrough Curve

Mathematical modeling has a very significant part in the scale-up process of laboratory experimental study to industrial scale. Different empirical models have been used to describe the biosorption process in dynamic study. However, the models are mostly applied in a sorption process consisting of a single metal ion. Researchers have complemented column study analysis with the development of mechanistic models and computer simulation as an efficient tool for explaining the kinetic behavior of the fixed bed column, prediction of the breakthrough curves, and the scale-up technology. This approach has been applied to mono-component biosorption systems while binary and multi-component has not been explored (Arim *et al.* 2018).

Therefore, in this study, to describe the binary bio-sorption of Cu^{2+} and Pb^{2+} ions onto orange peels in a fixed bed column, a suitable model was developed to determine the mechanisms responsible for the bio-sorption process and predict the breakthrough curves of the metal ions. The model made use of the following assumptions.

(i) The physical characteristics of the fluid phase and the bio-sorbent are constant, no chemical reaction.
(ii) Constant flow rate axially dispersed plug flow with negligible radial dispersions.
(iii) Constant temperature and pressure
(iv) Constant column void fraction
(v) The mass transfer resistance in the outer film is negligible
(vi) The linear driving force (LDF) is used to explain the mass transfer.

Based on the above assumptions, the approach used to develop the model combined the mass balance of the fluid phase, the equilibrium isotherm, and the linear driving force (LDF). The mathematical model was developed from the mass balance equation of the solid and liquid phases based on the above assumptions in the fixed bed column. The mass balance around the section dz of the bed is expressed as.

$$\frac{\partial C(z,t)}{\partial t} + U_i \frac{\partial C(z,t)}{\partial z} + \frac{(1-\varepsilon)}{\varepsilon} \rho_p \frac{\partial \{q(z,t)\}}{\partial t} - D_L \frac{\partial^2 C(z,t)}{\partial^2 z} = 0 \qquad (3.4)$$

Where $C(z,t)$ is the concentration of the metal ion in the fluid phase (mg/L), t is the time (s), U_i is the superficial velocity (m/s), z is the axial position in the bed (m), ε is the bed porosity, ρ_p is the density of the adsorbent (Kg/m^3), $q(z,t)$ is the average adsorbed metal ion concentration (mg/Kg_{ads}) and D_L is the axial dispersion coefficient (m^2/s).

The linear driving force (LDF) model explained by Glueckauf (1955) was used to describe the intraparticle mass transfer,

$$\frac{\partial \{q(z,t)\}}{\partial t} = K_{LDF}[q^*(z,t) - \{q(z,t)\}] \qquad (3.5)$$

Where K_{LDF} is the LDF kinetic constant (s^{-1}) while q*(z, t) is the adsorbed phase concentration of the species in equilibrium with the bulk concentration (mg/Kg_{ads}). Danckwerts proposed

boundary conditions stated by Equation (3.3)-(3.4) for solving Equations (3.1) – (3.2) with the initial conditions stated in Equation (3.5).

$$z = 0: D_L \frac{\partial C(z,t)}{\partial z} = U_i(C(0,t) - C_E) \quad (3.6)$$

$$Z = L: \frac{\partial C(z,t)}{\partial z} = 0 \quad (3.7)$$

$$t = 0: C(z,0) = 0; \; <q(z,0)> = 0 \quad (3.8)$$

Where CE symbolizes the inlet concentration (mg/L) and L is the bed height (m).

The equilibrium isotherm described by Langmuir isotherm model is used to explain the adsorption capacity, q*(mg/g).

$$q^*_{e,i} = \frac{q_{m,i} K_{L,i} C_{e,i}}{1 + \sum_{j=1}^{N} K_{L,j} C_{e,j}} \quad (3.9)$$

The axial dispersion coefficient D_L was described by the correlation in Equation ….

$$\frac{U_0 d_p}{D_L} = (0.2 + 0.011 Re^{0.48}) \quad (3.10)$$

Where U_0 is the superficial velocity (m/s), d_p is the average particle diameter (m), and Reynolds number Re, as stated in Equation 3.8.

$$Re = \frac{U_0 \rho_f d_p}{\eta_f} \quad (3.11)$$

Where ρ_f is the fluid density (Kg/m3) and viscosity of the fluid η_f (Pa.s).

The parameter K_{LDF} based on LDF model describing homogenous and porous particles was used as stated in Equation 3.9.

$$K_{LDF} = \frac{\Omega D_{pe}}{r_p^2 \rho f_h \left(\frac{dq^*}{dC}\right)} \quad (3.12)$$

The mass balance equation of the solid and liquid phase consisting of partial differential equations (PDE) was converted to an ordinary differential equation (ODE) using the finite difference method. The numerical solution used to discretize the PDE is the central finite difference method. Then, code was written using MATLAB R2019a to solve the equations together with the intraparticle mass transfer.

3.7 Statistical Validity

The statistical validity evaluated the statistical and mathematical features of the applied models and compared the error values obtained to determine the best model that fitted the experimental data the most. The statistical validation is significant for evaluating the performance of the adsorption models. Three different error functions were examined in this study namely: mean absolute error, root mean square error, and the coefficient correlation as represented in **Table 3.4**. The best-fit model was chosen based on the error function that gave the lowest error distribution between the experimental and predicted model values while the highest coefficient of correlation was selected.

Table 3.4: Error functions used to statistically validate the performance of the models.

Error function	Abbreviation	Equation
Mean absolute error	MAE	$MAE = \frac{1}{n}\sum_{i=1}^{n}\left\|y_{e,exp} - y_{e,pred}\right\|$
Root mean square error	RMSE	$RMSE = \sqrt{\frac{1}{n}\sum_{i=1}^{n}\left(y_{e,exp} - y_{e,pred}\right)^2}$
Coefficient of correlation	R^2	$R^2 = \frac{\sum\left(y_{e,exp} - y_{e,pred}\right)^2}{\sum\left(y_{e,exp} - y_{e,pred}\right)^2 + \left(y_{e,exp} - y_{e,pred}\right)^2}$

CHAPTER 4

4 Results Obtained for Bio-sorbent Characterization

This chapter presents the characterization results of the bio-sorbents before and after adsorption studies. The point of zero charge (pHpzc), functional group analysis, surface morphological structure, elemental composition, and the crystalline nature of the bio-sorbents are discussed in detail.

4.1 Point of Zero Charge

The point of zero charges (pHpzc) is a surface property usually investigated to determine the potential of a bio-sorbent for the removal of metal ions from an aqueous solution. The point of zero charge of an adsorbent is the point at which the surface of the adsorbent has zero net charge (Pathak, Mandavgane and Kulkarni 2017). The pHpzc of an adsorbent gives insight into the ionization potential and the interactive effect between the adsorbent surface and the adsorbate. When the pHpzc is less than the solution pH, adsorption of cations is favoured and when the pHpzc is greater than the solution pH, the adsorption of anions is favoured.

As shown in **Figure 4.1**, the pHpzc of natural orange and banana peels gave 3.85 and 4.83 respectively. This means that the surfaces of orange and banana peels are acidic and therefore favour the adsorption of cations. This result is similar to what was reported by (Nascimento *et al.* 2014).

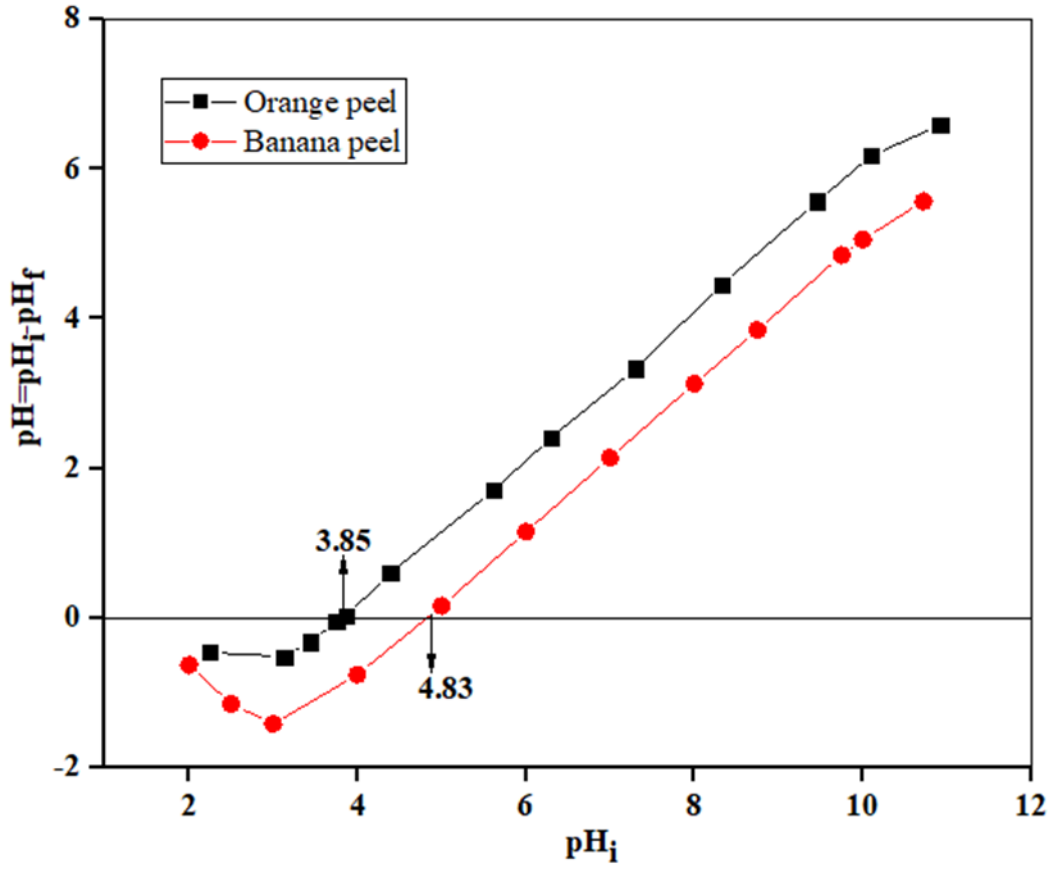

Figure 4.1: Point of zero charge of orange and banana peels

4.2 Functional Group Analysis

4.2.1 Before adsorption

The FTIR spectrum is used to identify the functional groups present on the surface of an adsorbent. Adsorption is a physical phenomenon that involves the interaction between the functional groups on the surface of a bio-sorbent and the metal ions in an aqueous solution. These functional groups provide active sites for the adsorption of the metal ions on the surface of the adsorbent. The FTIR spectra represented in **Figure 4.2** show the functional groups present on the surface of orange and banana peels before adsorption. The FTIR of natural orange and banana peels were obtained within the range of 500 to 4000 cm^{-1} wavenumber.

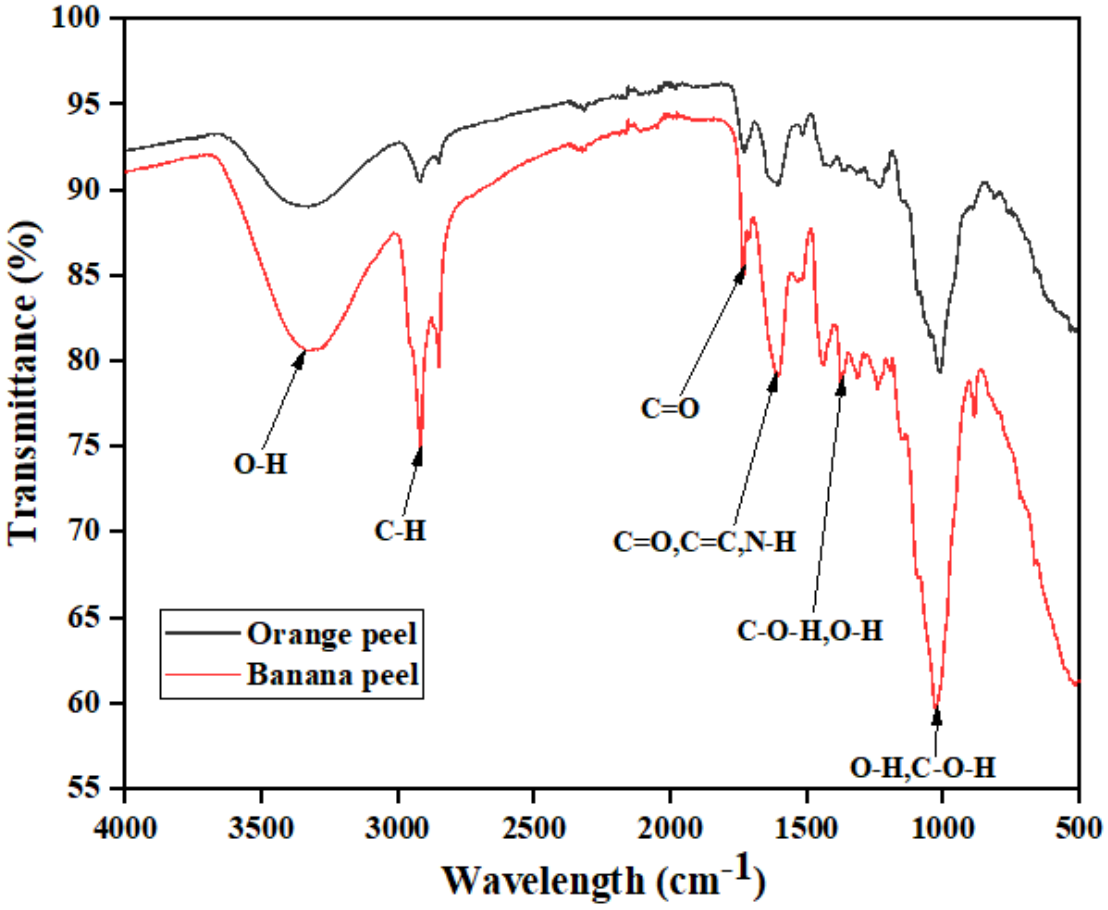

Figure 4.2: FTIR spectra of orange and banana peels before adsorption.

As shown in **Figure 4.2**, the spectrum of banana peel shows broader and more pronounced peaks than the orange peel probably because it has lower percentage transmittance. There are similarities in shape and band positions of the spectra of orange and banana peels but different percentage transmittance. The spectra of both bio-sorbents show the presence of a broad peak at 3382.62 cm^{-1}, which indicates the presence of an intermolecular bonded O-H group consisting of alcohols and phenols. The peaks at 2918.92 cm^{-1}, 2850.97 cm^{-1}, 1441.94cm^{-1}, 1374.74 $cm^{-1,}$ and 887.26 cm^{-1} indicate the presence of a saturated C-H substitution bond which can be likened to alkanes that are available in the pulp. The peaks at 1734.38 cm^{-1} and 1607.04 cm^{-1} reveal the presence of the carboxylic C=O bond and the unsaturated C=C bond respectively which are attributed to aldehydes and ketones. The peaks and functional groups observed on the surface of orange and banana peels are similar to the study reported by (Bhaumik and Mondal 2014; Oyewo, Onyango and Wolkersdorfer 2016; Deshmukh *et al.* 2017). The existence of a high quantity of hydroxyl and carboxyl groups on the surface of both

bio-sorbents suggest the tendency of these peels to adsorb positively charged metal ions. The presence of these functional groups plays an important role in the bio-sorption of heavy metals through electrostatic repulsive interaction. These acid groups become deprotonated at a solution pH above the pHpzc of the adsorbent hence, resulting in negatively charged adsorbent surface which favours uptake capacity of Cu^{2+} and Pb^{2+} ions which occurs as a result of the affinity of metal ions to the functional groups.

4.2.2 After adsorption

The functional groups present on the surface of orange and banana peels after adsorption are presented in **Figures 4.3** and **4.4** respectively. Each spectrum compares the FTIR of the bio-sorbent before adsorption, bio-sorbent loaded with Cu^{2+} and Pb^{2+} in both single and binary solute systems.

4.2.2.1 Orange peels after adsorption

A comparison of FTIR spectra of orange peels before and after adsorption is represented in **Figure 4.3**. All four patterns look similar which suggests that the same functional groups are present on the surface of the bio-sorbent before and after adsorption. However, there are significant shifts in the peaks and intensities of the spectrum. These shifts are attributed to the interaction between the functional groups present on the surface of the bio-sorbent and the copper and lead ions in the solution. The significant shift occurred in the monogram after adsorption in the peaks representing the O-H and C-O-H stretching which are peculiar to the adsorption of both copper and lead. This shows that hydroxyl and carboxyl groups played a major role in the adsorption of copper and lead. The percentage transmittance shows how much light was transmitted by the molecules. The percentage transmittance of natural orange peels started with 92 % which means 8 % was absorbed while the spectra representing after adsorption of copper, lead and binary solute of both metals started with 98 % transmittance suggesting 2 % was absorbed. Therefore, after the adsorption of metal ions, more light was transmitted by the molecules present in the bio-sorbent.

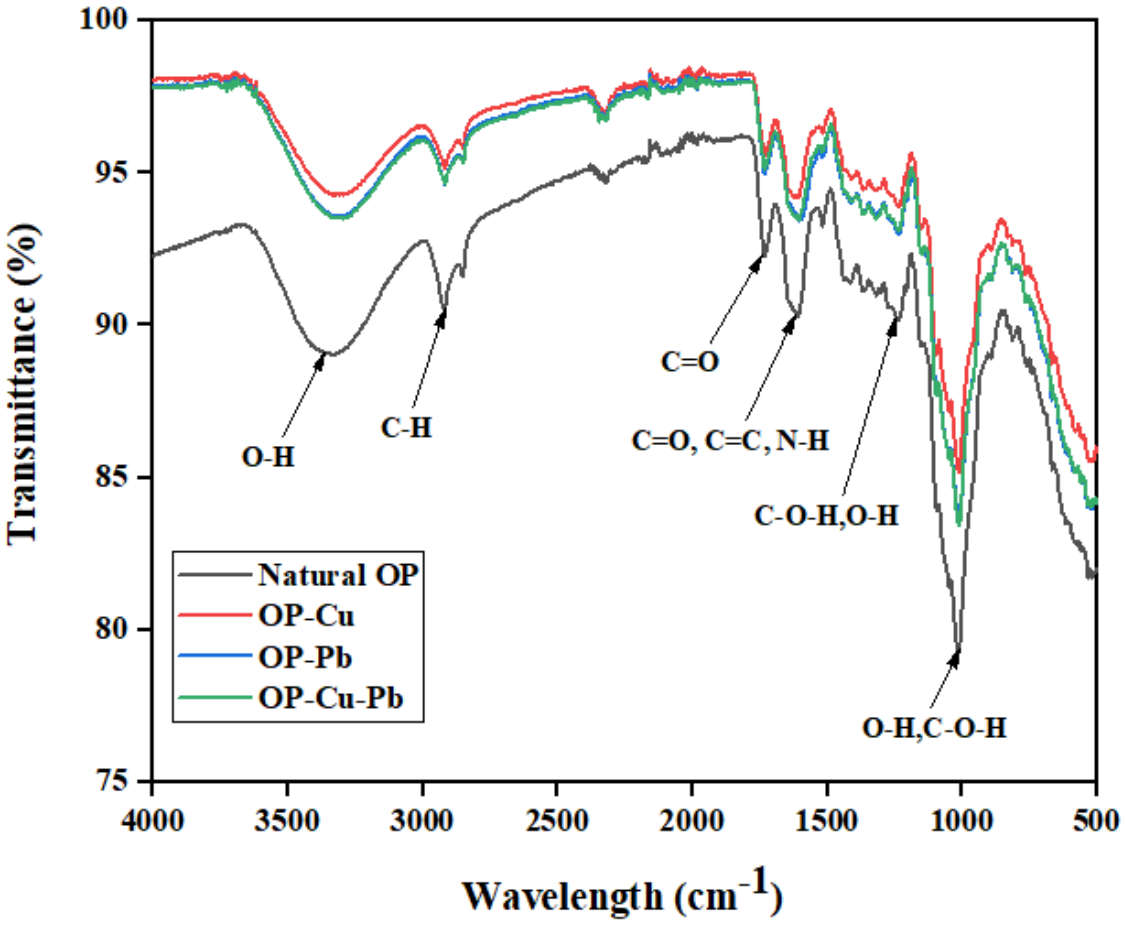

Figure 4.3: FTIR spectra of orange peels before and after adsorption

4.2.2.2 Banana peels after adsorption

Figure 4.4 depicts the FTIR spectra of banana peels before adsorption in comparison with after adsorption graphs. There are similarities in the shape and peak positions of the spectra after the adsorption of copper and lead in both single and binary systems. There are significant changes in the percentage transmittance of the peaks indicated on the spectra before and after the adsorption of copper and lead mostly represented by the hydroxylic and carboxylic groups. This reveals that there was an interaction between the metal ions in the solution and the surface of the bio-sorbent during the adsorption process through electrostatic attraction. In addition, the percentage transmittance of after adsorption spectra started at 98 % which is higher than natural banana peels with 91 %. This suggests that more light was transmitted by the molecules of the bio-sorbent after adsorption. Deshmukh *et al.* (2017) reported difference in transmittance at some peaks representing the carboxylic and hydroxyl groups of natural banana peels and the

banana peels loaded with cadmium, which indicted the importance of these functional groups in the binding mechanism.

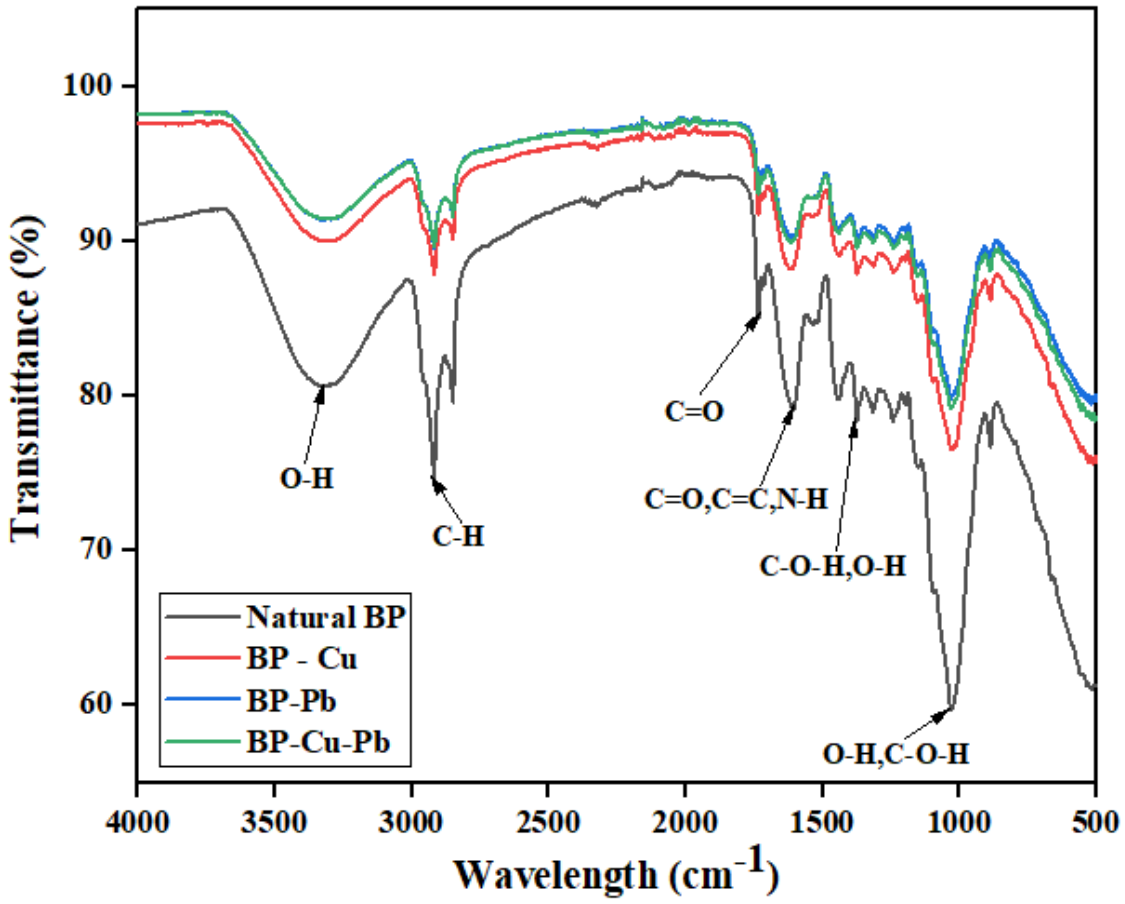

Figure 4.4: FTIR spectra of banana peels before and after adsorption.

4.3 Surface Morphology

The surface morphology helps to determine the surface structure of an adsorbent before and after adsorption using the scanning electron microscope (SEM). In this study, the surface morphology of orange and banana peels was determined before adsorption and after adsorption of copper and lead in both single and binary solute systems.

4.3.1 Surface morphology before adsorption

Figures 4.5 and **4.6** show the surface morphology images of orange and banana peels bio-sorbents before adsorption. The micrographs depicted in **Figure 4.5a**, and **Figure 4.5b** represent the 5 000 times and 10 000 times magnification of orange peel bio-sorbent before adsorption while a much closer view of the surface structure is displayed in **Figure 4.5b**. The surface of the orange peel revealed an uneven and highly irregular surface. In addition, the sharp and coarse particles with varying shapes and sizes can be seen deposited randomly on the surface of the bio-sorbent. Besides, some pores can be seen on the surface of the bio-sorbent in **Figure 4.5b**. The SEM images (**Figure 4.6a and Figure 4.6b**) show the surface structure of banana peel bio-sorbent before adsorption at the 5 000 times and 10 000 times magnification respectively. The surface reveals a rough and irregular shape, microporous with vast heterogeneity which can enhance the adsorption of copper and lead ions. Chen *et al.* (2018) investigated the adsorption capacity of four peels (litchi peel, orange peel, pomegranate peel and banana peel) in the removal of cadmium from an aqueous solution. The surface structure of the four peels were rough and loose with microporous structure. The surface of the peels revealed folds which greatly improved the adsorption capacity.

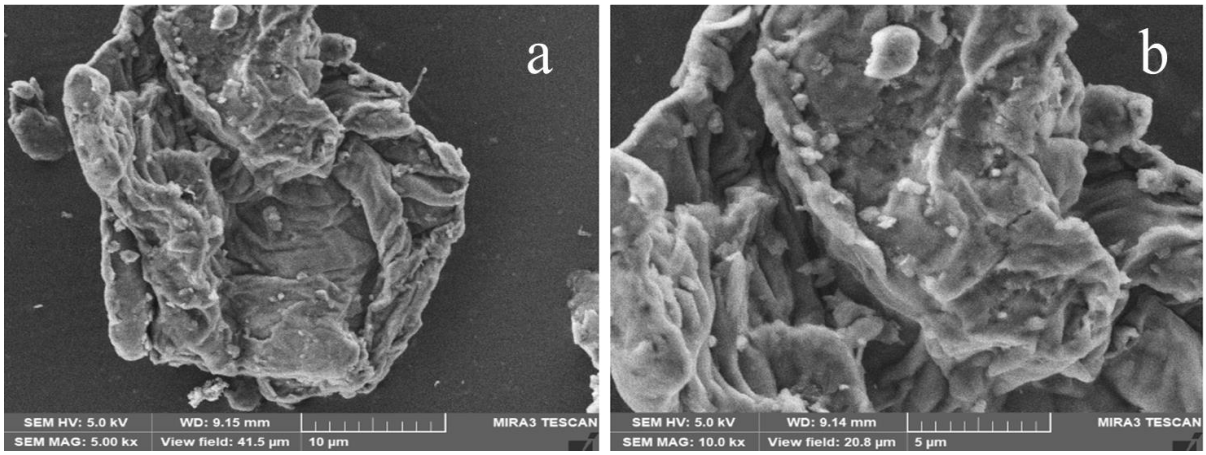

Figure 4.5: SEM images of orange peel powder before adsorption at (a) 5 000x and (b) 10 000x magnification

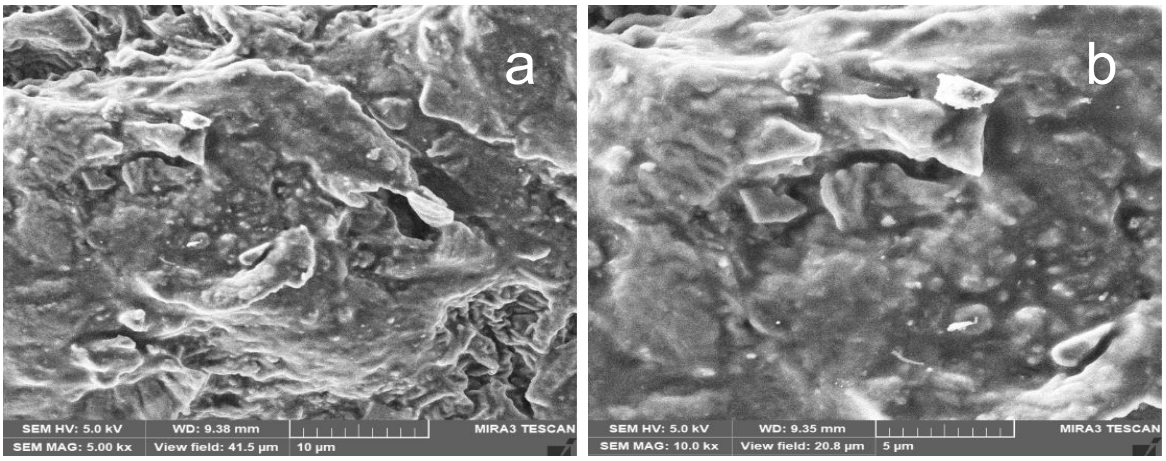

Figure 4.6: SEM images of banana peel powder before adsorption at (a) 5 000x and (b) 10 000x magnification

4.3.2 Surface morphology after adsorption

The micrographs displayed in **Figure 4.7** and **Figure 4.** ***8*** show the surface structure of orange and banana peel bio-sorbent after adsorption. The SEM images in **Figures 4.7a**, **4.7b** and **4.7c** represent the surface structure of orange peel after adsorption of Cu ions, Pb ions, and both Cu and Pb ions in binary solution, respectively. After adsorption of Cu and Pb ions, a highly significant change can be observed as shown in **Figures 4.7a** and **4.7b**. The roughness of the surface is more pronounced with reduced uneven particles distributed on the surface. Also, the surfaces of orange peels loaded with Cu and Pb ions appeared shiny which suggests physicochemical interactive effects of the metal ions with the functional groups present on the surface of the bio-sorbent. Amin, Alazba and Shafiq (2017b) reported rough asymmetric pores on the surface of banana peel biochar before adsorption, which enhanced the interactions between the biochar and the metal ions (Cu and Pb). After adsorption, the biochar surface became smooth and shiny with closed pore structures. However, **Figure 4.7c** representing the surface structure of orange peel bio-sorbent loaded with Cu and Pb ions in binary solution appeared rough with little deposit of irregular particles distributed on the surface, and less shiny surface was observed compared to **Figure 4.7a** and **4.7b**.

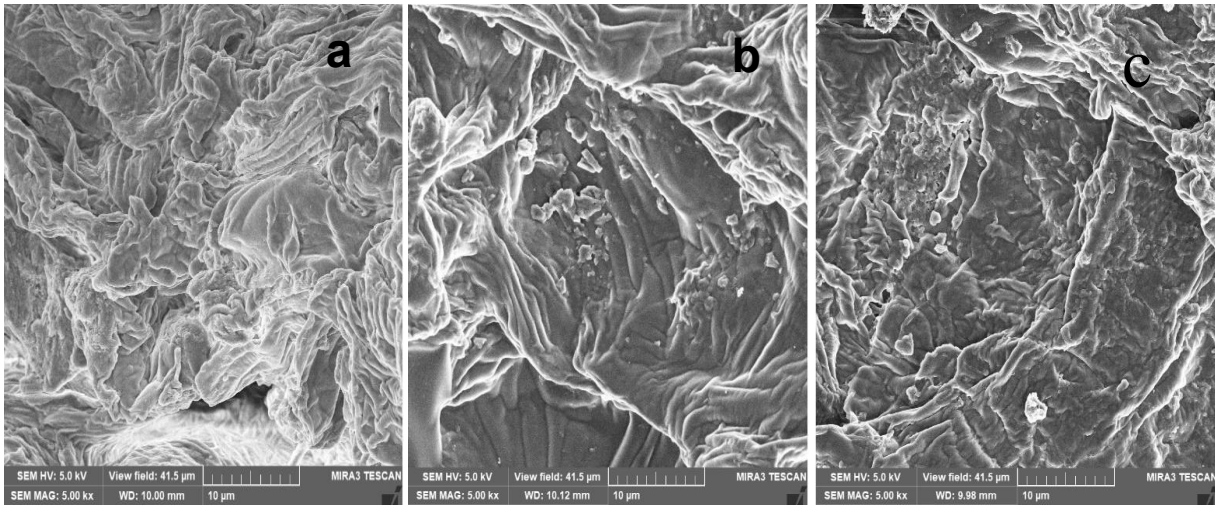

Figure 4.7: SEM images of orange peels bio-sorbent after adsorption at 5 000x magnification (a) OP loaded with Cu (b) OP loaded with Pb (c) OP loaded with Cu and Pb in binary solution.

The micrograph images of banana peels loaded with Cu ions, Pb ions, and Cu and Pb ions in binary solution were depicted in **Figures 4.8a**, **4.8b**, and **4.8c** respectively. Significant changes in the surface texture and structure of banana peels bio-sorbent can be observed after the adsorption of Cu^{2+} and Pb^{2+} ions. Besides, the fibrous structure of banana peel before adsorption disappeared, the surface became rougher, filled up, and irregular.

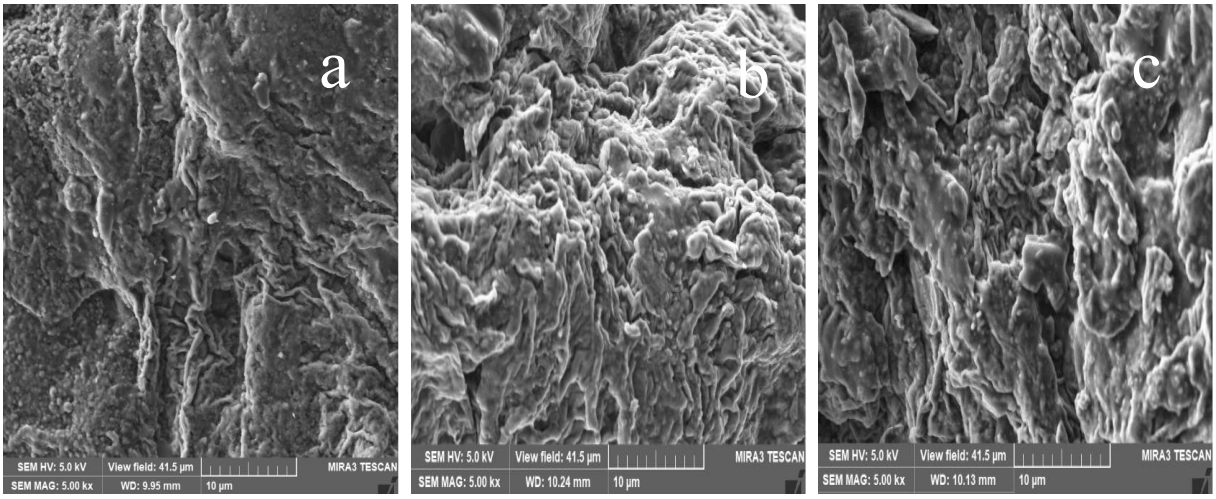

Figure 4. 8: SEM images of banana peels bio-sorbent after adsorption at 5 000x magnification (a) BP loaded with Cu (b) BP loaded with Pb (c) BP loaded with Cu and Pb in binary solution.

4.4 Energy-Dispersive X-ray Spectroscopy

EDX is an analytical instrument used to determine the elemental composition of substances. It is essential to know the elemental composition of adsorbents before and after adsorption to determine the adsorption mechanism and the functional groups that are responsible for the process.

4.4.1 EDX before adsorption

The EDX analysis of orange and banana peels bio-sorbents before adsorption is shown in **Figures 4.9a** and **4.9b** respectively. **Figure 4.9a** reveals the chemical composition of orange peel bio-sorbent, the surface indicated the presence of carbon, oxygen, magnesium, sulfur, potassium, and calcium. Carbon has the highest percentage composition followed by oxygen. This emphasizes the carboxyl and hydroxyl groups present on the surface of the bio-sorbent as revealed by the FTIR spectra. The EDX spectra of banana peel bio-sorbent showed the presence of carbon, oxygen, potassium, and silicon with carbon having the highest percentage composition followed by oxygen and silicon.

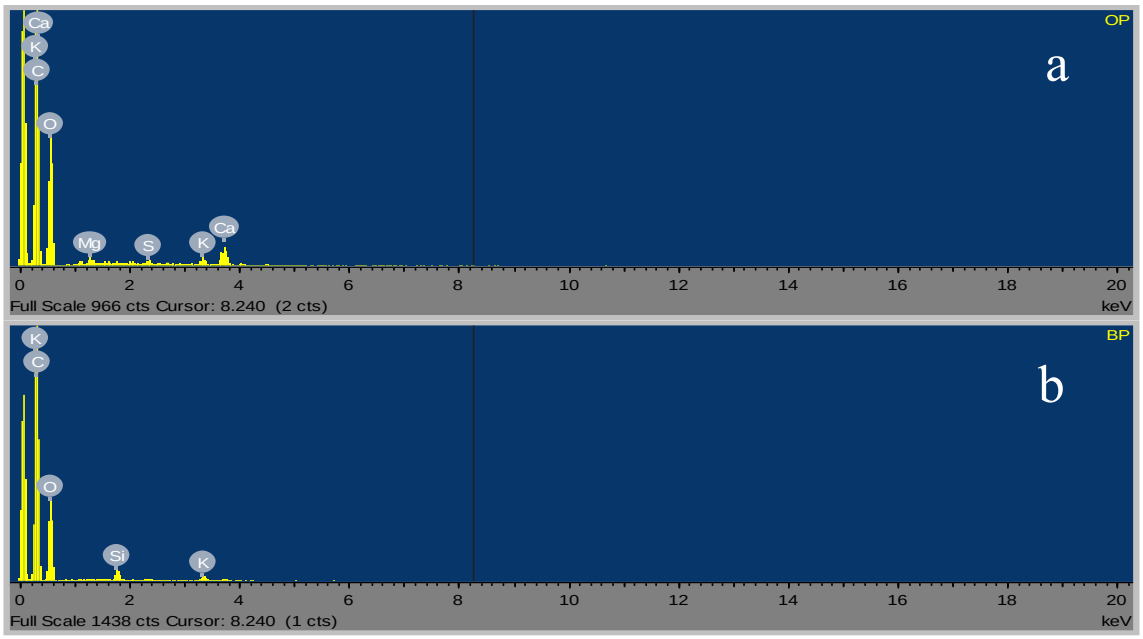

Figure 4.9: EDX image before adsorption (a) orange peel (OP) (b) banana peel (BP)

4.4.2 EDX after adsorption

The EDX spectra of orange and banana peels after adsorption of Cu ions and Pb ions in a single and binary system are shown in **Figures 4.10** and **4.11** respectively. The EDX spectra of orange peel loaded with copper (**Figure 4.10a**) showed an additional peak which confirmed the presence of copper being adsorbed on the surface of the bio-sorbent. Besides, there were changes in the peak intensities after adsorption while magnesium, potassium, and calcium peaks disappeared. This suggests ion-exchange took place on the surface of the bio-sorbent as a result of electrostatic interaction between the metal ions on the surface of the bio-sorbent and copper ions in the aqueous solution. In **Figure 4.10b**, the presence of Pb ion on the surface of the bio-sorbent after adsorption suggests that orange peel is capable of removing lead ions. Also, there was a disappearance of magnesium, sulphur, and potassium peaks suggesting the possibility of ion exchange between the sorbate and the adsorbent. However, Figure 4.10c representing EDX spectra of orange peel loaded with copper and lead ions in a binary system indicates the presence of only carbon and hydrogen with Cu and Pb peaks. It is apparent that all other elements except carbon and hydrogen disappeared and were replaced with Cu and Pb.

The percentage composition of Pb adsorbed on the surface of orange peel is more than Cu which suggests that orange peel bio-sorbent has more affinity for Pb^{2+} ions than Cu^{2+} ions.

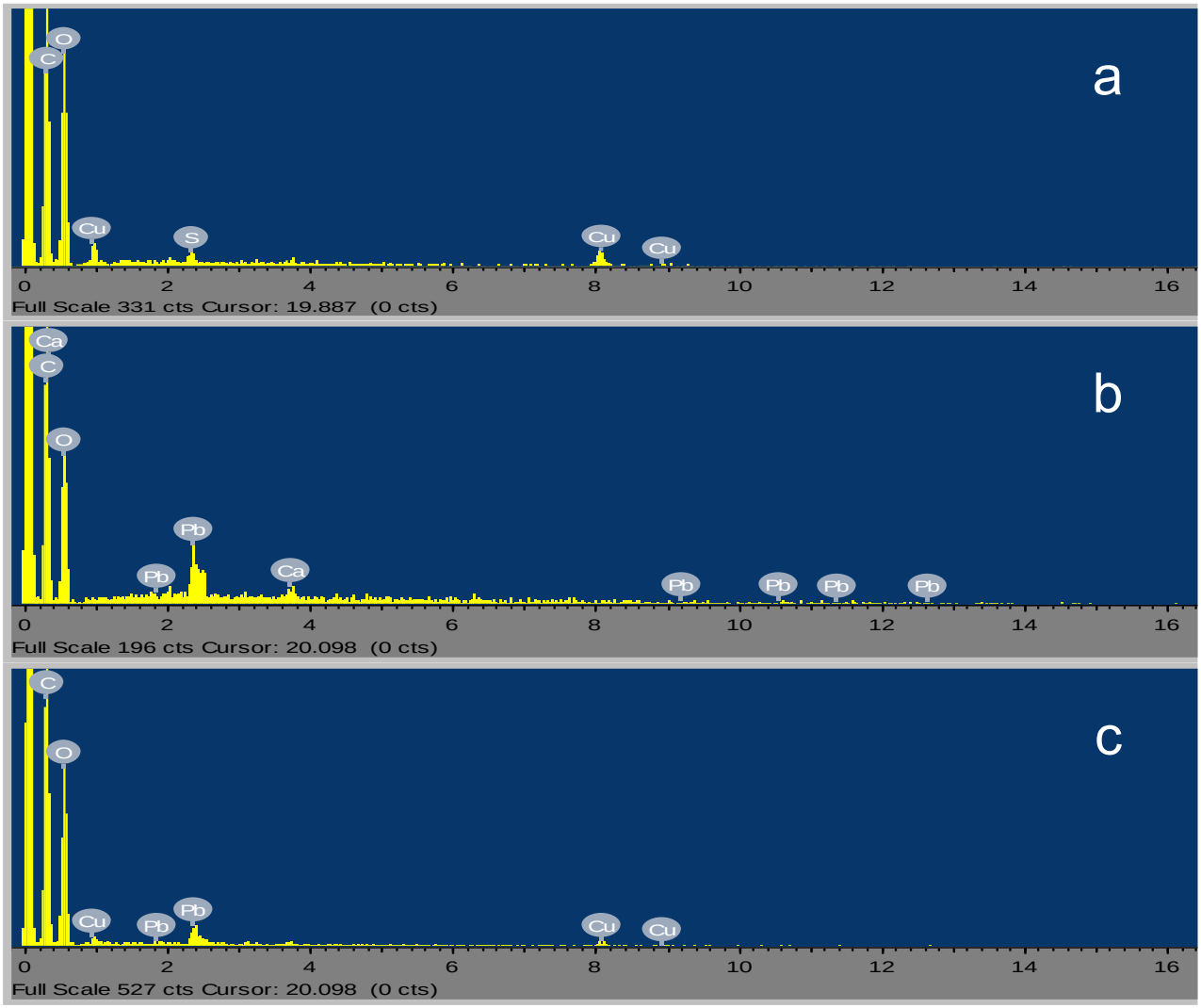

Figure 4.10: EDX spectra of orange peel after adsorption (a) OP loaded with Cu (b) OP loaded with Pb (c) OP loaded with both Cu and Pb.

The elemental analysis of banana peel after adsorption of Cu^{2+} ions and Pb^{2+} ions in the single and binary system is shown in **Figure 4.11**. The presence of elements such as carbon, silicon, and copper was observed on the surface of the bio-sorbent after adsorption (**Figure 4.11a**). However, as a result of copper ions adsorption onto the banana peel, the potassium peak disappeared suggesting ion exchange between the adsorbate and the adsorbent. Furthermore, the EDX spectra of banana peel loaded with Pb ions are represented in **Figure 4.11b**. The spectra revealed the presence of the Pb peak in addition to the peaks indicated before adsorption

except for potassium. The peaks representing calcium were seen on the spectra suggesting that a minute amount of calcium was present on the surface of the bio-sorbent. **Figure 4.11c** indicated the presence of elements such as carbon, silicon, copper, and lead on the surface of banana peels after adsorption of Cu and Pb ions in a binary system. Potassium was completely displaced because it is a highly reactive metal while silicon is a metalloid. It is evident that Cu^{2+} and Pb^{2+} were adsorbed and there was a slight difference between the percentage composition of Cu^{2+} and Pb^{2+} adsorbed. Pb^{2+} has a percentage composition of 0.76 % and Cu^{2+} has 0.7 %.

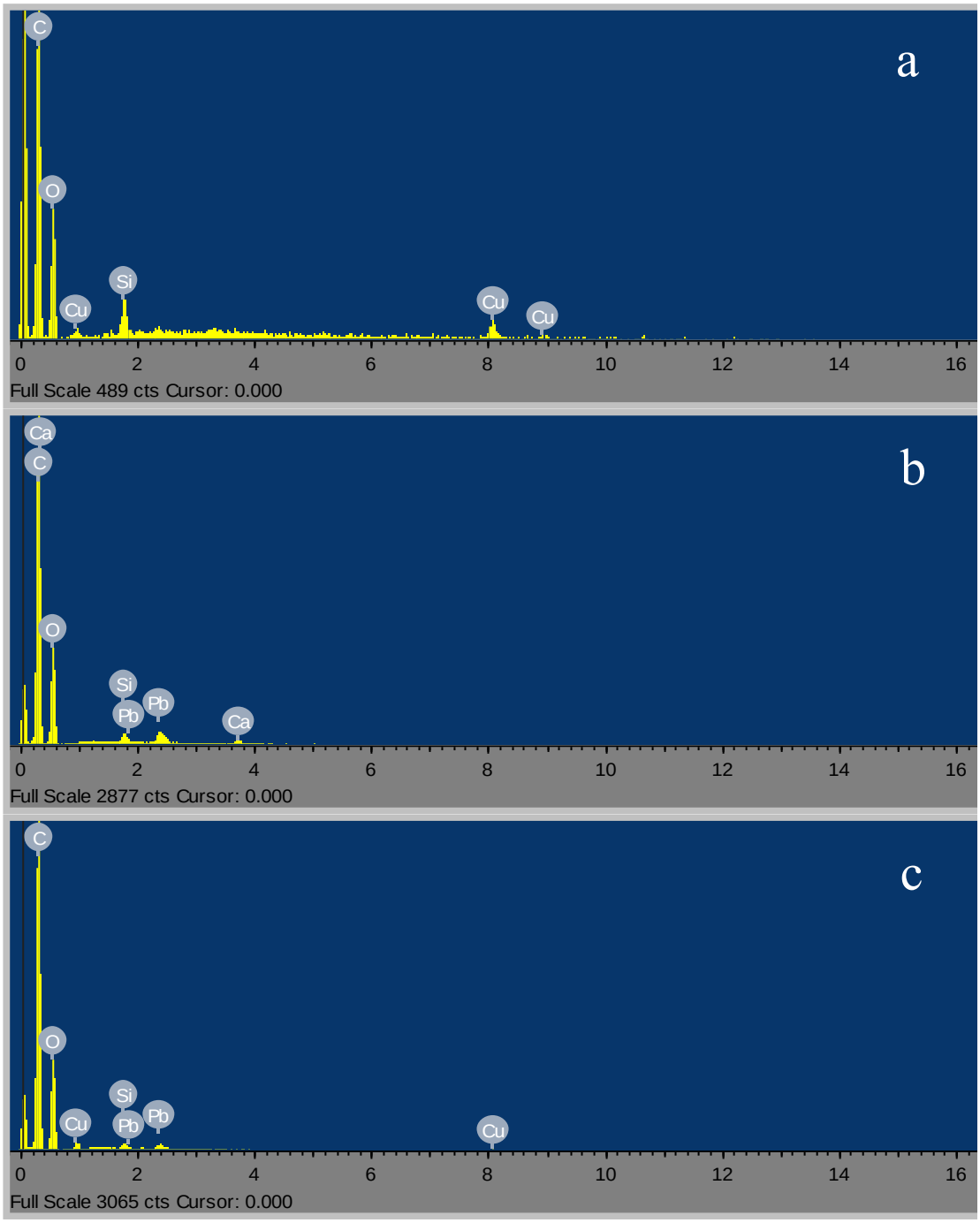

Figure 4.11: EDX spectra of banana peel after adsorption (a) BP loaded with Cu (b) BP loaded with Pb (c) BP loaded with both Cu and Pb.

4.5 X-Ray Diffraction Spectroscopy

The x-ray diffraction spectroscopy uses high-accuracy rays to determine the crystallinity of a material. The XRD pattern helps to identify the crystalline phase or amorphous materials present in the adsorbent. Hence, the XRD was used to determine the kind of phases that are available in the peels and explain how the phases will influence the adsorption of copper and

lead ions. This analysis was done before adsorption only. The results obtained from the XRD analysis of orange and banana peels are as shown in **Figures 4.12** and **4.13**, respectively.

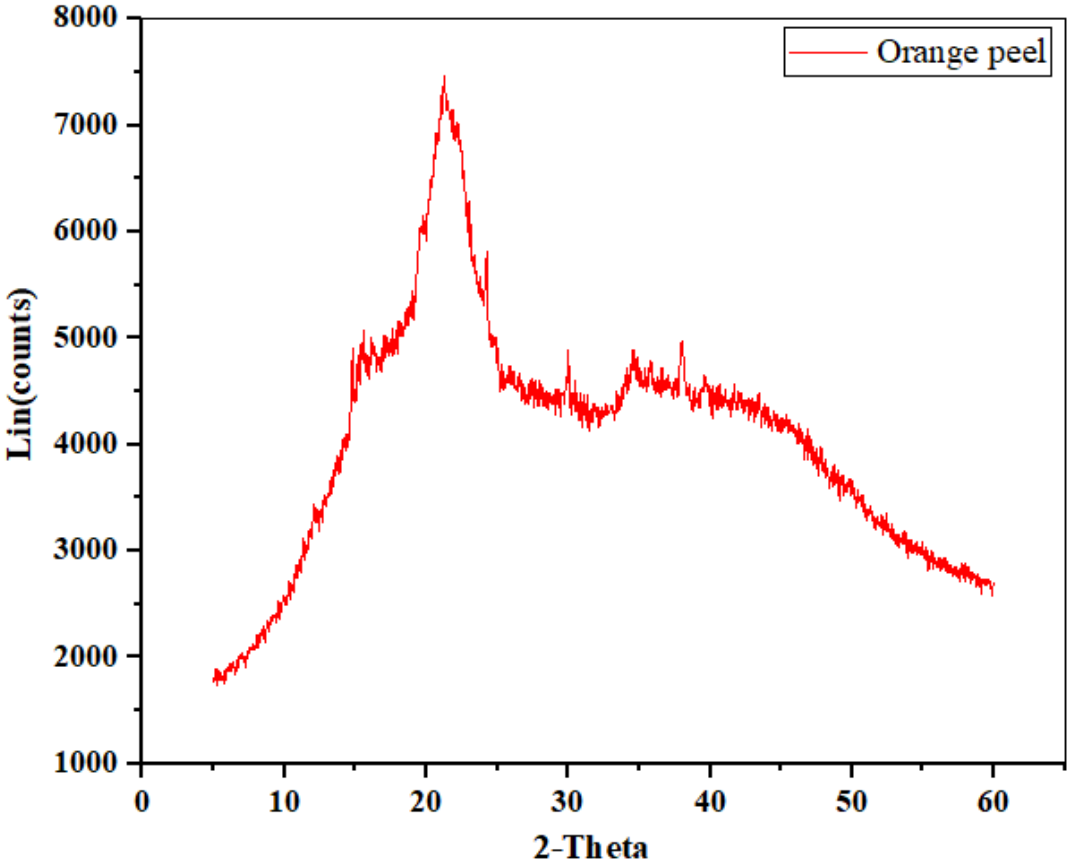

Figure 4.12: XRD analysis of orange peels before adsorption

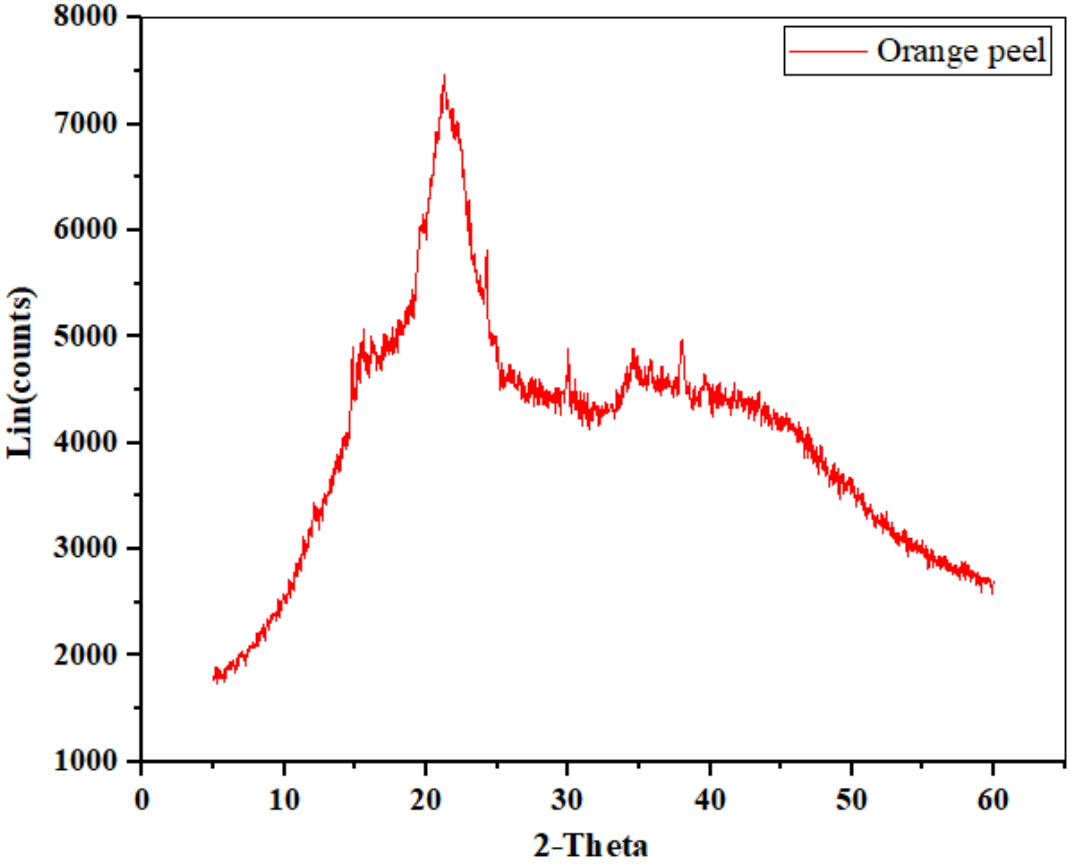

Figure 4.12 represents the diffractogram of orange peels, it reveals broadband between 30^0 and 50^0. The XRD spectra of orange and banana peels as represented in **Figures 4.12** and **4.13** respectively did not show well-defined peaks in any region of the spectra, hence no discrete mineral phase can be noticed. Therefore, the orange and banana peels showed a completely amorphous structure. The adsorption capacity of an adsorbent is affected by the structural arrangement of the adsorbent. The structure of orange and banana peels showed regions that are less ordered which can be observed in the SEM structure of the adsorbents. During adsorption, there is a tendency for an adsorbent that is more amorphous to adsorb better because the aqueous solution has more access to the large surface and the active sites. Amin, Alazba and Shafiq (2017b) reported that the XRD profile of banana peels revealed few peaks that were not excessively sharp suggesting that the structure is amorphous.

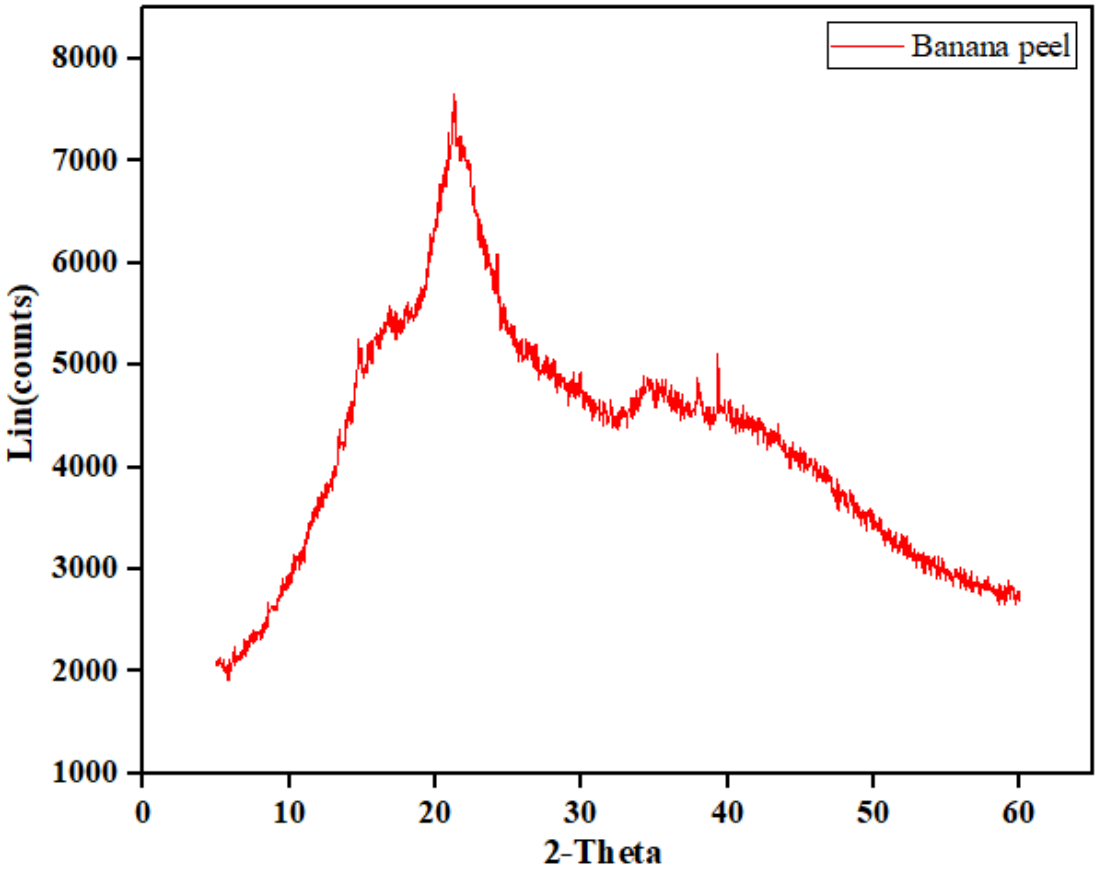

Figure 4.13: XRD analysis of banana peels before adsorption

4.6 BET Surface Area and Porosity

In this section, the surface area, pore size, and pore volume of the adsorbents are discussed. The results for both bio-sorbent are summarized in

Table 4.1 below. The pore structure of an adsorbent affects its behaviour, mechanical properties, and fluid flow.

Table 4.1: Surface properties of orange and banana peels.

Adsorbent Type	Adsorbent size (µm)	Surface Area (m^2/g)	Pore Size (nm)	Pore Volume (m^3/g)
Orange peel	75	9.8471	3.0768	0.01184
	255	6.6383	4.19216	0.00685
	455	3.5685	5.53014	0.00434
Banana peel	75	7.0768	5.41062	0.00059
	255	4.64141	3.42072	0.00045
	455	2.08572	2.94711	0.00039

The surface area is an inherent characteristic of a powdered material which explains the performance and the capacity of an adsorbent in an adsorption study. Both the internal and external surface area of an adsorbent plays an important role in the adsorption process. However, the internal surface area is referred to as the BET surface area and is also related to the pore system of an adsorbent. From

Table 4.1, it can be deduced that the orange peels had a larger surface area and pore size than banana peels across all the particle sizes of the bio-sorbents. Hence, it can be concluded that

orange peels are more porous than banana peels. The surface area of fruit peels is generally low (Pathak, Mandavgane and Kulkarni 2017) Pathak, Mandavgane and Kulkarni (2016) reported that the low surface area of fruit peels as compared to other bio-sorbents could be due to the operational complexity of degassing lignocellulosic samples.

4.7 Summary

The characteristics of orange and banana peels were studied to determine their physical, chemical, structural properties and also to determine their abilities to adsorb cations. The techniques used include; FTIR, SEM-EDS, XRD, and BET which were done before and after adsorption except for BET. The findings are summarized below;

- The FTIR showed the presence of functional groups (carboxyl, hydroxyl, carbonyl, and aminyl) which are responsible for the adsorption of Cu^{2+} and Pb^{2+}. There were significant shifts in the peaks representing the functional groups which suggest their role in the adsorption process.
- The SEM revealed that the surfaces of the bio-sorbents are rough, porous, and irregular before adsorption. However, the surfaces became covered and smooth after adsorption.
- The EDS revealed the presence of Cu^{2+} and Pb^{2+} on the surface of the bio-sorbents after adsorption which confirmed the adsorption of the heavy metals.
- The pHpzc of the bio-sorbents confirmed that they are suitable for cation adsorption.
- The BET and XRD confirmed that the bio-sorbents are porous and amorphous respectively.

CHAPTER 5

5 Batch Study on Interactive Effects of Operating Parameters and Optimization

This chapter explains the results of the interactive effects of operating parameters such as initial metal concentration, adsorbent dosage, pH, and particle size using orange and banana peels. The design of experiments was used to generate the experimental runs based on the range of the parameters. The design of experiments helps to study the interaction of many factors in a process that leads to a reduction in the number of experiments. This technique is completely different from the one-factor-at-a-time method which is also referred to as OFAT. The OFAT experimental design involves the study of one variable at a time while other factors are kept constant. This method has drawbacks such as waste of materials, it consumes time, doesn't give in-depth knowledge of the process, and is costly. Hence, the application of DOE is an efficient way of identifying significant process parameters with fewer experimental runs. Furthermore, DOE helps to determine optimum conditions suitable for the best performance of a process with many operating parameters.

In this chapter, findings from the interactive effect of the operating parameters in a single and binary solute system using orange and banana peels are elaborated. The chapter is divided into two sections; section **5.1** is based on the single solute system while section **5.2** is on the binary systems. The optimization study of the adsorption processes in the single and binary systems is also discussed. However, section **5.1.1** and section **5.1.2** results are not discussed in detail, part of the work presented in this chapter has been published (Afolabi, Musonge and Bakare 2021b; Afolabi, Musonge and Bakare 2021a). The abstract of the published papers is attached in **Appendix A.1** and **A.2** respectively. For the binary system in section **5.2**, the co-existence of the metal ions and effects on the operating parameters are explained. The interactive effects of operating parameters in the binary system were explained using surface plots generated by writing code in MATLAB. The sample of the code is provided in **Appendix A.3**.

5.1 Experimental Plan for Single Solute Adsorption using Design of Experiment (DOE)

The experimental design was done using face-centered CCD adapted from the RSM using four factors at three levels (-1, 0, +1) and six center points or replicate runs for the operating parameters as represented in **Table 3.2**. The Design-Expert version (11.1.0.1) was used to generate the design matrix which gave 30 experimental runs for the single solute system with the interaction of 4 operating parameters stated. The results obtained from the experiment were analyzed to determine the percentage yield and responses of each metal ion. The analysis of variance (ANOVA) was used to ascertain the relationship that exists between the input, responses, and the significance of the regression model. The interactive effects of the operating parameters were represented by 3D surface plots for each response. The experimental steps employed is as shown below in **Figure 5.1**.

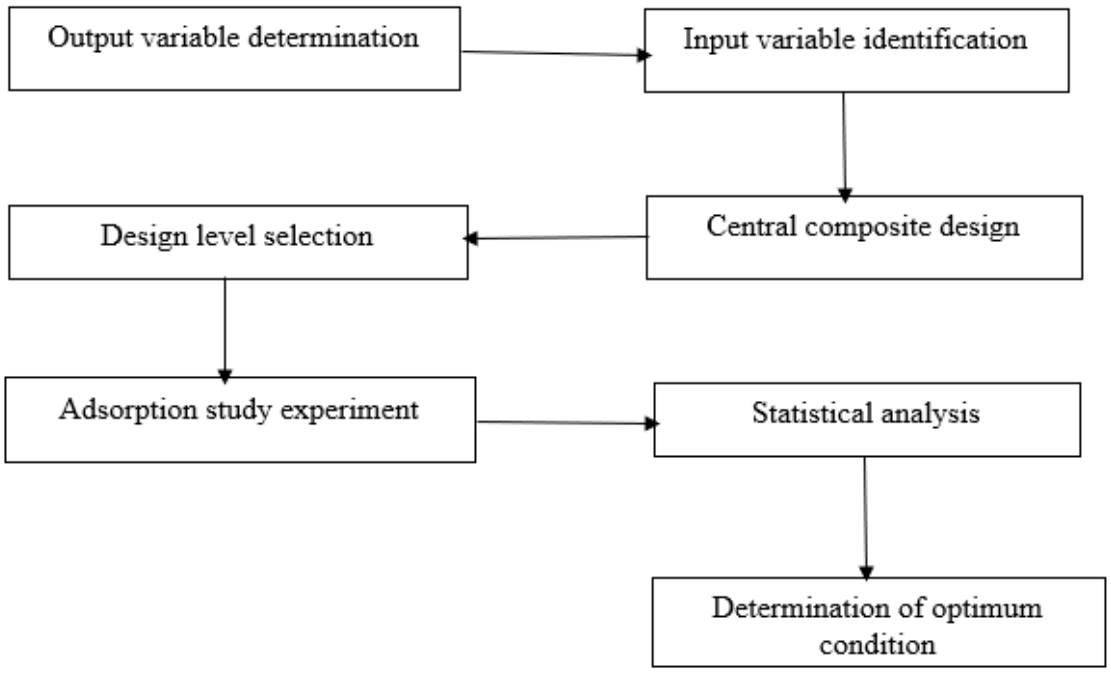

Figure 5.1: Experimental steps

5.1.1 Adsorption of Cu^{2+} and Pb^{2+} onto orange peels using CCD

The factorial experimental setup using 4 independent variables (initial concentration, pH, adsorbent dosage, and particle size) gave a total of 30 experimental runs with the percentage removal of copper and lead as the responses as shown in **Table 5.1**. The experimental matrix comprises 16 factorial points, 8 axial points, and 6 center points. In the case of Cu^{2+} bio-sorption, the main effect variables representing initial concentration, adsorbent dosage, pH, and particle size are significant while the initial concentration, adsorbent dosage, and pH are significant for Pb^{2+} bio-sorption. The regression models for the bio-sorption process are significant which indicates that the second-order polynomial model is in good agreement with the experimental data for the biosorption of Cu^{2+} and Pb^{2+}.

The model fitness was also checked by considering the closeness of the predicted and the experimental values known as the co-efficient of determination R^2 which gave 0.9852 and 0.9433 for the biosorption of Cu^{2+} and Pb^{2+} respectively. The highest percentage removal was achieved at pH 5.5, initial concentration of 100 mg/L, and adsorbent dosage of 1g for Cu^{2+} biosorption while particle size effect was marginal. This result is reasonable with the fact that at low initial concentration, little amount of adsorbent is needed for adsorption hence, adsorbent dosage increased with increasing initial metal ion concentration. Therefore, the initial metal concentration, pH, and adsorbent dosage are the important factors responsible for the biosorption of Cu^{2+} onto orange peels.

In the case of Pb^{2+} biosorption onto orange peels, the pH and adsorbent dosage had a greater influence on the adsorption process while initial concentration and particle size had marginal differences. The optimum conditions obtained for Cu^{2+} and Pb^{2+} gave 88 % and 90 % respectively with the initial concentration of 100 mg/L, pH 5.5 for Cu^{2+} and pH 6 for Pb^{2+}, an adsorbent dosage of 1 g and particle size 75 µm. The response surface diagrams, ANOVA, and the predicted against the actual value plot are shown in **Appendix A.1**. In conclusion, the adsorption mechanism of Cu^{2+} ad Pb^{2+} can be ascribed to the interaction of the operating parameters with the functional groups present on the surface of the bio-sorbent. Hence, ion exchange is the adsorption mechanism responsible for the bio-sorption of the metal ions.

Table 5.1: CCD matrix and responses (actual and predicted) results using orange peels

Std	Run	Initial conc. (mg/L)	pH	Adsorbent dosage (g)	Particle size (µm)	Responses			
						Copper % removal		Lead % removal	
						Exp	Pred	Exp	Pred
13	1	10	2	1	455	90.62	89.29	90.05	56.70
2	2	100	2	0.1	75	33.61	31.95	64.28	64.63
29	3	55	4	0.55	265	83.95	84.03	86.59	64.83
24	4	55	4	0.55	455	89.59	86.65	88.3	66.14
1	5	10	2	0.1	75	69.59	70.83	97.52	70.64
21	6	55	4	0.1	265	63.64	62.47	89.29	74.43
25	7	55	4	0.55	265	82.56	84.03	80.56	77.68
17	8	10	4	0.55	265	95.45	95.21	98.96	78.39
9	9	10	2	0.1	455	70.81	71.87	81.81	82.76
19	10	55	2	0.55	265	78.11	78.12	78.38	82.93
10	11	100	2	0.1	455	39.2	39.12	56.8	84.37
18	12	100	4	0.55	265	69.32	69.49	67.22	85.33
5	13	10	2	1	75	90.16	89.29	94.34	87.01
3	14	10	6	0.1	75	88.85	87.86	94.97	88.10
4	15	100	6	0.1	75	48.39	48.93	64.16	88.10
30	16	55	4	0.55	265	84.14	84.03	89.96	88.10
14	17	100	2	1	455	74.97	76.77	75.87	88.10
7	18	10	6	1	75	98.53	97.82	99.75	88.10
20	19	55	6	0.55	265	91.2	91.13	94.58	88.10
11	20	10	6	0.1	455	90.03	89.41	91.93	88.56
15	21	10	6	1	455	95.85	98.31	99.49	88.74
22	22	55	4	1	265	85.16	86.27	92.42	90.34
8	23	100	6	1	75	79.38	79.12	78.34	94.09
16	24	100	6	1	455	87.77	85.75	83.24	94.18
6	25	100	2	1	75	70.82	70.65	80.75	94.93
12	26	100	6	0.1	455	54.94	56.61	67.15	95.58
28	27	55	4	0.55	265	83.41	84.03	89.42	96.53
26	28	55	4	0.55	265	83.41	84.03	88.51	97.59

27	29	55	4	0.55	265	86.53	84.03	89.2	99.04
23	30	55	4	0.55	75	79.93	82.81	90.5	98.32

5.1.2 Adsorption of Cu^{2+} and Pb^{2+} onto banana peels using CCD

This section explains the investigation carried out using RSM with CCD to study the interaction and relationship that exists between the independent variables (initial concentration, pH, adsorbent dosage, and particle size) and the responses. The CCD matrix of Cu^{2+} and Pb^{2+} onto banana peels and the responses are presented. The adsorbent dosage, pH, and particle size have a great influence on the adsorption process of Cu^{2+}. The coefficient of determination (R^2) which shows the relationship between the actual and predicted values for the bio-sorption efficiency of Cu^{2+} gave 0.9889. The highest experimental result was obtained at the highest concentration of 100 mg/L with a percentage removal of 98 % with a pH range of 4-5.5. The optimum conditions for the biosorption of Cu^{2+} using banana peels gave 92.92% with an initial concentration of 100 mg/L, adsorbent dosage 1g, pH 5, and particle size of 75 µm. The desirability of the condition gave 1.000 which implies the optimum condition is reasonably acceptable.

It can be deduced that there is strong agreement between the predicted and the experimental yield with little difference in the percentage removal. The p-value which measures the significance of the model parameters showed that pH, adsorbent dosage and initial metal ion concentration have a great influence on the adsorption process of Pb^{2+} onto banana peels (Afolabi, Musonge and Bakare 2021b). The result showed that maximum removal of Pb^{2+} was obtained between pH 4-5 with a percentage removal of 99.32 % and the percentage removal increased with increasing pH. In addition, the percentage removal of Pb^{2+} increased with increasing adsorbent dosage and initial concentration. The optimum conditions obtained were; initial concentration 100 mg/L, pH 5, adsorbent dosage 0.55 g, and particle size 75µm with percentage removal of 98.146 % while the desirability gave 1.000. The response surface diagrams, ANOVA, and the predicted versus the actual plot are presented in **Appendix A.2**.

In conclusion, the bio-sorption mechanism of Cu^{2+} and Pb^{2+} onto banana peels revealed that there was an exchange of ions between the copper ions and lead ions in the solution and the ions present on the surface of banana peels.

Table 5.2: CCD matrix and responses (actual and predicted) results using banana peels

Std	Run	Initial Conc. (mg/L)	Adsorbent dosage (g)	pH	Particle size (µm)	Responses			
						Copper % removal		Lead % removal	
						Exp	Pred	Exp	Pred
8	1	100	1	6	75	92.65	91.84	98.59	96.93
28	2	55	0.55	4	250	94.20	93.39	88.28	91.99
18	3	100	0.55	4	250	98.12	97.42	99.32	94.32
30	4	55	0.55	4	250	92.80	93.39	88.30	91.99
5	5	10	0.1	6	75	96.25	96.05	98.98	94.04
11	6	10	1	2	455	85.50	84.06	74.30	70.38
7	7	10	1	6	75	91.71	92.44	85.40	86.60
16	8	100	1	6	455	94.52	94.34	98.96	97.50
13	9	10	0.1	6	455	80.10	78.51	76.80	76.56
14	10	100	0.1	6	455	81.67	82.75	80.24	81.90
19	11	55	0.1	4	250	82.21	83.11	78.01	77.13
20	12	55	1	4	250	94.78	95.01	85.03	89.04
2	13	100	0.1	2	75	59.95	60.43	54.93	54.54
6	14	100	0.1	6	75	86.05	86.46	81.77	85.74
17	15	10	0.55	4	250	95.04	96.87	80.20	88.33
29	16	55	0.55	4	250	92.98	93.39	98.89	91.99
9	17	10	0.1	2	455	63.55	65.17	56.30	57.39
3	18	10	1	2	75	84.51	84.17	76.50	74.02
27	19	55	0.55	4	250	92.96	93.39	98.87	91.99
1	20	10	0.1	2	75	72.38	71.47	64.20	65.44
4	21	100	1	2	75	81.57	82.13	81.56	81.75
15	22	10	1	6	455	80.80	81.10	73.60	73.52
21	23	55	0.55	2	250	81.85	82.71	79.91	81.48
12	24	100	1	2	455	94.91	95.86	87.55	91.76
23	25	55	0.55	4	75	88.30	88.38	88.30	91.18
26	26	55	0.55	4	250	95.01	93.39	88.01	91.99
10	27	100	0.1	2	455	69.75	67.96	61.64	60.13

24	28	55	0.55	4	455	85.41	86.47	87.20	87.44
22	29	55	0.55	6	250	94.41	94.68	97.47	99.03
25	30	55	0.55	4	250	95.78	93.39	98.96	91.99

5.2 Experimental Plan for Binary Solute Adsorption using Design of Experiment (DOE)

The effect of the co-existence of Cu^{2+} and Pb^{2+} was studied using the mixture of the metal ions in a solution. It is important to study the effect of the co-existence of the metal ions because it is very rare for wastewater to contain a single metal ion. Also, for industrial-scale treatment of wastewater, the study of the co-existence of metal ions with the operating parameters is important. This study investigated the application of RSM for the prediction and optimization of the bio-sorption capacity of orange and banana peels for the binary removal of Cu^{2+} and Pb^{2+} ions from wastewater.

5.2.1 Central composite design for the binary solute system

The bio-sorbent and synthetic solution preparation were explained in sections **3.1.1** and **3.1.2** of chapter three respectively. The pH of the solutions was maintained in the range 5.5-6 being the optimized pH value for the single metal system. The design expert software (11.1.0.1) was used to generate the statistical design of the experimental runs. For the binary solute system, three operating parameters were selected for the biosorption of Cu^{2+} and Pb^{2+} ions onto orange and banana peels, namely; initial metal ion concentration, adsorbent dosage, and particle size at specified factor levels (**Table 3.2**). The CCD generated a total of 20 experimental runs with 3 operating parameters using face-centered design. In the optimization study, the second-order polynomial equation was used to explain the interactive effects of the independent variables. The quadratic model used to optimize the process variables is shown below.

$$Y = \beta_o + \sum_{i=1}^{k} \beta_i X_i + \sum_{i=1}^{k} \beta_{ii} X_i^2 + \sum_{i=1} \sum_{j=i+1} \beta_{ij} X_i X_j + \varepsilon \qquad (5.1)$$

where Y is the predicted response, X_i and X_j are the independent variables, β_o, β_i, β_{ii}, and β_{ij} are the regression coefficient and ε is the residual error. The interpretation of the experimental

results and the significant variables are explained using mathematical functions called the analysis of variance (ANOVA).

5.2.2 Adsorption of Cu^{2+} and Pb^{2+} onto orange peels in binary solute using CCD

The experimental design matrix for the biosorption of Cu^{2+} and Pb^{2+} ions onto orange peels is presented in

Table 5.3 with the predicted and experimental responses. The second-order polynomial Equation 5.1 with multiple regression analysis was used to generate the responses (percentage removal of Cu^{2+} and Pb^{2+}) using the three design factors.

Table 5.3: CCD experimental matrix and responses of Pb^{2+} and Cu^{2+} removal onto orange peels.

Std	Run	Initial Conc. (mg/L)	Adsorbent dosage (g)	Particle size (µm)	Responses			
					Lead % removal		Copper % removal	
					Exp	Pred	Exp	Pred
15	1	55	0.55	265	83.75	83.93	72.89	71.48
5	2	10	0.1	455	80.34	80.56	59.1	59.06
2	3	100	0.1	75	62.07	61.95	79.5	78.69
17	4	55	0.55	265	82.86	83.93	70.17	71.48
12	5	55	1	265	90.47	91.18	85.06	86.55
4	6	100	1	75	88.12	88.04	84.72	84.77
6	7	100	0.1	455	70.86	71.13	59.95	60.57
20	8	55	0.55	265	84.15	83.93	73.72	71.48
9	9	10	0.55	265	90.12	88.88	72.82	70.86
3	10	10	1	75	98.85	98.71	86.2	85.60
16	11	55	0.55	265	84.45	83.93	72.1	71.48
1	12	10	0.1	75	77.97	78.86	68.98	70.76
19	13	55	0.55	265	83.21	83.93	69.65	71.48
8	14	100	1	455	84.78	84.03	82.65	80.89
18	15	55	0.55	265	84.05	83.93	70.25	71.48
10	16	100	0.55	265	78.15	78.83	69.29	71.19

14	17	55	0.55	455	81.75	81.75	65.98	66.34
13	18	55	0.55	75	83.45	82.90	74.55	74.13
11	19	55	0.1	265	76.06	74.80	70.53	68.98
7	20	10	1	455	86.95	87.21	87.32	88.14

The quadratic regression model showing the model parameters generated for the responses; percentage removal of Pb (Y_1) and percentage removal of Cu (Y_2) written for coded factors as a function of initial concentration (A), adsorbent dosage (B), and the particle size (C) are represented in Equations 5.2 and 5.3 respectively.

$$Y_1(Pb) = 83.93 - 5.03A + 8.19B - 0.578C + 1.56AB + 1.87AC - 3.3BC - 0.0709A^2 - 0.9409B^2 - 1.61C^2 \quad (5.2)$$

$$Y_2(Cu) = 71.48 + 0.169A + 8.79B - 3.89C - 2.19AB - 1.61AC + 3.56BC - 0.4577A^2 + 6.28B^2 - 1.25C^2 \quad (5.3)$$

The model equations 5.2 and 5.3 comprise three main effects (A, B, C), three interactive effects (AB, AC, BC), and three quadratic effects (A^2, B^2, C^2). The order of the interactive factors to increase the percentage removal of Pb^{2+} is as AC > AB > BC while for percentage removal of Cu^{2+} is BC > AC > AB.

5.2.2.1 Analysis of variance (ANOVA) for the models

The regression models were evaluated using ANOVA to determine the significant factors that fitted well with the models as presented in

Table 5.*4* and **Table 5.5**. The ANOVA helps to identify the factors that had no significant influence on the model and the adsorption process. The models gave a 95 % confidence level, 5 % significance level, and a degree of freedom of 9. All the model features; the sum of squares, F-values (Fisher variation ratio), P-values, adequate precision, and the lack of fit values was acceptable and show the significance of the models. The P-values of less than 0.05 shows that the regression model terms are highly significant. The P-values of the regression models representing percentage removal of Pb^{2+} and Cu^{2+} gave <0.0001 which implies that the

regression model equation fitted well with the experimental data. The lack of fit value greater than 0.05 signifies that the models have one or more terms that have no significant influence on the regression models because of pure error or noise. However, such terms were included in the model to justify the parent terms and the interactive behaviour. In the case of percentage removal of Pb^{2+}, the significant model parameters are initial concertation A, adsorbent dosage B, interactive terms (AB, AC, BC), and quadratic term C^2 while particle size C, quadratic terms (A^2 and B^2) are not significant. The significant model parameters for the percentage removal of Cu^{2+} are adsorbent dosage B and particle size C which have the first-order main effect, interactive terms (AB, AC, BC), and quadratic term B^2 while initial concentration A and quadratic terms (A^2, and C^2) are not significant.

The overall performance of the models was evaluated based on the regression coefficient of determination (R^2), the adjusted R^2, and the predicted R^2. The R^2 helps to ascertain the closeness of the experimental values to the predicted values which range from 0 to 1, where 0 denotes no correlation between the data. The R^2 obtained for the regression models was found to be close to 1, which implies a good fit between the experimental and the predicted data as represented in **Figure 5.2** The predicted R^2 and the adjusted R^2 for the regression models of Pb^{2+} and Cu^{2+} are in reasonable agreement with a difference of less than 0.2, which validates the significance of the models. The R^2 values for the models were found to be 0.9927 and 0.9725 for percentage Pb^{2+} removal and percentage Cu^{2+} removal respectively. The adequate precision of the models, which is a measure of the signal to noise ratio, was desirable for a ratio greater than 4.

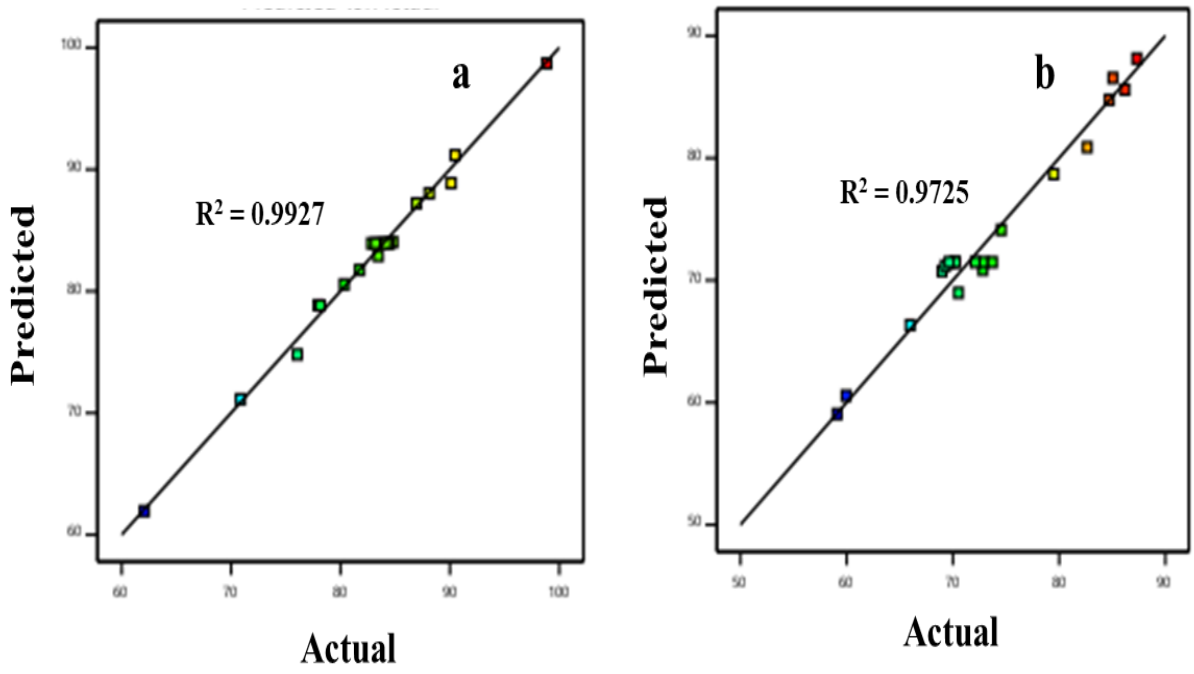

Figure 5.2: Predicted versus actual plots (a) Pb^{2+} and (b) Cu^{2+} removal using orange peels.

Table 5.4: ANOVA for % Pb removal using orange peels

Source	Sum of squares	Df	Mean square	F-value	P-value Prob>F	Comments
Pb Model	1088.25	9	120.92	151.21	< 0.0001	significant
A-Initial concentration	252.51	1	252.51	315.76	< 0.0001	
B-Adsorbent dosage	670.27	1	670.27	838.17	< 0.0001	
C-Particle size	3.34	1	3.34	4.18	0.0682	
AB	19.47	1	19.47	24.35	0.0006	
AC	28.05	1	28.05	35.08	0.0001	
BC	87.12	1	87.12	108.94	< 0.0001	
A^2	0.0138	1	0.0138	0.0173	0.8980	
B^2	2.43	1	2.43	3.04	0.1116	
C^2	7.09	1	7.09	8.87	0.0139	
Residual	8.00	10	0.7997			
Lack of Fit	6.17	5	1.23	3.39	0.1034	not significant
Pure Error	1.82	5	0.3647			
Cor Total	1096.25	19				

Std. Dev.	R^2	Adjusted	Predicted	Adeq.	Mean	C. V. %
0.8942	0.9927	R^2 0.9861	R^2 0.9483	Precision 58.15	82.62	1.08

Table 5.5: ANOVA for % Cu removal using orange peels.

Source	Sum of squares	Df	Mean square	F-value	P-value Prob>F	Comments
Cu Model	1230.20	9	136.69	39.32	< 0.0001	significant
A-Initial concentration	0.2856	1	0.2856	0.0822	0.7802	
B-Adsorbent dosage	772.47	1	772.47	222.22	< 0.0001	
C-Particle size	151.71	1	151.71	43.64	< 0.0001	
AB	38.37	1	38.37	11.04	0.0077	
AC	20.67	1	20.67	5.95	0.0349	
BC	101.39	1	101.39	29.17	0.0003	
A^2	0.5762	1	0.5762	0.1658	0.6925	
B^2	108.53	1	108.53	31.22	0.0002	
C^2	4.28	1	4.28	1.23	0.2931	
Residual	34.76	10	3.48			
Lack of Fit	20.79	5	4.16	1.49	0.3365	not significant
Pure Error	13.97	5	2.79			
Cor Total	1264.96	19				
Std. Dev.	**R^2**	**Adjusted**	**Predicted**	**Adeq.**	**Mean**	**C. V. %**
1.86	**0.9725**	**R^2 0.9478**	**R^2 0.7934**	**Precision 22.06**	**73.77**	**2.53**

5.2.2.2 3D representation of the interactive effects on the responses

The graphical representation of the interactive effects of the model parameters on each of the responses is shown in 3D plots depicted in

Figure 5.3 to **Figure 5.5**. The surface plots were generated by writing code using MATLAB (MATLAB R2019a).

Figure 5.3 shows the interaction between initial concentration and adsorbent dosage with the percentage removal of Pb^{2+} and Cu^{2+} ions. The bio-sorption capacity of Pb^{2+} increased with increasing adsorbent dosage while an increase in the initial concentration had no significant changes on the adsorption capacity. This suggests that the surface of the bio-sorbent has

reached the saturation point. In the case of the percentage removal of Cu^{2+}, the initial concentration and the adsorbent dosage increased with increasing percentage removal. The percentage removal of Pb^{2+} and Cu^{2+} increased with the increasing dosage of orange peels. This result is reasonable because a little amount of bio-sorbent relates to a small active site, since the surface of the bio-sorbent is acidic more active sites must be occupied for proton metal ion competition.

Figure 5.4 shows the interactive effect of initial concentration and particle size on the percentage removal of Pb^{2+} and Cu^{2+}. The highest bio-sorption capacity of Pb^{2+} was obtained at the initial concentration of 10 mg/L, while the particle size had no significant changes on the adsorption process. On the contrary, the percentage removal of Cu^{2+} increased with increasing initial concentration and particle size.

Figure 5.5 depicts the interaction between the adsorbent dosage and the particle size on the percentage removal of Pb^{2+} and Cu^{2+}. The bio-sorption capacity of Pb^{2+} and Cu^{2+} ions increased with increasing adsorbent dosage while the particle size had little effect on the adsorption efficiency of the metal ions. The intersection of the two graphs shows that the maximum percentage removal of Pb^{2+} and Cu^{2+} ions in the binary system was reached with particle size of 75 microns. This result is significant because smaller particle sizes have a larger surface area and enhances adsorption capacity than bigger particle sizes. Furthermore,

Figure 5.3 to

Figure 5.5 showed that the percentage removal of Pb^{2+} was higher than Cu^{2+} with all the interactions which are as a result of higher reactivity of Pb^{2+} than Cu^{2+} (Martín-Lara *et al.* 2016). Hence, Pb^{2+} ions were more adsorbed in the binary system than Cu^{2+} ions, as represented in

Table 5.*3*. In conclusion, adsorbent dosage had the highest influence on the percentage removal of Pb^{2+} and Cu^{2+} ions in the binary system followed by the initial concentration while particle size had little or no significant effect.

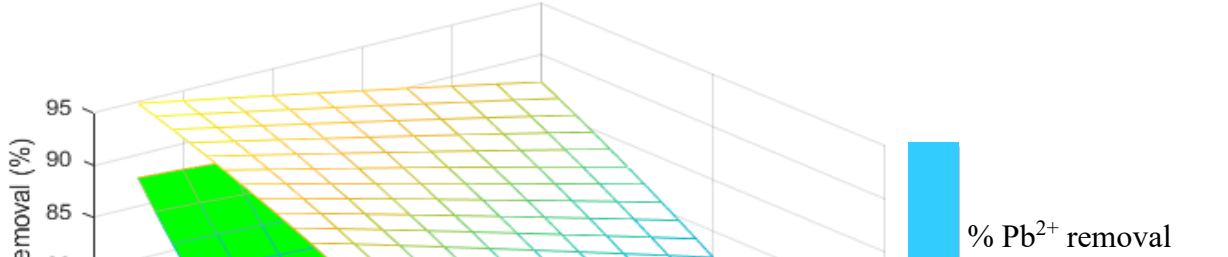

Figure 5.3: Effect of initial concentration and dosage on % Pb^{2+} and % Cu^{2+} removal

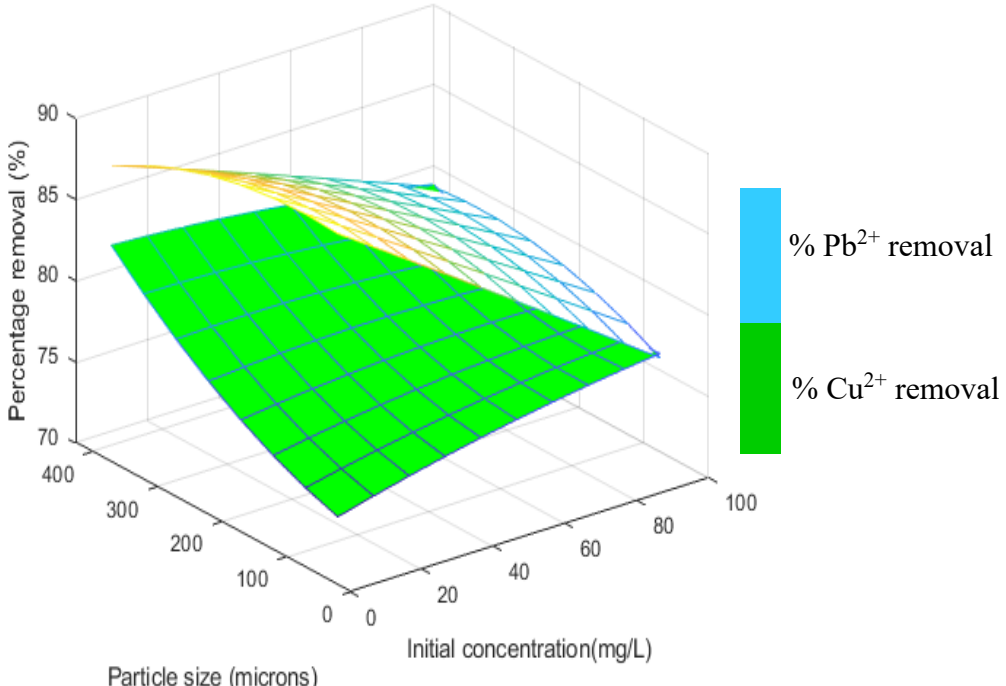

Figure 5.4: Effect of initial concentration and particle size on % Pb^{2+} and Cu^{2+} removal

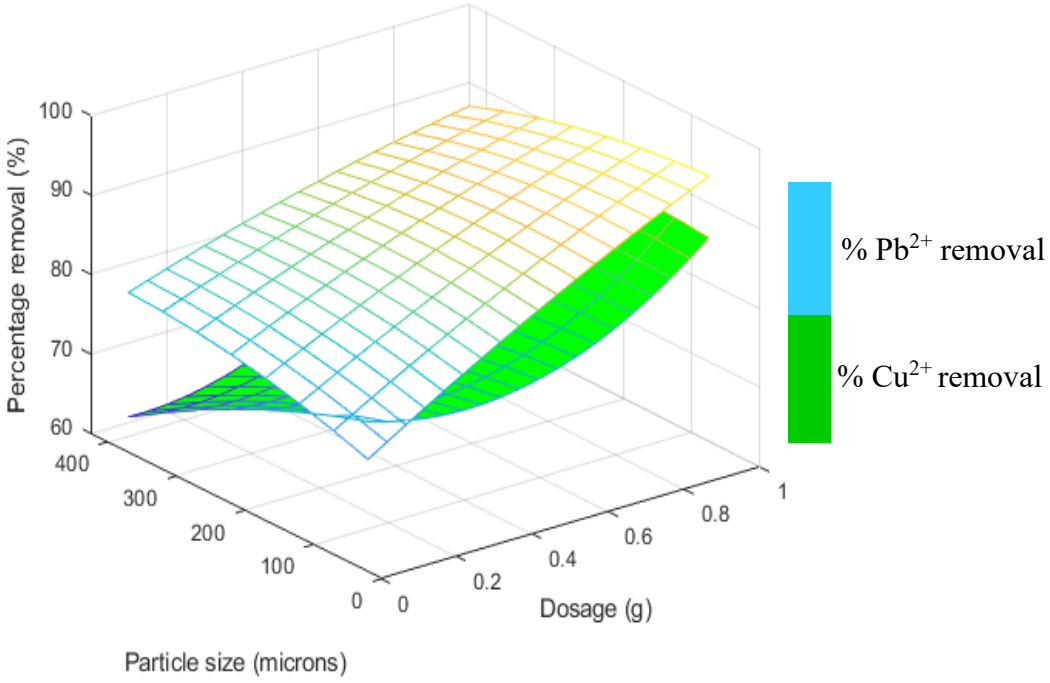

Figure 5.5: Effect of dosage and particle size on the % Pb^{2+} and % Cu^{2+} removal

5.2.2.3 Optimization of parameters for the biosorption of Cu^{2+} and Pb^{2+} ions.

The goal of optimization is to obtain the optimal values for the operating parameters involved in a process. The purpose is to maximize the percentage removal of the metal ions to achieve the highest optimum removal. The desirability of the solution is used to evaluate the suitability of the optimum condition obtained. The optimization will also help to determine the performance and capacity of the adsorbent in the binary solute system. The optimized variable condition for the biosorption of Cu^{2+} and Pb^{2+} ions in the binary system using orange peels gave 92.039 % and 86.77 % removal for Pb^{2+} and Cu^{2+} ions respectively, with an initial concentration of 100 mg/L, an adsorbent dosage of 1 g and particle size of 75 µm. The

desirability of the solution gave 0.895 which signifies that the optimum condition is reasonably acceptable.

5.2.3 Adsorption of Cu^{2+} and Pb^{2+} onto banana peels in binary solute using CCD

The experimental design matrix for the biosorption of Pb^{2+} and Cu^{2+} ions onto banana peels is presented in **Table 5.6** which shows the experimental data simulated together with corresponding predicted responses. The second-order polynomial (Equation 5.1) with multiple regression analysis was used to generate the responses (percentage removal of Pb^{2+} and Cu^{2+}) using the three design factors.

Table 5.6: CCD experimental matrix and responses of Pb^{2+} and Cu^{2+} removal onto banana peels.

Std	Run	Initial Conc. (mg/L)	Adsorbent dosage (g)	Particle size (µm)	Responses			
					Lead % removal		Copper % removal	
					Exp	Pred	Exp	Pred
15	1	55	0.55	265	86.4	86.36	79.62	80.43
5	2	10	0.1	455	85.05	84.57	60.9	60.58
2	3	100	0.1	75	72.04	71.58	80.19	80.46
17	4	55	0.55	265	86.24	86.36	79.6	80.39
12	5	55	1	265	91.2	91.05	82.4	82.35
4	6	100	1	75	92.1	92.48	86.49	86.72
6	7	100	0.1	455	83.89	83.97	81.58	81.58
20	8	55	0.55	265	86.1	86.36	85.26	81.43
9	9	10	0.55	265	87.65	87.61	84.16	85.27
3	10	10	1	75	91.63	91.46	97.6	97.51
16	11	55	0.55	265	86.68	86.36	79.62	80.39
1	12	10	0.1	75	80.64	80.97	76.01	75.67
19	13	55	0.55	265	87.2	86.36	79.59	80.01
8	14	100	1	455	97.85	97.43	87.21	87.47
18	15	55	0.55	265	86.15	86.32	79.61	80.09
10	16	100	0.55	265	87.4	87.82	91.14	90.38
14	17	55	0.55	455	87.9	88.35	75.12	75.54
13	18	55	0.55	75	84.15	84.08	82.79	82.72

11	19	55	0.1	265	78.54	79.07	68.09	68.49
7	20	10	1	455	87.25	87.62	82.41	82.05

The experimental results obtained were analyzed with the second-order polynomial equation which gave the responses (% Pb^{2+} and % Cu^{2+} removal). The Design Expert software gave quadratic model for the responses which were expressed as a function of three main effects; initial concentration (A), adsorbent dosage (B) and particle size (C), together with three quadratic effects (A^2, B^2, C^2) and three interactive effects (AB, AC, BC). The order of the influence of the interactive effect on the yield of Pb^{2+} removal is AB > AC > BC and AC > BC > AB in the case of percentage removal of Cu^{2+}. The quadratic regression model equations for % Pb^{2+} and % Cu^{2+} removal are expressed in terms of coded factors as indicated in Equations 5.4 to 5.5 respectively.

$$Y_1(Pb) = 86.36 + 0.106A0 + 5.99B + 2.14C + 2.6AB + 2.2BC - 1.86BC + 1.35A^2 - 1.3B^2 - 0.1495C^2 \quad (5.4)$$

$$Y_2(Cu) = 80.43 + 2.55A + 6.93B - 3.59C - 3.9AB + 4.05AC - 0.0938BC + 7.39A^2 - 5.01B^2 - 1.3C^2 \quad (5.5)$$

5.2.3.1 Analysis of variance (ANOVA) for the models

The ANOVA was used to determine the significant variables that fitted well with the regression models as presented in **Table 5.7** and **Table 5.8**. The ANOVA helps to identify the relationship between the main, quadratic, and interactive effects and the responses. The models gave a high level of confidence (95 %) with a 5 % significance level and a degree of freedom of 9. The significance of the models was evaluated with the sum of squares, F-values, P-values, adequate precision, and the lack of fit values were all within limits and in reasonable agreement. The P-values of the models gave <0.0001 which shows a good fit between the regression models and the experimental data. In the case of percentage removal of Pb^{2+}, the significant terms with P-values < 0.05 are B, C, AB, AC, BC, $A^{2,}$ and B^2 while A and C^2 are not significant. The lack of fit (LOF) F-value of the model was greater than 0.05 which implies that one or more model terms are not significant. Besides, the significant terms for the percentage removal of Cu^{2+} are A, B, C, AB, AC, A^2, and B^2 while BC, and C^2 are not significant. Also, the LOF F-value of 0.10 implies the Lack of Fit is not significant relative to the pure error.

Furthermore, the overall performance of the models was evaluated based on the coefficient of determination (R^2) together with the values of the adjusted R^2 and the predicted R^2. All the R^2 values of the models were found to be close to 1, which suggests a reasonable agreement between the data presented with a straight line in **Figure 5.6**.

The regression models showed that the predicted R^2 is in reasonable agreement with adjusted R^2 with a difference of less than 0.2. The coefficient of determination R^2 for the percentage removal of Pb^{2+} and Cu^{2+} ions gave 0.995 and 0.9738 respectively.

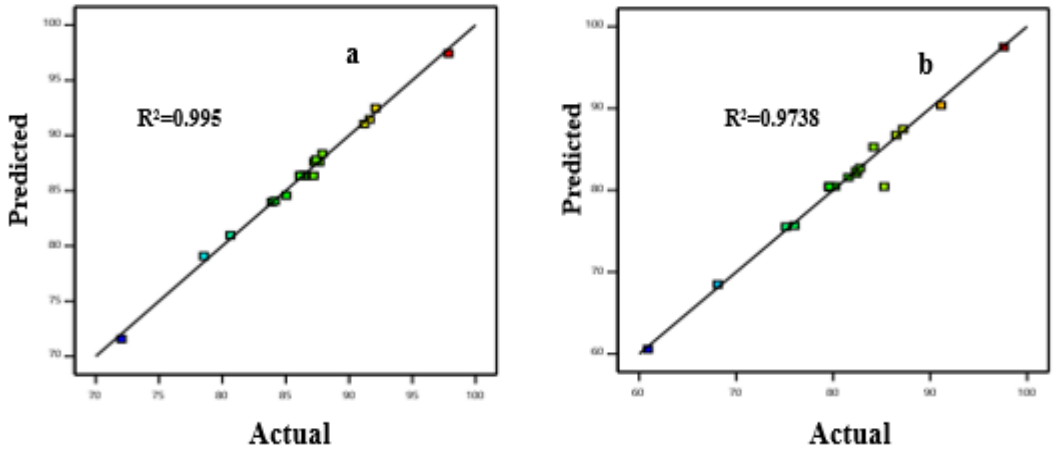

Figure 5.6: Predicted versus actual plots (a) Pb^{2+} and (b) Cu^{2+} removal using banana peels.

Table 5.7: ANOVA for % Pb removal using banana peels

Source	Sum of squares	Df	Mean square	F-value	P-value Prob>F	Comments
Pb Model	531.93	9	59.10	222.70	< 0.0001	significant
A-Initial concentration	0.1124	1	0.1124	0.4234	0.5299	
B-Adsorbent dosage	358.44	1	358.44	1350.59	< 0.0001	
C-Particle size	45.71	1	45.71	172.23	< 0.0001	
AB	54.24	1	54.24	204.36	< 0.0001	
AC	38.59	1	38.59	145.40	< 0.0001	
BC	27.71	1	27.71	104.42	< 0.0001	
A^2	5.02	1	5.02	18.90	0.0015	
B^2	4.68	1	4.68	17.63	0.0018	

C^2	0.0615	1	0.0615	0.2317	0.6406	
Residual	2.65	10	0.2654			
Lack of Fit	1.83	5	0.3660	2.22	0.2009	not significant
Pure Error	0.8241	5	0.1648			
Cor Total	534.58	19				
Std. Dev. 0.515	**R^2 0.9950**	**Adjusted R^2 0.9906**	**Predicted R^2 0.9472**	**Adeq. Precision 70.96**	**Mean 86.31**	**C. V. % 0.596**

Table 5.8: ANOVA for % Cu removal using banana peels

Source	Sum of squares	Df	Mean square	F-value	P-value Prob>F	Comments
Cu Model	1093.77	9	121.53	41.31	< 0.0001	significant
A-Initial concentration	65.18	1	65.18	22.16	0.0008	
B-Adsorbent dosage	480.80	1	480.80	163.45	< 0.0001	
C-Particle size	128.59	1	128.59	43.72	< 0.0001	
AB	121.45	1	121.45	41.29	< 0.0001	
AC	131.30	1	131.30	44.64	< 0.0001	
BC	0.0703	1	0.0703	0.0239	0.8802	
A^2	150.20	1	150.20	51.06	< 0.0001	
B^2	69.15	1	69.15	23.51	0.0007	
C^2	4.68	1	4.68	1.59	0.2358	
Residual	29.42	10	2.94			
Lack of Fit	2.79	5	0.5588	0.1050	0.9864	not significant
Pure Error	26.62	5	5.32			
Cor Total	1123.18	19				
Std. Dev. 1.72	**R^2 0.9738**	**Adjusted R^2 0.9502**	**Predicted R^2 0.9505**	**Adeq. Precision 30.45**	**Mean 80.97**	**C. V. % 2.12**

5.2.3.2 3D representation of the interactive effects on the responses

The 3D graphical representations of the interactive effects of the operating parameters on the responses are presented in **Figure 5.7** to **Figure 5.9**. The plots depict the percentage removal of Pb^{2+} and Cu^{2+} in a binary system with the interaction of the operating parameters. The graphs were obtained with the aid of MATLAB (MATLAB 2019a). **Figure 5.7** represents the

interaction between initial concentration and adsorbent dosage with percentage removal of Pb^{2+} and Cu^{2+} ions. The percentage removal of Pb^{2+} and Cu^{2+} increased with increasing adsorbent dosage. The graph depicting the percentage removal of Cu^{2+} showed a saddle point which implies that the highest bio-sorption capacity lies between the maximum and the minimum points. However, increased initial concentration led to an increase in the removal of Cu^{2+} ions.

Figure 5.8 shows the interactive effects of initial concentration and particle size on the bio-sorption capacity of Pb^{2+} and Cu^{2+}. The percentage removal of Pb^{2+} increased slightly with an increase in initial concentration while no changes occurred with increasing particle size for Pb^{2+} and Cu^{2+} removal. The percentage removal of Cu^{2+} increased significantly with increasing initial concentration. This shows that initial concentration and adsorbent dosage greatly influenced the bio-sorption efficiency of Cu^{2+}.

Figure 5.9 shows the interaction between the adsorbent dosage and the particle size on the bio-sorption efficiency of Pb^{2+} and Cu^{2+}. The percentage removal of Pb^{2+} and Cu^{2+} increased with increasing adsorbent dosage. This result is acceptable because an increase in adsorbent dosage increases the active sites thus enhancing the efficiency of the bio-sorbent. Also, the bio-sorption of Pb^{2+} increased slightly with increasing particle size while particle size had no changes on the biosorption of Cu^{2+}.

In conclusion, the adsorption efficiency of Pb^{2+} and Cu^{2+} in a binary system onto banana peels was greatly influenced by adsorbent dosage then followed by the initial concentration while the particle size had little or no significant impact on the process.

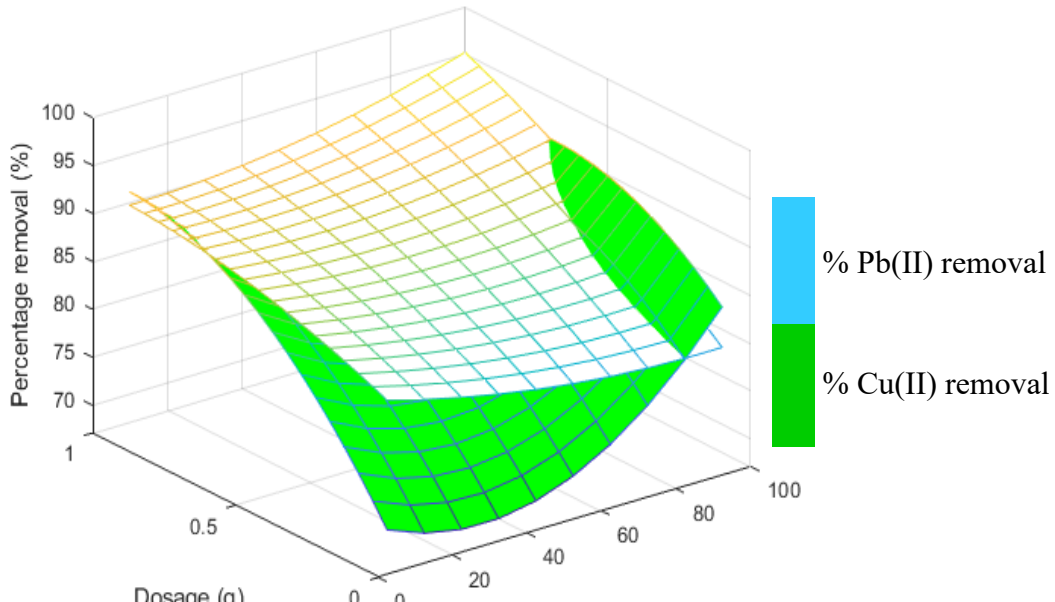

Figure 5.7: Effect of initial concentration and dosage on % Pb^{2+} and % Cu^{2+} removal in a binary system onto banana peels.

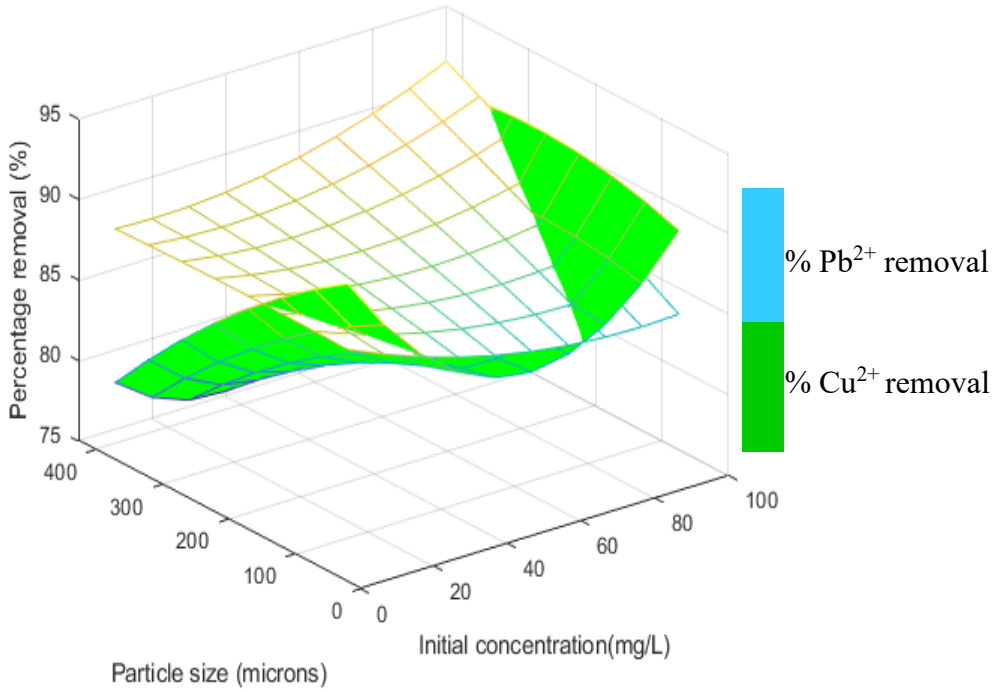

Figure 5.8: Effect of initial concentration and particle size on % Pb^{2+} and % Cu^{2+} removal in a binary system onto banana peels.

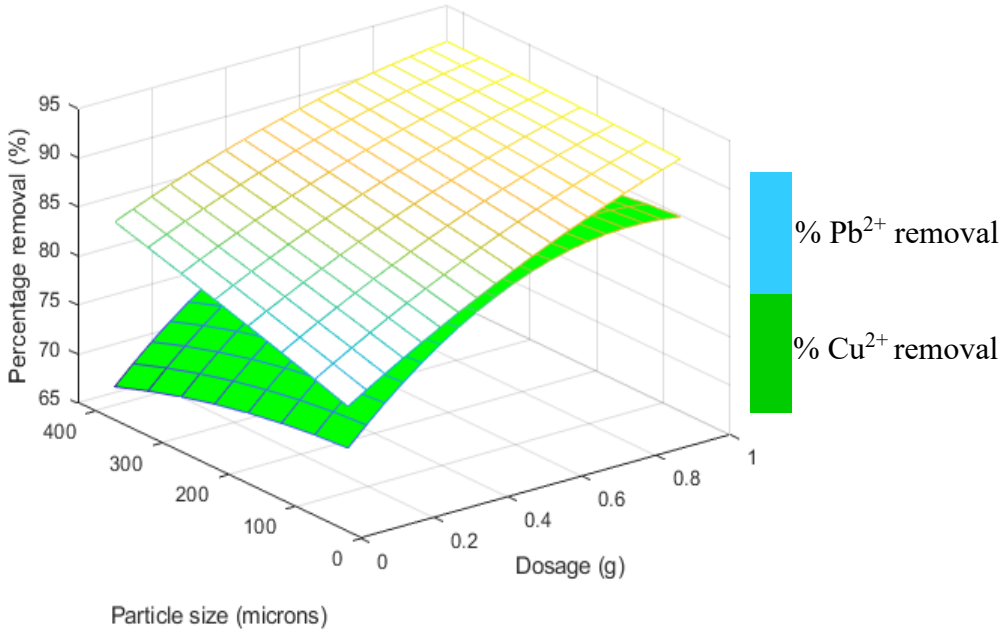

Figure 5.9: Effect of adsorbent dosages and particle size on % Pb^{2+} and % Cu^{2+} removal in a binary system onto banana peels.

5.2.3.3 Optimization of variables for the biosorption of Cu^{2+} and Pb^{2+} ions.

The optimization of operating variables for the biosorption of Pb^{2+} and Cu^{2+} ions using banana peels gave 88.483 % and 84.724 % respectively, with an initial concentration of 100 mg/L, an adsorbent dosage of 1g, and particle size of 75 µm. The desirability of the solution gave 0.890 which is acceptable since it is close to 1.

5.3 Summary

The interactive effect of operating variables was studied in single and binary systems using RSM. For the single solute system, a similar trend was observed in the bio-sorption of Cu^{2+} and Pb^{2+} using orange and banana peels. The adsorption of Pb^{2+} was higher than Cu^{2+} which showed that both bio-sorbents have a higher affinity for Pb^{2+} however, orange peels adsorbed better than banana peels. The adsorption process was greatly influenced by the pH and

adsorbent dosage. The optimum condition gave a pH of 5, initial concentration 100 mg/L, adsorbent dosage 1g, and particle size 75 µm. The percentage removal increased with an increase in adsorbent dosage. The ANOVA showed that the regression model was significant with a low probability (p-value).

The effect of the co-existence of Cu^{2+} and Pb^{2+} ions in solution and the interactive effect with the operating variables showed that Pb^{2+} was more adsorbed than Cu^{2+} for both bio-sorbents. However, orange peels had a higher adsorption rate of 98.85 % than banana peels with an adsorption rate of 97.85 %. The agreement between the experimental and predicted values confirmed the validity of second-order polynomial equations for the biosorption of Cu^{2+} and Pb^{2+} in binary systems using both bio-sorbents.

CHAPTER 6

6 Adsorption Isotherm Modeling of Single and Binary Solute Systems

The isotherm study is carried out to explain the interaction of the solute molecules with the adsorbent active sites during the adsorption process. Equilibrium isotherm is determined to know the capacity of the bio-sorbent for metal ions adsorption. It helps to compare the mathematical and statistical behavior of the adsorption process using experimental data analyzed by Langmuir and Freundlich isotherm which are the well-known isotherm models. The isotherm results were discussed, and the best fit model was determined. This section presents the isotherm studies using orange and banana peels in both single and binary systems. The section is subdivided into two namely, section **6.1** and section **6.2** for single and binary isotherm study using orange and banana peels respectively. Some of the results in this chapter have been published (Afolabi, Musonge P and B.F 2020; Afolabi *et al.* 2021).

6.1 Single and Binary Adsorption using Orange Peels

The experimental methods used are explained in section **3.2**. In this section, the adsorption process experimental data of Cu^{2+} and Pb^{2+} onto orange peels were fitted with Langmuir and Freundlich isotherm models. The linear model Equations 3.11 and 3.14 were used to determine the model parameters for Langmuir and Freundlich isotherm respectively. A very important guide to determining the best isotherm is to fit the experimental data into different isotherm models for estimation and then compare the correlation coefficient (R^2) values obtained (Foo and Hameed 2010). Hence, Langmuir and Freundlich isotherm models were used to analyze the data.

6.1.1 Langmuir isotherm of single and binary systems using orange peels

The Langmuir isotherm model is a semi-empirical model that explains the adsorption mechanism based on the assumption that the surface of the bio-sorbent is energetically homogenous and adsorption energy is uniform for all sites (Hossain *et al.* 2012). The isotherm studies were performed with a fixed amount of bio-sorbent but varying initial concentrations. The quantity adsorbed for both single and binary adsorption systems of Pb^{2+} and Cu^{2+} using orange peels were analyzed using Equation 3.1. The linear isotherm model parameters are presented in **Table 6.1**.

Table 6.1: Langmuir and Freundlich isotherm parameters

Ion	System	Langmuir				Freundlich		
		b (L/mg)	q_m (mg/g)	R^2	R_L	K_f	n	R^2
Cu^{2+}	Single	0.16	31.62	0.972	0.38	5.40	2.11	0.888
Cu^{2+}	Binary	0.15	40.18	0.988	0.4	5.19	1.56	0.934
Pb^{2+}	Single	0.59	59.14	0.985	0.14	20.18	1.34	0.954
Pb^{2+}	Binary	0.77	38.05	0.998	0.02	24.06	4.29	0.898

Figure 6.1 shows the experimental data for the adsorption isotherm of Pb^{2+} under single and binary systems as well as the linear fits for the Langmuir isotherm model. The adsorption of Pb^{2+} in both systems increased with increasing initial metal ion concentrations. As presented in **Table 6.1**, the maximum adsorption capacity of Pb^{2+} with the value 59.14 mg/g in a single system is higher than the binary system with the value 38.05 mg/g suggesting that the presence of Cu^{2+} in the binary system affected the adsorption of Pb^{2+}. The Langmuir isotherm constant "b" is higher for Pb^{2+} (0.59 and 0.77 L/mg) than Cu^{2+} (0.16 and 0.15 L/mg) in the single and binary system respectively, which buttress the fact that Pb^{2+} was more adsorbed than Cu^{2+}. Therefore, Pb^{2+} has a higher affinity for the active sites on the surface of orange peels.

Comparing the correlation coefficient R^2 value for Langmuir and Freundlich isotherm models in both single and binary systems (**Table 6.1**), it is obvious that Langmuir isotherm fitted the experimental data well for both Cu^{2+} and Pb^{2+} with values of R^2 very close to 1.

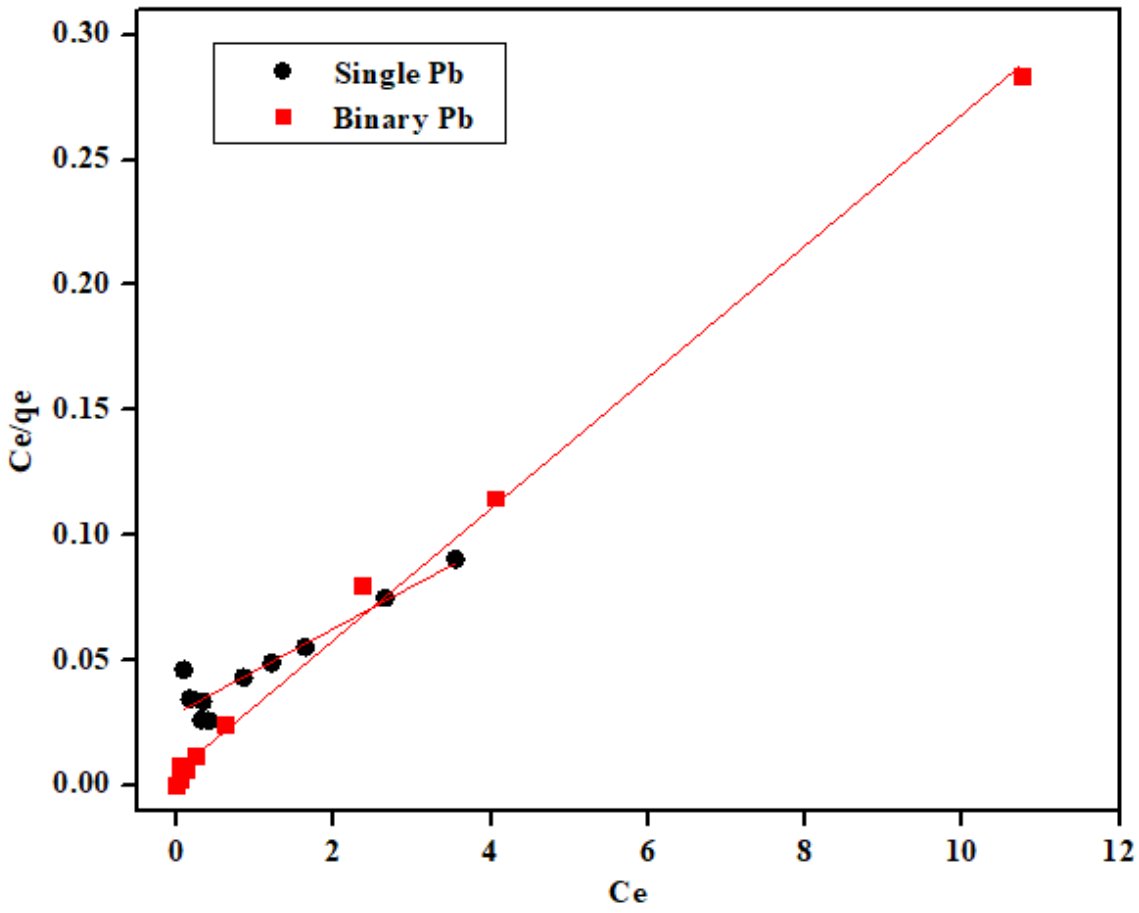

Figure 6.1: Langmuir adsorption isotherm of Pb^{2+} adsorption in both single and binary systems on orange peels (initial concentration 10 – 200 mg/L, adsorbent dose 0.5 g and pH 5)

The linear isotherm plot and experimental data for the adsorption of Cu^{2+} in single and binary systems onto orange peels are presented in **Figure 6.1**. The adsorption of Cu^{2+} increased with increasing initial metal concentration for both systems. As shown in **Table 6.1**, the maximum adsorption capacity of Cu^{2+} in the binary system is higher than the single system and higher than the maximum adsorption capacity of Pb^{2+} in the binary system. This suggests that the presence of Pb^{2+} in the binary system did not affect the adsorption of Cu^{2+}. However, from the experimental data, the quantity adsorbed for Cu^{2+} at the initial concentration of 125 mg/L increased from 19.72 mg/g in a single system to 23.98 mg/g in the binary system. This means at the stated initial concentration, Pb^{2+} has reached equilibrium and there was less competition for the active sites. Therefore, at lower initial concentrations, Cu^{2+} was sensitive to the presence of Pb^{2+} in the binary system.

Furthermore, the coefficient of correlation R^2 value for Langmuir isotherm fitted the experimental data well for single and binary adsorption of Cu^{2+} onto orange peels.

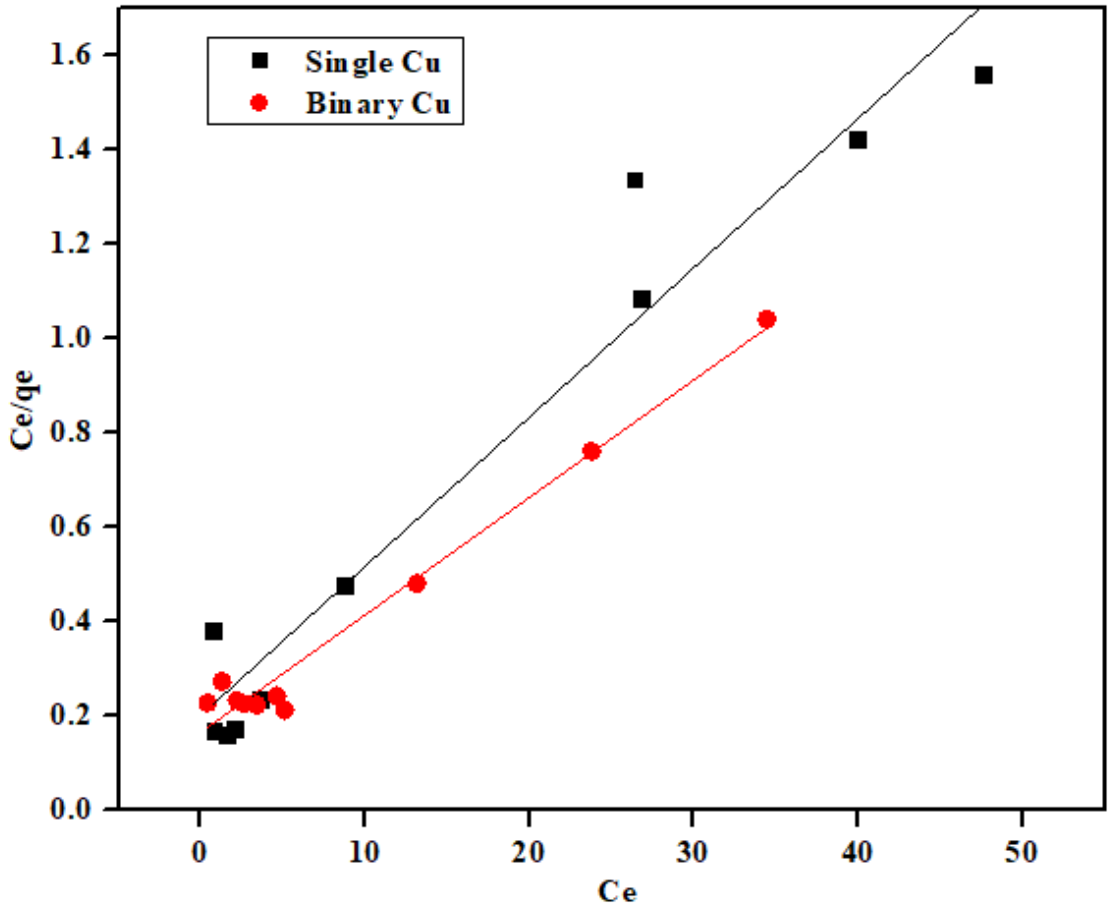

Figure 6.2: Langmuir adsorption isotherm of Cu^{2+} adsorption in both single and binary systems on orange peels. (Initial concentration 10 – 200 mg/L, adsorbent dose 0.5 g and pH 5)

Another important characteristic of the Langmuir isotherm model can be represented by a dimensionless factor R_L, also known as the separation factor. This is used to determine the adsorption behavior of the bio-sorbent as presented in **Table 6.2**. The separation factor, R_L for the adsorption of Pb^{2+} and Cu^{2+} in both single and binary systems onto orange peels falls within the range of $0<R_L<1$, which implies that the adsorption process is favorable within the concentration range studied. Hence, the orange peel is efficient for the adsorption of Pb^{2+} and Cu^{2+} ions from aqueous solutions.

Table 6.2: The separation factor R_L for an adsorption process.

Parameters	Adsorption behaviour
$R_L > 1$	Unfavourable
$R_L = 1$	Linear
$0 < R_L < 1$	Favourable
$R_L = 0$	Irreversible

6.1.2 Freundlich isotherm of single and binary systems using orange peels

The Freundlich isotherm assumes the surface of an adsorbent is heterogeneous and adsorption energy is exponentially distributed (Hossain *et al.* 2014).

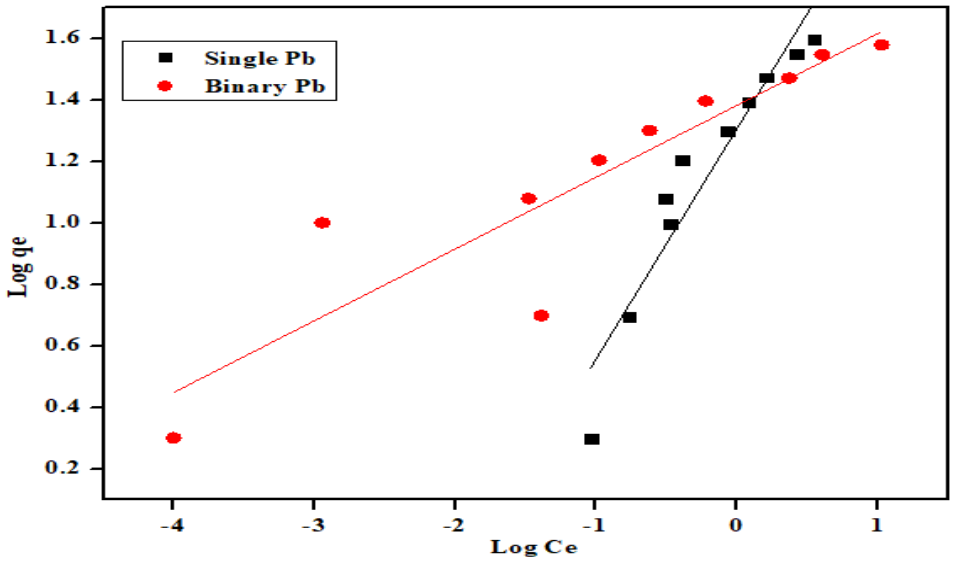

Figure 6.3: Freundlich adsorption isotherm of Pb^{2+} adsorption in both single and binary systems on orange peels (Initial concentration 10 – 200 mg/L, adsorbent dose 0.5 g and pH 5)

Figure 6.3 and **Figure 6.4** represent the plots of the experimental data and the linear fit for Pb^{2+} and Cu^{2+} respectively in both single and binary systems. Freundlich isotherm Equation 3.14 was used, and the equation parameters are presented in **Table 6.2**. The parameters K_F and n are the Freundlich isotherm constants describing the adsorption capacity and intensity, respectively.

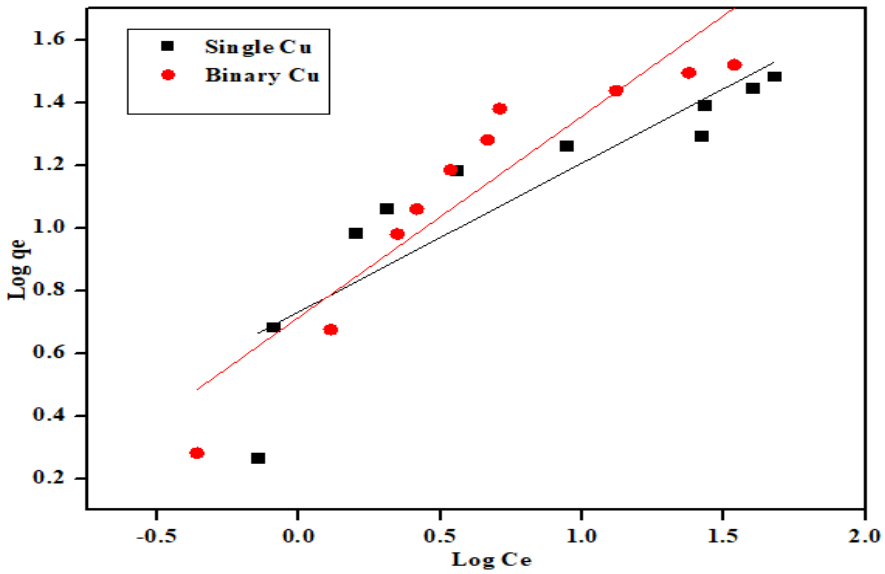

Figure 6.4: Freundlich adsorption isotherm of Cu^{2+} adsorption in both single and binary systems on orange peels. (initial concentration 10 – 200 mg/L, adsorbent dose 0.5 g and pH 5)

The measure of the exponent 'n' explains the adsorbent – sorbent phenomenon capacity and favorability (Dada *et al.* 2012). **Table 6.3** shows the values of n and the interpretation. The Freundlich isotherm constant "n" which evaluates the adsorption intensity of the metal ions was determined to be greater than 1 and in the range $1 < n < 10$ for Pb^{2+} and Cu^{2+} in both single and binary systems. This shows that the adsorption process is favorable. Furthermore, the values of 1/n for Pb^{2+} and Cu^{2+} in both single and binary systems; single Cu (0.47), binary Cu (0.64), single Pb (0.75), and binary Pb (0.23) are less than 1 suggesting that the systems are favorable and highly chemisorption. This implies there exist great bonds between the adsorbent and the adsorbate because of the chemisorption reactions.

Table 6.3: The Freundlich isotherm constant n for an adsorption process

Parameters	Type of system
$n > 1$	Favourable
$1 < n < 10$	Favourable
$1/n < 1$	Highly chemisorption
$1/n \sim 1$	Heterogenous
$1/n > 1$	Cooperative adsorption

6.2 Single and binary adsorption using banana peels

The experimental methods used in this section is the same as in section 3.2. The adsorption experimental data of Pb^{2+} and Cu^{2+} onto banana peels in both single and binary systems were fitted with Langmuir and Freundlich isotherm models.

6.2.1 Langmuir isotherm of single and binary systems using banana peels

Table 6.4: Isotherm parameters for the sorption of Pb^{2+} and Cu^{2+} from single and binary systems solution using banana peels

	Adsorbate system	q_{max} (mg/g)	R_L	b(L/mg)	R^2
Langmuir	Single Pb^{2+}	66.67	0.29	0.24	0.984
	Binary Pb^{2+}	37.69	0.01	7.87	0.999
	Single Cu^{2+}	28.56	0.37	0.17	0.979
	Binary Cu^{2+}	26.89	0.18	0.45	0.999
	Adsorbate	1/n	N	K_f	R^2
Freundlich	Single Pb^{2+}	0.90	1.11	12.27	0.981
	Binary Pb^{2+}	0.14	7.22	23.82	0.791
	Single Cu^{2+}	0.45	2.21	5.09	0.907
	Binary Cu^{2+}	0.40	2.51	7.12	0.930

Table 6.4 presents the model parameters obtained for the Langmuir and Freundlich isotherm for the adsorption of Pb^{2+} and Cu^{2+} in single and binary systems onto banana peels. A similar trend was observed in the adsorption behavior of orange peels with that of banana peels. The quantity adsorbed increased with increasing initial concentration. The maximum adsorption capacity of the single metal solutions was higher than the binary metal systems. However, the maximum adsorption capacity of Pb^{2+} and Cu^{2+} in both single and binary systems onto orange peels was higher than banana peels. The maximum adsorption capacity followed the order: single Pb^{2+} > binary Pb^{2+} > single Cu^{2+} > binary Cu^{2+} with values 66.67, 37.69, 28.56, and 26.89 mg/g respectively.

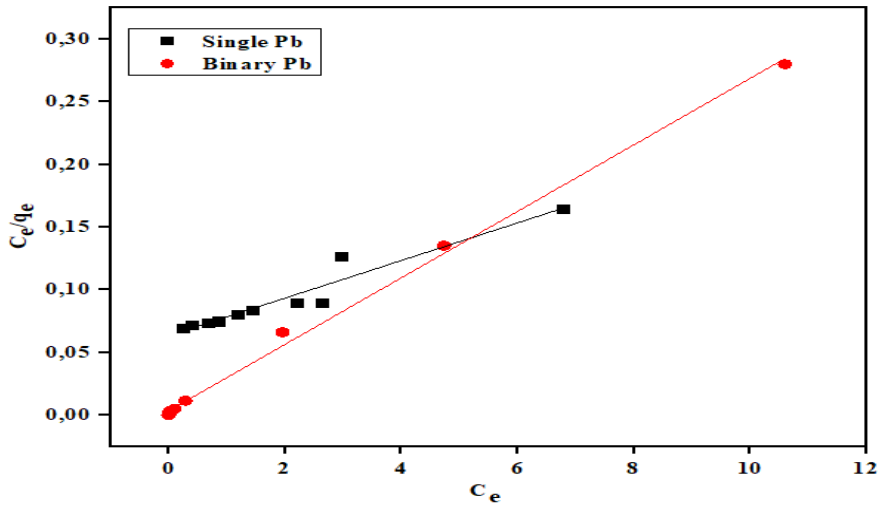

Figure 6.5: Langmuir adsorption isotherm of Pb^{2+} adsorption in both single and binary systems on banana peels. (initial concentration 10 – 200 mg/L, adsorbent dose 0.5 g and pH 5).

Figure 6.5 shows the experimental data and Langmuir linear fit for Pb^{2+} in a single and binary system onto banana peels. The maximum adsorption capacity of the single Pb^{2+} system with the value 66.67 mg/g is higher than binary Pb^{2+} with the value 37.69 mg/g which suggests that the co-existence of the two metals reduced the adsorption of Pb^{2+} in the binary system. The values of 'b' for Pb^{2+} (0.24, 7.89 L/mg for single and binary system respectively) were higher than Cu^{2+} (0.17, 0.45 L/mg for single and binary system respectively) which suggests that Pb^{2+} has a higher affinity for the active sites on the surface of banana peels.

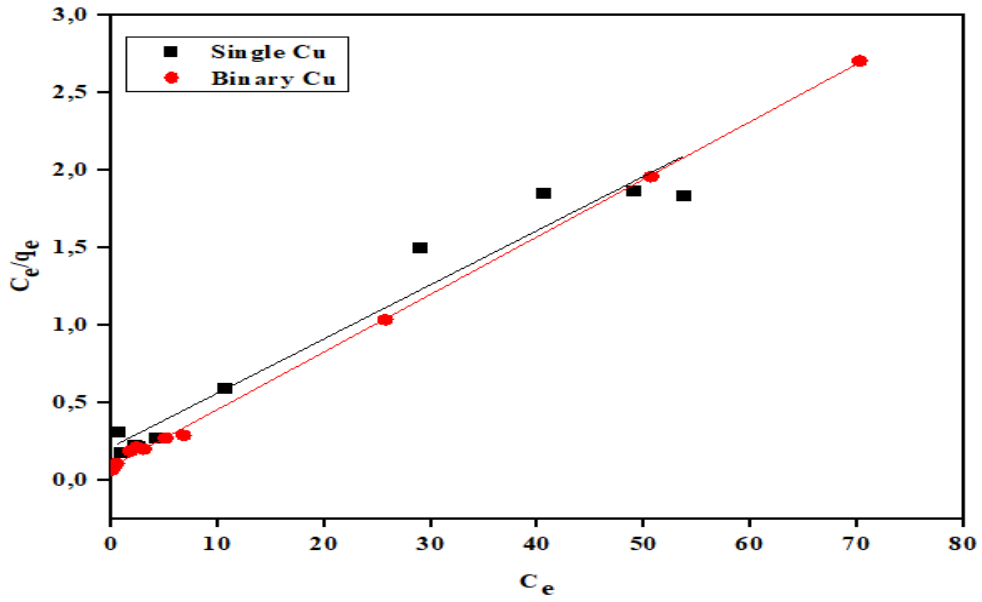

Figure 6.6: Langmuir adsorption isotherm of Cu^{2+} adsorption in both single and binary systems on banana peels. .(initial concentration 10 – 200 mg/L, adsorbent dose 0.5 g and pH 5)

The linear isotherm plot and experimental data for the adsorption of Cu^{2+} in single and binary systems onto banana peels are presented in **Figure 6.6**. The maximum adsorption capacity of single Cu^{2+} was higher than binary Cu^{2+} which implies that the co-existence of the two metal ions in solution reduced the adsorption capacity. The correlation coefficients obtained for Langmuir isotherm were higher in all cases compared to the Freundlich isotherm. The R^2 values for the Langmuir isotherm were: 0.984, 0.999, 0.979 and 0.999 for single Pb^{2+}, binary Pb^{2+}, single Cu^{2+} and binary Cu^{2+} respectively. The corresponding R^2 values obtained for the Freundlich isotherm in all the cases were: 0.981, 0.791, 0.907, and 0.930 for single Pb^{2+}, binary Pb^{2+}, single $Cu^{2+,}$ and binary Cu^{2+} respectively. Based on the values of R^2 obtained, it was concluded that the experimental data fitted the Langmuir isotherm for all the adsorbate systems.

The dimensionless factor R_L which measures the efficiency of the adsorption process and explains the performance of the sorbent-sorbate system was observed to be less than 1 for the adsorbate systems

Table 6.*4*. This shows that the adsorption process is favorable.

6.2.2 Freundlich isotherm of single and binary systems using banana peels

Figure 6.7 and **Figure 6.8** represent the experimental and Freundlich linear fit for Pb^{2+} and Cu^{2+} in both single and binary systems respectively. The Freundlich isotherm is used to explain the adsorption mechanism on a heterogenous surface. Again, just as in the case of Langmuir isotherm, K_F is an isotherm constant which explains the adsorption capacity for the Freundlich model; while 'n' is the adsorption intensity for the Freundlich model. As illustrated in **Table 6.3**, adsorption generally occurs readily when the value of n is between 1 and 10. Therefore, from

Table 6.4, it was evaluated that the values of n were below 10 thus suggesting favorable adsorption. In addition, the values of 1/n for Pb^{2+} and Cu^{2+} in both single and binary systems; single Pb (0.90), binary Pb (0.14), single Cu (0.45), and binary Cu (0.40) again are less than 1 suggesting that the systems are favorable and highly chemisorption for the adsorption onto banana peels. This implies the existence of strong bonds between the adsorbent and the adsorbate because of the chemisorption reactions.

There are variations in the adsorption capacities obtained for both adsorbents in this study as compared with other studies. This could be because of variations in the range of the operating parameters such as the adsorbent dosage, initial metal ion concentration, and pH differing from other studies. Hence, instead of the above-mentioned factors, different adsorption capacities have been reported. However, the results obtained in this study followed the general trend reported for fruit peels bio-sorbent (Pathak Pranav, Mandavgane Sachin and Kulkarni Bhaskar 2015; Obike *et al.* 2018).

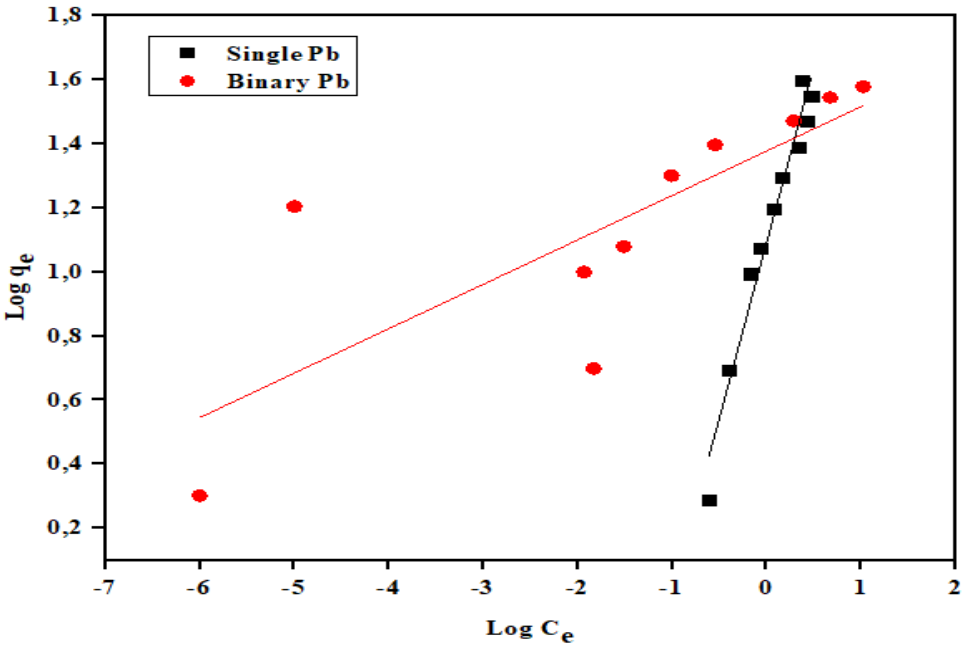

Figure 6.7: Freundlich adsorption isotherm of Pb^{2+} adsorption in both single and binary systems on banana peels. (Initial concentration 10 – 200 mg/L, adsorbent dose 0.5 g and pH 5)

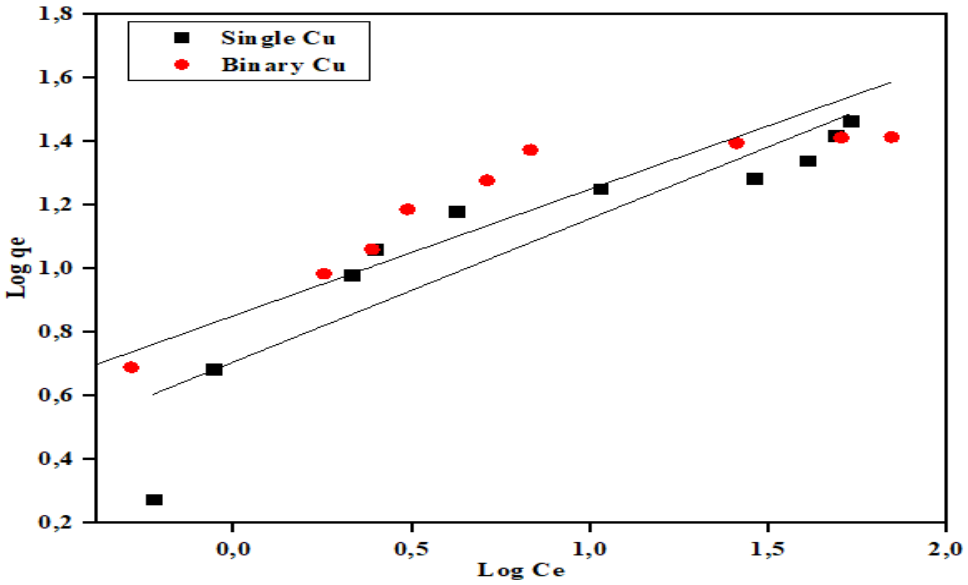

Figure 6.8: Freundlich adsorption isotherm of Cu^{2+} adsorption in both single and binary systems on banana peels. (Initial concentration 10 – 200 mg/L, adsorbent dose 0.5 g and pH 5)

6.3 Statistical Validation

This section explained the mathematical and statistical validation of the results obtained using the isotherm models and compared the errors to determine the best performing or best fit model based on the experimental information. Three different error functions were investigated in this study. The error functions studied are summarized in **Table 6.5** below. The error function that has the lowest error distribution between the experimental and predicted values was chosen as the best fit while selecting the highest value for the coefficient of determination.

Table 6.5: Statistical error functions used to determine the best fit isotherm model

Error function	Abbreviation	Equation
Mean Absolute Error	MAE	$MAE = \frac{1}{n}\sum_{i=1}^{n}\left\|q_{e,exp} - q_{e,pred}\right\|$
Root Mean Square Error	RMSE	$RMSE = \sqrt{\frac{1}{n}\sum_{i=1}^{n}\left(q_{e,exp} - q_{e,pred}\right)^2}$
Coefficient of determination	R^2	$R^2 = \frac{\sum\left(q_{e,exp} - q_{e,pred}\right)^2}{\sum\left(q_{e,exp} - q_{e,pred}\right)^2 + \left(q_{e,exp} - q_{e,pred}\right)^2}$

Where n is the number of experimental data points, $q_{e,exp}$ (mg/g) is the experimental adsorption capacity at equilibrium and $q_{e,pred}$ (mg/g) is the predicted or theoretical adsorption capacity at equilibrium.

The values of the statistical error analysis for orange and banana peels are shown in **Table 6.6** and **Table 6.7** respectively. The values represented in **Table 6.6** and **Table 6.7** show that the Langmuir isotherm model has lower error values as compared with the Freundlich isotherm model and therefore statistically suitable for describing the biosorption of Pb^{2+} and Cu^{2+} in a single and binary system onto both orange and banana peels respectively. The higher R^2 values and lower MAE and RMSE values were obtained for Langmuir isotherm equilibrium data modelling. Langmuir isotherm model is a commonly used model which gives the best fit as

reported by many researchers and explains the adsorption capacity and thermodynamic energy (Dada *et al.* 2017).

Table 6.6: The values of the error functions comparing isotherm models using orange peels.

Isotherm Model	Adsorbate systems	Error function		
		MAE	**RMSE**	**R^2**
Langmuir	Single Pb	1.092	1.712	0.985
	Binary Pb	2.371	3.471	0.998
	Single Cu	2.370	2.917	0.972
	Binary Cu	1.526	2.386	0.988
Freundlich	Single Pb	3.476	5.025	0.954
	Binary Pb	3.732	4.326	0.898
	Single Cu	3.129	3.532	0.888
	Binary Cu	4.930	7.042	0.934

Table 6.7: The values of the error functions comparing isotherm models using banana peels.

Isotherm Model	Adsorbate systems	Error function		
		MAE	**RMSE**	**R^2**
Langmuir	Single Pb	2.939	3.922	0.984
	Binary Pb	4.329	5.160	0.999
	Single Cu	2.241	2.609	0.979
	Binary Cu	0.971	1.546	0.999
Freundlich	Single Pb	3.045	4.176	0.981
	Binary Pb	4.798	6.154	0.791
	Single Cu	3.117	3.494	0.907
	Binary Cu	4.371	5.926	0.930

6.4 Summary

From the studies conducted, it can be concluded that orange peels performed better as an adsorbent in the adsorption of Pb^{2+} and Cu^{2+} in both single and binary systems than banana peels. The Langmuir and Freundlich isotherm models gave the following insights into the adsorption mechanism onto orange and banana peels.

- Pb^{2+} was more adsorbed than Cu^{2+} in both systems and bio-sorbents. For orange peels, Pb^{2+} quantity adsorbed gave 59.14 and 38.05 mg/g, Cu^{2+} quantity adsorbed gave 31.62

and 40.18 mg/g for single and binary systems respectively. For banana peels, Pb^{2+} quantity adsorbed gave 66.67 and 37.69 mg/g, Cu^{2+} gave 28.56 and 26.89 mg/g respectively for single and binary systems. This suggests that Pb^{2+} has more affinity for the active sites on the bio-sorbent surface.

- The adsorption of Pb^{2+} and Cu^{2+} in both single and binary systems for the two bio-sorbents followed the Langmuir isotherm with higher coefficients of correlation.
- The Langmuir isotherm suggests that adsorption occurred on the monolayer.
- The statistical error analysis showed that Langmuir isotherm model fitted the experimental data for both bio-sorbents.
- Based on the results obtained in this study, orange peels were chosen for the column study to investigate the applicability and performance of industrial wastewater treatment.

CHAPTER 7

7 Adsorption Kinetic Study in Single and Binary Solute Systems

The kinetic study is conducted to determine the rate of the adsorption process. It investigates the rate of change of an adsorption process with time. It is highly essential to determine the rate of adsorption of copper and lead onto orange and banana peels as it helps in the design of a fixed-bed column. For industrial scale, the reaction efficiency is a function of the rate of adsorption and the sorption capacity. The fixed-bed column design parameter, the shape of the breakthrough curve, and the breakthrough time are functions of the rate of adsorption (Afroze and Sen 2018). Therefore, for process design and the control of the adsorption phenomenon, it is important to determine the adsorption kinetics and the mechanism of adsorption.

Kinetic studies provide extensive information on the adsorbate capacity uptake rate and the rate-controlling steps such as intraparticle mass transfer, external mass transfer, the diffusivity of solute, and adsorptive reactions which helps with the selection of the best process conditions for the full-scale process operation. The pseudo-first and pseudo-second-order models are used to study the sorption mechanism and to determine the rate-controlling steps in this study. These two models are the most used to determine adsorption mechanisms in adsorption studies. Some of the results discussed in this chapter have been published (Afolabi *et al.* 2021).

7.1 Adsorption Kinetic Modelling of Pb^{2+} and Cu^{2+} onto Orange Peels.

In this section, the kinetic study of Pb^{2+} and Cu^{2+} onto orange peels in single and binary systems with the effect of time at different initial concentrations (10, 55, and 100 mg/L) were investigated using the pseudo-first and pseudo-second-order model. The linearized form of the models as stated in Equations 3.5 and 3.8 respectively.

7.1.1 Pseudo-first-order model

The calculated constant parameters obtained from the pseudo-first-order linear model using orange peels are presented in **Table 7.1**. The effect of time on different initial concentrations was studied in a single and binary system containing Cu^{2+} and Pb^{2+}. **Figures 7.1** and **7.2** represent the plot of $\log(q_e - q_t)$ against t for the single and binary systems of Cu^{2+} and Pb^{2+} using orange peels. From **Table 7.1**, the pseudo-first-order constant K_1 is higher for the binary system than the single system for both Cu^{2+} and Pb^{2+}. The correlation coefficient (R^2) for the single solute Cu^{2+} and Pb^{2+} pseudo-first-order model was in the range 0.903 to 0.986 while the binary system was in the range 0.762 to 0.958.

Table 7.1: Pseudo-first-order model parameters for the adsorption of Cu^{2+} and Pb^{2+} using orange peels.

Metal ion concentration		Cu			Pb		
		10 mg/L	55 mg/L	100 mg/L	10 mg/L	55 mg/L	100 mg/L
Pseudo-first order	Single						
q_e		0.34	2.20	2.16	0.34	1.07	1.28
K_1		0.06	3.31	2.81	7.46	3.70	1.13
R^2		0.905	0.903	0.913	0.957	0.941	0.986
Pseudo-first order	Binary						
q_e		6.83E6	465.27	2087.37	0.05	14.72	2.18
K_1		48.96	6.96	10.59	8.83	11.06	0.33
R^2		0.958	0.762	0.897	0.970	0.891	0.924

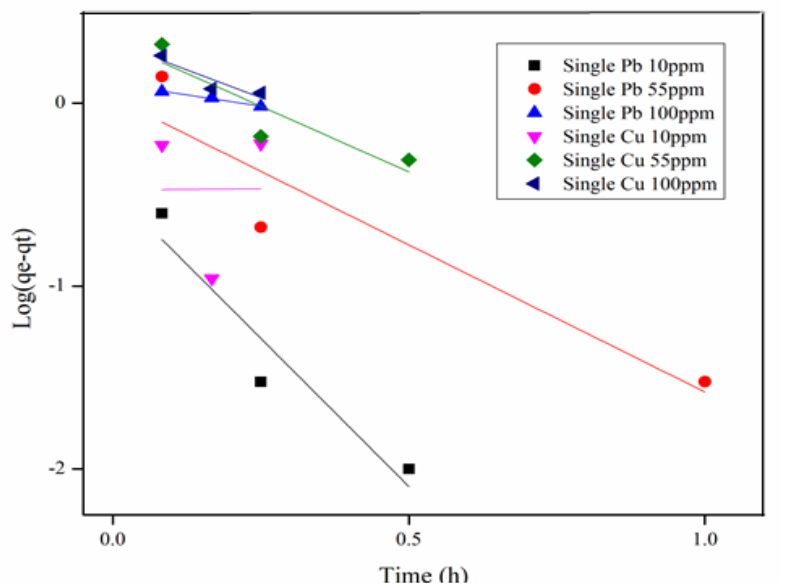

Figure 7.1: Pseudo-first-order kinetic model graph of single Cu^{2+} and Pb^{2+} at different initial concentrations. (Initial concentration 10 – 100 mg/L, adsorbent dose 1 g and pH 5)

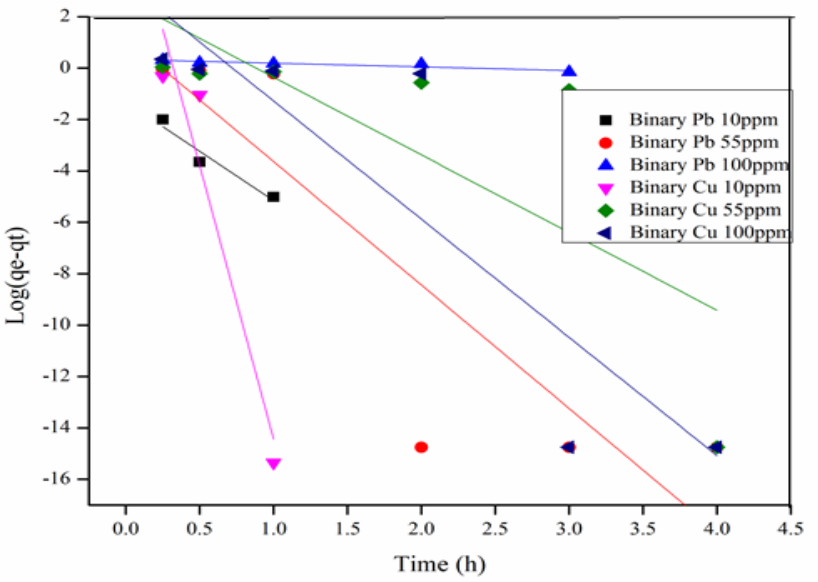

Figure 7.2: Pseudo-first-order kinetic model graph of binary Cu^{2+} and Pb^{2+} at different initial concentrations. (Initial concentration 10 – 100 mg/L, adsorbent dose 1 g and pH 5)

7.1.2 Pseudo-second-order model

The pseudo-second-order model parameters are represented in **Table 7.2**. The quantity adsorbed for Cu^{2+} and Pb^{2+} in a single system at the different initial concentrations is higher

than the quantity adsorbed in the binary system. However, the quantity of Pb^{2+} adsorbed in both single and binary systems is higher than Cu^{2+} for all the initial concentrations. The pseudo-second-order constant K_2 value for Pb^{2+} under the binary system was higher than Cu^{2+} signifying adsorption of Cu^{2+} is negatively affected in the coexistence of Pb^{2+}. The correlation coefficient for the pseudo-second-order was observed to be very close to 1 for Cu^{2+} and Pb^{2+} in both systems at the different initial concentrations, which suggests that the adsorption rate is chemically controlled.

Table 7.2: The pseudo-second-order model parameters for the adsorption of Cu^{2+} and Pb^{2+} using orange peels.

Metal ion concentration		Cu			Pb		
		10 mg/L	55 mg/L	100 mg/L	10 mg/L	55 mg/L	100 mg/L
Pseudo-second order	Single						
q_e		7.32	13.15	37.19	9.93	39.41	48.97
K_2		0.65	0.94	0.02	13.69	0.05	0.40
R^2		0.999	0.999	0.991	1.000	0.999	0.999
Pseudo-second order	Binary						
q_e		42.48	9.49	13.39	3.82	15.96	17.09
K_2		0.02	0.44	0.04	10.71	0.55	0.30
R^2		0.999	0.999	0.999	1.000	0.999	0.999

Figure 7.3 and **Figure 7.4** show the graphs representing the linear form of the pseudo-second-order model of Cu^{2+} and Pb^{2+} in single and binary systems using orange peels. It can be observed that the graphs for both single and binary systems started from the origin, indicating the good fit of the model. According to Afroze and Sen (2018), the pseudo-second-order model is more suitable and most appropriate for the prediction of adsorption mechanism and it suggests chemical adsorption (chemisorption). Obike *et al.* (2018) studied the equilibrium and kinetic studies of Cu^{2+}, Cd^{2+}, $Pb^{2+,}$ and Fe^{2+} adsorption from an aqueous solution using cocoa pod husk. The kinetic data fitted well to the pseudo-second-order model. In addition, Semerjian (2018) also investigated the equilibrium and kinetic process of the removal of Cu^{2+} and Pb^{2+} from aqueous solutions using pine sawdust. The author reported that the metal adsorption kinetics was very well described by the pseudo-second-order model.

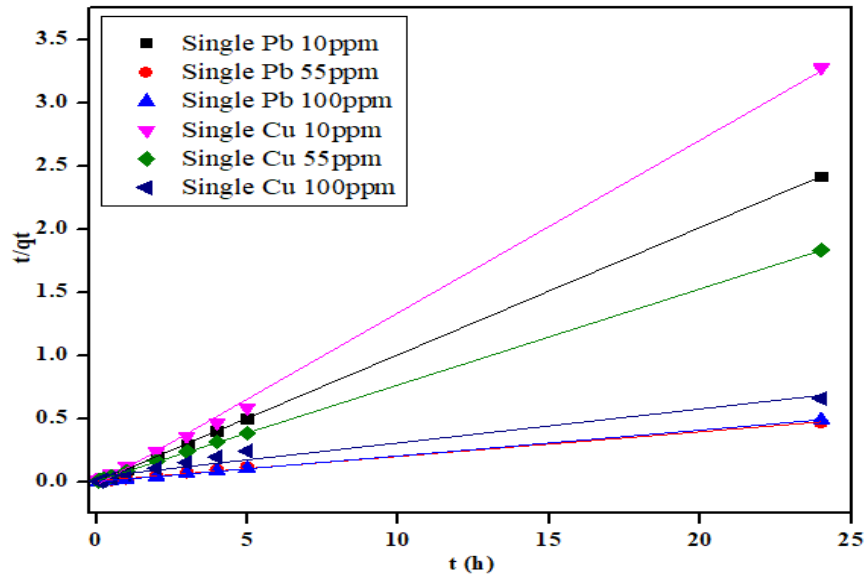

Figure 7.3: Pseudo-second-order kinetic model graph of single Cu^{2+} and Pb^{2+} at different initial concentrations using orange peels. (Initial concentration 10 – 100 mg/L, adsorbent dose 1 g and pH 5)

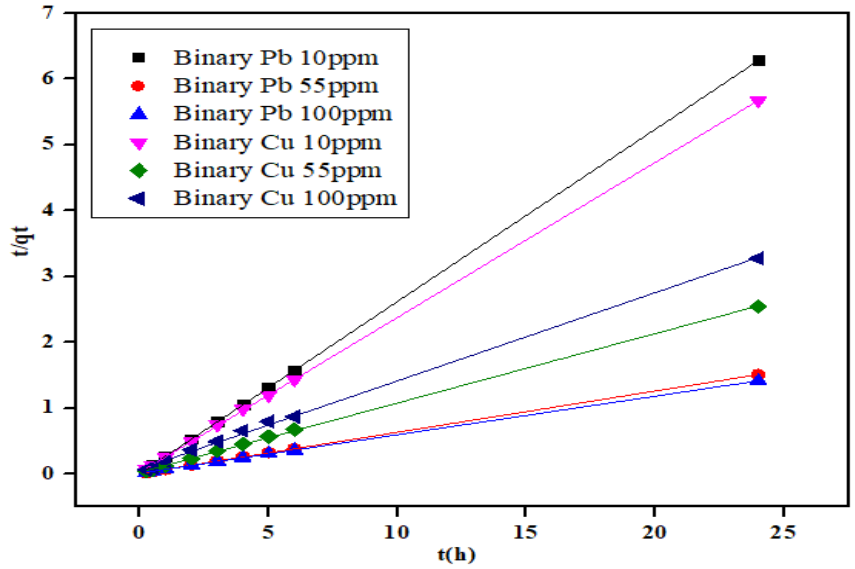

Figure 7.4: Pseudo-second-order kinetic model graph of binary Cu^{2+} and Pb^{2+} at different initial concentrations using orange peels. (Initial concentration 10 – 100 mg/L, adsorbent dose 1 g and pH 5)

7.2 Adsorption kinetic modelling of Pb^{2+} and Cu^{2+} onto banana peels.

The kinetic study of Pb^{2+} and Cu^{2+} onto banana peels in a single and binary system at different initial metal ion concentrations was investigated using linear pseudo-first-order and pseudo-second-order models. The rate of adsorption was studied and the adsorption capacity at the equilibrium of the metal ions was compared.

7.2.1 Pseudo-first-order model

The model parameters of the pseudo-first-order model are presented in **Table 7.3** below. The adsorption capacity of Cu^{2+} and Pb^{2+} in a single solute system was higher than the binary system at the different initial concentrations. The pseudo-first-order constant K_1 was also higher in the single solute system than the binary system this indicates the interaction between the metal ions during coexistence.

Table 7.3: Pseudo-first-order model parameters for the adsorption of Cu^{2+} and Pb^{2+} using banana peels.

Metal ion concentration		Cu			Pb		
		10 mg/L	55 mg/L	100 mg/L	10 mg/L	55 mg/L	100 mg/L
Pseudo-first order	Single						
q_e		0.93	2.79	5.86	0.53	14.79	31.84
K_1		2.73	18.06	14.52	7.13	2.55	6.88
R^2		0.704	0.899	0.999	0.999	0.972	0.985
Pseudo-first order	Binary						
q_e		0.25	1.65	0.96	0.16	0.78	1.13
K_1		0.23	1.89	1.38	5.53	0.39	1.59
R^2		0.998	0.961	0.935	0.992	0.995	0.951

The pseudo-first-order single and binary graphical representations are shown in **Figure 7.** and **Figure 7.6** respectively. The graphs show that the pseudo-first-order model is not suitable to predict the adsorption process as the linear plots do not pass through the origin.

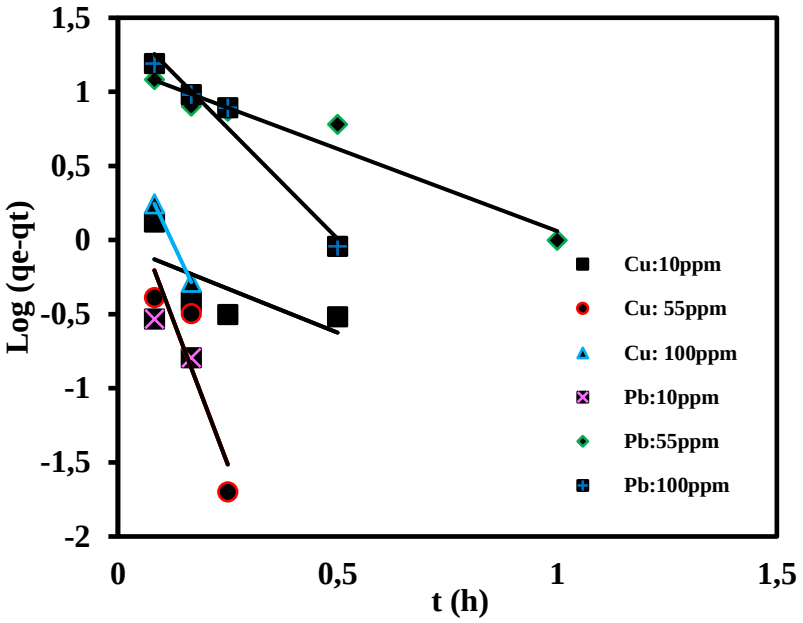

Figure 7.5: Pseudo-first-order kinetic model graph of single Cu^{2+} and Pb^{2+} at different initial concentrations. (Initial concentration 10 – 100 mg/L, adsorbent dose 1 g and pH 5)

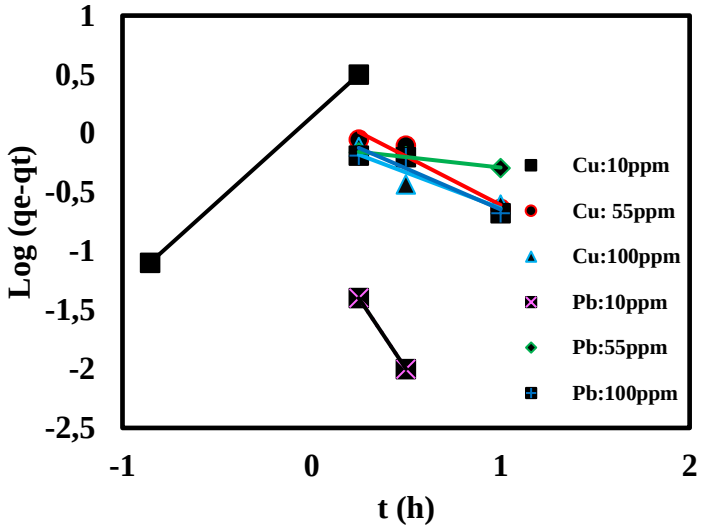

Figure 7.5: Pseudo-first-order kinetic model graph of binary Cu^{2+} and Pb^{2+} at different initial concentrations. (Initial concentration 10 – 100 mg/L, adsorbent dose 1 g and pH 5)

7.2.2 Pseudo-second-order model

The pseudo-second-order model parameters are presented in **Table 7.4** below. The equilibrium adsorption capacity of Pb^{2+} increased with increasing initial concentration for both single and binary systems. The adsorption capacity of Pb^{2+} is higher than Cu^{2+} in both single and binary systems. This suggests that banana peels have a higher affinity for Pb^{2+} than Cu^{2+}. Also, the adsorption capacity of the metal ions is reduced in the binary system which shows the effect of the co-existence of metal ions in the solution. The lower values of K_2 for Cu^{2+} in the binary system as compared to Pb^{2+} suggest that the adsorption rate of Cu^{2+} is negatively affected in the presence of Pb^{2+}. The adsorption kinetics of Cu^{2+} and Pb^{2+} in both systems at various initial concentrations fitted the pseudo-second-order model with correlation coefficient (R^2) very close to 1, which suggests that the adsorption rate is controlled by the chemical adsorption process.

Table 7.4: The pseudo-second-order model parameters for the adsorption of Cu^{2+} and Pb^{2+} using banana peels.

Metal ion concentration		Cu			Pb		
		10 mg/L	55 mg/L	100 mg/L	10 mg/L	55 mg/L	100 mg/L
Pseudo-second order	Single						
q_e		13.25	3.63	7.18	9.73	19.71	42.35
K_2		6.80	5.50	0.71	26.65	0.20	0.41
R^2		0.999	0.999	0.984	1.000	0.996	0.999
Pseudo-second order	Binary						
q_e		4.09	7.03	6.08	3.77	14.85	17.45
K_2		20.54	2.24	2.30	116.34	3.22	3.22
R^2		1.000	0.999	0.999	1.000	0.999	0.999

The graphs representing the pseudo-second-order model of Cu^{2+} and Pb^{2+} in single and binary systems at different initial metal ion concentrations using banana peels are shown in **Figure 7.6** and **Figure 7.7** respectively. The linear fit of the graphs starts from the origin which indicates a good fit of the model. This also suggests that the adsorption process favours the pseudo-second-order model which suggests that the adsorption mechanism is chemically controlled (chemisorption).

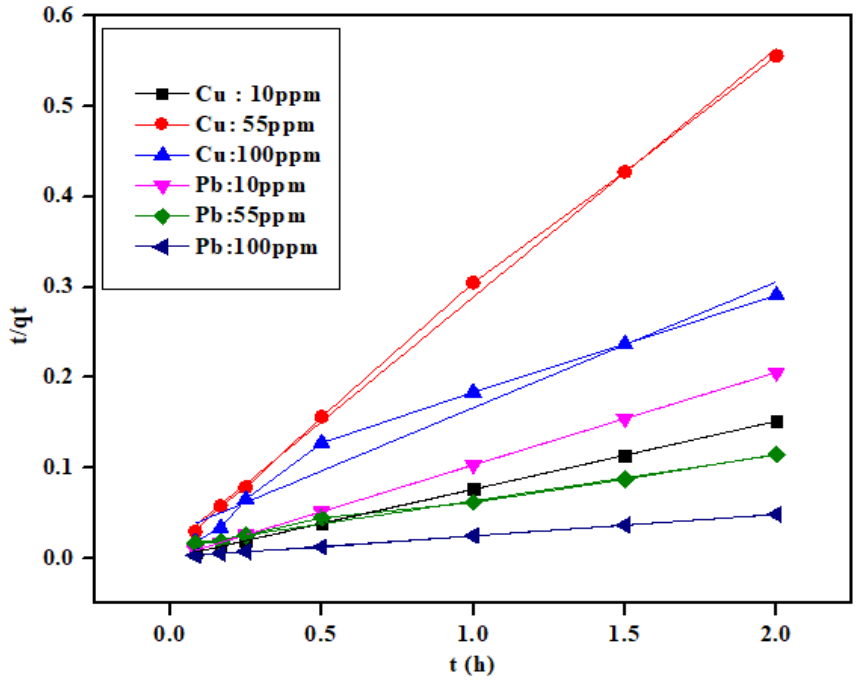

Figure 7.6: Pseudo-second-order kinetic model graph of single Cu^{2+} and Pb^{2+} at different initial concentrations using banana peels. (Initial concentration 10 – 100 mg/L, adsorbent dose 1 g and pH 5)

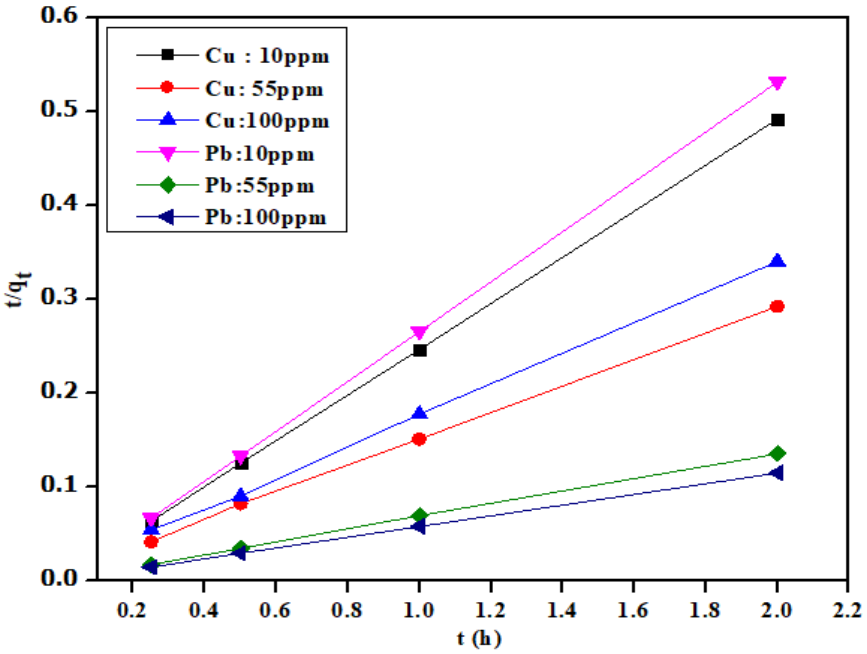

Figure 7.7: Pseudo-second-order kinetic model graph of single Cu^{2+} and Pb^{2+} at different initial concentrations using banana peels.

The adsorption of Cu^{2+} and Pb^{2+} using orange and banana peels in both single and binary systems revealed that the adsorption capacity of Pb^{2+} is higher than Cu^{2+} which suggests that Pb^{2+} could bind with more functional groups on the surface of the bio-sorbents. Hossain *et al.* (2014) reported that the functional groups on the surface of the bio-sorbents are responsible for the higher uptake of Pb^{2+} when compared with other metals in solution.

The values of k_1 and K_2 are time-dependent and help to determine the reaction rate of an adsorption process to reach equilibrium. They are also factors of process parameters such as the particle size, pH, initial concentration, adsorbent dosage, temperature, and agitation speed (Chen *et al.* 2018). In the binary system of Cu^{2+} and Pb^{2+} using the orange and banana peels, it was observed that the K_2 values at the initial concentrations 10, 50 and 100 mg/L gave (20.54, 2.24, and 2.30) respectively for the Cu^{2+} which were lower than values (116.34, 3.22 and 3.22) obtained for Pb^{2+}. This suggests that Pb^{2+} was more adsorbed than Cu^{2+} at the different initial concentrations.

The adsorption mechanism of Pb^{2+} and Cu^{2+} in single and binary systems using orange and banana peels followed the pseudo-second-order model, which suggests that the adsorption process is chemisorption. This was also noticeable in the correlation coefficient of the pseudo-second-order model. Although, the correlation coefficients for both pseudo-first-order and pseudo-second-order in Cu^{2+} and Pb^{2+} adsorption were both closer to 1 in some cases, however, the pseudo-second-order were higher. Therefore, the pseudo-second-order model has a higher tendency to predict the adsorption process of the adsorbates onto orange and banana peels. Sikarwar and Jain (2016) and Afroze and Sen (2018) affirmed that the pseudo-second-order model is more suitable for predicting the adsorption process, which means chemical adsorption or chemisorption has occurred. Chemisorption is promoted by chemical forces of attraction or chemical bond between the adsorbent and the adsorbate which leads to the formation of a unilayer of adsorbate in solution on the adsorbent and therefore results in to increase in the enthalpy of the adsorption process. This result agrees with the isotherm study which showed that adsorption occurred on monolayer for both single and binary solute of Pb^{2+} and Cu^{2+}.

7.3 Summary

The studies carried out showed that both orange and banana peels are capable of adsorbing Cu^{2+} and Pb^{2+} in both single and binary systems. Both the pseudo-first-order and pseudo-second-order models gave some information and insights into the adsorption mechanism of the bio-sorbents.

- Orange and banana peels performed well in the adsorption of Cu^{2+} and Pb^{2+} in both single and binary systems.
- The adsorption capacity of orange peels for Cu^{2+} and Pb^{2+} in both single and binary systems is higher than banana peels.
- Pb^{2+} was more adsorbed than Cu^{2+} in both single and binary systems using both bio-sorbents.
- The adsorption capacities of both bio-sorbents in the binary system were reduced as compared with the single solute system.
- The experimental data fitted the pseudo-second-order model for both single and binary systems of Cu^{2+} and Pb^{2+} suggesting chemisorption as the adsorption mechanism.
- The adsorption capacities of orange peels for both isotherm and kinetic models were consistently higher than banana peels in both single and binary systems. Hence, orange peels were chosen for column studies.
- This chapter, therefore, concludes the investigation on the adsorption capacity of orange and banana peels in the batch mode. The information gotten from this section is important to determine the bio-sorbent that will be used for column studies.

CHAPTER 8

8 Results Obtained from the Fixed-bed Adsorption Column Studies

8.1 Introduction

The previous chapters (chapter 5, 6, and 7) discussed the results obtained from the batch studies on the removal of copper and lead from aqueous solution using orange and banana peels. The chapters presented information on the performance of the adsorbents and the adsorption mechanisms involved. These results however not applicable for the treatment of wastewater on an industrial scale. The batch studies are not viable economically and cannot be used for the design and in the practice of industrial adsorption column (Chatterjee, Mondal and De 2018). The data obtained in the batch studies are not relatively applicable in the continuous adsorption system where the contact time between the adsorbate and adsorbent is not sufficient for equilibrium to be reached (Afroze and Sen 2018). Hence, it is important to study the performance of adsorbents to remove heavy metals in a continuous process to ascertain their applicability on an industrial scale. In addition, the study of continuous adsorption processes via the fixed-bed column allows more proper utilization of the adsorption efficiency than the batch studies and can explore the major influencing operating parameters such as bed height, flow rate and the initial metal ion concentration, etc., that is paramount to the design of a fixed-bed adsorber.

This study aimed to explore the efficiency of orange peels for the removal of Cu^{2+} and Pb^{2+} in the single and binary system in a fixed-bed column. Orange peels were chosen for the column study because of its performance in the batch study. The orange peels were used in their natural form, there was no pretreatment whatsoever before used.

The most crucial consideration for the design of a fixed-bed adsorption column is the proper generation of breakthrough curves through the service time of column operation which determines the process life span of the bed. The shape of the breakthrough curve and the breakthrough time features can be obtained through changes of various column operating parameters such as inlet solution flow rate , initial metal ion concentration and the bed height or mass of the adsorbent which influence the shape of the breakthrough curve. The adsorption breakthrough curve is defined as the concentration of the column effluent over time. In

adsorption studies, the breakthrough curve mostly observed is an “S” shape in nature when the flow is fully developed.

8.2 Breakthrough Curve Analysis

8.2.1 Effect of flow rate

The inlet flow rate of the metal solution is an essential operating parameter that must be investigated in the performance and efficiency of an adsorption column in a fixed bed (Abdolali *et al.* 2017). The effect of flow rate on the adsorbent efficiency was conducted by considering the flow rate 1 mL/min and 3 mL/min of copper and lead single solute solution with an initial metal concentration (50 mg/L) and bed height (2 cm) which were kept constant. The breakthrough curves obtained from the experimental results of copper and lead sorption at the flow rates are represented in **Figure 8.1**. The summary of the breakthrough curve parameters such as; breakthrough adsorption capacity (Q_b), breakthrough exhaustion time (t_e), breakthrough time (t_b), the volume of aqueous solution treated at breakthrough (V_b) and exhaustion time (V_e) were determined and represented in **Table 8.1** for both Cu^{2+} and Pb^{2+} bio-sorption. In this study, the breakthrough time for copper and lead was obtained when the effluent concentration reached 1 mg/L, which is according to the World Health Organization (WHO) and the South African National Standards (SANS) (Araujo *et al.* 2013).

From **Table 8.1**, a low flow rate resulted in more processing time to reach both the breakthrough and exhaustion points. Therefore, the volume of aqueous solution-processed at breakthrough decreased as the flow rate increased while the volume treated at exhaustion increased with increased flow rate. These were observed for both copper and lead breakthrough curves. Notably, the breakthrough time for the lead at 1 mL/min and 3 mL/min are 928 min and 277 min respectively. This shows a decrease in the breakthrough time as the flow rate increased. The breakthrough time for copper however decreased from 360 min to 36 min at flow rate 1 mL/min and 3mL/min respectively. This is because, at a high flow rate, the residence time reduces which shortens the adsorbate-adsorbent contact time. The volume of aqueous solution treated at breakthrough decreased for both copper and lead from 0.36 L to 0.108 L for copper and 0.928 L to 0.831 L for the lead at 1 mL/min and 3 mL/min respectively. The bed performance/efficiency decreased with increased flow rate, which can be as a result of shortened adsorbent-adsorbate contact time at a high flow rate (Abdolali *et al.* 2017). The increase in flow rate also gave steeper breakthrough curves, the breakthrough curve shifted

closer to the origin. This also shortens the mass transfer zone thus reducing the residence time in the column.

As a result of the reduction in mass transfer zone, the adsorption capacity at the breakthrough point decreased from 30 to 26 mg/g for lead bio-sorption and 17.25 to 15.25 mg/g for copper bio-sorption for 1 mL/min and 3 mL/min respectively. These results are reasonable and agree with the findings reported in similar studies (Abdolali *et al.* 2017; Yahya *et al.* 2020a; Yahya *et al.* 2020b). Yahya *et al.* (2020a) reported that the breakthrough curve formed a steep gradient at a higher flow rate for Cr^{3+} and Cu^{2+}.

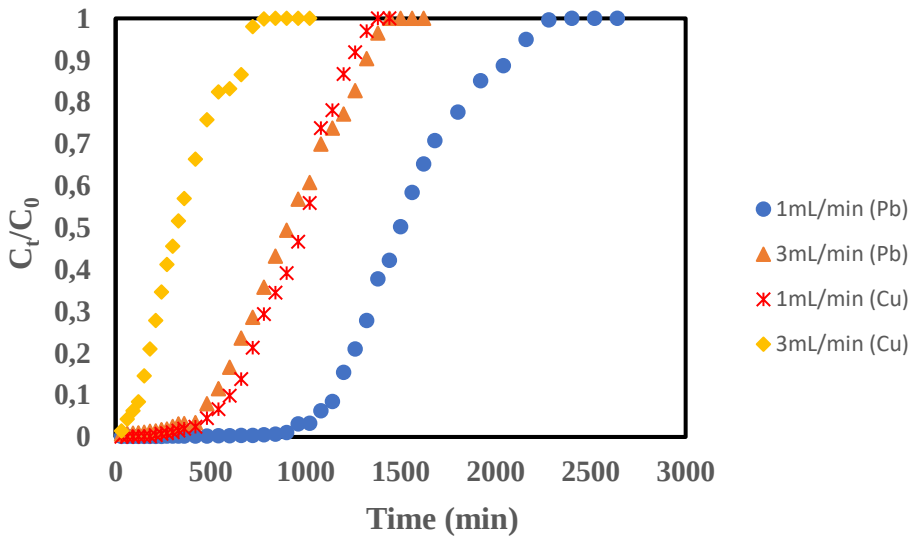

Figure 8.1: Breakthrough curves for the removal of lead and copper using orange peels at different flow rates (initial concentration = 50 mg/L; bed height = 3 cm).

Table 8.1: Summary of the fixed bed parameters at breakthrough and exhaustion points for lead and copper sorption in a single solute at different flow rates.

Sorbate	Flow rate (mL/min)	Q_b (mg/g)	Breakthrough time t_b (min)	Volume processed at t_b (L)	Exhaustion Time t_e (min)	Volume processed at t_e (L)
Pb	1	30	928	0.928	2160	2.16
	3	26	277	0.831	1365	4.10
Cu	1	17.25	360	0.360	1297	1.30
	3	15.22	36	0.108	704	2.11

8.2.2 Effect of Bed Height

The effect of bed height is an important operating parameter in the continuous operation of fixed-bed columns. It is highly essential for column design and scale-up. The effect of the bed height for investigating the adsorbent performance was conducted at bed height of 1 cm and 3 cm at an initial concentration of 50 mg/L and flow rate of 3 mL/min. When the bed height is varied in an adsorption process, it means the active sites on the adsorbent and the contact time between the adsorbate and the adsorbent are varied (Afroze and Sen 2018). The breakthrough curve of copper and lead bio-sorption at different bed heights is depicted in **Figure 8.2**.

The breakthrough capacity (Q_b), breakthrough time (t_b), the exhaustion time (t_e), the volume of aqueous solution treated at breakthrough (V_b), and exhaustion (V_e) times for the bio-sorption of copper and lead in a single solute solution as determined from the breakthrough curves are summarized in **Table 8.1**. The breakthrough time for both copper and lead increased with an increase in bed height resulting in a similar breakthrough profile. This shows that at a high bed height, there are more active sites available on the surface of the adsorbent, hence resulting in a longer breakthrough time and more volumes of the aqueous solution being treated at the breakthrough point. The breakthrough time for lead bio-sorption increased from 53 min to 1003 min while it increased from 36 min to 341 min for copper bio-sorption for 1 cm and 3 cm bed height respectively. This is reasonable because a smaller bed height suggests a smaller quantity of adsorbent. An increase in the bed height means the metal ion has additional time to interact with the adsorbent leading to greater uptake of Cu^{2+} and Pb^{2+} in the column.

The adsorption capacity of copper and lead at the breakthrough point increased with increasing bed height from 37 to 44 mg/g for lead and 22 to 36 mg/g for copper at 1 cm and 3 cm bed height respectively. An increase in bed height broadens the mass transfer zone which results in the availability of more sorption sites on the surface of the adsorbent (Yahya *et al.* 2020b). In addition, when the bed height is increased, the diffusion mass transfer predominates in comparison with the axial dispersion phenomenon. Therefore, a great increase in the breakthrough time was observed. Abdolali *et al.* (2017) revealed that a high bed height is more desirable for more active binding sites to be provided and for better performance of a fixed-bed column.

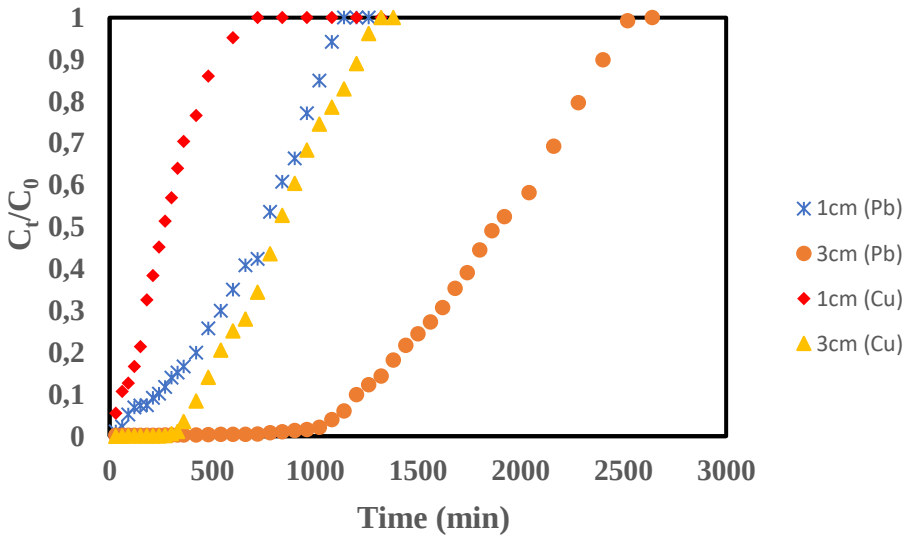

Figure 8.2: Breakthrough curves for the removal of lead and copper in single solute using orange peels at different bed heights (initial concentration of 50mg/L; flow rate of 3mL/min).

Table 8.2: Summary of the fixed bed parameters at breakthrough and exhaustion points for lead and copper sorption in single solute at different bed heights.

Sorbate	Bed height (cm)	Qb (mg/g)	Breakthrough time t_b (min)	Volume processed at t_b (L)	Exhaustion Time t_e (min)	Volume processed at t_e (L)
Pb	1	37	53	0.106	1088	2.18
	3	44	1003	2.0	2465	4.93
Cu	1	22	15	0.03	600	1.2
	3	36	341	0.682	1250	2.5

8.2.3 Effect of initial concentration

The effect of initial concentration is an essential operating parameter in a fixed-bed column adsorption study. It helps to determine the adsorption capacity of an adsorbent. The effect of varying initial concentrations of lead and copper ions in a single solute solution was studied in the range of 10 to 100 mg/L at a constant bed height of 3 cm and flow rate of 3 mL/min. The breakthrough curves are depicted in **Figure 8.3**. The breakthrough capacity (Q_b), breakthrough time (t_b), the exhaustion time (t_e), the volume of aqueous solution treated at breakthrough (V_b), and exhaustion (V_e) times for the bio-sorption of copper and lead in a single solute solution on the effect of initial concentration as determined from the breakthrough curves are summarized in **Table 8.3**.

Observation of **Figure 8.3** shows that orange peels were spent faster at higher inlet concentrations for both copper and lead. A preliminary breakthrough point was observed at high concentrations. The breakpoint time of lead was obtained after 1241, 700, and 15 min while it was observed at 616, 129, and 15 min for copper at 10, 50, and 100 mg/L respectively. A decrease in the inlet concentration resulted in a prolonged breakthrough curve, suggesting that a high volume of the aqueous solution is treated. This means a low concentration gradient leads to a lengthier journey through the column due to a reduction in mass transfer coefficient (Yahya *et al.* 2020a). Specifically, from **Table 8.3**, the adsorption capacity of copper and lead increased with increasing inlet concentration. For copper, at inlet concentrations of 10, 50, and 100 mg/L the adsorption capacity gave 10.2, 22.6, and 39 mg/g while for lead adsorption capacity gave 10.8, 53.5, and 84 mg/g respectively. The increase in adsorption capacity at high inlet concentration occurred because of an increase in the solid-liquid phase, a driving force for the column adsorption. This will enhance the scale-up when the column is operating at an optimum condition.

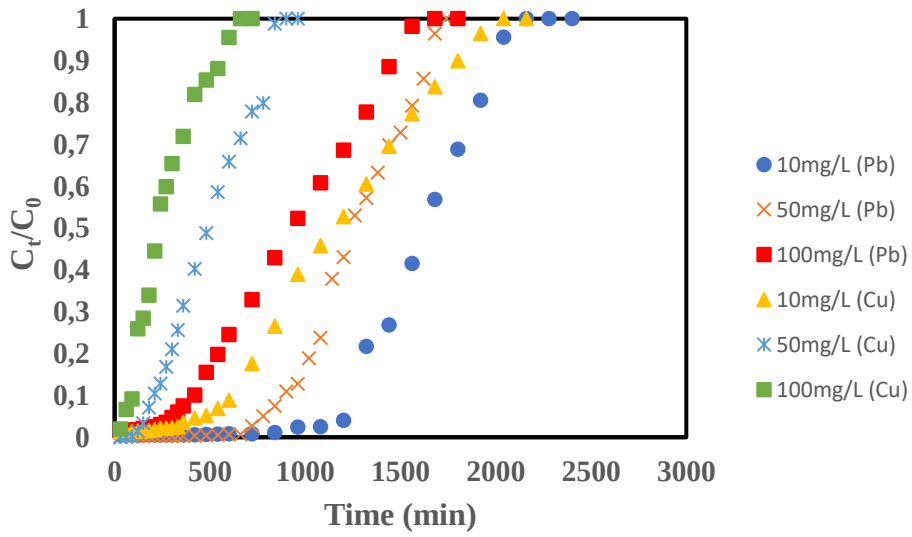

Figure 8.3: Breakthrough curves for the removal of lead and copper in a single solute using orange peels at different initial concentrations (bed height of 3cm; flow rate of 3mL/min).

Table 8.3: Summary of the fixed bed parameters at breakthrough and exhaustion points for lead and copper sorption in single solute at different initial concentrations.

Sorbate	Initial concentration (mg/L)	Q_b (mg/g)	Breakthrough time t_b (min)	Volume processed at t_b (L)	Exhaustion Time t_e (min)	Volume processed at t_e (L)
Pb	10	10.8	1241	2.48	2035	4.07
	50	53.5	700	1.4	1672	3.34
	100	84	15	0.03	1520	3.04
Cu	10	10.2	616	1.23	1894	3.79
	50	22.6	129	0.258	828	1.656
	100	39	15	0.03	596	1.19

8.3 Application of Breakthrough Models

Breakthrough curves are defined as the concentration-time graph which shows the ratio of the effluent concentration to the inlet concentration over time. To analyze the fixed-bed column characteristics and to scale up for industrial operations, a suitable dynamic model must be applied. Many simple mathematical dynamic models have been developed to analyze and predict the dynamic characteristic and behavior of the fixed-bed performance. Therefore, to determine the breakthrough performance, to analyze and calculate the column adsorption kinetic parameters, and to evaluate the bed capacity, the following models are widely used in column dynamic analysis; Thomas, Yoon Nelson, and Adams Bohart model. Hence, these models were applied to the experimental results to evaluate the adsorption capacity and performance of the fixed-bed column in this study.

8.3.1 Thomas Model

The Thomas model is one of the widely used dynamic models for describing fixed-bed column performance and predicting the breakthrough curve operating parameters. The model assumes plug flow in the bed and makes use of Langmuir kinetics of adsorption (Thomas 1944). The linearized form of the Thomas model is represented in Equation 3-22. The K_{Th} and q_o values calculated from the slope and intercepts of the linear graph of ln[(C0/Ct)-1] against time obtained from the experimental data are shown in **Appendix B1**. The model parameters representing the different operating parameters studied are summarized in **Table 8.4** and **Table 8.5** respectively for lead and copper bio-sorption.

From **Table 8.4**, the values of K_{Th} and q_o increased with an increase in flow rate. Abdolali *et al.* (2017) and Ali Gh. Khamseh and Ghorbanian (2018) reported an increase in the value of K_{Th} as the flow rate increased. The increase in q_o value with an increase in flow rate agrees with the work by (Amin, Alazba and Shafiq 2017a; Yahya *et al.* 2020a). The K_{Th} and q_o values decreased with an increase in bed height. This agrees with the work reported by other researchers (Amin, Alazba and Shafiq 2017a; Ali Gh. Khamseh and Ghorbanian 2018; Musonge 2020). Meanwhile, an increase in initial concentration gave a decrease in the value of K_{Th} and an increase in the value of q_o. This result corresponds with the result reported by (Amin, Alazba and Shafiq 2017a).

Table 8.4: Summary of Thomas model parameters for lead sorption using orange peels in a fixed bed column

Parameter	**Thomas Model**		
Flow rate (mL/min)	**K_{Th} *10^{-4} (Lmin^{-1}mg^{-1})**	**q_o (mg/g)**	**R^2**
1	1.02	19.35	0.953
3	1.16	34.33	0.991
Bed height (cm)	**K_{Th} *10^{-4} (Lmin^{-1}mg^{-1})**	**q_o (mg/g)**	**R^2**
1	1.04	34.71	0.957
3	0.78	30.48	0.960
Initial concentration (mg/L)	**K_{Th} *10^{-4} (Lmin^{-1}mg^{-1})**	**q_o (mg/g)**	**R^2**
10	3.7	8.55	0.905
50	1.12	32.61	0.962
100	0.48	46.05	0.976

From **Table 8.5** an increase in flow rate resulted in a corresponding increase in the values of K_{Th} and q_o. Ali Gh. Khamseh and Ghorbanian (2018) studied the breakthrough modeling of thorium bio-sorption on orange peels in a fixed-bed column. The effects of flow rate, bed height, and feed inlet concentration were investigated. The breakthrough point decreased with decreasing bed height, increasing feed inlet concentration, and increasing the flow rate while the sorption capacity increased with decreasing bed height. The experimental results were fitted with Thomas and Yoon Nelson. Abdolali *et al.* (2017) studied the performance of a multi-metal binding bio-sorbent (MMBB) for removing cadmium, copper, lead, and zinc in a continuous fixed-bed column. The effect of influent flow rate, metal concentration, and bed depth were investigated. The results showed that the total metal adsorption reduced with increasing influent flow rate. The Thomas model better described the column dynamic behaviour than the

Yoon Nelson models. In addition, an increase in bed height gave a corresponding decrease in the values of K_{Th} and q_o. This result corresponds to what was obtained by other researchers (Muhamad, Doan and Lohi 2010; Amin, Alazba and Shafiq 2017a). An increase in initial concentration resulted in a decrease in the value of K_{Th} and an increase in the values of q_o. This is similar to the result obtained by (Amin, Alazba and Shafiq 2017a). The Thomas model parameters for the sorption of lead and copper onto orange peels followed the same trend. However, the adsorbed capacity for lead biosorption is higher than copper in all conditions. The high correlation coefficient R^2 values in **Table 8.4** and **Table 8.5** show that the Thomas model was well fitted with the experimental data.

Table 8.5: Summary of Thomas model parameters for copper sorption using orange peels in a fixed bed column

Parameter	**Thomas Model**		
Flow rate (mL/min)	**KTh *10^{-4} (Lmin^{-1}mg^{-1})**	**qo (mg/g)**	**R^2**
1	1.58	11.60	0.980
3	2.14	12.84	0.909
Bed height (cm)	**KTh *10^{-4} (Lmin^{-1}mg^{-1})**	**qo (mg/g)**	**R^2**
1	1.94	14.02	0.988
3	1.9	13.34	0.939
Initial concentration (mg/L)	**KTh *10^{-4} (Lmin^{-1}mg^{-1})**	**qo (mg/g)**	**R^2**
10	4.0	5.91	0.992
50	2.28	13.01	0.829
100	1.02	13.85	0.913

8.3.2 Yoon Nelson Model

Yoon Nelson model is regarded as a simplified model because it does not require data like characteristics of adsorbate, type of adsorbent, and the physical properties of the bed (Afroze and Sen 2018). The assumption of this model is based on the rate of decrease in the adsorption probability of each adsorbate is proportional to the adsorbate adsorption probability and the probability of adsorbate breakthrough on the adsorbent (Yoon and NELSON 1984). The

linearized form of the model as expressed in Equation 3-23 was applied. The plot of $\ln(C_t/C_o-C_t)$ against time gave a straight line with a slope of K_{YN} and intercept $K_{YN}\tau$. The graphs of the experimental data are represented in **Appendix B2**. The model parameters for lead and copper sorption are summarized in Table 8.6 and Table 8.7 respectively.

From **Table 8.6**, an increase in the flow rate gave an increase in the values of K_{YN} and a decrease in the value of τ while an increase in the bed height resulted in a decrease in the values of K_{YN} and an increase in the value of τ. Basu, Guha and Ray (2019) used a fixed-bed column bioreactor for the adsorption of lead using lentil husk as bio-sorbent. The adsorption capacity increased with increasing bed height and feed concentration while the experimental data were well described by Thomas and Yoon Nelson model. The bed height delayed 50 % adsorbate breakthrough time τ increased with increasing bed height. Alalwan, Kadhom and Alminshid (2020) examined the use of rice husk for removing thallium ions from aqueous solutions using a fixed-bed adsorption column. The effects of bed height, flow rate, initial concentration, and solution pH on the breakthrough curves were analyzed. The experimental results were compared with the Thomas and Yoon Nelson models. The results showed that increasing the bed height, decreasing the flow rate and the initial concentration improved the removal capacity of the bio-sorbent. In addition, an increase in initial concentration resulted in a corresponding increase in K_{YN} and a decrease in τ. This result is similar to the findings reported by (Lakshmipathy and Sarada 2015; Alalwan, Kadhom and Alminshid 2020)

Table 8.6: Summary of Yoon Nelson model parameters for lead sorption using orange peels in a fixed bed column

	Yoon Nelson Model		
Flow rate (mL/min)	**K_{YN} (min^{-1})**	**τ (min)**	**R^2**
1	0.0051	1547.63	0.951
3	0.0058	915.5	0.990
Bed height (cm)	**K_{YN} (min^{-1})**	**τ (min)**	**R^2**
1	0.0052	694.11	0.955
3	0.0039	1828.72	0.958
Initial concentration (mg/L)	**K_{YN} (min^{-1})**	**τ (min)**	**R^2**
10	0.0037	1709.24	0.905
50	0.0048	1304.46	0.960
100	0.0049	920.92	0.975

From **Table 8.7**, an increase in flow rate resulted in an increase in K_{YN} values and a decrease in the values of τ while an increase in bed height gave a decrease in the value of K_{YN} and an increase in the values of τ. Aranda-Garcia and Cristiani-Urbina (2020) carried out a continuous fixed-bed column study using acorn shells from Quercus crassipes Humb to remove chromium from an aqueous solution. The effects of influent solution pH, flow rate, bed height, and initial concentration were investigated. The adsorption of chromium increased with increasing bed height, flow rate, and influent concentration of chromium. The results showed that τ decreased with increasing flow rate while K_{YN} increased with increasing initial concentration. An increase in initial concentration resulted in an increase in the values of K_{YN} and a decrease in the values of τ. This is similar to the results obtained by other researchers (Lakshmipathy and Sarada 2015). The values of the correlation coefficient R^2 obtained in **Table 8.6** and **Table 8.7** are close to 1, this suggests that the experimental data are well fitted with the Yoon Nelson model.

Table 8.7: Summary of Yoon Nelson model parameters for copper sorption using orange peels in a fixed bed column

	Yoon Nelson Model		
Flow rate (mL/min)	**K_{YN} (min^{-1})**	**τ (min)**	**R^2**
1	0.0079	928.35	0.978
3	0.0107	342.38	0.905
Bed height (cm)	**K_{YN} (min^{-1})**	**τ (min)**	**R^2**
1	0.0097	280.40	0.985
3	0.0095	860.33	0.937
Initial concentration (mg/L)	**K_{YN} (min^{-1})**	**τ (min)**	**R^2**
10	0.004	1182.43	0.990
50	0.0102	520.44	0.827
100	0.0114	276.92	0.910

8.3.3 Bohart-Adams Model

This model is based on assumption that equilibrium is not instantaneous, which implies that the adsorption rate is proportional to the adsorbent residual capacity and the concentration of the dissolved species (Bohart and Adams 1920). The linear form of the model as expressed in Equation 3-24 was applied to the experimental data. The values of K_{AB} and N_o were obtained from the linear plot of $\ln(C_t/C_o)$ against time as depicted in **Appendix B3**. The model

parameters for the sorption of lead and copper using orange peels are summarized in **Table 8.8** and **Table 8.9** respectively.

From **Table 8.8** and **Table 8.9**, the trends observed by the model parameters are the same for both lead and copper sorption. An increase in flow rate increased both K_{BA} and N_o while an increase in bed height resulted in an increase in K_{BA} and a decrease in N_o. Basu, Guha and Ray (2019) used a fixed-bed column bioreactor for the adsorption of lead in continuous mode with lentil husk as bio-sorbent. An increase in the initial concentration resulted in a decrease in K_{BA} and an increase in the values of No (Basu, Guha and Ray 2019). However, a low correlation coefficient ($R^2 < 0.9$) was obtained for most of the parameter conditions specifically in the case of copper sorption. This suggests that the Bohart-Admas model does not fit the experimental data well enough.

Table 8.8: Summary of Bohart-Adams model parameters for lead sorption using orange peels in a fixed bed column

	Bohart-Adams Model		
Flow rate (mL/min)	**KBA*10-4 ($Lmin^{-1}mg^{-1}$)**	**No (mg/L)**	**R^2**
1	0.68	12331.81	0.905
3	0.7	23711.51	0.914
Bed height (cm)	**KBA*10-4 ($Lmin^{-1}mg^{-1}$)**	**No (mg/L)**	**R^2**
1	0.56	26581.51	0.884
3	0.6	17680.02	0.948
Initial concentration (mg/L)	**KBA*10-4 ($Lmin^{-1}mg^{-1}$)**	**No (mg/L)**	**R^2**
10	2.8	5091.72	0.945
50	0.82	19579.23	0.938
100	0.25	36218.79	0.871

Table 8.9: Summary of Bohart-Adams model parameters for copper sorption using orange peels in a fixed bed column

	Bohart-Adams Model		
Flow rate (mL/min)	**KBA*10-4 ($Lmin^{-1}mg^{-1}$)**	**No (mg/L)**	**R^2**
1	1.12	7102.10	0.901
3	0.62	13854.83	0.668
Bed height (cm)	**KBA*10-4 ($Lmin^{-1}mg^{-1}$)**	**No (mg/L)**	**R^2**
1	0.3	23923.82	0.561
3	1.3	8962.79	0.812
Initial concentration (mg/L)	**KBA*10-4 ($Lmin^{-1}mg^{-1}$)**	**No (mg/L)**	**R^2**
10	2.2	4483.53	0.894
50	1.3	9164.32	0.598
100	0.25	17727.24	0.556

8.3.4 Statistical Validity

The section evaluated the statistical and mathematical features of the applied models and compared the error values obtained to determine the best model that fitted the experimental data the most. The statistical validation is significant for evaluating the performance of dynamic adsorption models. Three different error functions were examined in this study namely: mean absolute error, root mean square error, and the coefficient correlation as represented in **Table 8.10**. The error values corresponding to the models used for the sorption of lead and copper are summarized in **Table 8.11** and **Table 8.12** respectively. The best-fit model was chosen based on the error function that gave the lowest error distribution between the experimental and predicted model values while the highest coefficient of correlation was selected.

Table 8.10: Error functions used to statistically validate the performance of the models.

Error function	Abbreviation	Equation
Mean absolute error	MAE	$MAE = \frac{1}{n}\sum_{i=1}^{n}\lvert y_{e,exp} - y_{e,pred}\rvert$
Root mean square error	RMSE	$RMSE = \sqrt{\frac{1}{n}\sum_{i=1}^{n}\left(y_{e,exp} - y_{e,pred}\right)^2}$
Coefficient of correlation	R^2	$R^2 = \frac{\sum\left(y_{e,exp} - y_{e,pred}\right)^2}{\sum\left(y_{e,exp} - y_{e,pred}\right)^2 + \left(y_{e,exp} - y_{e,pred}\right)^2}$

From **Table 8.11** and **Table 8.12**, the error functions showed good agreement between the experimental and predicted values for the three models with RMSE and MAE < 1 in most cases. The highest values of R^2 and lowest values of RMSE and MAE were obtained. The best model chosen had the highest value of R^2 and lowest values of RMSE and MAE, which suggests that the Thomas and Yoon Nelson models performed well.

Table 8.11: Breakthrough curves regression and error analysis for lead sorption

Parameters	**Thomas**			**Yoon Nelson**			**Bohart -Adams**		
single solute Pb	**RMSE**	**MAE**	**R^2**	**RMSE**	**MAE**	**R^2**	**RMSE**	**MAE**	**R^2**
Flow rate (mL/min)									
1	0.027	0.017	0.953	0.028	0.018	0.951	1.242	0.422	0.905
3	0.028	0.020	0.991	0.028	0.020	0.990	0.470	0.227	0.914
Bed height (cm)									
1	0.045	0.035	0.957	0.045	0.035	0.955	0.208	0.111	0.884
3	0.030	0.018	0.960	0.031	0.019	0.958	0.501	0.168	0.948
Concentration (mg/L)									
10	0.065	0.039	0.907	0.065	0.040	0.905	0.266	0.114	0.945
50	0.034	0.021	0.962	0.035	0.021	0.960	0.511	0.215	0.938
100	0.040	0.027	0.976	0.040	0.027	0.975	0.438	0.203	0.871s

Table 8.12: Breakthrough curves regression and error analysis for copper sorption

Parameters	Thomas			Yoon Nelson			Bohart -Adams		
single solute Cu	RMSE	MAE	R^2	RMSE	MAE	R^2	RMSE	MAE	R^2
Flow rate (mL/min)									
1	0.037	0.024	0.980	0.037	0.024	0.978	0.754	0.296	0.901
3	0.055	0.040	0.909	0.055	0.040	0.905	0.368	0.254	0.668
Bed height (cm)									
1	0.023	0.016	0.988	0.023	0.016	0.985	0.323	0.246	0.561
3	0.075	0.049	0.939	0.075	0.049	0.937	1.662	0.661	0.812
Concentration (mg/L)									
10	0.029	0.018	0.992	0.030	0.019	0.990	0.539	0.245	0.894
50	0.088	0.067	0.829	0.088	0.066	0.827	1.130	0.522	0.598
100	0.062	0.045	0.913	0.062	0.045	0.910	0.359	0.275	0.556

8.5 Summary

The major aim of this section of the study was to evaluate the performance of natural orange peels in the removal of Cu^{2+} and Pb^{2+} in a fixed-bed column. Each metal ion was examined individually in the continuous flow setup. The experimental results showed that the performance of the bed was improved with an increase in the bed height, the quantity adsorbed increased from 37 mg/g to 44 mg/g for Pb^{2+} and from 22 mg/g to 36 mg/g for Cu^{2+} as the bed height was increased from 1 cm to 3 cm. The volume of solution treated at breakthrough decreased with an increase in flow rate for both metals. The volume treated at breakthrough for Pb^{2+} decreased from 0.928 to 0.831 mL and Cu^{2+} decreased from 0.360 to 0.108 mL when the flow rate was increased from 1 to 3 mL/min. The significant factors used to measure the performance of an adsorbent such as breakthrough adsorption capacity (Q_b) and the breakthrough time (t_b) were analyzed for both metal ions. However, similar trends were observed for both metals though Pb^{2+} performance was better than Cu^{2+} with all the parameters. The Q_b and t_b decreased with an increase in flow rate while it increased with an increase in bed height for both metal ions. Also, the Q_b increased with an increase in the initial metal ion concentration and a consequent decrease in t_b for both metal ions. The quantity adsorbed for Pb^{2+} increased from 10.8 to 84 mg/g and 10.2 to 33 mg/g for Cu^{2+} as the initial concentration increased from 10 to 100 mg/L. It is important to note that the adsorption capacity of Pb^{2+} was higher than Cu^{2+} which complements the findings reported in the batch studies.

The experimental data obtained were fitted into the Thomas, Yoon Nelson, and the Bohart-Adams models to determine the best fit and the well-performed model. For all the parameters considered, the Thomas and Yoon Nelson models performed well with a high coefficient of correlation ($R^2 > 0.9$). The models were also validated using some statistical error analysis, which showed that the Thomas and Yoon Nelson models fitted the experimental data fairly well.

CHAPTER 9

9 Modelling of Bi-Solute Adsorption Column Systems.

9.1 Introduction

In this section, the binary solute system of Cu^{2+} and Pb^{2+} was investigated in a column study using orange peels. It is very crucial to evaluate the performance of orange peels when the metal ions co-exist in a continuous mode. In the application of the bio-sorption process for industrial-scale treatment of wastewater, it is essential to study the effect of the co-existence of metal ions because it is very rare for wastewater to contain a single metal ion. Many operating parameters are very important for industrial treatment application and scale-up however, only initial concentration was considered for this study. In addition, the existing dynamic models (Thomas, Yoon Nelson, and Bohart-Adams) were applied to the experimental data.

9.2 Effect of initial concentration on the binary system of Cu^{2+} and Pb^{2+}

The study of the effect of initial concentration on the binary system of Cu^{2+} and Pb^{2+} was carried out using the same set-up as stated in chapter 8. The initial concentrations considered were 10 mg/L, 50 mg/L, and 100 mg/L of Cu^{2+} and Pb^{2+} at ratio 1:1 with a constant bed height of 3 cm and flow rate of 3 mL/min. The comparison of the breakthrough curves representing the binary systems of Cu^{2+} and Pb^{2+} are depicted in **Figure 9.1** to **Figure 9.3**. The breakthrough curves are represented by the normal concentration (ratio of effluent metal ion concentration to the influent metal ion concentration) against the time profile which depicts the typical S-shapes.

The breakthrough curves for the binary solution of Cu^{2+} and Pb^{2+} showed a slightly different shape than those reported for the single solute solution Figure 8.3. This can be ascribed to the influence of the co-existence of metal ions which led to competition for the limited binding sites on the bio-sorbent. The binary breakthrough curves for Cu^{2+} and Pb^{2+} showed that the biosorption capacity for each metal ion differs and the curves denote a higher affinity of Pb^{2+} for orange peels. The bio-sorption capacity of Pb^{2+} was consistently higher than the biosorption capacity of Cu^{2+} for all the initial concentrations chosen. This confirms the higher affinity of Pb^{2+} for orange peels irrespective of the initial metal ion concentration. This was also reported for the single metal ions as well as the batch experiments.

Considering **Figure 9.1** to **Figure 9.3**, the breakthrough time decreased with an increased initial concentration for both metal ions. An increase in the influent metal ion concentration resulted in a steeper breakthrough curve which drew the breakthrough curve closer to the origin as the binding sites were quickly saturated. Furthermore, complete breakthrough curves were obtained for both metal ions at the different initial concentrations chosen. The breakthrough curves representing Cu^{2+} bio-sorption reached a breakthrough point faster than Pb^{2+}. These results are similar to the findings reported by (Martín-Lara *et al.* 2016). The authors studied the binary biosorption of copper and lead onto pine cone shells in batch reactors and fixed-bed columns at initial concentrations 50/50 and 100/100, and observed that the breakthrough curves of Cu^{2+} reached breakthrough point faster than Pb^{2+} because of lower affinity for the binding sites on the bio-sorbent. Escudero-Oñate, Poch and Villaescusa (2017) also reported that the breakthrough curve of Cu^{2+} reached breakthrough point faster than Pb^{2+} in the modelling competitive breakthrough curves of Cu^{2+}, Ni^{2+}, Pb^{2+} and Cd^{2+} ternary mixtures using grape stalks wastes. Vilar *et al.* (2008) reported that Cu^{2+} bio-sorption reached a breakthrough point faster than Pb^{2+} in the study of continuous bio-sorption of Pb^{2+} and Cu^{2+} in a fixed-bed column using algae *Gelidium* and granulated algal wastes. This claim was also supported by (Hawari and Mulligan 2007) in the study of the effect of the presence of lead on the bio-sorption of Cu^{2+}, Cd^{2+}, and Ni^{2+} by anaerobic biomass. The authors observed that the breakthrough curve of Cu^{2+} reached a breakthrough point faster than Pb^{2+} in a flow-through column.

Furthermore, the behavior of Pb^{2+} and Cu^{2+} in a binary system can be explained using parameters characterizing the binding strength of the metal ions such as crystal radius, hydrated ionic radius, and covalent binding. The values of these parameters for Pb^{2+} and Cu^{2+} are represented in **Table 9.1** below.

Table 9.1: Parameters characterizing the binding strength of Pb^{2+} and Cu^{2+}

Parameters	Pb	Cu
Ionic radius, r	1.19	0.73
Hydrated ion radius, r_{hyd}	4.01	4.19
Covalent binding, $X^2(r_{cryst} + 0.85)$	7.18	6.41
Electronegativity, X_m	2.33	1.90

Table 9.1 shows that the hydrated radii of both metals are larger than the ionic radius. A change in the inclination of the hydrated water molecules relates to the electrostatic binding of metal ions. If the hydrated water molecules are not strongly held by the metal ion, there can be a change of state and the metal ion can accumulate at the interface of the bio-sorbent (Martín-Lara *et al.* 2016). Generally, when comparing crystal radii of ions with the same charge such as Pb^{2+} and Cu^{2+}, larger ions that are less strongly hydrated are mostly accumulated at the interface. In essence, Pb^{2+} which has a higher affinity for adsorption on bio-sorbent has a lower hydration ion radius when compared to Cu^{2+}. This explains the fact that less strongly hydrated ions tend to accumulate at the interface. In addition, the greater the covalent binding index, the greater the tendency and potential of the metal ion to form covalent bonds with the functional groups present on the surface of the bio-sorbent. Hence, larger ions can fit into a binding site and bind simultaneously to several groups on an adsorbent surface. This explains the higher affinity of Pb^{2+} for orange peels. Similar results have been reported for some cations by (Hawari and Mulligan 2007; Shoaib, Badar and Aslam 2011; Chatterjee and Schiewer 2014; Martín-Lara *et al.* 2016). It can therefore be concluded that the tendency of Pb^{2+} greater binding and affinity is due to higher covalent binding and ionic radius with lower hydrated radius.

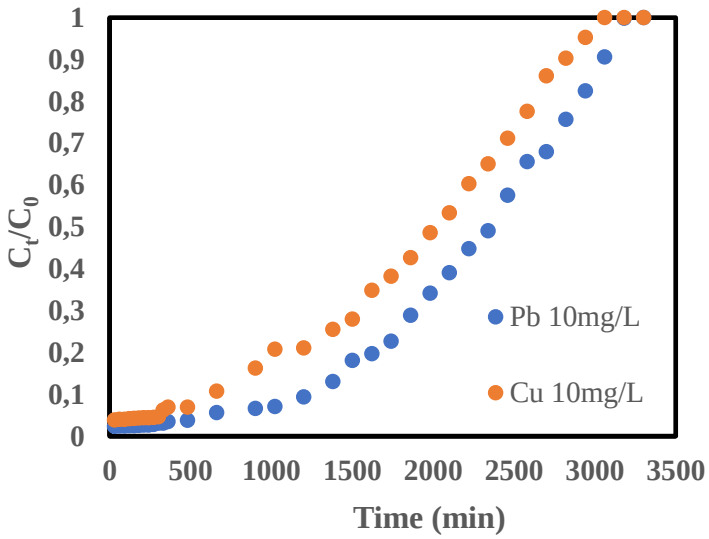

Figure 9.1: Experimental breakthrough curves of Cu^{2+} and Pb^{2+} in binary solution using orange peels.

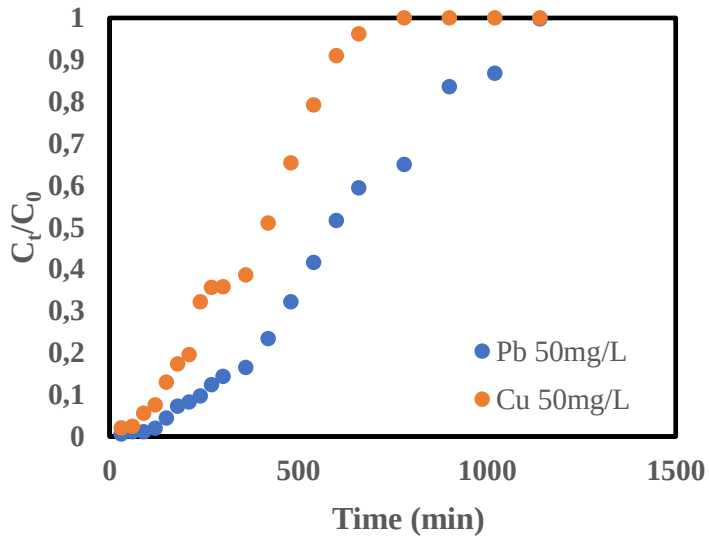

Figure 9.2: Experimental breakthrough curves of Cu^{2+} and Pb^{2+} in binary solution using orange peels.

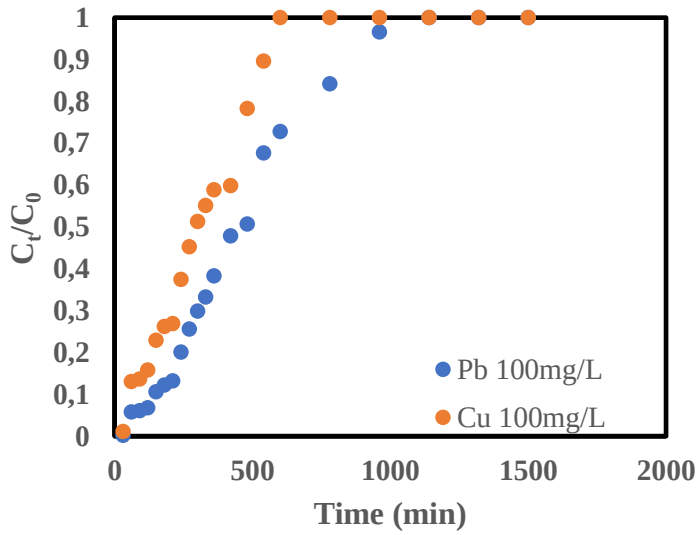

Figure 9.3: Experimental breakthrough curves of Cu^{2+} and Pb^{2+} in binary solution using orange peels.

9.3 Application of breakthrough curve models to the binary system of Cu^{2+} and Pb^{2+}

The breakthrough curves obtained from the binary systems of Cu^{2+} and Pb^{2+} for the various initial concentrations studied were fitted with the existing models namely; Thomas, Yoon Nelson, and Bohart Adams model. The values obtained for the model parameters are summarized in **Table 9.2** below.

The Thomas model showed that an increase in initial concentration resulted in a decrease in the values of K_{Th} and a corresponding increase in the values of q_o. This trend is observed for both cu^{2+} and Pb^{2+} as the initial concentration increased. The values of K_{Th} for Pb^{2+} at each condition are lower than Cu^{2+} while the values of q_o for Pb^{2+} is higher than Cu^{2+} in all the different initial concentrations. The high correlation coefficients ($R^2 > 0.9$) were obtained at the initial concentrations of 10 mg/L and 50 mg/L for Thomas and Yoon Nelson models while the R^2 for 100 mg/L was less than 0.9. This suggests that the experimental data agree well with the Thomas and Yoon Nelson models at lower concentrations.

Table 9.2: Breakthrough model data for binary bio-sorption of Cu^{2+} and Pb^{2+}.

Parameter	Thomas model			Yoon Nelson model			Bohart Adams model		
	KTh *10^{-4} (Lmin^{-1}mg^{-1})	**qo (mg/g)**	**R^2**	**KYN (min^{-1})**	**τ (min)**	**R^2**	**KBA*10 -4 (Lmin^{-1}mg^{-1})**	**No (mg/L)**	**R^2**
Metal ion concentration (10mg/L)									
Pb	2.1	10.092	0.955	0.0021	2018.38	0.952	1.3	7089.11	0.913
Cu	2.4	9.073	0.979	0.0024	1814.53	0.977	1.7	6438.03	0.966
Metal ion concentration (50mg/L)									
Pb	1.54	14.781	0.926	0.0077	591.26	0.924	0.86	10690.64	0.807
Cu	2.0	9.338	0.965	0.0100	373.50	0.962	1.14	6731.49	0.841
Metal ion concentration (100mg/L)									
Pb	0.77	23.556	0.861	0.0077	471.12	0.860	0.45	17012.46	0.606
Cu	0.95	15.95	0.875	0.0095	319	0.873	0.59	11182.03	0.692

9.4 Summary

In this chapter, the fixed-bed column study of binary bio-sorption of Cu^{2+} and Pb^{2+} was investigated. The adsorption capacity of orange peels in the presence of both metal ions was explained. The findings are summarized below.

- The breakthrough curves of binary systems of Cu^{2+} and Pb^{2+} are different from the single system which explains the interaction of the metal ions.
- An increase in the influent metal ion concentration resulted in a steeper breakthrough curve which drew the breakthrough curve closer to the origin as the binding site was quickly saturated.
- The breakthrough time decreased with increased initial concentration for both metals.
- The breakthrough curves of Cu^{2+} reached a breakthrough point faster than Pb^{2+} which suggests that Cu^{2+} has less affinity for the binding sites on the surface of the bio-sorbent.

- The adsorption capacity of Pb^{2+} was consistently higher than Cu^{2+} for all the initial concentrations considered, which was influenced by the binding strength of Pb^{2+}.
- The Thomas and Yoon Nelson models performed well with the experimental data for initial concentrations 10 mg/L and 50 mg/L.
- Although the fitting through the empirical models (Thomas and Yoon Nelson) performed well. The equilibrium isotherm data obtained from batch study can be used to predict the adsorption breakthrough curve for the binary solute system of copper and lead in a fixed-bed column.

CHAPTER 10

10 Model Development for the Binary Solute System of Copper and Lead Removal in a Fixed-Bed Column

10.1 Introduction

Mathematical modelling has a very significant part in the scale-up process of laboratory experimental study to industrial scale. Different empirical models have been used to describe the bio-sorption process in the dynamic study as demonstrated in chapter 9. Many studies have been reported on the removal of heavy metal ions from an aqueous solution using a fixed-bed column. Most of these studies are based on single metal systems only while few of these works have applied phenomenological mathematical modelling which is a significant tool for the industrial application of the process. The development of the mathematical model to describe the fixed-bed adsorption process is tedious because it involves the estimation of equilibrium and kinetic data and other necessary parameters. This approach is more tedious and complex for multicomponent systems due to an increase in the parameters required to solve the model. Researchers have complemented column study analysis with the development of mechanistic models and computer simulation as an efficient tool for explaining the kinetic behaviour of the fixed bed column, prediction of the breakthrough curves, and the scale-up technology.

Therefore, in this chapter, a mathematical model is developed to describe the binary bio-sorption of Cu^{2+} and Pb^{2+} ions onto orange peels in a fixed bed column.

10.2 Mathematical Modelling

In developing a mathematical model to describe the adsorption of Cu-Pb in a binary system using a fixed-bed column with orange peels some assumptions were considered as stated below.

i. The physical characteristics of the fluid phase and the bio-sorbent are constant, with no chemical reaction.
ii. Constant flow rate axially dispersed plug flow with negligible radial dispersions.
iii. Constant temperature and pressure
iv. Constant column void fraction

v. The mass transfer resistance in the outer film is negligible

vi. The linear driving force (LDF) is used to explain the mass transfer.

vii. The Langmuir isotherm is used to describe the bio-sorption equilibrium.

The mathematical model was developed from the mass balance equation of the solid and liquid phases based on the above assumptions in the fixed bed column. The mass balance of a section dz length of the bed is expressed as.

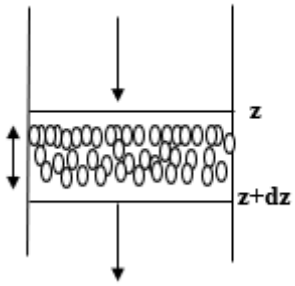

Figure 10.1. Mass balance in the element of a fixed bed column

Figure 10.1 depicts an elemental portion of the fixed bed column that was considered to develop a mathematical model to describe the dynamics of a fixed bed adsorption column. A mass balance is taken around the elemental section of the column following the principle of conservation of mass.

$$Rate\ of\ material\ in - Rate\ of\ material\ out + Rate\ of\ material\ generation\ by\ adsorption = Rate\ of\ material\ accumulation \quad (10.1)$$

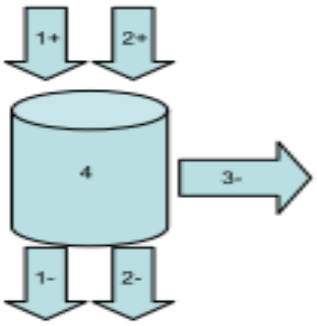

Figure 10.2. Mass conservation of the elemental section of the column

i. Convective mass transfer: (+1) - (1-) = $-U\frac{\partial C}{\partial z}$

Where; U is the superficial velocity, ms^{-1}

C is the adsorbate concentration in the mobile phase, mg/L

Z is the axial coordinate, m

ii. Axial dispersion: (2+) – (2-) = $D_L\frac{\partial^2 C}{\partial Z^2}$

D_L is the axial dispersion coefficient, m^2s^{-1}

iii. Material adsorbed by adsorbent: (3-) = $\frac{(1-\varepsilon)}{\varepsilon}\rho\frac{\partial q}{\partial t}$

Ɛ is the bed porosity

P is the particle density, Kgm^{-3}

q is the average solid-phase adsorbate concentration, mg/g

T is the Time, sec

iv. Accumulation of the adsorbate: (4) = $\frac{\partial C}{\partial t}$

$$\frac{\partial C(z,t)}{\partial t} + U\frac{\partial C(z,t)}{\partial z} + \frac{(1-\varepsilon)}{\varepsilon}\rho_p\frac{\partial\{q(z,t)\}}{\partial t} - D_L\frac{\partial^2 C(z,t)}{\partial^2 z} = 0 \qquad (10.2)$$

The linear driving force (LDF) was used to describe the intraparticle mass transfer,

$$\frac{\partial\{q(z,t)\}}{\partial t} = K_{LDF}[q^*(z,t) - \{q(z,t)\}] \qquad (10.3)$$

To solve this mathematical model, other model parameters are required namely D_L and K_{LDF}in Equation (10.2) and (10.3) respectively. The values of the parameters were obtained by using Equations 3.32 to 3.35.

The design of an efficient adsorption process for binary solute needs the development of a model that can describe the dynamic behavior in a fixed bed column with the selected adsorbent. The prediction of column dynamics behavior requires the simultaneous solution of partial differential equations (PDE) representing the material balance around the elemental section of the adsorption bed. The simultaneous solution of the PDE is tedious and time-consuming hence, (10.2 was converted to ordinary differential equations (ODE) using the finite difference approximation method. The ODE was solved using an ode solver (ODE15s) in

MATLAB, this was then followed by a code written using MATLAB R2019a to solve the numerical equations together with the intraparticle mass transfer. **Table 10.1** shows the properties and parameters used in solving the ode.

Table 10.1: Properties and parameters used for solving ODE.

Adsorbent	Bed properties	Equilibrium (Afolabi, Musonge P and B.F 2020)	Mass transfer
ρ=571-615kgm^{-3}	L=3cm	q_{maxCu}=40.18	D_{peCu}=2.8x10^{-7}cm^{2}s^{-1}
d_p=0.69x10^{-6} -1.43x10^{-6}m	Ɛ=0.58	b_{cu}=0.15	D_{pePb}=6.0x10^{-8}cm^{2}s-1
	d=2.3cm	q_{max}=38.05	D_{ax}=2.74x10^{-8}cms^{-1}-5.68x10^{-8}cms^{-1}
	Q=0.05cm^{3}s^{-1}	b_{Pb}=4.77	
	Uo=1.2x10-^{4}ms^{-1}	K_{LCu}=0.167L/mg	
		K_{LPb}=0.092L/mg	
		dq/dc_{Cu}=8.0206	
		dq/dc_{Pb}=3.1059	

10.3 Finite Difference Approximation Method

The finite-difference approximation gives a function expression at different points that approximate a partial derivative (Erdogan Madenci and Guven 2015). To approximate a partial difference equation, an approximation of various derivatives of the PDE at different mesh points is done. The boundary and initial conditions associated with the PDEs are incorporated to generate linear systems of equations which gives the actual solution approximation at the mesh points. Therefore, this method is used to solve ordinary differential equations ODEs – Bounded value problems (BVP). To solve this problem using the finite difference method, we divide the interval of the bed into 'n' subintervals.

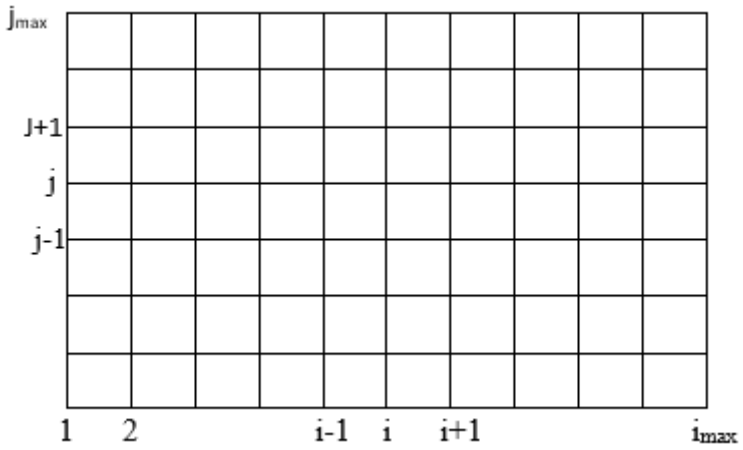

Figure 10.3. Discrete difference grid

The finite approximation is applied to the first and second-order PDE derivatives. From Figure 10.3, 'j' is the mesh point along with the discretized domain, where j = 0, 1, 2, ….., n. The column length 'L' and the number of the mesh points 'n' are defined below.

$$Spatial\ step\ size\ dz = \frac{L}{n} \tag{10.4}$$

Discretization of PDE derivatives for component 'i' along the j-direction of the specified domain.

The forward difference;

$$\frac{\partial Ci}{\partial z} = \frac{C_{i,j+1} - C_{i,j}}{z} \tag{10.5}$$

The backward difference;

$$\frac{\partial Ci}{\partial z} = \frac{C_{i,j} - C_{i,j-1}}{z} \tag{10.6}$$

The forward and backward difference;

$$\frac{\partial^2 Ci}{\partial z^2} = \frac{\left.\frac{\partial Ci}{\partial z}\right|_{FD} - \left.\frac{\partial Ci}{\partial z}\right|_{BD}}{z} \tag{10.7}$$

$$\frac{\partial^2 C_i}{\partial z^2} = \frac{\frac{C_{i,j+1} - C_{i,j}}{z} - \frac{C_{i,j} - C_{i,j-1}}{z}}{z} \quad (10.8)$$

$$\frac{\partial^2 C_i}{\partial z^2} = \frac{C_{i,j+1} - 2C_{i,j} + C_{i,j-1}}{z^2} \quad (10.9)$$

The central difference;

$$\frac{\partial Ci}{\partial z} = \frac{C_{i,j+1} - C_{i,j-1}}{2z} \quad (10.10)$$

10.4 MATLAB Code

MATLAB is one of the most used engineering applications for the numerical solution of ordinary differential equations (ODEs). It has various ODE solvers which ensure odes are solved accurately and more efficiently based on the stiffness of the ODE. A differential equation is said to be stiff if the solution changes significantly when close to the point of integration. Hence, this type of solution employs a numerical technique that uses smaller integration intervals rather than large intervals. The choice of solver and stiffness is mainly influenced by the efficiency of the solution. To increase the efficiency while solving the ODE equation, a solver that makes use of the largest step and sustains an accurate solution is selected. Therefore, ode15s is chosen for the numerical solution of the ODEs obtained in this study. The code developed for solving the discretized equation followed the steps as shown in the flow diagram below. To execute the ode solver, the code is divided into two sections namely; the function script and the main program file. The scripts are compiled in **Appendix C1**.

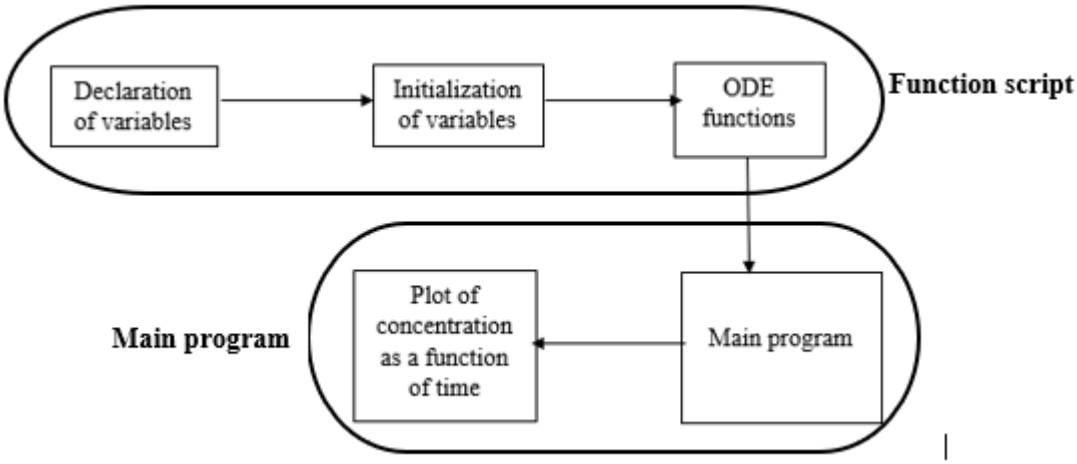

Figure 10.4. Flow diagram of the MATLAB execution

10.4.1 Function Script

In the execution of the function, the variables are declared, the initial conditions are stated and the selected ODE solver is defined.

10.4.1.1 Declaration of variables

In this section, the variables in the equation are declared.

cFeed = 50 Feed concentration

L = 3 Column length

t0 = 0 Initial Time

tf = 4000 Final time

dt = 0.5 Time step

z = 0:0.005:L Mesh generation

t = t0:dt:tf Time vector

n = numel(z) Size of mesh grid

10.4.1.2 Initialization of Variables

The initial and boundary conditions are stated in this section.

c0 = zeros(n,1)

c0(1) = cFeed

q0 = zeros(n,1) t = 0, q = 0 for all z,

y0 = [c0 ; q0]

10.4.1.3 ODE function

The ODE function to be used is stated here and the variables to be plotted are determined.

ODE15S Solver

[T, Y] = ode15s(@(t,y) MyFun(t,y,z,n),t,y0);

10.4.2 Main Program

The main program comprises the function, definition of constants in the equation, allocation of variables and the constraints.

10.4.2.1 Function

The chosen function is called.

function DyDt=MyFun(~, y, z, n)

10.4.2.2 Definition of variables

In this section, the constants as specified in the equation are defined.

D = Axial Dispersion coefficient

U = Superficial velocity

Ɛ = Voidage fraction

K_L = Mass Transfer Coefficient

q_{max}= Langmuir parameter

b= Langmuir constant

10.4.2.3 Allocation of variables

The initial variables are defined here with necessary allocations.

c = zeros(n,1)

q = zeros(n,1)

DcDt = zeros(n,1)

DqDt = zeros(n,1)

10.5 Mathematical Model Results

The results obtained from the mathematical model solved based on the linear driving force model together with the experimental data are shown in **Figure 10.5** to **Figure 10.7**. The breakthrough time decreased with an increasing initial concentration which suggests that the bio-sorbent gets saturated with an increasing initial concentration hence the breakthrough curves move closer to the origin. Also, the breakthrough curves of copper bio-sorption reached breakthrough point faster than lead for all the initial concentrations considered which supports the experimental results. The model results showed that the mathematical model can be used to describe the binary solute breakthrough adsorption curves however the model did not perform well at a low initial concentration as shown in **Figure 10.5**. Although the development of a mathematical model for the column adsorption of binary solute is tedious and laborious, these results have shown that batch results can be incorporated into the model development to predict breakthrough adsorption curves, especially at high initial concentrations.

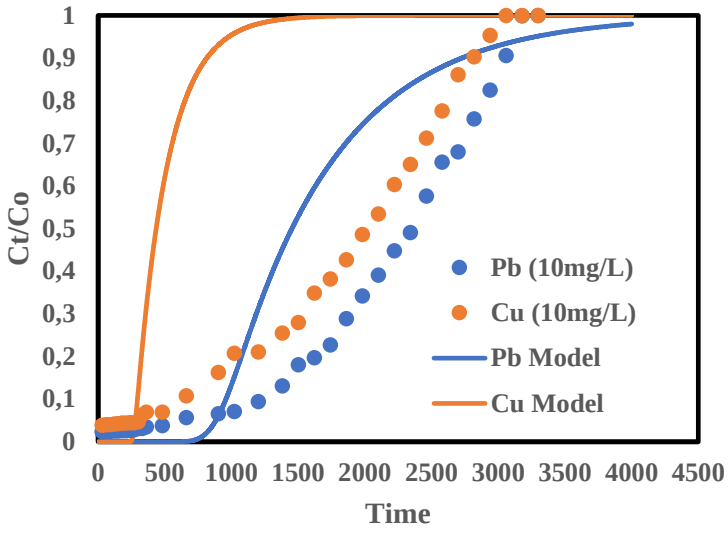

Figure 10.5. Experimental and mathematical model breakthrough curves of copper and lead in binary solute solution with initial concentration 10 mg/L.

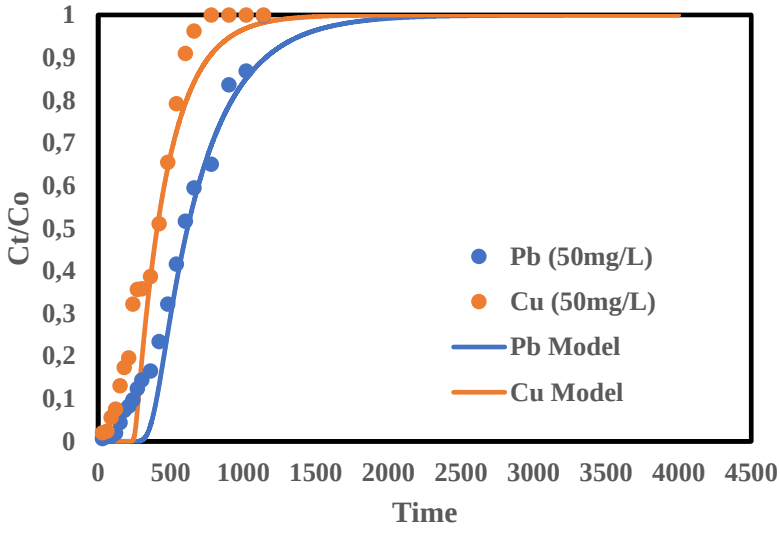

Figure 10.6. Experimental and mathematical model breakthrough curves of copper and lead in binary solute solution with initial concentration 50 mg/L.

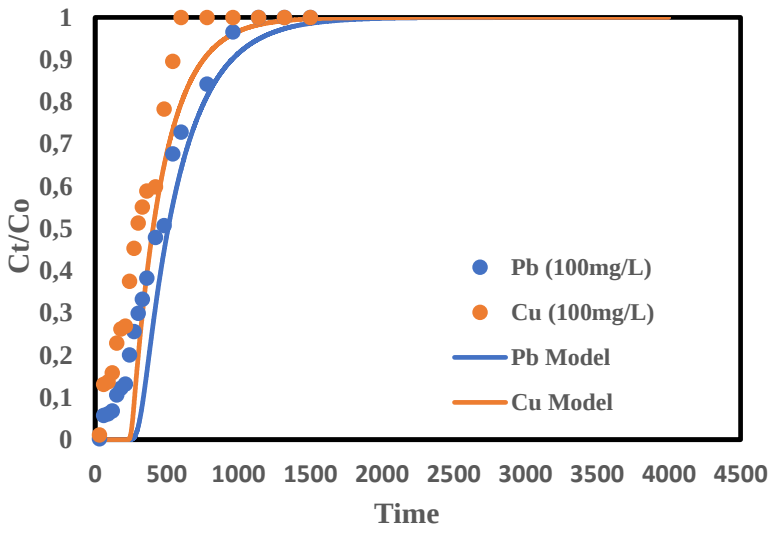

Figure 10.7. Experimental and mathematical model breakthrough curves of copper and lead in binary solute solution with initial concentration 100 mg/L.

10.6 Comparison of the Performance of the Existing Model with the Developed Model .

The Thomas model has been proven to be more efficient and accurate than other existing column adsorption models (Musonge 2020) and is therefore used to compare with the developed mathematical model. The graphical representations are shown in **Figures 10.8** to **10.10**. The Thomas model followed a similar trend with the experimental and developed models, such that the breakthrough curves of copper bio-sorption reached breakthrough point faster than lead. However, the Thomas model fitted the experimental data better than the developed model. This could be because of approximation and iterations involved in the mathematical model.

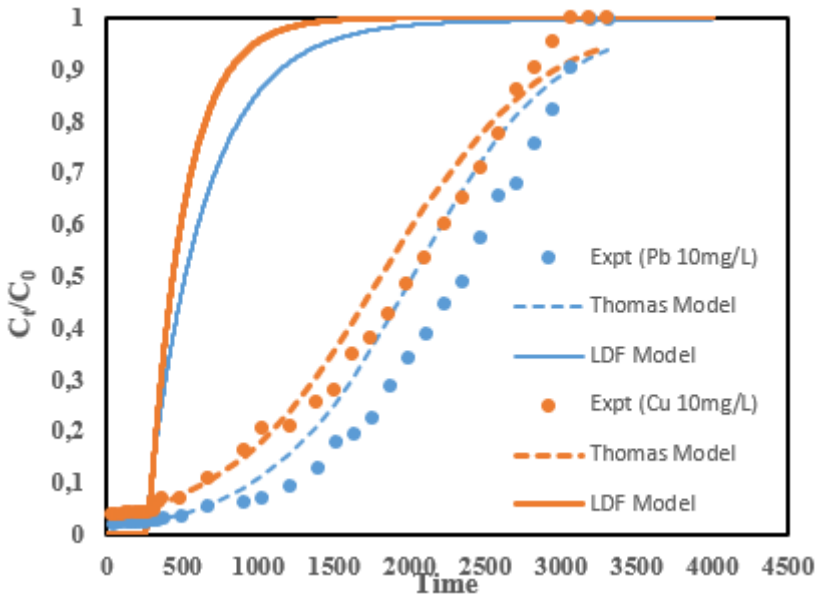

Figure 10.8. Experimental, Thomas and mathematical model breakthrough curves of copper and lead in binary solute solution with initial concentration 10 mg/L

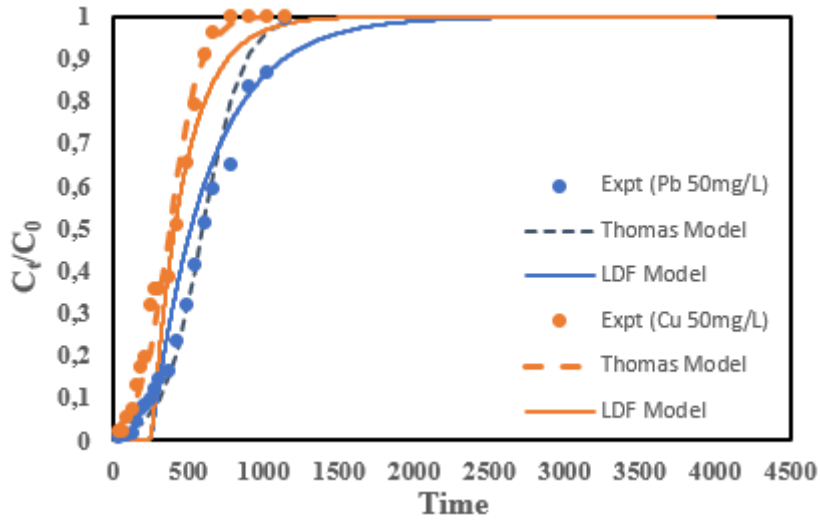

Figure 10.9. Experimental, Thomas and mathematical model breakthrough curves of copper and lead in binary solute solution with initial concentration 50 mg/L

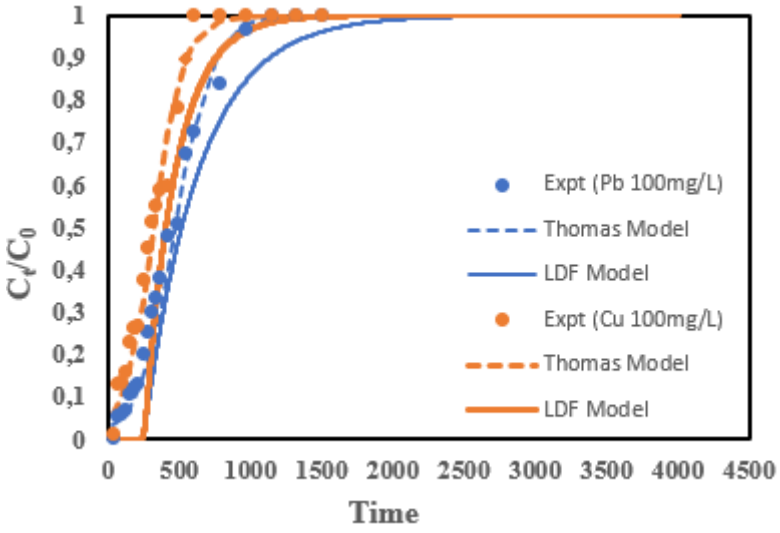

Figure 10.10. Experimental, Thomas and mathematical model breakthrough curves of copper and lead in binary solute solution with initial concentration 10 mg/L

10.7 Statistical Validity

The statistical validation was used to evaluate the performance of the Thomas and the mathematical model. Three different error functions were examined in this study namely: mean absolute error, root mean square error, and the coefficient correlation as represented in **Table 8.10**. The Thomas model gave the lowest mean absolute error (MAE) value of 0,08 while the mathematical model gave the MAE value of 0,9 which explains the deviations of the models from the experimental results.

Table 10.2: Breakthrough curves regression and error analysis for Thomas and developed models

Parameters	**Thomas**			**Developed model**		
Binary solute Pb-Cu	**RMSE**	**MAE**	**R^2**	**RMSE**	**MAE**	**R^2**
Concentration 10mg/L						
Pb	0.081	0.058	0.955	0.697	0.583	0.735
Cu	0.050	0.037	0.979	0.306	0.124	0.736
Concentration 50mg/L						
Pb	0.051	0.035	0.926	0.883	0.822	0.736
Cu	0.053	0.038	0.965	0.924	0.882	0.733
Concentration 100mg/L						
Pb	0.048	0.036	0.861	0.904	0.854	0.735
Cu	0.047	0.035	0.875	0.925	0.884	0.734

10.8 Summary

In this chapter, a mechanistic model was developed from the mass balance equation to explain the behaviour of the breakthrough curve of copper and lead in a binary solute system. The effect of varying initial concentrations of the metal ions was investigated. The findings and performance of the model are outlined below.

- Complete breakthrough curves were obtained for both metal ions at the different initial concentrations chosen.
- The breakthrough time decreased with increasing initial concentration for both metal ions.
- The breakthrough curves representing copper reached breakthrough point faster than lead at the different initial concentrations. This suggests that copper has a lower affinity for the binding sites on the surface of the bio-sorbent.
- The mathematical model described the experimental results well for higher initial concentrations while there are deviations at a lower initial concentration (10mg/L).

- The mathematical model has shown beyond reasonable doubt that equilibrium isotherm studies carried out in the batch experiments are important for describing breakthrough adsorption curves.
- Therefore, the mathematical model developed for the binary system is suitable for predicting the breakthrough curves using batch experimental results.

CHAPTER 11

11. Conclusions and Recommendations

11.1 Main Findings and Conclusions

This study investigated the following specific objectives as outlined in Chapter 1:

- To determine the characteristics of the bio-sorbents before and after adsorption using analytical techniques (FTIR, SEM-EDS, XRD, and BET) and the point of zero charges of the bio-sorbents.
- To optimize the interactive effects of operating parameters such as pH, initial concentration, adsorbent dosage, and particle size on the single and binary solute adsorption of Cu^{2+} and Pb^{2+} using orange and banana peels
- To determine the equilibrium and kinetic parameters of single and binary bio-sorption of Cu^{2+} and Pb^{2+} using orange and banana peels.
- To study the effect of initial concentration, flow rate, and bed height on the single and binary bio-sorption of Cu^{2+} and Pb^{2+} using a fixed-bed column.
- To develop a suitable model for binary solute competitive adsorption breakthrough curves.

The main findings obtained for each of the objectives are discussed below:

On the first objective, orange and banana peels adsorbents were analyzed to determine their physical and chemical properties, surface morphology, surface charge, functional group, surface area, and pore size. These analyses were done using analytical techniques; SEM-EDS, FTIR, XRD, and BET. The FTIR spectra of both bio-sorbents contain hydroxyl, phenol, carbonyl, carboxyl, and aminyl groups before adsorption. There were significant shifts in the peaks representing hydroxyl and carboxyl groups after adsorption of copper and lead, which was common to both bio-sorbents. This showed the role of hydroxylic and carboxylic groups in the adsorption of copper and lead in single and binary systems. The SEM analysis was used to explain the morphological structure of the bio-sorbents before and after adsorption. The surface of banana peels showed a rough, irregular, and porous surface before adsorption. While the surface became uniform, smooth, and covered after adsorption of copper and lead which showed the presence of the metal ions on the surface of the bio-sorbent. The surface structure

of orange peels before adsorption was rough, non-uniform and there was the presence of pores while the surface became smooth, pores were covered and shiny after adsorption of copper and lead. The elemental composition (EDS) of banana peels revealed the presence of carbon, oxygen, silicon, and potassium on the surface of the bio-sorbents before adsorption. After adsorption, there was a significant change in the percentage composition of the elements and the presence of adsorbed metal ions (copper and lead) was evident. The EDS of orange peels bio-sorbent revealed the presence of carbon, oxygen, and minute amounts of naturally occurring metals (magnesium, potassium, and calcium) and sulphur. The naturally occurring metals disappeared after adsorption and were displaced with the adsorbed metal ions. XRD was used to determine the crystallinity of the bio-sorbents. There was no discrete mineral phase identified on the surface of orange and banana peels which showed that both bio-sorbents are completely amorphous. The pHpzc of both bio-sorbents showed that they are acidic and therefore suitable for cation adsorption.

With regards to objective two, the interactive effect of operating parameters in the adsorption of copper and lead for single and binary systems was investigated. The experimental design was done using face-centered CCD adapted from the RSM using four factors (initial concentration, pH, adsorbent dosage, and particle size) in the single systems adsorption onto the bio-sorbents. The model fitness for the bio-sorption of copper and lead using orange and banana peels showed closeness between the predicted and experimental values. The regression models obtained for the bio-sorption of copper and lead using both bio-sorbents are significant. The bio-sorption mechanism of Cu^{2+} and Pb^{2+} onto orange and banana peels revealed that there was an exchange of ions between the copper ions and lead ions in the solution and the ions present on the surface of bio-sorbents.

For the binary solute, the interactive effect of three factors (initial concentration, adsorbent dosage, and particle size) were studied using both bio-sorbents. The validity of the regression model and the agreement between the experimental and predicted values confirmed the validity of the second-order polynomial equation for the binary bio-sorption of copper and lead using orange and banana peels. Pb^{2+} ions were more adsorbed in the binary system than Cu^{2+} ions for both bio-sorbents. The adsorption efficiency of Pb^{2+} and Cu^{2+} in the binary system onto orange and banana peels was greatly influenced by adsorbent dosage then followed by an initial concentration while the particle size had little or no significant impact on the process.

Considering objective three, the isotherm and kinetic studies were conducted to determine the capacity of orange and banana peels for the removal of copper and lead in the single and binary systems and to determine the effect of co-existence of these metals ions in the adsorption process. In the single and binary systems using both bio-sorbents, the adsorption uptake of lead was higher than copper, suggesting that the bio-sorbents have a greater affinity for lead ions. The adsorption equilibrium was well described by the Langmuir isotherm model for both single and binary systems of the metal ions. The kinetic model followed pseudo-second-order for both single and binary systems which suggests that the adsorption mechanism is chemisorption. From the batch results, it can be concluded that orange peels bio-sorbent performed better than banana peels hence, orange peels were selected for column study.

Objective four was explored to determine the performance of orange peels in the removal of copper and lead in a fixed-bed column. The effects of operating parameters such as flow rate, initial concentration, and bed height were studied with a single metal ion. The breakthrough adsorption capacity (Q_b) and the breakthrough time (t_b) decreased with an increase in flow rate while it increased with an increase in bed height for both metal ions. The Q_b increased with an increase in the initial metal ion concentration and a consequent decrease in t_b for both metal ions. A similar trend was observed in the behaviour of both metal ions however, the performance of lead was better than copper for all the parameters. The experimental data were fitted with the empirical models (Thomas, Yoon Nelson, and Bohart-Adams) to ascertain the best-performed model. Thomas and Yoon Nelson's models performed well with a high coefficient of correlation ($R^2 > 0.9$).

Finally, the last objective studied the binary solute adsorption of copper and lead in a fixed-bed column and the development of a mathematical model to explain the behaviour of the breakthrough curves. For this purpose, the effect of initial concentration was investigated in the ratio 1:1. The bio-sorption capacity of Pb^{2+} was consistently higher than the biosorption capacity of Cu^{2+} for all the initial concentrations. This confirms the higher affinity of Pb^{2+} for orange peels irrespective of the initial metal ion concentration.

In addition, the mathematical model developed gave breakthrough curves which described the experimental breakthrough curves fairly well. The mathematical model results followed a similar trend with the experimental results such that the breakthrough curve of copper reached breakthrough point faster than lead for all the initial concentrations considered. Although the

development of a mathematical model for the column adsorption of multicomponent is tedious and laborious, these results have shown that batch results can be used to predict breakthrough adsorption curves. In conclusion, the batch and column results showed that both bio-sorbents have a higher affinity for lead than copper. This is because lead which has a higher affinity for adsorption on bio-sorbent has a lower hydration ion radius when compared to copper.

11.2 Implications of the study

This section discusses the implications of the major results obtained in this study. orange and banana peels are microporous bio-sorbents with functional groups capable of removing copper and lead from wastewater. Generally, fruit peels contain high hydrogen and carbon content (Pathak, Mandavgane and Kulkarni 2017). Most fruit peels have an acidic surface charge thereby enhancing the adsorption of cations from aqueous solution. In the presence of copper and lead ions in a solution, the bio-sorbents have more affinity for lead ions than copper ions because of their higher ionic radius. The solution pH, adsorbent dosage, and the initial concertation are significant operating parameters that mostly influence the adsorption capacity of fruit peels. Pathak Pranav, Mandavgane Sachin and Kulkarni Bhaskar (2015) reported that solution pH is the most important parameter in an adsorption process using fruit peels. It affects the solution chemistry, the functional group activities, and the composition of the adsorbate. The adsorbent dosage determines the extent of active sites available for adsorption and also decides the percentage removal of the adsorbate while the initial concentration provides the required driving force to overcome the mass transfer resistance between the adsorbate and the adsorbate. Shafiee, Akbari and Ghiassimehr (2018) investigated the removal of lead from wastewater using Lawsonia inermis (Henna). The effect of operating parameters such as initial metal concentration, solution pH, and adsorbent dosage was studied. Adesanmi *et al.* (2020) investigated the effect of pH, adsorbent dosage, and initial concentration on the removal of heavy metal ions from an aqueous solution using banana and orange peels. Kumar *et al.* (2018) reported the effect of pH, adsorbate concentration, and adsorbent dosage on the removal of copper using dried orange peels. To the best of the author's knowledge, no work has been reported on the interaction of these operating parameters in the presence of multi-solute. Therefore, this study has investigated the interactive effects of the operating parameters in the binary solute system since, it is very unlikely that wastewater will contain a single solute.

The equilibrium and kinetic studies in both single and binary systems using orange and banana peels were well fitted with Langmuir and pseudo-second-order models respectively. the Langmuir isotherm model suggests adsorption occurred on monolayer while pseudo-second-order kinetic model implies that the adsorption mechanism is chemisorption. Deshmukh *et al.* (2017) used dried banana peels as an adsorbent for the removal of cadmium from wastewater. The equilibrium and kinetic experimental data were well fitted with Langmuir and the pseudo-second-order model. Shafiee, Akbari and Ghiassimehr (2018) reported that Freundlich isotherm model performed better than Langmuir isotherm in the adsorption of lead using Hienna while the pseudo-second-order kinetic model fitted the experimental data. Obike *et al.* (2018) reported the equilibrium experimental data of copper, cadmium, lead, and iron adsorption onto cocoa pod fitted well with Langmuir model while the kinetic fitted well with pseudo-second-order model. Saravanan *et al.* (2021) reported the kinetic and equilibrium studies of Cr(VI) removal from synthetic solution using mixed fruit peels. The equilibrium and kinetic data were best fitted with Langmuir and pseudo-second-order model respectively. Binauhan *et al.* (2021) investigated and compared the adsorption capacity of fruit peels for the removal of Al(III) and Cu(II) ions in single and binary aqueous systems. The kinetic and isotherm experimental data were best fitted with pseudo-second-order and Langmuir isotherm model respectively. Babapoor *et al.* (2022) studied the removal of chromium and iron from contaminated solutions using tangerine peel, bovine gut, tea waste, and sunflower seed hull. The adsorption isotherms were well fitted with Langmuir and Freundlich isotherm models while the adsorption kinetics were well validated with the pseudo-second-order kinetic model.

The flow rate, bed height, and initial metal ion concentration are the most studied operating parameters in a fixed-bed column (Patel 2019). There are many kinetic models used to describe the dynamic behavior in a column, however, the Thomas model has been reported by many researchers as the best-performed model (Musonge 2020). The adsorption capacity of copper and lead using orange peels in a fixed-bed column decreased with increasing flow rate while the adsorption capacity increased with increasing bed height and initial metal ion concentration. The experimental data for both single and binary systems of copper and lead were well fitted with Thomas and Yoon Nelson model. Abdolali *et al.* (2017) studied the effect of influent flow rate, metal concentration, and bed depth for the removal of cadmium, copper, lead, and zinc using multi metal-binding bio-sorbent in a fixed-bed column. The amount of metal adsorbed decreased with increasing flow rate and increased with increasing initial concentration. The

Thomas model described the dynamic behavior better than other models. Vera *et al.* (2018) reported the biosorption of lead and cadmium with sugarcane bagasse in a fixed-bed column. The Thomas and Yoon Nelson models successfully fitted with the experimental data. Mitra and Das (2019) investigated the removal of chromium using *Psidium guajava* leaves in a column study. The authors studied the effect of operating parameters such as flow rate, bed depth, and initial concentration. The metal uptake increased with increasing initial concentration while the experimental data fitted well with the Thomas model.

The existing dynamic kinetic models were developed based on a single solute system, however, wastewater contains more than one solute. Martín-Lara *et al.* (2016) studied binary biosorption of copper and lead in a packed bed reactor using a pinecone shell. The adsorption of lead was higher than copper which confirmed higher selectivity of pinecone shell for lead. However, no kinetic model was used to describe the dynamic behavior of the breakthrough curves. In this study, a mathematical model was developed to describe the behavior of the breakthrough curve in a binary system. the developed model made use of results obtained from the batch experimental studies which were substituted into the linear driving force model to quantify the adsorption capacity of the system.

11.3 Recommendations

Despite milestones attained in this study, there are still more and future works to be done. Therefore, the following outlined areas can be investigated for further research works.

- The bio-sorbents used in this study were explored in their natural form. Many physical treatment techniques can be applied to modify the surface structure of the bio-sorbents thereby enhancing their performance without creating other disposal problems. This can also allow for a study on adsorbent regeneration.
- This research work focused on the single and binary adsorption of heavy metals using synthesized wastewater. Future work should focus on the use of real wastewater with multi-metal ions to determine the practical application of the findings.
- The binary solute adsorption system used a ratio of 1:1 for all initial metal ion concentrations. Future work should also investigate a variation in the ratio of the metal ion.

- The height of the laboratory scale column should be increased progressively to a pilot-scale size of about 1m, to establish a fully developed flow to obtain design parameters for scale-up.
- The design of columns in series should be investigated to eliminate wastage in terms of unused adsorbed.

12. REFERENCES

A. Streitwieser and C. H. Heathcock. 1989. *Quimica Organica*. 3rd ed. Mexico: McGraw-Hill.

Abbas, S. H., Ismail, I. M., Mostafa, T. M. and Sulaymon, A. H. 2014. Biosorption of heavy metals: a review. *J. Chem. Sci. Technol*, 3 (4): 74-102.

Abd-Talib, N., Chuong, C. S., Mohd-Setapar, S. H., Asli, U. A., Pa'ee, K. F. and Len, K. Y. T. 2020. Trends in Adsorption Mechanisms of Fruit Peel Adsorbents to Remove Wastewater Pollutants (Cu (II), Cd (II) and Pb (II)). *Journal of Water and Environment Technology*, 18 (5): 290-313.

Abdolali, A., Ngo, H. H., Guo, W., Zhou, J. L., Zhang, J., Liang, S., Chang, S. W., Nguyen, D. D. and Liu, Y. 2017. Application of a breakthrough biosorbent for removing heavy metals from synthetic and real wastewaters in a lab-scale continuous fixed-bed column. *Bioresource Technology*, 229: 78-87.

Adesanmi, A. S., Evuti, A. M., Aladeitan, Y. M. and Abba, A. H. 2020. Utilization of waste in solving environmental problem: Application of banana and orange peels for the removal of lead (II) ions from aqueous solution of lead nitrate. *Nigeria Journal of Engineering Science and Technology Research*, 6 (1): 18-33.

Afolabi, F. O., Musonge P and B.F, B. 2020. Bio-sorption of CU2+ and PB2+ Ions onto Citrus Sinensis (Orange) Peel. Paper presented at the *SETWM-20, ACBES-20 & EEHSS-20 Nov. 16-17, 2020 Johannesburg (SA)*.

Afolabi, F. O., Musonge, P. and Bakare, B. F. 2021a. Application of the Response Surface Methodology in the Removal of Cu2+ and Pb2+ from Aqueous Solutions Using Orange Peels. *Scientific African*, 13

Afolabi, F. O., Musonge, P. and Bakare, B. F. 2021b. Evaluation of Lead (II) Removal from Wastewater Using Banana Peels: Optimization Study. *Polish Journal of Environmental Studies*, 30 (2): 1-10.

Afolabi, F. O., Musonge, P., Bakare, B. F. and Arellano-Garcia, H. 2021. Bio-sorption of copper and lead ions in single and binary systems onto banana peels. *Cogent Engineering*, 8 (1)

Afroze, S. and Sen, T. K. 2018. A review on heavy metal ions and dye adsorption from water by agricultural solid waste adsorbents. *Water, Air, & Soil Pollution*, 229 (7): 1-50.

Ahmad, H., Ee, C. J. and Baharudin, N. S. 2016. A preliminary study for removal of heavy metals from acidic synthetic wastewater by using pressmud-rice husk mixtures. *IOP Conference Series: Earth and Environmental Science*, 36: 1-8.

Ahmed, M. J. K. and Ahmaruzzaman, M. 2016. A review on potential usage of industrial waste materials for binding heavy metal ions from aqueous solutions. *Journal of Water Process Engineering*, 10: 39-47.

Akpomie, K. G. and Conradie, J. 2020. Banana peel as a biosorbent for the decontamination of water pollutants. A review. *Environmental Chemistry Letters*, 18 (4): 1085-1112.

Aksu, Z. and Gönen, F. 2004. Biosorption of phenol by immobilized activated sludge in a continuous packed bed: prediction of breakthrough curves. *Process Biochemistry*, 39 (5): 599-613.

Alalwan, H. A., Kadhom, M. A. and Alminshid, A. H. 2020. Removal of heavy metals from wastewater using agricultural byproducts. *Journal of Water Supply: Research and Technology—AQUA*, 69 (2): 99-112.

Ali Gh. Khamseh and Ghorbanian, S. A. 2018. Experimental and modeling investigation of thorium biosorption by orange peel in a continuous fixed-bed column. *Journal of Radioanalytical and Nuclear Chemistry*, 317: 871-879.

Amarasinghe, B. and Williams, R. 2007. Tea waste as a low cost adsorbent for the removal of Cu and Pb from wastewater. *Chemical Engineering Journal*, 132 (1-3): 299-309.

Amin, M., Alazba, A. and Amin, M. 2017. Absorption Behaviours of Copper, Lead, and Arsenic in Aqueous Solution Using Date Palm Fibres and Orange Peel: Kinetics and Thermodynamics. *Polish Journal of Environmental Studies*, 26 (2): 543-557.

Amin, M., Alazba, A. and Shafiq, M. 2017a. Batch and fixed-bed column studies for the biosorption of Cu (II) and Pb (II) by raw and treated date palm leaves and orange peel. *Global Nest Journal*, 19: 464-478.

Amin, M. T., Alazba, A. A. and Shafiq, M. 2017b. Removal of Copper and Lead using Banana Biochar in Batch Adsorption Systems: Isotherms and Kinetic Studies. *Arabian Journal for Science and Engineering*, 43 (11): 5711-5722.

Anwar, J., Shafique, U., Waheed uz, Z., Salman, M., Dar, A. and Anwar, S. 2010. Removal of Pb(II) and Cd(II) from water by adsorption on peels of banana. *Bioresource Technology*, 101 (6): 1752-1755.

Aranda-Garcia, E. and Cristiani-Urbina, E. 2020. Hexavalent chromium removal and total chromium biosorption from aqueous solution by Quercus crassipes acorn shell in a continuous up-flow fixed-bed column: Influencing parameters, kinetics, and mechanism. *PloS One*, 15 (1): e0227953.

Araujo, C. S. T., Carvalho, D. C., Rezende, H. C., Almeida, I. L. S., Coelho, L. M., Coelho, N. M. M., Marques, T. L. and Alves, V. N. 2013. *Bioremediation of Waters Contaminated with Heavy Metals Using Moringa oleifera Seeds as Biosorbent*. INTECH.

Arim, A. L., Neves, K., Quina, M. J. and Gando-Ferreira, L. M. J. J. o. C. P. 2018. Experimental and mathematical modelling of Cr (III) sorption in fixed-bed column using modified pine bark. 183: 272-281.

Arunakumara, K., Walpola, B. C. and Yoon, M.-H. 2013. Banana Peel: A Green Solution for Metal Removal from Contaminated Waters. *Korean Journal of Environmental Agriculture*, 32 (2): 108-116.

Asante-Sackey, D., Rathilal, S., V. Pillay, L. and Kweinor Tetteh, E. 2020. Ion Exchange Dialysis for Aluminium Transport through a Face-Centred Central Composite Design Approach. *Processes*, 8 (2)

Ashraf, M. A., Wajid, A., Mahmood, K., Maah, M. J. and Yusoff, I. 2011. Removal of heavy metals from aqueous solution by using mango biomass. *African Journal of Biotechnology*, 10 (11): 2163-2177.

B. Imelik and J. C. Vedrine. 1994. *Catalyst Characterization : Physical Techniques for Solid Materials*. New York: Plenum Press.

Babapoor, A., Rafiei, O., Mousavi, Y., Azizi, M. M., Paar, M., Nuri, A. and Kwapiński, W. 2022. Comparison and Optimization of Operational Parameters in Removal of Heavy Metal Ions from Aqueous Solutions by Low-Cost Adsorbents. *International Journal of Chemical Engineering*, 2022: 1-21.

Babarinde, N. A., Babalola, J. O. and Sanni, R. A. 2006. Biosorption of lead ions from aqueous solution by maize leaf. *International Journal of Physical Sciences*, 1 (1): 23-26.

Badessa, T. S., Wakuma, E. and Yimer, A. M. 2020. Bio-sorption for effective removal of chromium(VI) from wastewater using Moringa stenopetala seed powder (MSSP) and banana peel powder (BPP). *BMC Chem*, 14 (1): 71.

Barakat, M. A. 2011. New trends in removing heavy metals from industrial wastewater. *Arabian Journal of Chemistry*, 4 (4): 361-377.

Barquilha, C. E. R., Cossich, E. S., Tavares, C. R. G. and Silva, E. A. 2017. Biosorption of nickel(II) and copper(II) ions in batch and fixed-bed columns by free and immobilized marine algae Sargassum sp. *Journal of Cleaner Production*, 150: 58-64.

Basu, M., Guha, A. K. and Ray, L. 2019. Adsorption of Lead on Lentil Husk in Fixed Bed Column Bioreactor. *Bioresource Technology*, 283: 86-95.

Beni, A. A. and Esmaeili, A. 2020. Biosorption, an efficient method for removing heavy metals from industrial effluents: a review. *Environmental Technology & Innovation*, 17: 100503.

Bera, S. P., Godhaniya, M. and Kothari, C. 2021. Emerging and advanced membrane technology for wastewater treatment: A review. *Journal of Basic Microbiology*,

Bhatnagar, A. and Minocha, A. 2010. Biosorption optimization of nickel removal from water using Punica granatum peel waste. *Colloids and Surfaces B: Biointerfaces*, 76 (2): 544-548.

Bhatnagar, A., Minocha, A. K. and Sillanpää, M. 2010. Adsorptive removal of cobalt from aqueous solution by utilizing lemon peel as biosorbent. *Biochemical Engineering Journal*, 48 (2): 181-186.

Bhatt, P. K. and Singh, R. P. 2018. The Effects of Toxic Agricultural Wastes on the Environment and Their Manangement. *Cosmos An International Journal of Art & Higher Education* 7(1): 1-7.

Bhaumik, R. and Mondal, N. K. 2014. Optimizing adsorption of fluoride from water by modified banana peel dust using response surface modelling approach. *Applied Water Science*, 6 (2): 115-135.

Bilal, M., Ihsanullah, I., Younas, M. and Ul Hassan Shah, M. 2021. Recent advances in applications of low-cost adsorbents for the removal of heavy metals from water: A critical review. *Separation and Purification Technology*, 278

Bilal, M., Shah, J. A., Ashfaq, T., Gardazi, S. M., Tahir, A. A., Pervez, A., Haroon, H. and Mahmood, Q. 2013. Waste biomass adsorbents for copper removal from industrial wastewater--a review. *Journal of Hazardous materials*, 263 Pt 2: 322-333.

Binauhan, M. G., Adornado, A. P., Tayo, L. L., Soriano, A. N. and C. Rubi, R. V. 2021. Kinetics and Equilibrium Modeling of Single and Binary Adsorption of Aluminum(III) and Copper(II) Onto Calamansi (Citrofortunella microcarpa) Fruit Peels. *Applied Science and Engineering Progress*,

Biswas, S. and Mishra, U. 2015. Continuous Fixed-Bed Column Study and Adsorption Modeling: Removal of Lead Ion from Aqueous Solution by Charcoal Originated from Chemical Carbonization of Rubber Wood Sawdust. *Journal of Chemistry*, 2015: 9.

Bohart, G. and Adams, E. 1920. Adsorption in columns. *Journal of the American Chemical Society*, 42: 523-544.

Box, G. E. and Wilson, K. B. 1951. On the experimental attainment of optimum conditions. *Journal of the Royal Statistical Society: Series B (Methodological)*, 13 (1): 1-38.

Burakov, A. E., Galunin, E. V., Burakova, I. V., Kucherova, A. E., Agarwal, S., Tkachev, A. G. and Gupta, V. K. 2018. Adsorption of heavy metals on conventional and nanostructured materials for wastewater treatment purposes: A review. *Ecotoxicology and environmental safety*, 148: 702-712.

Calero, M., Hernainz, F., Blazquez, G., Tenorio, G. and Martin-Lara, M. A. 2009. Study of Cr (III) biosorption in a fixed-bed column. *Journal of Hazardous materials*, 171 (1-3): 886-893.

Cao, Y.-r., Liu, Z., Cheng, G.-l., Jing, X.-b. and Xu, H. 2010. Exploring single and multi-metal biosorption by immobilized spent Tricholoma lobayense using multi-step response surface methodology. *Chemical Engineering Journal*, 164 (1): 183-195.

Chao, H.-P., Chang, C.-C. and Nieva, A. 2014. Biosorption of heavy metals on Citrus maxima peel, passion fruit shell, and sugarcane bagasse in a fixed-bed column. *Journal of Industrial and Engineering Chemistry*, 20 (5): 3408-3414.

Chatterjee, A. and Schiewer, S. 2011. Biosorption of Cadmium(II) Ions by Citrus Peels in a Packed Bed Column: Effect of Process Parameters and Comparison of Different Breakthrough Curve Models. *CLEAN - Soil, Air, Water*, 39 (9): 874-881.

Chatterjee, A. and Schiewer, S. 2014. Effect of Competing Cations (Pb, Cd, Zn, and Ca) in Fixed-Bed Column Biosorption and Desorption from Citrus Peels. *Water, Air, & Soil Pollution*, 225 (2)

Chatterjee, S., Mondal, S. and De, S. 2018. Design and scaling up of fixed bed adsorption columns for lead removal by treated laterite. *Journal of Cleaner Production*, 177: 760-774.

Chen, Y., Wang, H., Zhao, W. and Huang, S. 2018. Four different kinds of peels as adsorbents for the removal of Cd (II) from aqueous solution: Kinetics, isotherm and mechanism. *Journal of the Taiwan Institute of Chemical Engineers*, 88: 146-151.

Chiban, M., Zerbet, M., Carja, G. and Sinan, F. 2012. Application of low-cost adsorbents for arsenic removal: A review. *Journal of Environmental Chemistry and Ecotoxicology*, 4 (5): 91-102.

Chu, K. H. 2010. Fixed bed sorption: setting the record straight on the Bohart-Adams and Thomas models. *Journal of Hazardous materials*, 177 (1-3): 1006-1012.

Corda, N. and Kini, M. S. 2019. Recent studies in adsorption of Pb(II), Zn(II) and Co(II) using conventional and modified materials:a review. *Separation Science and Technology*, 55 (15): 2679-2698.

Dąbrowski, A., Podkościelny, P., Hubicki, Z. and Barczak, M. 2005. Adsorption of phenolic compounds by activated carbon—a critical review. *Journal of Chemosphere*, 58 (8): 1049-1070.

Dada, A. O., Adekola, F. A., Odebunmi, E. O. and Shon, Y.-S. 2017. Kinetics, mechanism, isotherm and thermodynamic studies of liquid phase adsorption of Pb2+ onto wood activated carbon supported zerovalent iron (WAC-ZVI) nanocomposite. *Cogent Chemistry*, 3 (1)

Dada, A. O., Olalekan, A. P., Olatunya, A. M. and Dada, O. 2012. Langmuir, Freundlich, Temkin and Dubini-Radushkevich Isotherms Studies of Equilibrium Sorption of Zn2+ Unto Phosphoric Acid Modified Rice Husk. *IOSR Journal of Applied Chemistry*, 3 (1): 38-45.

De Gisi, S., Lofrano, G., Grassi, M. and Notarnicola, M. 2016. Characteristics and adsorption capacities of low-cost sorbents for wastewater treatment: a review. *Journal of Sustainable Materials*, 9: 10-40.

Demirbas, A. 2008. Heavy metals adsorption onto agro-based waste materials *Journal of Hazardous Materials*, 157: 220-229.

Deshmukh, P. D., Khadse, G. K., Shinde, V. M. and Labhasetwar, P. 2017. Cadmium Removal from Aqueous Solutions Using Dried Banana Peels as An Adsorbent: Kinetics and Equilibrium Modeling. *Journal of Bioremediation & Biodegradation*, 08 (03): 395.

Dong, Y. and Lin, H. 2017. Competitive adsorption of Pb(II) and Zn(II) from aqueous solution by modified beer lees in a fixed bed column. *Process Safety and Environmental Protection*, 111: 263-269.

Erdogan Madenci and Guven, I. 2015. The Finite element method and Applications in Engineering using ANSYS.

Escudero-Oñate, C., Poch, J. and Villaescusa, I. 2017. Adsorption of Cu(II), Ni(II), Pb(II) and Cd(II) from Ternary Mixtures: Modelling Competitive Breakthrough Curves and Assessment of Sensitivity. *Environmental Processes*, 4 (4): 833-849.

Febrianto, J., Kosasih, A. N., Sunarso, J., Ju, Y.-H., Indraswati, N. and Ismadji, S. 2009. Equilibrium and kinetic studies in adsorption of heavy metals using biosorbent: a summary of recent studies. *Journal of Hazardous materials*, 162 (2-3): 616-645.

Foo, K. Y. and Hameed, B. H. 2010. Insights into the modeling of adsorption isotherm systems. *Chemical Engineering Journal*, 156 (1): 2-10.

Giri, D. D., Jha, J. M., Tiwari, A. K., Srivastava, N., Hashem, A., Alqarawi, A. A., Abd Allah, E. F. and Pal, D. B. 2021. Java plum and amaltash seed biomass based bio-adsorbents for synthetic wastewater treatment. *Environ Pollut*, 280: 116890.

Glueckauf, E. 1955. Theory of chromatography. Part 10.—Formulæ for diffusion into spheres and their application to chromatography. *Trans. Faraday Soc.*, 51 (0): 1540-1551.

Gönen, F. and Serin, D. S. 2012. Adsorption study on orange peel: removal of Ni (II) ions from aqueous solution. *African Journal of Biotechnology*, 11 (5): 1250-1258.

Gorman-Lewis, D., Martens-Habbena, W. and Stahl, D. A. 2019. Cu(II) adsorption onto ammonia-oxidizing bacteria and archaea. *Geochimica et Cosmochimica Acta*, 255: 127-143.

Guechi, E.-K. and Hamdaoui. 2016. Evaluation of potato peel as a novel adsorbent for the removal of Cu (II) from aqueous solutions: equilibrium, kinetic, and thermodynamic studies. *Journal of desalination and water treatment*, 57 (23): 10677-10688.

Guiza, S. 2017. Biosorption of heavy metal from aqueous solution using cellulosic waste orange peel. *Ecological Engineering*, 99: 134-140.

Gunatilake, S. K. 2015. Methods of removing heavy metals from industrial wastewater. *Journal of Methods*, 1 (1): 12-18.

Gupta, S., Kumar, D. and Gaur, J. 2009. Kinetic and isotherm modeling of lead (II) sorption onto some waste plant materials. *Chemical Engineering Journal*, 148 (2-3): 226-233.

Gupta, S., Sireesha, S., Sreedhar, I., Patel, C. M. and Anitha, K. L. 2020. Latest trends in heavy metal removal from wastewater by biochar based sorbents. *Journal of Water Process Engineering*, 38

Gupta, V., Carrott, P., Ribeiro Carrott, M. and Suhas. 2009. Low-cost adsorbents: growing approach to wastewater treatment—a review. *Critical Reviews in Environmental Science and Technology*, 39 (10): 783-842.

Gupta, V., Carrott, P., Singh, R., Chaudhary, M. and Kushwaha, S. 2016. Cellulose: a review as natural, modified and activated carbon adsorbent. *Journal of Bioresource Technology*, 216: 1066-1076.

Harripersadth, C. 2021. Evaluating the Performance of an Eggshell-Bagasse Biosorption system in removing Lead and Cadmium from Aqueous Solutions.

Harripersadth, C., Musonge, P., Makarfi Isa, Y., Morales, M. G. and Sayago, A. 2020. The application of eggshells and sugarcane bagasse as potential biomaterials in the removal of heavy metals from aqueous solutions. *South African Journal of Chemical Engineering*, 34: 142-150.

Hawari, A. H. and Mulligan, C. N. 2007. Effect of the presence of lead on the biosorption of copper, cadmium and nickel by anaerobic biomass. *Process Biochemistry*, 42 (11): 1546-1552.

Hong, Y.-S., Kim, C.-J., Sin, K.-R. and Pak, J.-S. 2018. A new adsorption rate equation in batch system. *Chemical Physics Letters*, 706: 196-201.

Hossain, M., Ngo, H. H., Guo, W. and Nguyen, T. 2012. Removal of copper from water by adsorption onto banana peel as bioadsorbent. *International Journal of Geomate*, 2 (2): 227-234.

Hossain, M. A., Ngo, H. H., Guo, W. S., Nghiem, L. D., Hai, F. I., Vigneswaran, S. and Nguyen, T. V. 2014. Competitive adsorption of metals on cabbage waste from multi-metal solutions. *Bioresource Technology*, 160: 79-88.

Huang, J., Huang, Z.-L., Zhou, J.-X., Li, C.-Z., Yang, Z.-H., Ruan, M., Li, H., Zhang, X., Wu, Z.-J., Qin, X.-L., Hu, J.-H. and Zhou, K. 2019. Enhancement of heavy metals removal by microbial flocculant produced by Paenibacillus polymyxa combined with an insufficient hydroxide precipitation. *Chemical Engineering Journal*, 374: 880-894.

Ismael, I. S., Melegy, A. and Kratochvíl, T. 2012. Lead removal from aqueous solution by natural and pretreated zeolites. *Geotechnical and Geological Engineering*, 30 (1): 253-262.

Issabayeva, G., Aroua, M. K. and Sulaiman, N. M. 2008. Continuous adsorption of lead ions in a column packed with palm shell activated carbon. *Journal of Hazardous materials*, 155 (1-2): 109-113.

J. I. Goldstein, D. E. Newbury, D. C. Joy, C. E. Lyman, P. Echlin, E. Lifshin, L. Sawyer and Michael, J. R. 2003. *Scanning Electron Microscopy and X-Ray Microanalysis*. 3rd ed. New York: Kluwer Academia/Plenum Publishers.

Juang, R., Wu, F. and Tseng, R. 1997. The ability of activated clay for the adsorption of dyes from aqueous solutions. *Journal of Environmental Technology*, 18 (5): 525-531.

Kamsonlian, S., Suresh, S., Majumder, C. and Chand, S. 2011. Characterization of banana and orange peels: Biosorption mechanism. *International Journal of Science Technology & Management*, 2 (4): 1-7.

Khamparia, S. and Jaspal, D. K. 2017. Adsorption in combination with ozonation for the treatment of textile waste water: a critical review. *Frontiers of Environmental Science & Engineering*, 11 (1)

Krstić, V., Urošević, T. and Pešovski, B. 2018. A review on adsorbents for treatment of water and wastewaters containing copper ions. *Chemical Engineering Science*, 192: 273-287.

Kumar, A. and Jena, H. M. 2016. Removal of methylene blue and phenol onto prepared activated carbon from Fox nutshell by chemical activation in batch and fixed-bed column. *Journal of Cleaner Production*, 137: 1246-1259.

Kumar, K., Patavardhan, S. S., Lobo, S. and Gonsalves, R. 2018. Equilibrium study of dried orange peel for its efficiency in removal of cupric ions from water. *International Journal of Phytoremediation*, 20 (6): 593-598.

Kumar, P. S., Ramalingam, S., Kirupha, S. D., Murugesan, A., Vidhyadevi, T. and Sivanesan, S. 2011. Adsorption behavior of nickel (II) onto cashew nut shell: Equilibrium, thermodynamics, kinetics, mechanism and process design. *Journal of Chemical Engineering* 167 (1): 122-131.

Kurniawan, T. A., Chan, G. Y., Lo, W. H. and Babel, S. 2006. Comparisons of low-cost adsorbents for treating wastewaters laden with heavy metals. *Science of the Total Environment*, 366 (2-3): 409-426.

Kweinor Tetteh, E. and Rathilal, S. 2018. Evaluation of the coagulation floatation process for industrial mineral oil wastewater treatment using response surface methodology (rsm). *International Journal of Environmental Impacts: Management, Mitigation and Recovery*, 1 (4): 491-502.

Lagergren, S. 1898. About the theory of so-called adsorption of soluble substances. *Kungliga Svenska Vetenskapsakad. Handingarl*, 24: 1-39.

Lakshmipathy, R. and Sarada, N. C. 2015. A fixed bed column study for the removal of Pb2+ ions by watermelon rind. *Environmental Science: Water Research & Technology*, 1 (2): 244-250.

Lathan, N., Edwards, S., Thomas, C. and Agwaramgbo, L. 2013. Comparative Study of Lead Removal by Extracts of Spinach, Coffee, and Tea. *Journal of Environmental Protection*, 04 (03): 250-257.

Li, Q., Ji, M., Li, X., Song, H., Wang, G., Qi, C. and Li, A. 2019. Efficient co-removal of copper and tetracycline from aqueous solution by using permanent magnetic cation exchange resin. *Bioresource Technology*, 293: 122068.

Liu, C., Ngo, H. H., Guo, W. and Tung, K.-L. 2012. Optimal conditions for preparation of banana peels, sugarcane bagasse and watermelon rind in removing copper from water. *Bioresource Technology*, 119: 349-354.

Liu, J., Yang, H., Gosling, S. N., Kummu, M., Flörke, M., Pfister, S., Hanasaki, N., Wada, Y., Zhang, X. and Zheng, C. 2017. Water scarcity assessments in the past, present, and future. *Earth's Future*, 5 (6): 545-559.

Liu, R. and Lian, B. 2019. Non-competitive and competitive adsorption of Cd(2+), Ni(2+), and Cu(2+) by biogenic vaterite. *Science of the Total Environment*, 659: 122-130.

Mahmoud, M. A. 2016. Kinetics studies of uranium sorption by powdered corn cob in batch and fixed bed system. *J Adv Res*, 7 (1): 79-87.

Malik, D., Jain, C. and Yadav, A. K. 2017. Removal of heavy metals from emerging cellulosic low-cost adsorbents: a review. *Applied water science*, 7 (5): 2113-2136.

Marín, A. B. P., Ortuño, J. F., Aguilar, M. I., Meseguer, V. F., Sáez, J. and Lloréns, M. 2010. Use of chemical modification to determine the binding of Cd(II), Zn(II) and Cr(III) ions by orange waste. *Biochemical Engineering Journal*, 53 (1): 2-6.

Martín-Lara, M. A., Blázquez, G., Calero, M., Almendros, A. I. and Ronda, A. 2016. Binary biosorption of copper and lead onto pine cone shell in batch reactors and in fixed bed columns. *International Journal of Mineral Processing*, 148: 72-82.

Matouq, M., Jildeh, N., Qtaishat, M., Hindiyeh, M. and Al Syouf, M. Q. 2015a. The adsorption kinetics and modeling for heavy metals removal from wastewater by Moringa pods. *Journal of Environmental Chemical Engineering*, 3 (2): 775-784.

Matouq, M., Jildeh, N., Qtaishat, M., Hindiyeh, M. and Al Syouf, M. Q. 2015b. The adsorption kinetics and modeling for heavy metals removal from wastewater by Moringa pods. *Journal of Environmental Chemical Engineering*, 3 (2): 775-784.

Medellin-Castillo, N. A., Padilla-Ortega, E., Regules-Martínez, M. C., Leyva-Ramos, R., Ocampo-Pérez, R. and Carranza-Alvarez, C. 2017. Single and competitive adsorption of Cd(II) and Pb(II) ions from aqueous solutions onto industrial chili seeds (C apsicum annuum) waste. *Sustainable Environment Research*, 27 (2): 61-69.

Medina, T. J., Arredondo, S. P., Corral, R., Jacobo, A., Zárraga, R. A., Rosas, C. A., Cabrera, F. G. and Bernal, J. M. 2020. Microstructure and Pb2+ Adsorption Properties of Blast Furnace Slag and Fly Ash based Geopolymers. *Minerals*, 10 (9)

Mella, B., Barcellos, B. S. d. C., da Silva Costa, D. E. and Gutterres, M. 2017. Treatment of Leather Dyeing Wastewater with Associated Process of Coagulation-Flocculation/Adsorption/Ozonation. *Ozone: Science & Engineering*, 40 (2): 133-140.

Memon, J. R., Memon, S. Q., Bhanger, M., Memon, G. Z., El-Turki, A. and Allen, G. C. 2008. Characterization of banana peel by scanning electron microscopy and FT-IR spectroscopy and its use for cadmium removal. *Colloids and Surfaces B: Biointerfaces*, 66 (2): 260-265.

Mihalache, R., Peleanu, I., Meghea, I. and Tudorache, A. 1998. Competitive adsorption models of organic pollutants from bi-and tri-solute systems on activated carbon. *Journal of Radioanalytical and Nuclear Chemistry*, 229 (1-2): B133-138.

Mitra, T. and Das, S. K. 2019. Cr (VI) removal from aqueous solution using Psidium guajava leaves as green adsorbent: column studies. *Applied Water Science*, 9 (7): 1-8.

Mondal, N. K. 2016. Natural Banana (Musa acuminate) Peel: an Unconventional Adsorbent for Removal of Fluoride from Aqueous Solution through Batch Study. *Water Conservation Science and Engineering*, 1 (4): 223-232.

Mondal, N. K. and Roy, A. 2018. Potentiality of a fruit peel (banana peel) toward abatement of fluoride from synthetic and underground water samples collected from fluoride affected villages of Birbhum district. *Applied Water Science*, 8 (3)

Montgomery, D. C. 2009. *Design and analysis of experiments*. 7th ed. Hoboken, N.J: Wiley.

Moyo, M., Pakade, V. E. and Modise, S. J. 2017. Biosorption of lead(II) by chemically modified Mangifera indica seed shells: Adsorbent preparation, characterization and performance assessment. *Process Safety and Environmental Protection*, 111: 40-51.

Muhamad, H., Doan, H. and Lohi, A. 2010. Batch and continuous fixed-bed column biosorption of Cd2+ and Cu2+. *Chemical Engineering Journal*, 158 (3): 369-377.

Musonge, P. 2020. Statistical Evaluation of Models for the Removal of Heavy Metals in Adsorption Columns Using Bio-Waste Materials. *International Journal of Engineering Research and Technology*, 13 (10)

Myers, R. H., Montgomery, D. C. and Anderson-Cook, C. M. 2016. *Response Surface Methodology*. Wiley.

Naidu, G., Ryu, S., Thiruvenkatachari, R., Choi, Y., Jeong, S. and Vigneswaran, S. 2019. A critical review on remediation, reuse, and resource recovery from acid mine drainage. *Environ Pollut*, 247: 1110-1124.

Nascimento, G. E. d., Duarte, M. M. M. B., Campos, N. F., Rocha, O. R. S. d. and Silva, V. L. d. 2014. Adsorption of azo dyes using peanut hull and orange peel: a comparative study. *Environmental Technology*, 35 (11): 1436-1453.

Nguyen, T. A. H., Ngo, H. H., Guo, W. S., Zhang, J., Liang, S., Yue, Q. Y., Li, Q. and Nguyen, T. V. 2013. Applicability of agricultural waste and by-products for adsorptive removal of heavy metals from wastewater. *Bioresource Technology*, 148: 574-585.

Nguyen, T. C., Loganathan, P., Nguyen, T. V., Kandasamy, J., Naidu, R. and Vigneswaran, S. 2018. Adsorptive removal of five heavy metals from water using blast furnace slag and fly ash. *Environmental Science and Pollution Research International*, 25 (21): 20430-20438.

Nleya, Y., Simate, G. S. and Ndlovu, S. 2016. Sustainability assessment of the recovery and utilisation of acid from acid mine drainage. *Journal of Cleaner Production*, 113: 17-27.

Nour T. Abdel-Ghani and El-Chaghaby, G. A. 2014. Biosorption for metal ions removal from aqueous solutions: A review of recent studeis. *international Journal of Latest Research in Science and Technology*, 3 (1): 24 - 42.

Obike, A. I., Igwe, J. C., Emeruwa, C. N. and Uwakwe, K. J. 2018. Equilibrium and kinetic studies of Cu (II), Cd (II), Pb (II) and Fe (II) adsorption from aqueous solution using cocoa (Theobroma cacao) pod husk. *Journal of Applied Sciences and Environmental Management*, 22 (2)

Obotey Ezugbe, E. and Rathilal, S. 2020. Membrane Technologies in Wastewater Treatment: A Review. *Membranes (Basel)*, 10 (5)

Orts, F., del;, R. A. I., J.;, M., J.;, B. and F;, C. 2019. Study of the Reuse of Industrial Wastewater After Electrochemical Treatment of Textile Effluents without External Addition of Chloride. *International Journal of Electrochemical Science*: 1733-1750.

Oyewo, O. A., Onyango, M. S. and Wolkersdorfer, C. 2016. Application of banana peels nanosorbent for the removal of radioactive minerals from real mine water. *J Environ Radioact*, 164: 369-376.

P. J. Goodhew, J. Humphreys and Beanland, R. 2001. *Electron Microscopy and Analysis*. 3rd ed. London: Taylor and Francis.

Padilla-Ortega, E., Leyva-Ramos, R. and Flores-Cano, J. 2013. Binary adsorption of heavy metals from aqueous solution onto natural clays. *Journal of Chemical Engineering Journal*, 225: 535-546.

Pala, S. L., Kebede Biftu, W., Suneetha, M. and Ravindhranath, K. 2021. Simultaneous removal of lead and cadmium ions from simulant and industrial waste water: using Calophyllum Inophyllum plant materials as sorbents. *International Journal of Phytoremediation*: 1-15.

Pap, S., Bezanovic, V., Radonic, J., Babic, A., Saric, S., Adamovic, D. and Turk Sekulic, M. 2018. Synthesis of highly-efficient functionalized biochars from fruit industry waste biomass for the removal of chromium and lead. *Journal of Molecular Liquids*, 268: 315-325.

Park, D., Yun, Y.-S. and Park, J. M. 2010. The past, present, and future trends of biosorption. *Biotechnology and Bioprocess Engineering*, 15 (1): 86-102.

Patel, H. 2019. Fixed-bed column adsorption study: a comprehensive review. *Applied Water Science*, 9 (3)

Pathak, P. D., Mandavgane, S. A. and Kulkarni, B. D. 2016. Characterizing fruit and vegetable peels as bioadsorbents. *Current Science (00113891)*, 110 (11): 2114-2123.

Pathak, P. D., Mandavgane, S. A. and Kulkarni, B. D. 2017. Fruit peel waste: characterization and its potential uses. *Curr. Sci*, 113 (3): 444-454.

Pathak Pranav, D., Mandavgane Sachin, A. and Kulkarni Bhaskar, D. 2015. *Fruit peel waste as a novel low-cost bio adsorbent*. Available: https://www.degruyter.com/view/j/revce.2015.31.issue-4/revce-2014-0041/revce-2014-0041.xml.

Perez-Marin, A. B., Zapata, V. M., Ortuno, J. F., Aguilar, M., Saez, J. and Llorens, M. 2007. Removal of cadmium from aqueous solutions by adsorption onto orange waste. *Journal of Hazardous Materials*, 139 (1): 122-131.

Pérez Marín, A. B., Aguilar, M. I., Meseguer, V. F., Ortuño, J. F., Sáez, J. and Lloréns, M. 2009. Biosorption of chromium (III) by orange (Citrus cinensis) waste: Batch and continuous studies. *Chemical Engineering Journal*, 155 (1-2): 199-206.

Podstawczyk, D., Witek-Krowiak, A., Dawiec, A. and Bhatnagar, A. 2015. Biosorption of copper(II) ions by flax meal: Empirical modeling and process optimization by response surface methodology (RSM) and artificial neural network (ANN) simulation. *Ecological Engineering*, 83: 364-379.

Qiu, B., Tao, X., Wang, H., Li, W., Ding, X. and Chu, H. 2021. Biochar as a low-cost adsorbent for aqueous heavy metal removal: A review. *Journal of Analytical and Applied Pyrolysis*, 155

R. W. Cahn Frs. 2005. *Concise Encyclopedia of Materials Characterization*. 2nd ed. Oxford: Elsevier Ltd.

Rajput, M. S., Sharma, A., Sharma, S. and Verma, S. 2015. Removal of Lead (II) from aqueous solutions by orange peel. *International Journal of Applied Research*, 1 (9): 411-413.

Raouf MS, A. and Raheim ARM, A. 2016. Removal of Heavy Metals from Industrial Waste Water by Biomass-Based Materials: A Review. *Journal of Pollution Effects & Control*, 05 (01)

Regti, A., Laamari, M. R., Stiriba, S.-E. and El Haddad, M. 2017. Use of response factorial design for process optimization of basic dye adsorption onto activated carbon derived from Persea species. *Microchemical Journal*, 130: 129-136.

Ronda, A., Martín-Lara, M., Dionisio, E., Blázquez, G. and Calero, M. 2013. Effect of lead in biosorption of copper by almond shell. *Journal of the Taiwan Institute of Chemical Engineers*, 44 (3): 466-473.

Saka, C., Şahin, Ö. and Küçük, M. M. 2012. Applications on agricultural and forest waste adsorbents for the removal of lead (II) from contaminated waters. *International Journal of Environmental Science and Technology*, 9 (2): 379-394.

Sala, M. and Gutiérrez-Bouzán, M. C. 2014. Electrochemical treatment of industrial wastewater and effluent reuse at laboratory and semi-industrial scale. *Journal of Cleaner Production*, 65: 458-464.

Salman H. Abbas, Ibrahim M. Ismail, Tarek M. Mostafa and Sulaymon, A. H. 2014. Biosorption of heavy metals: A review. *Journal of Chemical Science and Technology*, 3 (4): 74 - 102.

Saravanan, A., Kumar, P. S. and Yaswanthraj, M. 2017. Modeling and analysis of a packed-bed column for the effective removal of zinc from aqueous solution using dual surface-modified biomass. *Particulate Science and Technology*, 36 (8): 934-944.

Saravanan, A., Senthil Kumar, P., Varjani, S., Karishma, S., Jeevanantham, S. and Yaashikaa, P. R. 2021. Effective removal of Cr(VI) ions from synthetic solution using mixed biomasses: Kinetic, equilibrium and thermodynamic study. *Journal of Water Process Engineering*, 40

Schiewer, S. and Balaria, A. 2009. Biosorption of Pb2+ by original and protonated citrus peels: Equilibrium, kinetics, and mechanism. *Chemical Engineering Journal*, 146 (2): 211-219.

Schrank, S. G., Gebhardt, W., José, H. J., Moreira, R. F. P. M. and Schröder, H. F. 2017. Ozone Treatment of Tannery Wastewater Monitored by Conventional and Substance Specific Wastewater Analyses. *Ozone: Science & Engineering*, 39 (3): 159-187.

Semerjian, L. 2018. Removal of heavy metals (Cu, Pb) from aqueous solutions using pine (Pinus halepensis) sawdust: Equilibrium, kinetic, and thermodynamic studies. *Journal of Environmental Technology Innovation*, 12: 91-103.

Sen, S., Prajapati, A. K., Bannatwala, A. and Pal, D. 2019. Electrocoagulation treatment of industrial wastewater including textile dying effluent – a review. *Desalination and Water Treatment*, 161: 21-34.

Shafiee, M., Akbari, A. and Ghiassimehr, B. 2018. Removal of Pb(II) from Wastewater Using Henna: Optimization of Operational Conditions. *Iranian Journal of Chemical Engineering*, 15 (4): 17-26.

Shi, J., Yang, Z., Dai, H., Lu, X., Peng, L., Tan, X., Shi, L. and Fahim, R. 2018. Preparation and application of modified zeolites as adsorbents in wastewater treatment. *Water Sci Technol*, 2017 (3): 621-635.

Shoaib, A., Badar, T. and Aslam, N. 2011. Removal of Pb(II), Cu(II) and Cd(II) from aqueous solution by some fungi and natural adsorbents in single and multiple metal systems. *Pak. J. Bot.*, 43 (6): 2997-3000.

Sikarwar, S. and Jain, R. 2016. Adsorption kinetics studies of an anti-inflammatory drug Mesalamine using Unsaturated Polyester Resin (UPR). *Journal of Molecular Liquids*, 224: 219-226.

Singh N.B, Nagpal Garima, Agrawal Sonal and Rachna. 2018. Water purification by using Adsorbents: A review. *Environmental Technology and Innovation*, 11: 187-240.

Sonune, A. and Ghate, R. 2004. Developments in wastewater treatment methods. *Journal of Desalination*, 167: 55-63.

Suhas, Gupta, V. K., Carrott, P. J., Singh, R., Chaudhary, M. and Kushwaha, S. 2016. Cellulose: A review as natural, modified and activated carbon adsorbent. *Bioresource Technology*, 216: 1066-1076.

Sulyman, M., Namiesnik, J. and Gierak, A. 2017. Low-cost Adsorbents Derived from Agricultural By-products/Wastes for Enhancing Contaminant Uptakes from Wastewater: A Review. *Polish Journal of Environmental Studies*, 26 (2): 479-510.

Tan, K. and Hameed, B. 2017. Insight into the adsorption kinetics models for the removal of contaminants from aqueous solutions. *Journal of the Taiwan Institute of Chemical Engineers*, 74: 25-48.

Tang, J., Zhang, C., Shi, X., Sun, J. and Cunningham, J. A. 2019. Municipal wastewater treatment plants coupled with electrochemical, biological and bio-electrochemical technologies: Opportunities and challenge toward energy self-sufficiency. *J Environ Manage*, 234: 396-403.

Tavana, M., Pahlavanzadeh, H. and Zarei, M. J. 2020. The novel usage of dead biomass of green algae of Schizomeris leibleinii for biosorption of copper(II) from aqueous solutions: Equilibrium, kinetics and thermodynamics. *Journal of Environmental Chemical Engineering*, 8 (5)

Thomas, H. C. 1944. Heterogeneous ion exchange in a flowing system. *Journal of the American Chemical Society*, 66 (10): 1664-1666.

Veglio, F. and Beolchini, F. 1997. Removal of metals by biosorption: a review. *Hydrometallurgy*, 44 (3): 301-316.

Vera, L. M., Bermejo, D., Uguña, M. F., Garcia, N., Flores, M. and González, E. 2018. Fixed bed column modeling of lead (II) and cadmium (II) ions biosorption on sugarcane bagasse. *Journal of Environmental Engineering Research*, 24 (1): 31-37.

Vilar, V. J., Loureiro, J. M., Botelho, C. M. and Boaventura, R. A. 2008. Continuous biosorption of Pb/Cu and Pb/Cd in fixed-bed column using algae Gelidium and granulated agar extraction algal waste. *Journal of Hazardous materials*, 154 (1-3): 1173-1182.

Volesky, B. 1990. Removal and recovery of heavy metals by biosorption. *Biosorption of heavy metals*: 7-43.

Witek-Krowiak, A., Chojnacka, K., Podstawczyk, D., Dawiec, A. and Pokomeda, K. 2014. Application of response surface methodology and artificial neural network methods in modelling and optimization of biosorption process. *Bioresource Technology*, 160: 150-160.

Worch, E. 2012. *Adsorption technology in water treatment: fundamentals, processes, and modeling*. Walter de Gruyter.

Yahya, M. D., Abubakar, H., Obayomi, K. S., Iyaka, Y. A. and Suleiman, B. 2020a. Simultaneous and continuous biosorption of Cr and Cu (II) ions from industrial tannery effluent using almond shell in a fixed bed column. *Results in Engineering*, 6

Yahya, M. D., Ihejirika, C. V., Iyaka, Y. A., Garba, U. and Olugbenga, A. G. 2020b. Continuous Sorption of Chromium Ions from Simulated Effluents using Citric Acid Modified Sweet Potato Peels. *Nigerian Journal of Technological Development*, 17 (1): 47-54.

Yakout, S. and El-Deen, G. S. 2016. Characterization of activated carbon prepared by phosphoric acid activation of olive stones. *Arabian Journal of Chemistry*, 9: S1155-S1162.

Ye, Y., Yang, J., Jiang, W., Kang, J., Hu, Y., Ngo, H. H., Guo, W. and Liu, Y. 2018. Fluoride removal from water using a magnesia-pullulan composite in a continuous fixed-bed column. *J Environ Manage*, 206: 929-937.

Yoon, Y. H. and NELSON, J. H. 1984. Application of gas adsorption kinetics I. A theoretical model for respirator cartridge service life. *American Industrial Hygiene Association Journal*, 45 (8): 509-516.

Younes, M. M., El-sharkawy, I. I., Kabeel, A. E., Uddin, K., Pal, A., Mitra, S., Thu, K. and Saha, B. B. 2019. Synthesis and characterization of silica gel composite with polymer binders for adsorption cooling applications. *International Journal of Refrigeration*, 98: 161-170.

Ys, H., Mckay, G., YS, H. and MCKAY, G. 1999. Pseudo-second order model for sorption processes. *Journal of Process Biochem*, 34 (5): 451-465.

Zou, W., Zhao, L. and Zhu, L. 2012. Adsorption of uranium(VI) by grapefruit peel in a fixed-bed column: experiments and prediction of breakthrough curves. *Journal of Radioanalytical and Nuclear Chemistry*, 295 (1): 717-727.

13. APPENDICES

13.1 Appendix A- Raw data for the batch studies and published paper

A.1: Batch studies using banana peels published paper

Pol. J. Environ. Stud. Vol. 30, No. 2 (2021), 1487-1496
DOI: *10.15244/pjoes/122449* ONLINE PUBLICATION DATE: 2020-11-27

Original Research

Evaluation of Lead (II) Removal from Wastewater Using Banana Peels: Optimization Study

Felicia O. Afolabi[1]*, Paul Musonge[2], Babatunde F. Bakare[3]

[1]Department of Chemical Engineering, Durban University of Technology, Durban, South Africa
[2]Institute of Systems Science, Durban University of Technology, Durban, South Africa
[3]Department of Chemical Engineering, Mangosuthu University of Technology, Umlazi, Durban, South Africa

Received: 19 March 2020
Accepted: 14 May 2020

Abstract

The response surface methodology was used to investigate the removal of Pb (II) from an aqueous solution using banana peel with varying operating parameters in a batch mode. The central composite design was used to study the interactive effects of the operating parameters (initial concentration, pH of the solution, adsorbent dosage and the particle size). The banana peel was characterized by FTIR which showed the functional groups, while SEM and EDS were used to study the morphology and elemental composition. The optimum removal of Pb(II) was 98.146 % at initial concentration 100 mg/L, pH 5, adsorbent dosage 0.55 g and particle size 75 µm. The deviation between the experimental and the model predicted percentage removal was 5.17 %. The analysis of variance showed that the regression model was significant with a low probability and the correlation coefficient R^2 value of 0.9153. The results showed that the biosorption of Pb(II) was highly influenced by the pH and the adsorbent dosage, while the particle size had little effect on the biosorption process.

Keywords: Banana peel; Bio-sorption; Lead removal; Optimization; Response surface methodology.

A.2: Batch studies using orange peels published paper

Scientific African 13 (2021) e00931

Contents lists available at ScienceDirect

Scientific African

journal homepage: www.elsevier.com/locate/sciaf

Application of the Response Surface Methodology in the Removal of Cu^{2+} and Pb^{2+} from Aqueous Solutions Using Orange Peels

Felicia Omolara Afolabi [a,*], Paul Musonge [a,b], Babatunde Femi Bakare [c]

[a] Institute of Systems Science, Durban University of Technology, Durban, South Africa
[b] Faculty of Engineering, Mangosuthu University of Technology, Durban, South Africa
[c] Department of Chemical Engineering, Mangosuthu University of Technology, Durban, South Africa

ARTICLE INFO

Article history:
Received 17 February 2021
Revised 2 August 2021
Accepted 3 August 2021

Editor: DR B Gyampoh

Keywords:
Bio-sorption
Wastewater
Central composite design
Optimization
Response surface methodology

ABSTRACT

Increasing industrialization and urbanization has led to increased wastewater effluents, which affect the environment if not properly treated before discharge into water bodies. Hence, it is important to adopt an efficient technique for treating wastewater before discharge into water bodies. This study investigated the interaction of initial concentration, pH, adsorbent dosage, and particle size with orange peels for the biosorption of Cu^{2+} and Pb^{2+} from aqueous solution using the response surface methodology (RSM) with the central composite design (CCD). The regression model ascertained the validity of the second-order polynomial equation for the biosorption of Cu^{2+} and Pb^{2+} using orange peels. The coefficient of determination (R^2) obtained from the analysis of variance (ANOVA) for Cu^{2+} and Pb^{2+} are 0.9852 and 0.9433, respectively. The maximum adsorption uptakes of Cu^{2+} and Pb^{2+} were 54.94 mg/g and 65.14 mg/g respectively, which suggests that orange peels have a higher affinity for Pb^{2+} than for Cu^{2+}. The maximum efficiencies of Cu^{2+} and Pb^{2+} under the optimum conditions of the process variables are 88% and 90%, respectively. The agreement between the experimental and predicted values shows that the quadratic model developed can be used to adequately determine the interaction between process parameters in the bio-sorption of Cu^{2+} and Pb^{2+} onto orange peels. The study contributes to the search for eco-friendly and sustainable solutions to the treatment of water contaminated with low concentrations of Cu^{2+} and Pb^{2+} metal ions.

A.3: MATLAB code for the binary bio-sorption of Cu^{2+} and Pb^{2+}

```
x = 10:10:100;

y = 2:0.2:6;

a = 0.55;

b = 265;

[X,Y]=meshgrid(x,y);

z1 = 67.518+0.177.*X+11.894.*Y+34.084.*a-0.175.*b-0.037.*X.*Y+0.051.*a.*X-
0.0001.*b.*X-1.384.*a.*Y+0.0004.*b.*Y-0.0065.*a.*b-0.0015.*X.^2-1.2654.*Y.^2-
7.983.*a.^2+0.0003.*b.^2;

z2 = -10.401+0.599.*X+10.348.*Y+53.68.*a+0.097.*b-0.028.*X.*Y-0.228.*a.*X-
0.0002.*b.*X-2.841.*Y.*a-0.011.*b.*Y-0.059.*a.*b-0.00003.*X.^2-
0.448.*Y.^2+0.233.*a.^2+4.32e-6.*b.^2;

figure

m1=mesh(X,Y,z1);

m1.FaceColor='red';

hold on

m2=mesh(X,Y,z2);

xlabel('pH');

ylabel('dosage (g)');

zlabel('Percentage removal (%)');

m2.FaceColor='green';
```

13.2 Appendix B - Column studies raw data

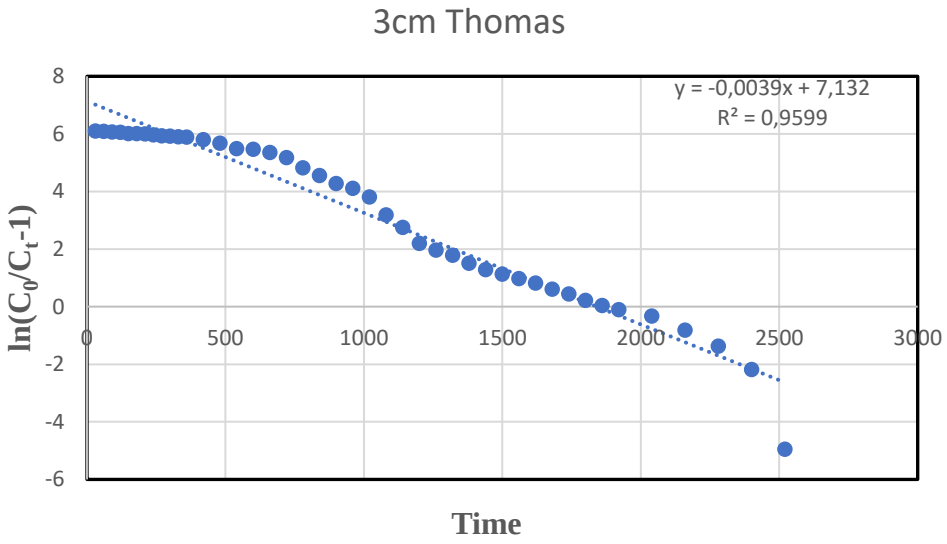

Figure B.1. Thomas model linear plot at 3cm bed height

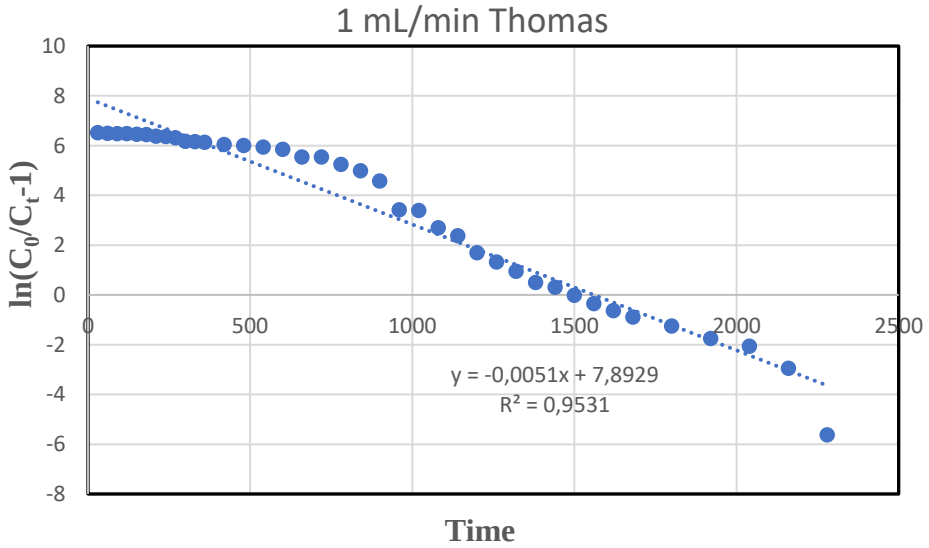

Figure B.2. Thomas model linear plot at 1 mL/min flow rate

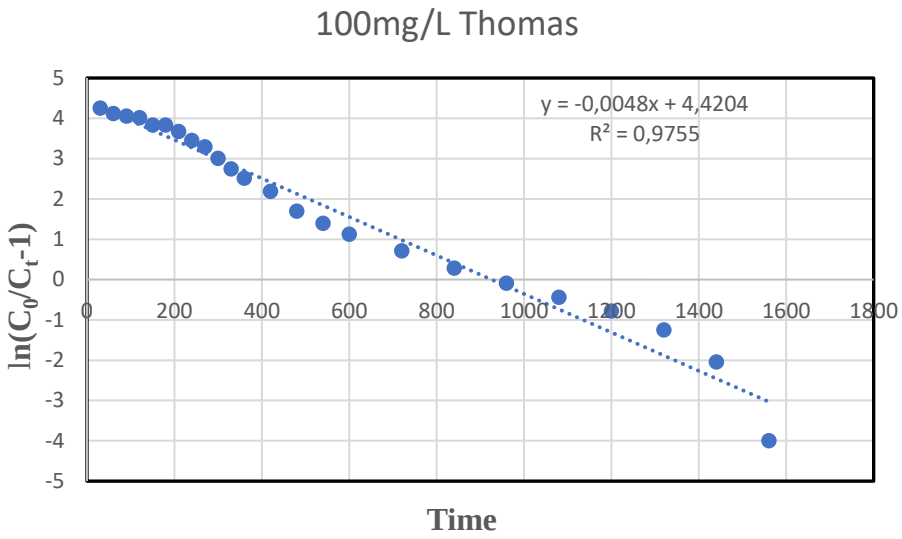

Figure B.3. Thomas model linear plot at 100 mg/L initial concentration

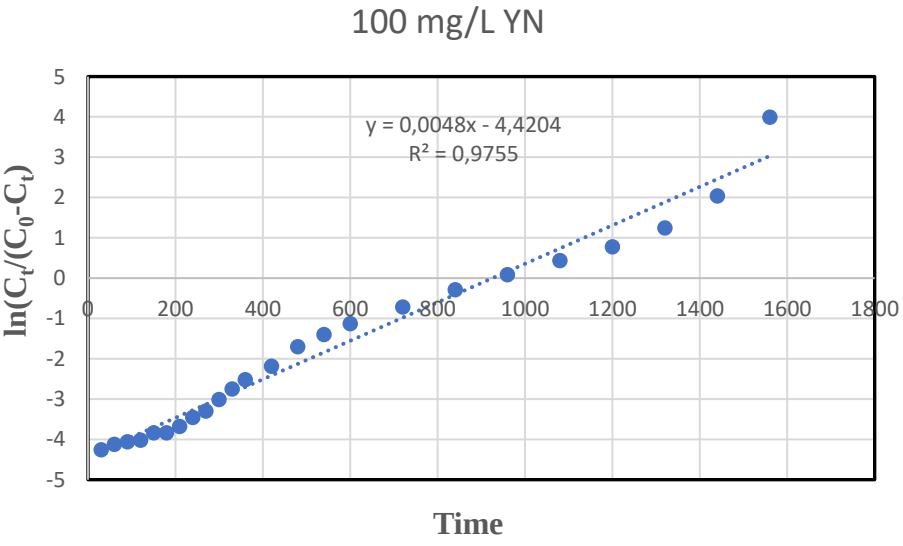

Figure B.4. Yoon Nelson model linear plot at 100 mg/L initial concentration

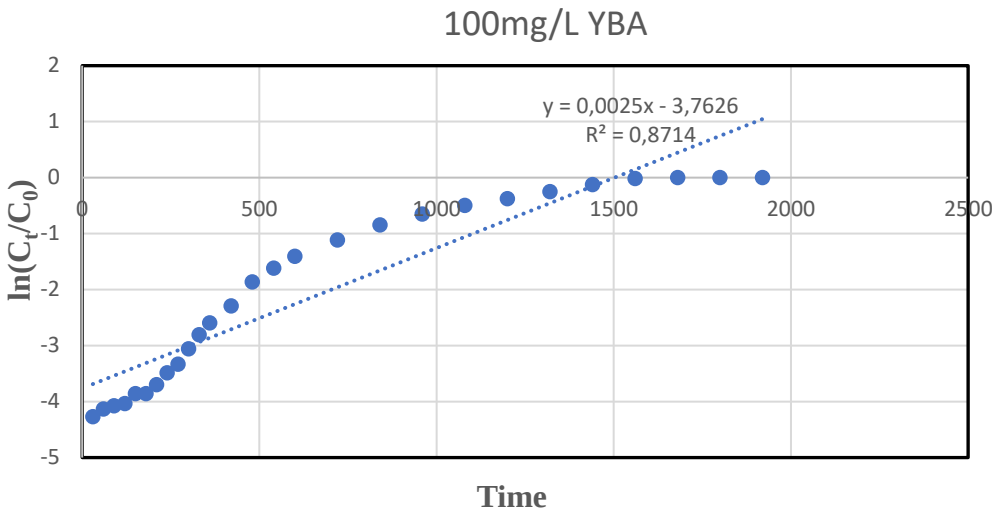

Figure B.5. Bohart Adams model linear plot at 100 mg/L initial concentration

13.3 Appendix C - Develop model script and data

C.1: Model parameter calculations

$$Flow\ rate\ Q = \frac{U_0 \pi d^2}{4}$$

Q = 3 mL/min = 0.05 cm^3/sec

Internal diameter d = 2.3

$$0.05 = \frac{U_0 (3.142) 2.3^2}{4}$$

Velocity U_0 = 1.2*10^{-2} cm/sec.

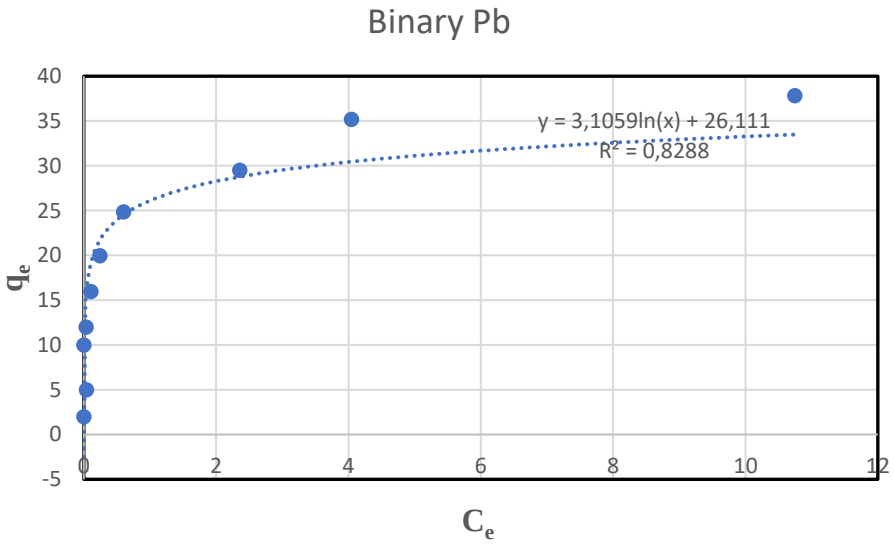

Figure C.1. Non-linear graph of binary Pb isotherm

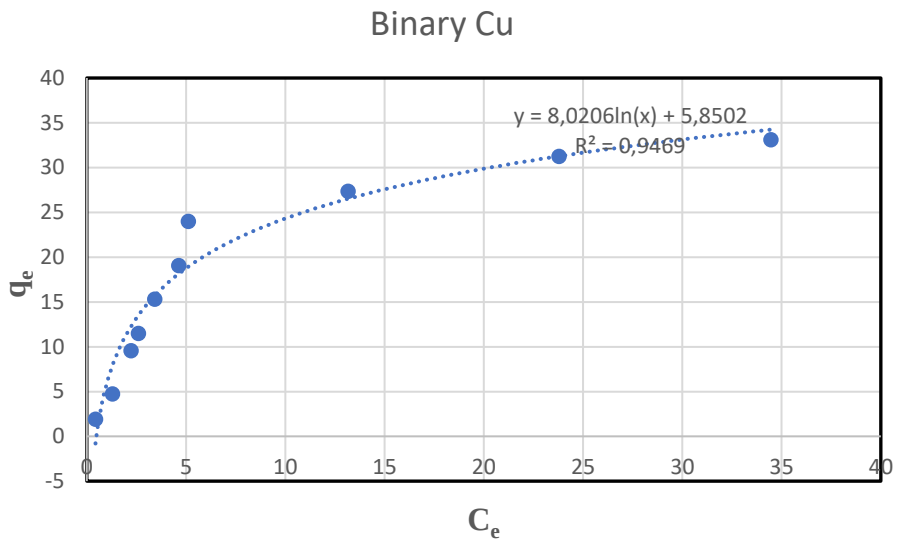

Figure C.2. Non-linear graph of binary Cu isotherm

C.2: Model code

```
cFeed = 10;      % Feed concentration
L = 3;           % Column length
t0 = 0;          % Initial Time
tf = 4000;       % Final time
dt = 0.5;        % Time step
z = 0:0.005:L;   % Mesh generation
t = t0:dt:tf;    % Time vector
n = numel(z);    % Size of mesh grid
%Initial Conditions / Vector Creation
c0 = zeros(n,1);
c0(1) = cFeed;
q0 = zeros(n,1);    % t = 0, q = 0 for all z, this makes sense to me
y0 = [c0 ; q0];     % Appends conditions together
```

C.3: Model data

Table C.1. Results of experimental, Thomas and developed model for the initial concentration of 10mg/L

Time	Experimental result		Thomas model		Developed model	
	Pb	Cu	Pb	Cu	Pb	Cu
30	0,024	0,039	0,015	0,325	1,44E-222	1,44E-222
150	0,025	0,042	0,019	0,041	7,08E-31	7,06E-31
300	0,031	0,063	0,024	0,053	0,123	0,123
900	0,066	0,163	0,087	0,149	0,814	0,817
1500	0,181	0,28	0,251	0,354	0,957	0,961
2700	0,68	0,861	0,807	0,843	0,993	0,998
3300	1	1	0,936	0,943	0,995	0,999
4000	1	1	1	1	0,995	0,999

Table C.2. Results of experimental, Thomas and developed model for the initial concentration of 50mg/L

Time	Experimental result		Thomas model		Developed model	
	Pb	Cu	Pb	Cu	Pb	Cu
30	0,006	0,02	0,013	0,031	5,10E-235	5,09E-235
150	0,044	0,13	0,032	0,097	1,49E-31	1,49E-31
300	0,144	0,358	0,095	0,324	0,123	0,123
600	0,516	0,91	0,517	0,906	0,599	0,599
900	0,836	1	0,915	0,994	0,817	0,817
1140	0,998	1	0,986	0,999	0,902	0,902
3300	1	1	1	1	0,996	0,999

4000	1	1	1	1	0,999	0,999

Table C.3. Results of experimental, Thomas and developed model for the initial concentration of 100mg/L

Time	**Experimental result**		**Thomas model**		**Developed model**	
	Pb	Cu	Pb	Cu	Pb	Cu
30	0,002	0,011	0,032	0,06	1,34E-237	1,34E-239
150	0,106	0,229	0,078	0,167	9,16E-32	9,16E-32
300	0,299	0,513	0,211	0,455	0,123	0,123
960	0,966	1	0,977	0,997	0,843	0,843
1500	1	1	0,999	0,999	0,961	0,961
2700	1	1	1	1	0,998	0,998
3300	1	1	1	1	0,999	0,999
4000	1	1	1	1	0,999	0,999